Cell signaling and functions mediated by a serine-threonine phosphatase regulatory subunit and related proteins in *Neurospora crassa*

A

thesis submitted in partial fulfillment of the

requirements for the award of the degree of

DOCTOR OF PHILOSOPHY

By

AVISHEK ROY

Department of Biosciences and Bioengineering

Indian Institute of Technology Guwahati

Guwahati – 781 039, Assam, India

January 2021

भारतीय प्रौद्योगिकी संस्थान गुवाहाटी
INDIAN INSTITUTE OF TECHNOLOGY GUWAHATI
Department of Biosciences and Bioengineering
Guwahati- 781 039

DECLARATION

I do hereby declare that the content embodied in this thesis entitled "**Cell signaling and functions mediated by a serine-threonine phosphatase regulatory subunit and related proteins in *Neurospora crassa***" is the result of investigations carried out by me in the Department of Biosciences and Bioengineering, Indian Institute of Technology Guwahati for the award of degree of Doctor of Philosophy, under the supervision of **Prof. Ranjan Tamuli**. The research presented in this thesis is original and has not been submitted in part or full for any degree or diploma to any other institute or university to the best of my knowledge and belief.

Avishek Roy

Guwahati
January, 2021

Avishek Roy
(Enrolment No. 156106025)

भारतीय प्रौद्योगिकी संस्थान गुवाहाटी
INDIAN INSTITUTE OF TECHNOLOGY GUWAHATI
Department of Biosciences and Bioengineering
Guwahati- 781 039

CERTIFICATE

This is to certify that the research work in this thesis entitled "**Cell signaling and functions mediated by a serine-threonine phosphatase regulatory subunit and related proteins in *Neurospora crassa***" by Avishek Roy (Roll No. 156106025) has been carried out at the Indian Institute of Technology Guwahati for the award of degree of Doctor of Philosophy in Biosciences and Bioengineering, under my supervision. The outcome of the research work presented in this thesis is original and has not been submitted in part or full for any degree or diploma to any other institute or university.

Guwahati
January, 2021

Thesis Supervisor: Prof. Ranjan Tamuli
Professor
Department of Biosciences & Bioengineering

Dedicated to

MA and BABA

List of Figures

List of Tables

Glossary

ANOVA	analysis of variance
bp	base pair
BLAST	basic local alignment search tool
BOD	biological oxygen demand
°C	degree Celsius
CA	California
CDD	Conserved Domain Database
cDNA	complementary deoxyribonucleic acid
ChIP	chromatin immunoprecipitation
cm	centimetre
DNA	deoxyribonucleic acid
EMSA	electrophoretic mobility shift assay
ExPASy	Expert Protein Analysis System
FGS	fructose glucose sorbose
FGSC	Fungal Genetics Stock centre
g	gram
g	relative centrifugal force
GFP	green fluorescent protein

h	hour
hph	hygromycin B resistance gene
Jm^{-2}	joule per square metre
KV	kilovolt
kb	kilo base pair
kDa	kilo Dalton
LG	linkage group
m	metre
M	molar
mA	milliampere
MEGA	Molecular Evolutionary Genetic Analysis
µg	microgram
µl	microlitre
µm	micrometre
µM	micromolar
ml	millilitre
mm	millimetre
mM	millimolar
N	normal
NCBI	National Center for Biotechnology Information

NCU	*Neurospora crassa* unit
NEB	New England Biolab
ng	nanogram
nM	nanomolar
NMR	nuclear magnetic resonance
Ω	ohm
OD	optical density
ORF	open reading frame
p	probability
PAGE	polyacrylamide gel electrophoresis
PCR	polymerase chain reaction
pm	picometre
psi	pound-force per square inch
qRT-PCR	quantitative real time polymerase chain reaction
RIP	repeat induced point mutation
RNA	ribonucleic acid
rpm	revolution per minute
RT-PCR	reverse transcription polymerase chain reaction
s	second
SCM	synthetic crossing media

SOB	super optimal broth
SOC	super optimal broth with Catabolite repression
UCR	University of California Riverside
USA	United States of America
UV	ultra violet
VM	Vogel's minimal media
VG	Vogel's glucose media
V	volt
w/v	weight/volume
w/w	weight/weight

Acknowledgments

Ph.D. is like a journey in a ship across the ocean, and we, the students, are like travelers with a goal to reach our destination safely and in time. For me, I got an opportunity to be a member of this wonderful ship named 'Neurospora Research Group' in the year 2015. From then onwards, I have been guided in every respect of my research work and emerge as an excellent professional to sail across the rough weather conditions, be it my research work, or to be an excellent professional by the captain of the ship Prof. Ranjan Tamuli. My heartiest respect, gratitude towards my supervisor Prof. Ranjan Tamuli without whose believe, support, guidance and motivation my thesis would not have seen the light of the day and I am also, thankful to him for his patience in going through the different versions of my thesis.

I would like to convey my sincere regards to my Doctoral committee members- Prof. Kannan Pakshirajan, Prof. Ajaikumar B Kunnumakara and Dr. Uttam Manna without whose suggestions and constructive criticism the thesis work would not have reached its completion.

I am thankful to the present and previous Directors of Indian Institute of Technology Guwahati (IITG) who have provided me such a vibrant and naturally rich campus to pursue my doctoral work and to the present and previous Heads of the Department of Biosciences and Bioengineering and other staff members of the department for providing me with the necessary support in terms of analytical instruments and other laboratory facilities for completion of my thesis work. I would like to pay my sincere regards to all the taxpayers of the country which enabled different funding agencies namely- MHRD, DBT and DST, Government of India for providing me with the fellowship and necessary project funding to my supervisor that aided and inspired me to culminate the research work into my thesis.

I would also like to thank Fungal Genetics Stock Centre (FGSC), University of Missouri, Kansas, USA for providing us with the *Neurospora* strains and generously waiving the charges for the same. Also, I will be ever grateful to Prof. Katherine A. Borkovich, Department of Plant Pathology and Microbiology, University of California, Riverside, USA for providing me with the *cnb-1*^{RIP} and 559 strains without which the research work would not have been possible.

Lab is a team and like in the game of football where coordination between all the players ensure victory of the team. In the similar way, I was lucky to have support, warmth and fun-loving environment provided by the members of the Neurospora Research group- Ajeet, Christy, Darshana. Serena, Rahul, Surabhi, Sangeeta and valuable suggestions and support by alumni members of this group- Dr. Rekha Deka, Dr. Ravi Kumar, Dr. Vijya Laxmi, Dr. Ananya Barman, Dr. Dibakar Gohain, Dr. Anand Tiwari, Manju, Pallavi, Shalini, Nayan and Divya. I would always cherish the company of- Darshana, Serena, Christy be it during the Tea breaks and other lighter moments we shared in the lab. I would like to mention especially about Dibakar da and Shasanka da with whom I have spent my major time during my Ph.D. tenure and explored various destinations to fulfill my bucketlist. They were not only my seniors but more like a family and we celebrated and spent many joyous occasions together and I will always cherish the bonding I share with them.

Friends are important assets for lifetime and I was lucky to have helpful friends and seniors in different spheres of life namely- Anurag, Abhijeet, Jon Jyoti, Aman, Anshuman, Krishna Kumar, Omkar, Madan, Ritirao, Sreeja, Srirupa, Adhiraj, Pulakeshwar, Langtuk, Abhirup, Sayantan, Bhaskar, Pratik, Narayan and seniors- Jahnu, Jintu, Madhurya, Babul, Shaad, Reshmi, Kamalesh, Prakash, Manash, Bandhan, Sourav, Chinmoy, Somdatta, Shweta, Souvik, Arka, Abhik, Rahul who have supported me throughout my entire professional career. I would like to especially mention about Sayantan, with whom I share almost 10 years of bonding right from my graduation days and was lucky to have him beside me in my PhD. tenure. The

memories of the lighter moments which we shared outside our routine research discussions will give me happiness throughout my life. I should mention about another important friend in my life – Daradi, who have seen me grow from an amateurish learner to a full-grown researcher and have always supported me through various ups and downs in both professional and personal life.

I would like to pay my heartiest regards and love towards my parents, relatives and cousins who have laid their sincere believe on me and supported me throughout my research work. I feel myself fortunate to have such wonderful supportive parents who have encouraged, motivated and guided me in every important decisions of my life which have helped me to successfully complete my research work. Thank you, Ma and Baba.

God, The Almighty has been kind to me showering his blessings and have shown me the correct path to tread on in different phases of my life and have provided me motivation to complete my research work successfully.

Lastly, I want to acknowledge the mess workers of the hostel and different eateries in and outside the campus which have provided me with their sumptuous delicacies that gave energy and kept me charged during the late working hours.

January, 2021 Avishek Roy

Synopsis

In this thesis work, I investigated cell functions mediated by the calcineurin B (CNB-1) subunit in *Neurospora crassa*. I studied how the mutations in the various EF-hand domains of CNB-1 result in diverse phenotypes under stress conditions, including calcium (Ca^{2+}) stress, thermotolerance, and regulation of the circadian clock in *N. crassa*. Furthermore, I established genetic interaction of *cnb-1* with the *nca-2, hsp80*, *crz-1*, *frequency* (*frq-1*), and *white-collar* (*wc-1*) genes in the regulation the heat shock, Ca^{2+} stress and circadian clock in *N. crassa*. Moreover, I found that the upregulation of *nca-2* during Ca^{2+} stress requires the binding of the transcription factor calcineurin responsive zinc-finger-1 (CRZ-1) to an 8 bp nucleotide sequence 5′-ACCGCGCC-3′, which is about 234 bp upstream of the ATG start codon of the *nca-2*. Furthermore, CRZ-1 physically binds to two other 8 bp nucleotide sequences 5´-CCTTCACA-3´ and 5′-AGCGGAGC-3′, which are about 1167 bp and 679 bp upstream of the ATG start codon in the promoter of *hsp80* under heat shock conditions in *N. crassa*. Therefore, the calcineruin-Crz-1 signaling cascade is important for cell survival under Ca^{2+} stress and heat shock conditions in *N. crassa*.

Thesis title: "Cell signaling and functions mediated by a serine-threonine phosphatase regulatory subunit and related proteins in *Neurospora crassa*"

Objectives:

1. Investigating the cell functions and regulatory mechanism of calcineurin B (CNB-1) subunit.
2. To identify the CNB-1 interacting partners and understanding their mechanism of action.
3. To establish a mechanistic model based on interacting partners and their role in different cell functions.

Chapters:

Chapter 1: Introduction

Chapter 2: Materials and Methods

Chapter 3: Cell functions and regulatory mechanism of calcineurin B (CNB-1) subunit

Chapter 4: Understanding the *cnb-1* transcriptional regulation and mechanism of action

Chapter 5: The calcineurin-CRZ-1 signaling pathway is required for the heat shock and calcium stress responses in *N. crassa*

Conclusions and future perspectives

Chapter 1: Introduction

Neurospora crassa is a filamentous fungus belonging to the ascomycetes family. *N. crassa* grows mainly on dead and burned vegetation in tropical and subtropical regions (Luque *et al.* 2012). *N. crassa* has been well established as an excellent eukaryotic model organism used for understanding various aspects of complex biological processes, including calcium (Ca^{2+}) signaling. Chapter 1 briefly describes about the historical timeline of *N. crassa* and how Ca^{2+} evolved as a universal signaling molecule. In eukaryotic organisms, Ca^{2+} plays a versatile role in regulating a wide array of cellular processes and adaptive responses (Berridge *et al.* 1998; Sanders *et al.* 2002; Davies and Terhzaz, 2009). The cytosolic free Ca^{2+} concentration ($[Ca^{2+}]_c$) is maintained ~100 nM at resting level and transiently rise to 1 μM or more to trigger Ca^{2+}-signaling (Chin and Means, 2000; Bootman *et al.* 2001).

Chapter 1 also briefly describes about another important Ca^{2+} signaling protein calcineurin, which plays a critical role in forming apical Ca^{2+} gradient, normal growth and development in *N. crassa* (Prokisch *et al.* 1997; Kothe and Free, 1998; Tamuli *et al.* 2016). In *N. crassa*, calcineurin is a heterodimer of a 63.9 kDa catalytic subunit calcineurin A (CNA-1) and a 19.8 kDa regulatory subunit calcineurin B (CNB-1), and these two subunits physically interact (Tamuli *et al.* 2016). CNB-1, the regulatory subunit of calcineurin is a Ca^{2+}-binding protein with four "EF-hand" Ca^{2+}-binding sites and a myristylation motif (Aitken et al. 1982). Moreover, transient rise in the $[Ca^{2+}]_c$ activates another EF-hand containing Ca^{2+} sensor calmodulin (CaM. CaM then activates calcineurin, which dephosphorylates calcineurin responsive zinc finger 1 (Crz1), which then enters into the nucleus and regulates target gene expression (Chen *et al.* 2010). Furthermore, the role of CNB-1 from lower to higher eukaryotes, including *N. crassa*, is discussed. Because *cnb-1* is an essential gene in *N. crassa*, conventional methods for generating knockout mutant and side directed mutagenesis of key amino acid residues are not possible due to lethality. Therefore, an inherent gene silencing

mechanism called repeat induced point (RIP) mutation (Cambareri et al. 1989) was used to generate viable *cnb-1*^{RIP} mutants, and their studies revealed important amino acid residues responsible for role of *cnb-1* during the sexual and asexual developmental stages, and in response to various environmental cues in *N. crassa* (Tamuli et al. 2016; Kumar et al. 2019). Finally, using chromatin immunoprecipitation (ChIP) and electrophoretic mobility shift assay (EMSA), I identified an 8 bp nucleotide sequence essential for the binding of CRZ-1 in the promoter of both *hsp80* and *nca-2* genes. CRZ-1 binds to this sequence to upregulate the *hsp80* and *nca-2* genes to cope with the heat shock and Ca^{2+} stress, respectively, in *N. crassa*.

Chapter 2: Materials and methods

Chapter 2 consists of the materials and methods used in the thesis work. *N. crassa* strains were grown, maintained and crossed as mentioned previously (Westergaard and Mitchell, 1947; Davis and de Serres, 1970). The wild type and different knockout mutants of *N. crassa* used for the study were obtained from the Fungal Genetics Stock Center (FGSC, Manhattan, KS). Some of the *N. crassa* strains were either generated in our laboratory or in Prof. Katherine A. Borkovich laboratory (University of California Riverside, USA). Chemicals and reagents were purchased from the standard suppliers, and used after being autoclaved or filter sterilized whenever required. Polymerase chain reaction (PCR), reverse transcriptase PCR, quantitative real time PCR, chromatin immunoprecipitation (ChIP), electrophoretic mobility shift assay (EMSA) and other molecular biology experiments were performed by using either the standard protocols (Sambrook and Russel, 2001) or according to manufacturer's instructions. All the statistical analyses of the experimental data and the graphs were plotted by using Microsoft Excel, Sigma Plot® (Systat Software, San Jose, CA).

Chapter 3: Cell functions and regulatory mechanism of calcineurin B (CNB-1) subunit

In this Chapter, I discussed about the effects of RIP-mutations in the different EF-hand domains of *cnb-1*. The analysis of the RIP-mutants lead to unravel the role of *cnb-1* in different stress conditions and development in *N. crassa*. Calcineurin is an essential gene, therefore, classical gene knockout approach is not viable. We therefore used repeat induced point (RIP) mutation, a gene silencing mechanism in *N. crassa* (Cambareri et al. 1989) to generate three RIP mutants of *cnb-1* (Tamuli et al. 2016). I studied the *cnb-1*^{RIP} mutants for its role in Ca^{2+} stress tolerance, where the *cnb-1*^{RIP} (602)-mutant displayed severe growth defect at the highest concentration of $CaCl_2$ (0.4 M) tested (Kumar et al. 2019). In addition, the *cnb-1*^{RIP} mutants showed inappropriate hyphal septation and branching in response to Ca^{2+} gradient. In addition, two *cnb-1*^{RIP} mutants 599 and 600 were sensitive to growth under osmotic stress conditions with an increasing concentration of sorbitol (Kumar et al. 2019). Furthermore, I found that the growth of the *cnb-1*^{RIP} mutants were reduced when exposed to a lethal temperature of 52 °C (Kumar et al. 2019). I also observed the role of *cnb-1* in the regulation of circadian clock in *N. crassa*. All the three mutants of *cnb-1* exhibited shorter period length in the circadian clock in comparison to the control *ras-1*^{bd} strain. Circadian clock shows insensitivity of its period length in response to variation in the growth temperature, a phenomenon known as temperature compensation (Q_{10}). However, the circadian clock of the *cnb-1*^{RIP} mutant strains remains temperature compensated in comparison with that of the positive control *ras-1*^{bd}.

Chapter 4: Understanding the *cnb-1* transcriptional regulation and mechanism of action

In this Chapter, I studied the molecular players that could have a probable genetic interaction with *cnb-1* for tolerance to the stress responses and developmental stages in *N. crassa*. The previous Chapter describes some of the important roles of *cnb-1* such as regulation of circadian clock, thermotolerance and Ca^{2+} mediated stress response in *N. crassa* (Kumar et al. 2019). Earlier studies identified several molecular players like *frequency* (*frq*) and *white-collar* (*wc-1* and *wc-2*) playing important roles in the *N. crassa* circadian clock (Dunlap and Lorros, 2004; Liu and Bell-Pedersen, 2006). Therefore, I also tested genetic interaction among the *cnb-1*, *frq-1* and *wc-1* genes and found that in the *cnb-1*^{RIP} mutants, at 20 ° and 25 °C, the *frq-1* gene exhibited reduced expression, whereas the *wc-1* levels were increased, indicating that the calcineurin pathway may regulate the transcription of the *frq-1* and *wc-1* genes. Calcineurin also has a role in thermotolerance, possibly with Hsp90 family of heat shock proteins (Hsps), and pathogenesis in *Cryptococcus neoformans*, *Candida glabrata*, and *Leishmania donovani* and (Singh et al. 2012). Calcineurin pathway activates downstream target crz-1 to regulate heat shock stress tolerance in C. *albicans* (Chen et al. 2012). The *N. crassa cnb-1*^{RIP} mutants were sensitive to growth at higher temperature, therefore, I investigated the molecular mechanism for the thermotolerance. I found that expression of *hsp80*, a class of heat shock protein belonging to the family of Hsp90, was increased under the heat shock conditions, indicating its involvement in the heat shock stress tolerance in *N. crassa cnb-1* mutants. Furthermore, to study genetic interaction between the calcineurin and *hsp80*, I used the calcineurin inhibitor FK506, which resulted in a reduced expression of the *hsp80*, *crz-1*, and *cnb-1*, suggesting a possible role of the calcineurin-crz1 pathway in the transcriptional regulation of *hsp80*. In addition, *cnb-1* has a role in the Ca^{2+} stress tolerance (Kumar et al. 2019), and earlier studies from our lab revealed a probable role of calcieneurin-crz-1 signal transduction pathway in the upregulation of *nca-2* (Gohain and Tamuli, 2019), a Ca^{2+}-ATPase

transporter that sequesters excess Ca^{2+} into the vacuoles or export them out of the cell to maintain Ca^{2+} homeostasis (Bowman et al. 2009, 2011). I also found that the expression of *nca-2* is reduced under the Ca^{2+} stress condition in the *cnb-1*^{RIP} mutants. Moreover, in the wild type strain, expression of *cnb-1*, *nca-2*, and *crz-1* under the Ca^{2+} stress was reduced on supplementation of FK506 in the standard VM media. Therefore, NCA-2 has a possible role in the calcineurin Ca^{2+} stress tolerance pathway.

Chapter 5: The calcineurin-CRZ-1 signaling pathway is required for the heat shock and calcium stress responses in *N. crassa*

In this Chapter, I studied the molecular mechanism leading to heat shock and Ca^{2+} stress tolerance in calcineurin. The ChIP analysis revealed that the transcription factor CRZ-1, a downstream target of calcineurin, binds to two separate sequences located 174 bp and 161 bp upstream of the *hsp80*, and the binding was more prominent under heat shock conditions. Therefore, binding of CRZ-1 appears to upregulate the expression of *hsp80* during heat shock stress tolerance. Furthermore, electrophoretic mobility shift assay (EMSA) revealed that 8 bp nucleotide sequences 5´-CCTTCACA-3´ and 5′-AGCGGAGC-3′, which are located about 1167 bp and 679 bp upstream of the ATG start codon in the promoter of *hsp80*, were responsible for the binding of CRZ-1 under the heat shock conditions. Additionally, ChIP analysis revealed that the CRZ-1 binds to 400 bp region in the promoter of *nca-2*. The Ca^{2+} ATPase transporter NCA-2 assists in sequestering Ca^{2+} into the vacuoles, thereby maintain Ca^{2+} homeostasis (Bowman et al. 2009, 2011), and the intensity of binding of CRZ-1 to the promoter of *nca-2* increases with the increasing concentration of Ca^{2+} ions. CRZ-1 binds to an 8 bp nucleotide sequence 5′-ACCGCGCC-3′, located about 234 bp upstream of ATG start codon, in the promoter of *nca-2* and upregulates its expression during Ca^{2+} stress. Therefore, the calcineurin-crz-1 signal transduction pathway has a role in the upregulation of both *hsp80*

and *nca-2*, and contributes in the survival under heat shock and Ca^{2+} stress conditions in *N. crassa*.

Conclusions and future perspectives:

This Chapter describes conclusions and future prospects of my thesis work. I also describe a model governing the regulation of *hsp80* and *nca-2* via calcineurin-CRZ-1 pathway. During Ca^{2+} or heat stress, the influx of Ca^{2+} to the cytoplasm increases via the Ca^{2+}-ATPase transporters and Ca^{2+} channel proteins, including NCA-2. The Ca^{2+} signaling machinery gets activated when $[Ca^{2+}]_c$ rises above a threshold level of about 1mM, Ca^{2+} binds to the Ca^{2+} sensors, including calmodulin (CaM) and calcineurin. Activated CaM is necessary for the full activation of Ca^{2+}-bound calcineurin, which subsequently dephosphorylates its downstream target CRZ-1 in the cytosol. The dephosphorylated CRZ-1 then shuttles into the nucleus and binds specific sequences in the promoter of *hsp80* and *nca-2*. HSP80 has a role in the cell survival under the heat shock condition, NCA-2 has a role in the survival under high Ca^{2+} possibly by transporting the excess Ca^{2+} into the internal stores or by mediating Ca^{2+} efflux from the cell, and therefore, NCA-2 is necessary for maintaining the Ca^{2+} homeostasis in the cell (Bowman *et al.* 2009, 2011; Zelter *et al.* 2004). Moreover, addition of the calcineurin inhibitor FK506 inhibits the downstream signaling cascade of calcineurin, resulting in the reduced expression of *nca-2*, *hsp80*, and *crz-1*.

Future perspectives of this research work:

This thesis work opens up several new avenues, such as (i) to determine the molecular interaction of Hsp80 and CNA-1, (ii) to identify additional molecular targets of calcineurin for its molecular mechanism behind the regulation of the circadian clock in *N. crassa*, and (iii) to

gain insight into the structure-function relationship of CNB-1 using nuclear magnetic resonance (NMR), and (iv) to determine an extensive molecular signaling network of calcineurin in *N. crassa*.

Chapter 1

An introduction to *Neurospora crassa* and calcium signaling

1.1 *Neurospora crassa*: a brief history of being established as an excellent model organism

The name '*Neurospora*' was given due to the characteristic nerve like striations present on the sexual spores (Fig. 1.1), also known as 'ascospores'. *Neurospora*, a filamentous fungus belonging to the phylum Ascomycota, was first documented as the organism responsible for orange bread mould infestations in French bakeries and reported as *Oidium aurantiacum* (Payen, 1843) and *Penicillium sitophilum* (Montagne, 1843) independently. In the mid-1920s, *N. crassa* was identified as a heterothallic fungus with two mating types, *A* and *a* with eight asci by Shear and Dodge, while Bernard Lodge and Carl Lindegren together demonstrated Mendelian inheritance in the individual asci (Shear and Dodge, 1927; Dodge, 1939; Perkins, 1992). George Beadle and Edward Tatum discovered that the typical function of a gene is to control a particular enzyme synthesis in *N. crassa*, which eventually led to the famous 'one gene one enzyme' hypothesis (Beadle and Tatum, 1941) for which they were awarded the Nobel Prize in "Physiology or Medicine" in 1958. Further, genome sequencing of *Neurospora crassa* was completed later in 2003 (Galagan et al. 2003). *N. crassa* has been extensively used as an model organism for understanding various biological processes such as cellular differentiation and development, DNA methylation and repair, genome defence mechanisms, mitochondrial transport, and post-transcriptional gene silencing (Davis, 2000; Davis and Perkins, 2002; Galagan et al. 2003).

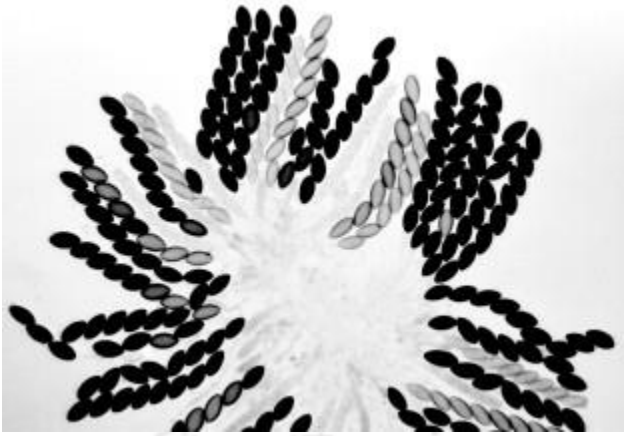

Fig. 1.1 Maturing rosette resulting from cross between two wild type strains of opposite mating type. The darker ascospores signify that they are more mature than the lighter ones resulted from the cross between two wild type strains in *N. crassa*. Figure is adapted from Raju, 1980.

N. crassa is a multicellular haploid organism having a genome size of about ~ 43 Mb and about 10,083- protein coding genes distributed into seven linkage groups (LG I-VII) that are of 4 to 10.3 Mb in size (Davis and de Serres, 1970; Davis and Perkins, 2002; Galagan et al. 2003). As a heterotroph, *N. crassa* can utilize a wide array of carbon and nitrogen sources, and only a few trace elements, simple salts, and a single vitamin called biotin are essential for its growth (Davis and de Serres, 1970; Burnett, 1975; Perkins and Davis, 2000). *Neurospora* possesses a wide range of genome defence mechanisms that functions in different life cycle phases, a reversible post-transcriptional gene silencing (PTGS) mechanism known as 'quelling' (Romano and Macino, 1992), which occurs during the vegetative phase, a transcriptional gene silencing (TGS) mechanism known as 'repeat-induced point mutation-RIP' (Cambareri et al. 1989) unique to fungi and occurs after fertilization and before karyogamy, another PTGS mechanism known as 'meiotic silencing' which occurs during its sexual phase (Shiu et al. 2001).

1.2 Life cycle of *N. crassa*

The multicellular fungus *N. crassa* has a complex life cycle compared to the unicellular yeasts, and consists of both asexual (vegetative) and sexual phases (Raju, 1992; Springer, 1993). In the nutrient-rich environment, *N. crassa* enters the asexual phase and produces branched multinucleated filaments or vegetative hyphae that runs parallel to the surface of the solid medium (Springer, 1993). The vegetative hyphae are segmented by incomplete internal cross walls or septa that allows the movement of cellular organelles like mitochondria, and other inclusion bodies amongst cells. A hyphal network is also called mycelium. Under nutrient-deprived condition or in the presence of an air-water interface, specialized aerial hyphae develop from the mycelium and give rise to conidiophores which subsequently produce uninucleate asexual spores called microconidia or multinucleate macroconidia (Springer, 1993). Macroconidia are primarily used as vegetative culture inoculum and also as fertilizing male parent in a sexual cross. Submerged cultures of *N. crassa* normally maintain vegetative hyphae without conidiation, however, certain environmental stimuli such as nitrogen or carbon starvation and exposure to high temperatures also lead to the formation of conidiophores or conidia in submerged cultures (Cortat and Turian, 1974; That and Turian, 1978; Plesofsky-Vig et al. 1983; Guignard et al. 1984).

N. crassa is a heterothallic filamentous fungus that contains two non-switching mating types, '*A*' and '*a*' determined by alternative DNA sequence known as idiomorphs. Starvation of nitrogen, low temperature, and light initiate the sexual cycle by forming female reproductive structure known as protoperithecium (Raju, 1992). A specialized receptor hypha (trichogyne) originating from the protoperithecium that initiates chemotropic growth towards a male element of the opposite mating type that is typically a hyphal fragment, macroconidium, or microconidium. Fusion of the trichogyne with the conidium is followed by transport of the male nucleus to the protoperithecium and initiates the development of the multicellular sexual

apparatus known as perithecium (matured protoperithecium). The male and female nuclei coexist as a dikaryon after plasmogamy in a specialized structure called ascogenous hypha. The paired male and female nuclei undergo a series of synchronous mitosis at the tip of a specialized hook-shaped structure called the crozier. During karyogamy, nuclei of the opposite mating type fuse and form a diploid zygote which undergoes two immediate meiotic divisions and post-meiotic mitosis producing an octad of eight spindle-shaped sexual spores known as ascospores that are packed in a linear fashion in the narrow ascus. After maturation, the ascospores are ejected through a beak (ostiole) at the tip of the perithecium in the direction of blue light. In the presence of suitable temperature and nutrients, the ejected ascospores can germinate and produce their own vegetative hyphae (Fig. 1.2; Raju, 1980; 1992; Springer, 1993; Kim et al. 2012).

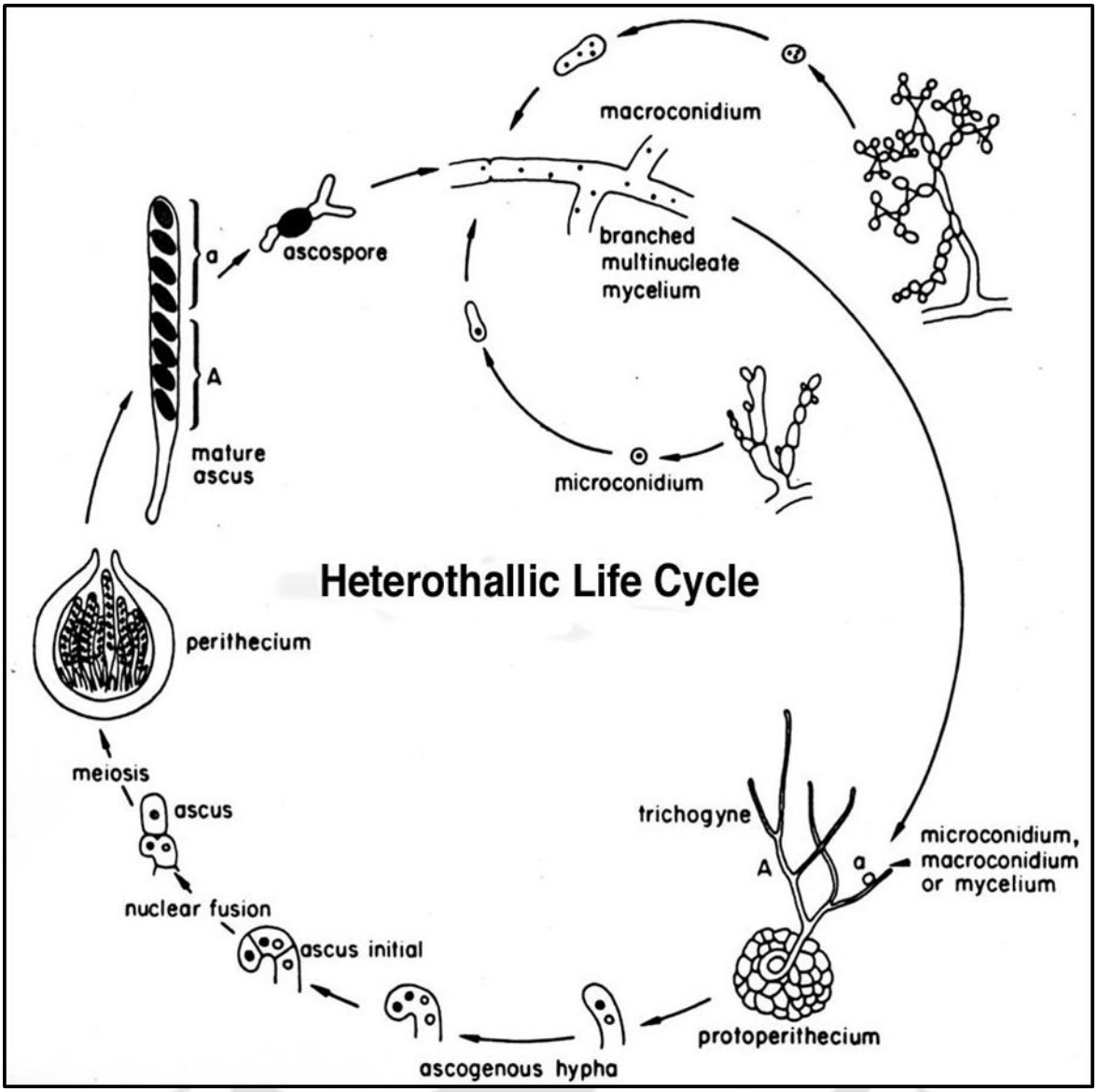

Fig. 1.2 The life cycle of *N. crassa*. During the asexual cycle, the multinucleate and branched vegetative mycelium develops into aerial hyphae and forms asexual spores, either multinucleate macroconidium or uninucleate microconidium that eventually germinate to form new mycelium. Sexual cycle is initiated with the formation of a female reproductive structure known as protoperithecium. It is fertilized by a conidium or mycelium of opposite mating type of a male parent and becomes matured perithecium which undergoes a series of mitosis and meiosis forming eight linearly ordered ascospores within an ascus. Once released, the mature pigmented multinucleate ascospores develops into new hyphae and forms the multicellular mycelium to complete the asexual cycle or functions as male or a female parent to undergo

another sexual cycle. Figure is adapted from FGSC (http://www.fgsc.net/Neurospora/sectionB2.htm).

1.3 Evolution of Calcium (Ca^{2+}) as a ubiquitous second messenger for signaling

Earth is covered by about 3 parts of water and one-part land. From the time of evolution of life on earth, both calcium (Ca^{2+}) and magnesium (Mg^{2+}) have evolved as divalent cations with a difference in the ability to form complex with water molecules. Ca^{2+} has a high degree of hydration and can accommodate 6 - 8 water molecules, and owing to its unique properties such as charge, ionic radius, polarizability and hydration energy, Ca^{2+} can easily interact with molecules of complex geometry such as proteins (Brini et al. 2013a; Brini et al. 2013b). The Ca^{2+} that enters the cytoplasm through Ca^{2+} channels, binds to a wide range of Ca^{2+} binding proteins through a characteristic Ca^{2+} binding helix-loop-helix structural motif known as EF-hand domain (Nakayama and Kretsinger, 1994; Clapham, 2007; Gifford et al. 2007). In the EF-hand domain, the Ca^{2+} binding loop between the two α-helices contains 12 amino acids rich in acidic residues provide negatively charged oxygen atoms for Ca^{2+} co-ordination (Fig. 1.3 A) in a pentagonal bipyramidal geometry (Fig.1.3 B), which is the most preferable co-ordination chemistry for Ca^{2+} (Gifford et al. 2007). From time immemorial, Ca^{2+} has evolved as a molecule for life and death, and played a critical role in the evolution of life on earth about 3.5 billion years ago (Plattner and Verkhratsky, 2014). Ca^{2+} in the primitive prokaryotes it seems to be regulated within the cells (Shermarova and Nesterov, 2005). It has been predicted that in the course of evolution, Ca^{2+} assisted in the stability of DNA or RNA molecules which exist as primitive stable molecules for the evolution of life (Jaiswal, 2001). From the time life evolved, ATP was considered as the central molecule which was responsible for formation of DNA/ RNA subsequently (Galimov, 2009; Ponnamperuma et al. 1963). Due to various chemical and biological reactions during cooling of earth caused the rising levels of extracellular free Ca^{2+} in the environment (Jaiswal, 2001). Therefore, the increasing levels of

Ca^{2+} acted as a selective pressure for the need of a Ca^{2+} homeostatic system that led to the evolution of various Ca^{2+} pumps, exchangers and internal Ca^{2+} stores, so that cells could maintain their cytosolic free Ca^{2+} ($[Ca^{2+}]c$) within the tolerable range (Jaiswal, 2001; Verkhratsky and Parpura, 2014). Even, the synthesis of ATP was dependent on low Ca^{2+} concentration, therefore Ca^{2+} evolved as an important signaling ion across the different forms of life. Right from the early days of bacteria and protozoan evolution, Ca^{2+} was considered as a molecule of cell signaling, much before it got established as a ubiquitous secondary messenger molecule in the eukaryotic system (Shemarova and Nesterov, 2005; Case et al. 2007).

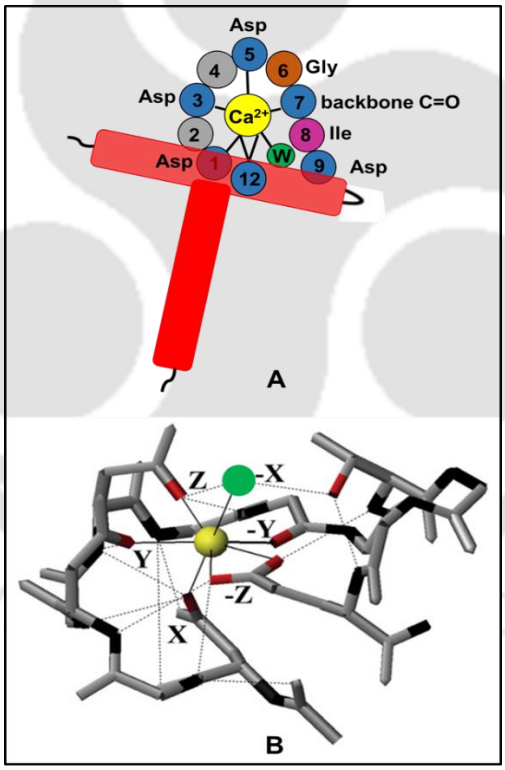

Fig. 1.3 Pictorial representation of the coordination sphere for Ca^{2+} binding EF-hand loop.

A. Schematic diagram of the co-ordination sphere where the two α-helices are shown in red, the co-ordinating amino acid ligands are shown in blue and water molecule (W) in green.

Conserved glycine (Gly) residues that provide the bend in the loop are shown in brown. The conserved hydrophobic amino acid residue that forms a short β-sheet in the paired EF-hand is shown in purple.

B. Ca^{2+} co-ordination in the canonical EF-hand domain 1 (EF-1) of calmodulin (CaM) showing both pentagonal bipyramidal Ca^{2+} co-ordination (continuous lines) and hydrogen bonding (dotted lines). Adapted from Gifford et al. 2007.

1.4 Ca^{2+} concentration gradient switches on the downstream Ca^{2+} signaling cascade in fungi

Outside the cell, the Ca^{2+} concentration is about 10^{-3} M (Chin and Means, 2000), whereas the cytosolic free $[Ca^{2+}]_c$ in resting condition is maintained at about ~100 nM, therefore a Ca^{2+} gradient of 10,000-fold is maintained by the cell across the plasma membrane (Berridge et al. 2003). The excess Ca^{2+} is stored in different intracellular stores, including endoplasmic reticulum (ER), mitochondria, and vacuoles (Cornelius and Nakashima, 1987). The Ca^{2+} concentration in the ER is maintained at several hundred µM. In addition, cell needs to maintain intracellular Ca^{2+} homeostasis to bypass the fluctuations in Ca^{2+} resulting in severe affects in the cell (Berridge et al. 2003). The entry of Ca^{2+} across the plasma membrane is mediated by specific receptors and Ca^{2+} channels in response to different stimuli such as membrane depolarization, mechanical stretch, and external agonists (Zeng et al. 2003; Mikoshiba et al. 2000). The mobilization of Ca^{2+} from the internal stores is primarily mediated by the IP_3 receptors (IP_3R; Zeng et al. 2003; Mikoshiba et al. 2000) and the ryanodine receptors (RyR; Hamilton et al. 2005). Several components like the plasma membrane Ca^{2+}-ATPase (PMCA), the sarcoplasmic/endoplasmic reticulum Ca^{2+}-ATPase (SERCA), the Na^+/Ca^{2+} exchanger, the mitochondrial uniporter are responsible for sequestering the excess Ca^{2+} from the cytosol by

transporting Ca^{2+} either to external medium or into different cellular compartments (Berridge et al. 2003).

N. crassa possesses a complex Ca^{2+} signaling system (Fig.1.4) consisting of forty-eight Ca^{2+} signaling proteins (Table 1.1; Borkovich et al. 2004; Tamuli et al. 2013). The Ca^{2+} signaling in *N. crassa* is significantly unique compared to that of plant and animal cells in terms of the second messenger systems associated with the Ca^{2+} release from the internal stores (Galagan et al. 2003; Borkovich et al. 2004; Zelter et al. 2004). *N. crassa* lacks inositol 1, 4, 5- trisphosphate (IP_3) receptors, ADP ribosyl cyclase and ryanodine receptors which are the key components of the mechanisms for Ca^{2+} release from internal stores in both plant and animal cells (Galagan et al. 2003; Borkovich et al. 2004). In addition, *N. crassa* also lacks extracellular Ca^{2+} sensing receptor proteins, as reported in animal cells for sensing changes in the extracellular Ca^{2+} concentration (Brown et al. 1993; Galagan et al. 2003; Borkovich et al. 2004). Interestingly *N. crassa* possesses both Ca^{2+}/Na^{+} and Ca^{2+}/H^{+} exchangers, while animals possess only Ca^{2+}/Na^{+} exchangers, and plants possess only Ca^{2+}/H^{+} exchangers, (Borkovich et al. 2004). These notable differences suggest that *N. crassa* might possess novel intracellular Ca^{2+} release mechanisms yet to be identified.

[a] Table 1.1 The list of Ca^{2+} signaling proteins in *N. crassa*

Sl. No.	NCU No.	Gene name	Protein name	Protein type	Best overall[b] (e-value; organism; protein name; accession number)
1	02762	*cch-1*	Cch-1	Ca^{2+} permeable channel	0; *Verticillium dahlia* (cch1); EGY18507.1

2	06703	*mid-1*	MID-1	Ca^{2+} permeable channel	2e-97; *Paracoccidioides brasiliensis* (MID1); EEH23338.1
3	11680[c]			Ca^{2+} permeable channel	0; *Ajellomyces dermatitidis* (Yvc1); EGE78766.1
4	03305	*nca-1*	NCA-1	Ca^{2+}-ATPase	0; *Trichophyton tonsurans* (SCA-1); EGD96734.1
5	04736	*nca-2*	NCA-2	Ca^{2+}-ATPase	0; *Magnaporthe oryzae* (Plasma membrane calcium transporting ATPase 3); EHA56671.1
6	05154	*nca-3*	NCA-3	Ca^{2+}-ATPase	0; *Glomerella graminicola* (Calcium translocating P-type ATPase); EFQ29373.1
7	03292	*pmr-1*	PMR-1	Ca^{2+}-ATPase	0; *Uncinocarpus reesii* (PMR1); XP_002541437.1
8	08147	*ph-7*	PH-7	Ca^{2+}-ATPase	0; *G. graminicola* (Potassium/sodium efflux Ptype ATPase); EFQ36596.1
9	04898	*trm-9*	TRM-9	Ca^{2+}-ATPase	0; *Cordyceps militaris* (Cation transporting ATPase 4); EGX91104.1
10	03818	*trm-10*	TRM-10	Ca^{2+}-ATPase	0; *V. dahlia* (Neo1p); EGY18069.1

11	07966	*trm-1*	TRM-1	Cation-ATPase	0; *T. tonsurans* (Cta3p); EGD97988.1
12	10143[d]	*atp-11*	ATP-11	Cation-ATPase	0; *C. militaris* (ATPase type 13A2); EGX92563.1
13	07075	*cax*	CAX	Ca^{2+}/H^{+} exchanger	0; *G. graminicola* (Calcium/proton exchanger); EFQ30300.1
14	00916	*trm-15*	TRM-15	Ca^{2+}/H^{+} exchanger	2e-176; *Aspergillus fumigatus* (membrane-bound cation transporter, XP_001481534.1)
15	00795	*trm-14*	TRM-14	Ca^{2+}/H^{+} exchanger	1e-149; *A. niger* (membrane-bound cation transporter, XP_001400827.2)
16	06366	*trm-18*	TRM-18	Ca^{2+}/H^{+} exchanger	0; *Sclerotinia sclerotiorum* (Ca^{2+}/H^{+} antiporter, XP_001589752.1)
17	07711	*trm-19*	TRM-19	Ca^{2+}/H^{+} exchanger	4e-160; *T. tonsurans* (vacuolar calcium ion transporter/H^{+} exchanger, EGD98067.1)
18	05360	*trm-17*	TRM-17	Ca^{2+}/H^{+} exchanger	0; *Metarhizium anisopliae* (calcium permease, EFY95914.1)

19	02826	*trm-16*	TRM-16	Ca^{2+}/Na^{+} exchanger	0; *Verticillium albo-atrum* (sodium/calcium exchanger protein, XP_003004985.1)
20	08490	*trm-20*	TRM-20	Ca^{2+}/Na^{+} exchanger	1e-83; *A. niger* (sodium/calcium transporter, XP_001397155.1)
21	01266	*plc-2*	PLC-2	Phospholipase C	0; *Sordaria macrospora* (phosphoinositide-specific phospholipase C, XP_003348116.1)
22	06245	*plc-1*	PLC-1	Phospholipase C	0; *G. graminicola* (phosphatidylinositol-specific phospholipase C, EFQ28596.1)
23	11415[e]	*inl-7*	INL-7	Phospholipase C	0; *G. graminicola* (Phosphatidylinositol-specific phospholipase C); EFQ31595.1
24	02175	*inl-15*	INL-15	Phospholipase C	3e-125; *Botryotinia fuckeliana* (BcPLC2); CCD34776.1
25	04120	*cmd*	CaM	Calmodulin	1e-103; *Gibberella zeae* (CaM); XP_382067.1

26	03804	*cna-1*	CNA-1	Ca^{2+} and/or CaM binding protein	0; *Sordaria macrospora* (Serine/threonine-protein phosphatase 2B catalytic subunit protein, XP_003352213.1)
27	03833	*cnb-1*	CNB-1	Ca^{2+} and/or CaM binding protein	2e-119; *Trichoderma reesei* (calcineurin, beta subunit, EGR44907.1)
28	09265	*cnx-1*	CNX-1	Ca^{2+} and/or CaM binding protein	0; *S. macrospora* (cnx1, XP_003347545.1)
29	05225[f]	*nde1*	NDE-1	Ca^{2+} and/or CaM binding protein	0; *M. oryzae* (mitochondrial NADH dehydrogenase, EHA47323.1)
30	02115			Ca^{2+} and/or CaM binding protein	0; *M. oryzae* (EF hand domain-containing protein, EHA48778.1)
31	01564	*mic-4*	MIC-4	Ca^{2+} and/or CaM binding protein	0; *M. oryzae* (calcium dependent mitochondrial carrier protein, EHA48778.1)
32	06948			Ca^{2+} and/or CaM binding protein	2e-54; *Mycosphaerella graminicola* (calcium ion binding, calmodulin, EGP88834.1)

33	04379	*ncs-1*	NCS-1	Ca^{2+} and/or CaM binding protein	4e-126; *Grosmannia clavigera* (neuronal calcium sensor 1, EFX03580.1)
34	02738	*pef-1*	PEF-1	Ca^{2+} and/or CaM binding protein	2e-130; *V. dahliae* (Peflin, EGY21808.1)
35	09871	*nup-34*	NUP-34	Ca^{2+} and/or CaM binding protein	4e-33; *V. dahliae* (Centrin-3,EGY16271.1)
36	01241	*mic-2*	MIC-2	Ca^{2+} and/or CaM binding protein	0; *T. reesei* (mitochondrial carrier protein, EGR44893.1)
37	06347	*ask-2*	ASK-2	Ca^{2+} and/or CaM binding protein	0; *S. macrospora* (actin cytoskeleton–regulatory complex protein, XP_003350109.1)
38	06617	*cdc4-2*	CDC4-2	Ca^{2+} and/or CaM binding protein	7e-93; *V. albo-atrum* (myosin regulatory light chain cdc4, XP_003009631.1)
39	03750	*cmd-2*	CMD-2	Ca^{2+} and/or CaM binding protein	8e-74; *B. fuckeliana* (calmodulin, XP_001560827.1)

40	08980	*nde-2*	NDE-2	Ca^{2+} and/or CaM binding protein	0; *G. clavigera* (alternative NADH-dehydrogenase, EFX03867.1)
41	02283	*camk-2*	CaMK-2	Ca^{2+} and/or CaM binding protein	0; *S. macrospora* (calcium/calmodulin-dependent protein kinase type I, XP_003344498.1)
42	09123	*camk-1*	CaMK-1	Ca^{2+} and/or CaM binding protein	0; *Sporothrix schenckii* (calcium/calmodulin-dependent kinase, AAV80434.1
43	09212	*camk-4*	CaMK-4	Ca^{2+} and/or CaM binding protein	0; *G. clavigera* (serine/threonine-protein kinase chk2, EFX01629.1)
44	02814	*prd-4*	PRD-4	Ca^{2+} and/or CaM binding protein	0; *V. dahliae* (serine/threonine-protein kinase srk1, EGY15110.1)
45	06650	*spp-3*	SPP-3	Ca^{2+} and/or CaM binding protein	3e-61; *Nectria haematococca* (phospholipase A2, XP_003042542.1)
46	02411			Ca^{2+} and/or CaM binding protein	0; *G. graminicola* (microtubule-associated protein, EFQ31793.1)

47	06177	*camk-3*	CaMK-3	Ca^{2+} and/or CaM binding protein	0; *M. grisea* (CMKK2, ACM41720.1)
48	04265	*inv*	INV	Ca^{2+} and/or CaM binding protein	7e-85; *Bacillus megaterium* (betafructosidase FruA, AEN90524.1)

[a]Adapted from Tamuli et al. 2013.

[b]BLASTp search was performed at NCBI (http://blast.ncbi.nlm.nih.gov/Blast.cgi; Altschul et al. 1990; Altschul et al. 1997; Altschul et al. 2005) with default parameters for each of the 48 Ca^{2+} signaling proteins against the non-redundant protein sequence databases and the respective best overall match in other organisms with *e*-value has been indicated.

[c]Split from NCU07605.1

[d]Split from NCU01437.1

[e]Split from NCU0955.1

[f]NCU05225 was indicated as NCU08980.1 in Borkovich et al. 2004.

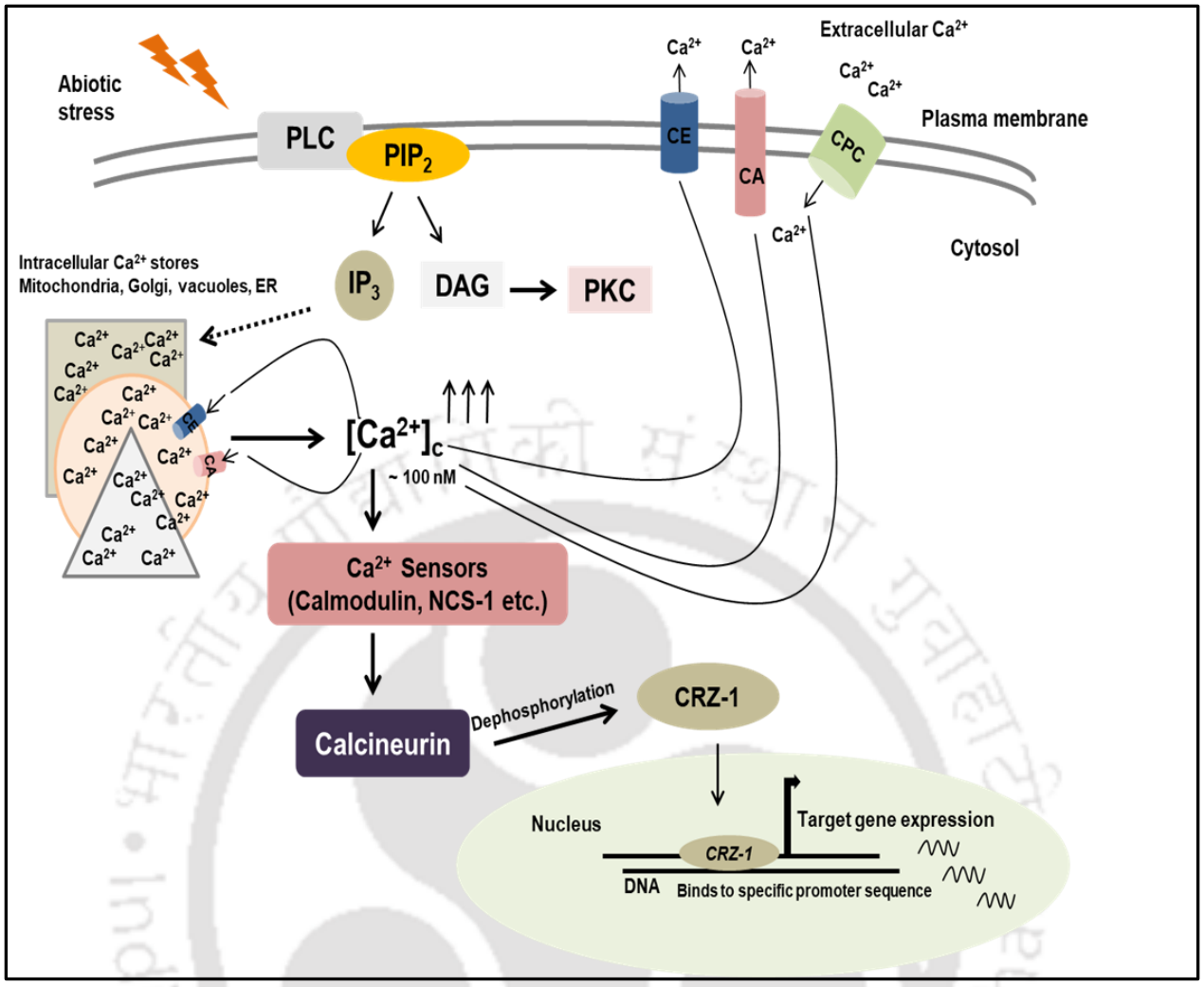

Fig. 1.4 Overview of the Ca^{2+} signaling mechanism in *N. crassa*.

Phospholipase C (PLC), localized to the membrane, hydrolyzes phosphatidylinositol-4, 5-bisphosphate (PIP_2) into two important second messenger molecules inositol 1,4,5-triphosphates (IP_3) and diacylglycerol (DAG). Furthermore, IP_3 induces Ca^{2+} release from the intracellular stores, including mitochondria, Golgi, vacuoles, and endoplasmic reticulum (ER). Then, DAG activates protein kinase C (PKC). The resting intracellular Ca^{2+} concentration ($[Ca^{2+}]_c$) is about 100 nM, a minute increase (shown using arrows pointing upward) of the $[Ca^{2+}]_c$ is detected by different Ca^{2+} sensing proteins such as calmodulin (CaM) and NCS-1, and activates the downstream signaling cascade. The activation of the downstream signaling cascade is depicted in the form of Calcineurin-Crz-1 signaling cascade. The serine/threonine

phosphatase calcineurin is activated by Ca^{2+} and CaM, and dephosphorylates the transcription factor CRZ-1 for its nuclear location and subsequent transcriptional activation of target genes in response to specific stimuli. Excess Ca^{2+} is removed from the cytosol by Ca^{2+} exchangers (CE) and Ca^{2+} -ATPases (CA) proteins, whereas Ca^{2+} permeable channels (CPC) are required for the influx of extracellular Ca^{2+} to maintain the cell Ca^{2+} homeostasis. Adapted from Roy et al. 2020.

1.5 Calcineurin, a serine/threonine phosphatase plays a key role in the Ca^{2+} mediated signal transduction from lower to higher eukaryotes

Calcineurin is the only serine/threonine protein phosphatase that depends on both Ca^{2+} and calmodulin for its activation (Mertz et al. 2000). Calcineurin is a heterodimer consisting of a catalytic subunit A (CNA) and a regulatory subunit B (CNB) (Geurini et al. 1997). Calcineurin was first detected in calmodulin affinity a column fraction that inhibited the calmodulin dependent cyclic nucleotide phosphodiesterase (Wang and Desai, 1976). The protein sequence and the crystallographic structure revealed that the catalytic subunit of calcineurin (CNA) has high homologies with other protein phosphatases, and the regulatory subunit (CNB) belongs to the EF-hand Ca^{2+} binding protein family (Lewit- Bentley and Rety, 2000). The domain structure of both CNA and CNB (Fig. 1.5) predicts that the former consists of a catalytic domain, a CaM binding, a calcineurin B binding, and an auto inhibitory domains, while CNB contains four EF hand domains that binds to four Ca^{2+} ions (Klee and Krinks, 1979).

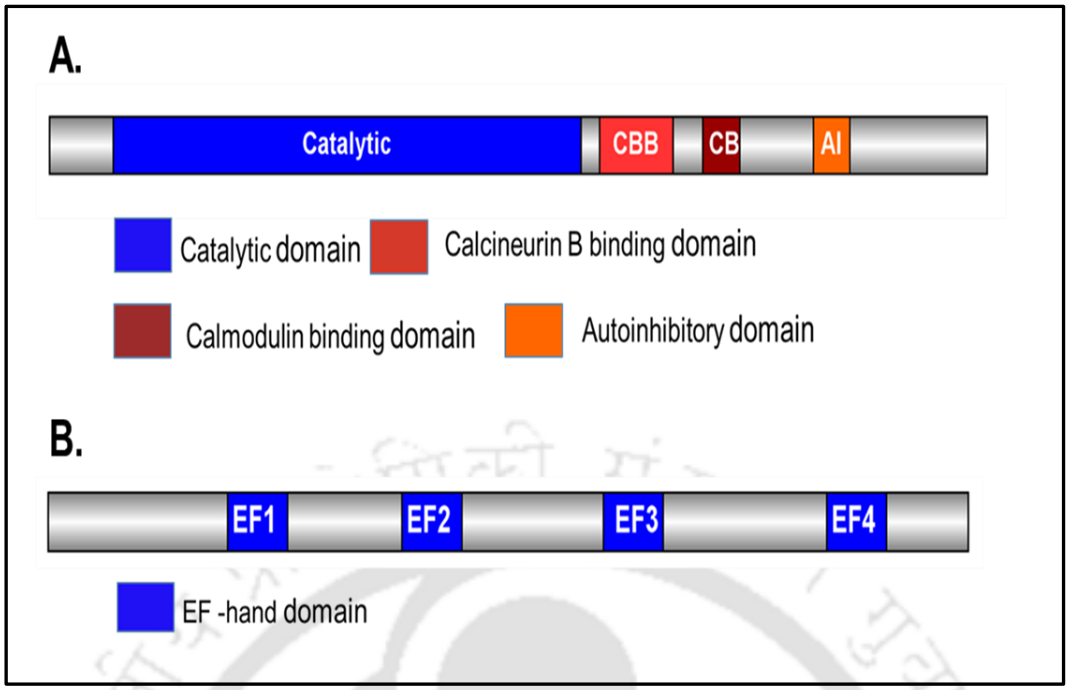

Fig. 1.5 Domain organization of calcineurin subunits. Schematic representation of different domains in CNA (A) and CNB (B) showing that (A) catalytic subunit (CNA) consists of catalytic domain, calcineruin B binding domain (CBB), calmodulin binding domain (CB) and autoinhibitory domain (AI) whereas, (B) regulatory subunit (CNB) comprises of four EF- hand domains (EF1, EF2, EF3 and EF4). The domain organization was done using IBS (Illustrator for biological sequences) http://ibs.biocuckoo.org/ (Liu et al. 2015).

1.5.1 Calcineurin A (CNA)

CNA is the catalytic subunit of calcineurin. It consists of four important domains, including a catalytic domain, a calcineurin B (CNB) binding domain, a calmodulin binding dom, and an auto inhibitory domain. The potent inhibitors of calcineurin are FKBP12 and FK506 (Griffith et al. 1995; Kissinger et al. 1995) and immunosuppressive drug cyclosporine A (CsA) (Huai et al. 2002). Inhibition of calcineurin using FK506 leads to suppression of T cell activation as they inhibit calcineurin mediated dephosphorylation of transcription factor known as nuclear factor of activated T cell (NFAT) in mammals (Shibasaki et al. 1996).

1.5.2 Calcineurin B (CNB)

Calcineurin B, the regulatory subunit of calcineurin, is a Ca^{2+-} binding protein with four EF-hand Ca^{2+}-binding sites and a myristoylation motif (Aitken et al. 1982). The CNB structure, determined by multidimensional NMR, is similar to that of calmodulin (Anglister et al. 1993).

Table 1.2 List of homologues of CNB-1 across different organisms ranging from lower to higher eukaryotes

Organism	Gene	Alternative Name	Tissue/Stage	Genebank entry	Chromosomal Location	References
Saccharomyces cerevisiae	CNB1			YSCCNB.Gb_pl1	XI	(Tanaka et al. 1991)
Arabidopsis thaliana	*SOS3* *CBL1* *CBL2* *CBL3*			AF060553 AF076251.Gb_pl2 AF076252.Gb_pl2 AF076253.Gb_pl2		(Luan et al. 1999; Mody et al. 1994)
Caenorhabditis elegans	*CeCnB*					(Hunter et al. 1999)
Neurospora crassa	*cnb-1*		Asexual Development	AF034089.Gb_pl1		(Free et al. 1998)
Drosophila melanogaster	*dCNB1*			DROCALCB.Gb_in	X chromosome, position 4F	(Klee et al. 1992)
Mus musculus	*Ppp3r1*h	*PP2Bβ 1*	Brain	CALB_MOUSE.SW		(Kincaid et al. 1992)
Rattus norvegicus	*Ppp3r1*h	*CNBα 1,*	Brain	RATCALCB.GB_RO		(Tanaka et al. 1994)

Homo sapiens	*PPP3R1*h		Brain	HUMCNR.Pr	2p16→p 15j	(Klee at al. 1992)

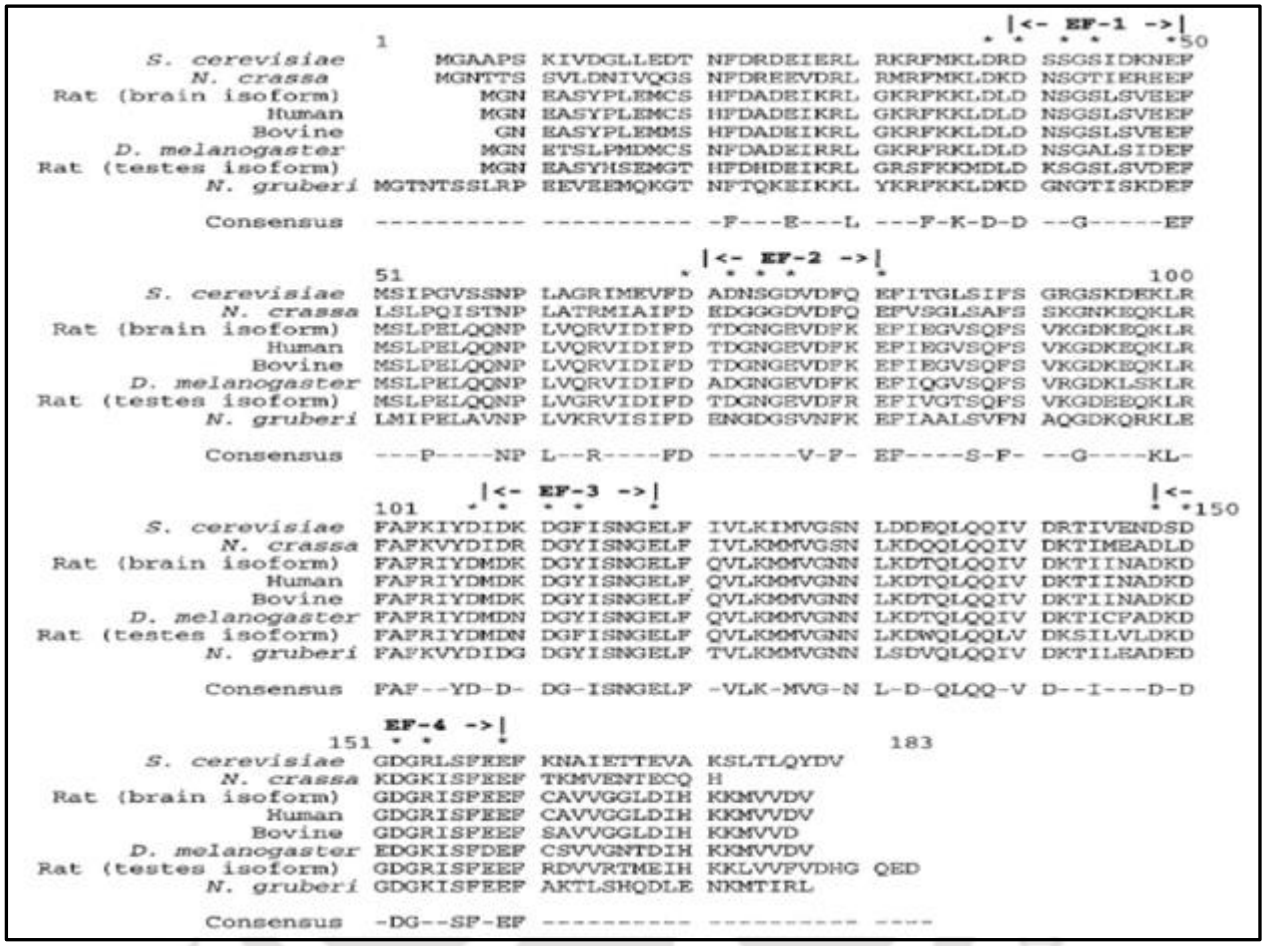

Fig. 1.6 Multiple sequence alignment of *cnb-1* from diverse organisms.

Calcineurin B sequences of *Saccharomyces cerevisiae* (Tanaka et al. 1991), *N. crassa* (Free et al. 1998), rat brain (Tanaka et al. 1994), rat testes (Tanaka et al. 1991), human (Klee et al. 1989), bovine (Cohen et al. 1994; Adachi et al. 1994), *Drosophila melanogaster* (Howells et al. 1996), and *Naegleria gruberi* (Fulton et al. 1995) were aligned using the multiple sequence alignment editor of the Wisconsin Package version 9.0 (https://www.drugdiscoveryonline.com/doc/gcggenetics-computer-group-0001) Genetics Computer Group (Madison, WI). The four Ca^{2+} binding EF-hand motifs are indicated. The residues that participate in Ca^{2+} coordination is noted by an asterisk. The consensus sequence is defined in which a residue is conserved in all 8 sequences. Figure is adapted from Mertz and Rusnak, 2000.

Calcineurin B subunit remains highly conserved throughout the evolution, and mammalian calcineurin B displays 86% amino acid sequence identity with the *Drosophila* homolog, whereas, 54% identity with the *S. cerevisiae* calcineurin B. Because calcineurin homologs are highly conserved, therefore, functional interchange of calcineurin B subunits between mammalian and *N. crassa* catalytic subunits was predicted (Kincaid and Ueki, 1993). The calcineurin B gene from the mammals encodes a protein of 170 amino acids comprising of four Ca^{2+}-binding EF-hand motifs (Cohen et al. 1993). There is absence of initiator methionine amino acid in the starting codon for transcription in the mature calcineurin B protein, and the new α-amino group of glycine at position 2 is acylated with myristic acid (Aitken et al. 1982). Th modification has been conserved throughout evolution from yeast to mammals, suggesting its importance in physiological processes (Cyert, 1993). Further, to explore how myristylation imparts a possible biological role for calcineurin, a mutant of calcineurin B with mutation at position 2 from glycine to alanine impaired myristylation (Zhu et al. 1995). Surprisingly, in *S. cerevisiae* for both wild-type and mutant calcineurin B proteins myristylation was not required either for membrane association or for the interaction with immunosuppressant drug complexes (Klee and Krinks, 1979). Klee and his colleagues in the year 1979 were the first to discover that calcineurin binds Ca^{2+} (Klee et al. 1979). Calcineurin B encompasses all the Ca^{2+} binding sites (Klee et al. 1979) and using flow dialysis, it was demonstrated that calcineurin B bind with high affinity to four Ca^{2+} having a dissociation constant (*K*d) $\geq 10^{-6}$ M. The amino acid sequence of calcineurin B depicted most of its homology with four Ca^{2+}-binding EF-hand motifs of calmodulin (35% identity) and troponin C (29% identity) (Cohen et al. 1984). There are about 39 subfamilies belonging to the family of EF-hand proteins each consisting of about two to eight EF-hand domains (Kreitsinger et al. 1995). With time greater number of Ca^{2+} binding proteins consisting of EF-hand domains have been identified, bearing homology to calcineurin B (Rusnak and Mertz, 2000). Neuronal calcium sensor (NCS-1) belonging to EF-

hand family of proteins isolated from *E. coli*, a have important roles in inhibition of rhodopsin phosphorylation in a Ca^{2+}dependent manner (Decastro et al. 1995), modulation of targets of calmodulin (Schaad et al. 1996), and regulation of exocytosis of granules required for the neurotransmission in *Drosophila* (McFerran et al. 1998). Another homolog of calcineurin B protein p22/CHP in rat is required for transducing downstream Ca^{2+} effectors thereby maintains a constitutive membrane trafficking in cell (Barroso et al. 1996). A protein which is homologous to calmodulin and calcineurin B thereby known as calcineurin B homologous protein (CHP) has been found to be ubiquitously expressed in human tissues binds to NHE1, a Na^{+}/H^{+} exchanger which on being phosphorylated have a role in inhibition of serum and GTPase based stimulation of NHEI activity (Lin and Barber, 1996). In CIB, a Ca^{2+}- and integrin-binding protein, is a 22-kDa Ca^{2+}-binding protein that interacts with the cytoplasmic tail of the integrin aIIb portion of the GPIIb/IIIa fibrinogen receptor (Naik et al. 1997), and SOS3 protein in *Arabidopsis thaliana* thereby imparting tolerance to salt stress in plants (Zhu et al. 1998). Calcineurin B bears a homology in the ranges of 27 to 31% with NCS-1, CIB, and SOS3 and to up to 43% for p22/CHP (Rusnak and Mertz, 2000).

1.5.3 (a) Role of calcineurin B in lower eukaryotes

Table 1.3 Functions of CNB in different lower eukaryotes

Organism	Function	References
Saccharomyces cerevisiae	Recovery from mating factor a-induced growth arrest, cation (e.g., Li^{+}, Na^{+}, Mn^{2+}) resistance, Ca^{2+} homeostasis, Ca^{2+}-mediated G2 arrest, onset of mitosis	Cyert, 1993; Thorner et al. 1993
Schizosaccharomyces pombe	Cytokinesis, mating, nuclear and spindle pole body positioning, polarized growth, proper septation, chloride homeostasis	Rasmussen et al. 1995; Moir et al. 1989

Neurospora crassa	Hyphal growth/conidiation, maintenance of apical Ca^{2+} gradient, proper septation	Free et al. 1998; Barthelmes et al. 1997
Cryptococcus neoformans	Virulence, pH and CO_2 homeostasis, temperature-sensitive growth, resistance to Li1	Heitman et al. 1997
Aspergillus nidulans	Cell cycle progression through G1/S, nuclear division, polarized growth, proper septation	Means et al. 1996; Means et al. 1994

(b) Role of calcineurin B in higher eukaryotes

Table 1.4 Functions of CNB in different higher eukaryotes

Organism	Function	References
Arabidopsis thaliana	Tolerance to high concentrations of Na^+	Zhu et al. 1998
Nicotiana tabacum	Tolerance to high concentrations of salt	Hasegawa et al. 1998
Homo sapiens	Important for programmed cell death of T and B lymphocytes, induction of cardiac morphogenesis and inducing cardiac hypertrophy	Bonnefoy-Berard et al. 1994; de La Pompa et al. 1998

1.6 Ca^{2+}- cation ATPases: an important class of transporters regulating Ca^{2+} signaling in fungi

In fungi, there are six major types of Ca^{2+} transporters, including Ca^{2+} pumps, Ca^{2+}/H^+ exchangers (Lange and Peiter, 2020), high-affinity Ca^{2+} system (HACS), low-affinity Ca^{2+} system (LACS), TRP-like Ca^{2+} channels, and mitochondrial Ca^{2+} uniporter (MCU) (Tisi et al. 2016). Among these Ca^{2+} transporters, HACS and LACS are two critical Ca^{2+} uptake systems

that are conserved across different fungi mediating the entry of Ca^{2+} in response to different cellular conditions (Martin et al. 2011). In the majority of fungi, release of Ca^{2+} from internal stores such as Golgi bodies, endoplasmic reticulum, vacuole, mitochondria are carried out by P-type Ca^{2+} ATPases driving the energy from the synthesis of ATP to transfer Ca^{2+} against the ion gradient (Li et al. 2019). In *A. fumigatus*, *McuA* is a Ca^{2+} uniporter localized to the mitochondrial membrane, and the deletion of *McuA* results in disruption of the mitochondrial Ca^{2+} homeostasis, suggesting its role in Ca^{2+} uptake (Song et al. 2016). In addition, *McuA* was overexpressed during environmental stress, indicating a dominant role in stress response in *A. fumigatus* (Song et al. 2016). The knockouts of *cchA*, *midA*, and *yvcA*, which are the *S. cerevisiae* homologs of *CCh1*, *MID1*, and *YVC1* were not virulent in mice model of invasive aspergillosis, suggesting that these transporters contribute to virulence in *A. fumigatus* (De Castro et al. 2014). In fungi, vacuoles are one of the major storehouse for Ca^{2+}, the Ca^{2+} ATPases and the Ca^{2+}/H^{+} exchangers are important transporters that guide the entry of Ca^{2+} into the vacuoles (Pittman, 2011). The *A. fumigatus pmcA*, *pmcB*, and *pmcC* Ca^{2+} transporters which are the homologs of the *S. cerevisiae PMC1*, and have a role in growth via activation of calcineurin during Ca^{2+} stress condition (Cunningham and Fink, 1994) are transcribed by the calcineurin-CrzA pathway. In *A. fumigatus*, the *pmcA* conditional mutant was not virulent in mice model of invasive aspergillosis; therefore, it imparts a role in conferring virulence and pathogenicity to the fungi, also it regulates the metabolism of Ca^{2+} and Mn^{2+} (Dinamarco et al. 2012). There are different classes of P-type Ca^{2+} ATPases that are named based on their localization to different organelles such as plasma membrane, Golgi apparatus, and endoplasmic reticulum, and classified as PMCA, SERCA, and SPCA (Sze et al. 2000; Carafoli, 2002; Ton and Rao, 2004). In *S. cerevisiae*, deletion of one of the Ca^{2+}-ATPase Pmr1p results in the lack of adequate amount of Ca^{2+} within the Golgi, an increase in the cytosolic Ca^{2+} concentration causing vacuolar fragmentation possibly to sequester excess Ca^{2+} (Kellermayer

et al. 2003). In *S. pombe*, Cps5p is the Pmr1p homolog, which plays a role in the cell wall formation, protein glycosylation, and maintains intracellular Ca^{2+} homeostasis by depletion of the excessive cytosolic Ca^{2+} via interaction with a vacuolar Ca^{2+}-ATPase homolog, Pmc1p (Cortés et al. 2004). In *C. albicans*, deletion of a Ca^{2+}-ATPase gene *CaPMR1*, the homolog of *PMR1* in *S. cerevisiae*, results in altered glycosylation, causing a defect in the cell wall formation and loss of virulence (Bates et al. 2005).

In *N. crassa*, deletion of a PMCA family of Ca^{2+} ATPase NCA-2 causes restricted growth, sensitivity to increasing concentration of Ca^{2+} in the media, and female sterile phenotype (Bowman et al. 2011; Deka and Tamuli, 2013). Moreover, the *nca-2* gene plays a role in carotenoid accumulation, regulation of the circadian clock with a Ca^{2+} sensor *ncs-1*, and thermotolerance with a cation-ATPase *trm-9* in *N. crassa* (Deka and Tamuli, 2013; Laxmi and Tamuli, 2015). Furthermore, *nca-2* might be transcriptionally upregulated via the calcineruin-Crz-1 signaling pathway under the high concentrations of Ca^{2+}, in *N. crassa* (Gohain and Tamuli, 2019).

1.7 Heat shock protein 90 (Hsp90) is one of the well-studied family of heat shock proteins (Hsps) in fungi

The Hsp90 family is one of the most evolutionarily conserved eukaryotic family of Hsps, having a major role in proper folding of several proteins and protects against harmful mutations in the proteins to prevent phenotypic change (Xu et al. 2011). The pathogenic fungi for infestation in human host require to survive at about 37 °C, whereas their niche temperature for growth is around 30 °C (Papagianni, 2004). Therefore, for survival of the pathogenic fungi in the higher temperature in the host, expression of Hsps are important for their chaperone activity necessary to evade stress response (Papagianni, 2004). Inhibition of Hsp90 leads to a decrease in spore formation, conidiation, hyphal growth, germination, suggesting its diverse roles in fungi (Kregel, 2002). At higher temperature such as 55 °C, Hsp90 gets localized to the

nuclei from the cytosol and assists in transcriptional regulation of various stress response genes in *A. fumigatus* (Lamoth et al. 2012). In *S. cerevisiae*, Hsp82 and Hsc82, two isoforms of Hsp90, shares 97% sequence identity, but Hsp82 is stable in stress conditions than the Hsc82 (Girstmair et al. 2019). Moreover, deletion studies demonstrated that the presence of Hsc82 isoforms is required for viability (Borkovich et al. 1989). Hsp90 in *S. cerevisiae* cross talks with Ste11, a homolog of Raf in mammals, and enters MAPK pathway for pheromone signaling (Louvion et al. 1998). Furthermore, the domain structure of Hsp90 (Fig. 1.7), revealed that it consists of three conserved domains including, N-terminal domain (NTD), middle domain, and C-terminal domain (CTD) (Lindquist and Whitesell, 2005). In addition, there is a charged domain acting as a linker between the middle and the NTD (Tsutsumi et al. 2005). Each of the domains have specific roles, NTD imparts role in binding of ATP, therefore, it is also known as nucleotide binding domain, whereas the CTD helps in dimerization of the proteins and it consists of the MEEVD motif that directs the localization of Hsp90 in cytoplasm or endoplasmic reticulum (ER) (Hoter et al. 2018). In the human fungal pathogen *Candida albicans*, the dimorphic switch from yeast to filamentous pathogenic form occurs via Ras-1 protein kinase A (PKA) pathway (Shapiro et al. 2009), the inhibition of Hsp90 using geldanamycin destabilizes Cdc28, one of the positive regulators of cell cycle, via this Ras-1 PKA signaling cascade (Senn et al. 2012). Therefore, Cdc28 interaction with Hsp90 is required for the virulence form of *C. albicans* that causes life threating diseases in immunocompromised individuals (Senn et al. 2012). In addition, inhibition of Hsp90 arrests biofilm formation (Robbins et al. 2011) and also increases the efficacy of antifungal azole drugs against *C. albicans* (Robbins et al. 2011; Singh et al., 2009). Moreover, Hsp90 inhibitors, such as NVP-AUY922 , NVP-HSP90 and NMS-E973 (E973) together with fluconazole (FLC) proves to be a potent therapeutic alternative against the increasing FLC drug resistance in *C. albicans* (Li et al. 2015). Another pathogenic species of fungi *Cryptococcus neoformans* or *Cryptococcus*

gattii causes cryptococcosis, a deadly disease leading to millions of deaths every year (Kwon-Chung et al. 2014). Inhibition of Hsp90 using one of the antifungal drugs radicicol (RAD) results in the reduced growth, cell membrane permeability, capsular volume and finally makes the *Crypococccus spp*. attenuated when infected in vivo using *Caenorhabditis elegans* (Cordeiro et al. 2016). Another study regarding Hsp90 revealed for the first time that antiviral drug ritonavir inhibits Hsp90, thereby, promoting the efficacy of the antifungal drugs and seems to open up new avenue for the therapeutic intervention in *C. neoformans* (Serafin et al. 2017).

In *N. crassa*, the presence of Hsp80, which belongs to the Hsp90 family heat shock proteins, has been identified (Borkovich et al. 2004). Studies on the heat shock proteins in *N. crassa* were limited to initial phenotypic characterization (Kumar et al. 2019). In addition, the upregulation of *Hsp80* was observed at 48 °C while the expression of other heat shock proteins was not significant in the same condition (Roy and Tamuli, unpublished). Hsp80 seem to constitute about 1-2 % of the protein content in the cytosol, thereby plays an important role in the viability of *N. crassa* (Colot et al. 2006).

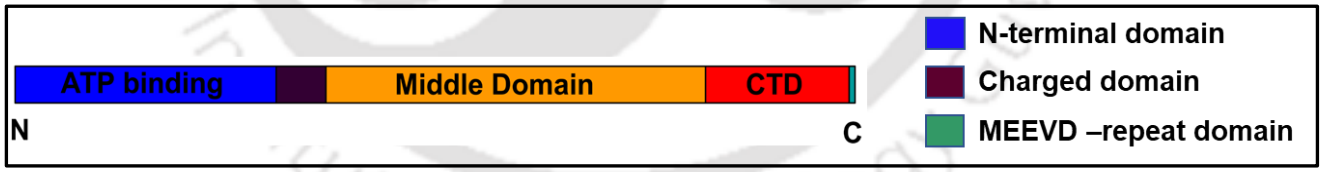

Fig. 1.7 Domain structure of Hsp90 in fungi

The domain structure of Hsp90 consists of a N-terminal domain for ATP binding, a charged domain that is a linker between the N-terminal domain (NTD) and the Middle domain, and a C-terminal domain (CTD) that consists of a repetitive MEEVD sequence responsible for the nuclear localization of Hsp90 for the regulation of chaperone activity and cellular functions.

1.8 Objectives of this study

Cnb-1, is an essential gene in *N. crassa*, therefore, conventional methods for generating knockout mutant and side directed mutagenesis of key amino acid residues are not possible due to lethality. Therefore, a gene silencing mechanism called repeat induced point (RIP) mutation (Cambareri et al. 1989) was used to generate viable RIP-induced *cnb-1* mutants, and earlier studies using the mutants revealed role of *cnb-1* in the regulation of hyphal differentiation and growth (Kothe and Free, 1998). Furthermore, in our laboratory, we generated *cnb-1*^{RIP} mutants (Tamuli et al. 2016), which revealed important amino acid residues responsible for *cnb-1* function in the regulation of different cellular functions in response to various environmental cues in *N. crassa*. In filamentous fungi, calcineurin interacts with the CRZ-1 transcription factor, and shown to regulate important cell functions such as thermotolerance (Heitman, 2005), virulence (Juvvadi et al. 2014), cell growth, antifungal drug resistance (Thewes, 2014). However, in *N. crassa* information regarding the cellular roles and molecular mechanism of CNB-1 was limited. Therefore, it will be interesting to know the putative interacting partners of CNB-1 and the molecular mechanism how these interacting partners can drive the cellular functions of CNB-1 in response to different stress conditions in *N. crassa*. Further, to understand the molecular mechanism behind CNB-1 functions in *N. crassa*, the thesis work was divided into three broad objectives which are stated below.

The broad objectives of the thesis are as follows:

1) Understanding the cell functions and regulatory mechanism of calcineurin B (CNB-1) subunit.
2) To identify the CNB-1 interacting partners and understanding their mechanism of action.

3) To establish a mechanistic model based on interacting partners and their role in different cell functions.

Chapter 2
Materials and Methods

2.1 Materials

2.1.1 Laboratory chemicals and other materials

Laboratory chemicals such as acrylamide (C_3H_5NO), ammonium iron (II) sulfate hexahydrate [$Fe(NH_4)_2(SO_4)_2.6H_2O$], ammonium nitrate (NH_4NO_3), ammonium persulphate [APS, $(NH_4)_2S_2O_8$], arginine, biotin, boric acid (H_3BO_3), calcium chloride ($CaCl_2.H_2O$), calcium D-pantothenate ($C_{18}H_{32}CaN_2O_{10}$), cetyltrimethyl ammonium bromide (CTAB, $C19H_{42}BrN$), chloroform ($CHCl_3$), citric acid ($C_6H_8O_7.H_2O$), diethyl pyrocarbonate (DEPC, $C_6H_{10}O_5$), dimethyl sulphoxide (DMSO, C_2H_6OS), absolute ethanol (C_2H_5OH), ethidium bromide (EtBr, $C_{21}H_{20}BrN_3$), ethylenediaminetetra acetic acid disodium salt dihydrate (EDTA, $C_{10}H_{14}N_2Na_2O_8.2H_2O$), ethylene glycol-bis (β-aminoethyl ether)-*N*,*N*,*N*′,*N*′-tetraacetic acid (EGTA, $C_{14}H_{24}N_2O_{10}$), ferrous sulphate heptahydrate ($FeSO_4.7H_2O$), formaldehyde (CH_2O), fructose($C_6H_{12}O_6$), glacial acetic acid (CH_3COOH), D-glucose ($C_6H_{12}O_6$), glutamine, glycerol ($C_3H_8O_3$), glycine, hydrochloric acid (HCL), 2-[4- (2-hydroxyethyl) piperazin-1-yl] ethanesulfonic acid (HEPES, $C_8H_{18}N_2O_4S$), isopropanol (C_3H_7OH), lithium chloride (LiCl), magnesium chloride ($MgCl_2$) magnesium sulphate heptahydrate ($MgSO_4.7H_2O$), manganous chloride tetrahydrate ($MnCl_2.4H_2O$), manganous sulphate ($MnSO_4.H_2O$), methanol (CH_3OH), *N*,*N*′-Methylenebisacrylamide ($C_7H_{10}N_2O_2$), (β-mercaptoethanol (C_2H_6OS), 3-Morpholinopropane-1-sulfonic acid (MOPS, $C_7H_{15}NO_4S$), 1,4-Piperazinediethanesulfonic acid (PIPES, $C_8H_{18}N_2O_6S_2$), Phenol: Chloroform: Isoamyl mixture (25:24:1), phenylmethylsulphonyl fluoride (PMSF, $C_7H_7FO_2S$), potassium acetate (CH_3COOK), potassium hydroxide (KOH), potassium nitrate (KNO_3), potassium phosphate dibasic (K_2HPO_4), potassium phosphate monobasic (KH_2PO_4), silica gel (6-12 mesh), sodium bicarbonate ($NaHCO_3$), sodium chloride (NaCl), sodium citrate dihydrate ($Na_3C_6H_5O_7.2H_2O$), sodium deoxycholate ($C_{24}H_{40}O_4$), sodium dodecyl sulphate (SDS, $NaC_{12}H_{25}SO_4$), sodium hydroxide (NaOH), sodium molybdate ($Na_2MoO_4.2H_2O$), sodium nitrate ($NaNO_3$), D-sorbitol

($C_6H_{14}O_6$), sorbose ($C_6H_{12}O_6$), sucrose ($C_{12}H_{22}O_{11}$), tetramethylethylenediamine [TEMED, $(CH_3)_2NCH_2CH_2N(CH_3)_2$], Tris base ($C_4H_{11}NO_3$), triethanoleamine ($C_6H_{15}NO_3$), Triton X-100, Tween 20, Tween 80 were procured from various manufacturers such as Himedia (Mumbai, India), Loba Chemie (Mumbai, India), Merck (Mumbai, India), and SRL (Mumbai, India). Bathocuproinedisulfonic acid disodium salt (BCS; $C_{26}H_{18}N_2Na_2O_6S_2$), dimethyl pimelimidate (DMP; $C_9H_{18}N_2O_2$), fungal protease inhibitor cocktail (FPIC) were procured from Sigma Aldrich (USA). Reagents for protein work namely- Prestained Protein ladder; Bradford Reagent; and Coomassie Brilliant Blue G-250 (CBB) dye were obtained from Himedia (Mumbai, India). All the antibodies, agarose, EMSA kit, TRIzol™ reagent, SYBR Green Real-Time PCR Master Mix, Dynabeads® Protein A magnetic beads, and nuclease-free water were purchased from Life Technologies (USA). All restriction enzymes, DNA size markers, Blue Gel Loading Dye (6X), routine Taq DNA polymerase, Phusion® High-Fidelity DNA Polymerase for PCRs were purchased from New England Biolabs (USA). Plasmid DNA isolation, Gel purification and PCR Clean-up kits were obtained from Qiagen (USA) as well as from GCC Biotech (Kolkata, India). Pancreatic RNAase A, proteinase K, and herring sperm DNA was purchased from Promega (Madison, USA). Verso cDNA Synthesis Kit was purchased from Thermo Fisher Scientific (Waltham, USA). Custom made Oligonucleotide primers were procured from Bioserve, Hyderabad, India. Glassware was obtained from Borosil (Mumbai, India) and Jain scientific glass works (Ambala, India). Plasticware was procured from Tarsons (Kolkata, India) and Genaxy (New Delhi, India). Rest of the chemicals were procured from local manufacturers and were of analytical grade.

2.1.2 *Neurospora crassa* strains

N. crassa strains were obtained from the Fungal Genetics Stock Centre and the University of California Riverside, and also generated in our laboratory.

1. **Strains acquired from the Fungal Genetics Stock Centre (FGSC):** *N. crassa* wild type, *ras-1*^{bd}, Δ*nca-2*, Δ*cax*, Δ*trm-9* and Δ*mus-52* knockout, and *his-3* mutant strains (Table 2.1) were obtained from the Fungal Genetics Stock Center (FGSC), University of Missouri, Kansas City, MO 64110 (McCluskey, 2003; McCluskey *et al.*, 2010).
2. **Strains obtained from University of California Riverside (UCR):** 599 A, 600 A, 602 A, 559 a and pccg-1_GFP strains (Table 2.1) were generated and obtained from the laboratory of Prof. Katherine A. Borkovich (University of California Riverside, USA).
3. **Strains generated in our laboratory:** Δ*trm-9*Δ*cax*, Δ*cnb-1; cnb-1*^{RIP}*; ras-1*^{bd} *(599-1),* Δ*cnb-1; cnb-1*^{RIP}*; ras-1*^{bd} *(600-8) and* Δ*cnb-1; cnb-1*^{RIP}*; ras-1*^{bd} *(602-82)*-strains (Table 2.1) were generated in this study.

Table 2.1. *Neurospora crassa* strains used in this study

Sl. No.	Strains	Strain type or NCU no.	Genotype	Reference
1	74-OR23-IVA	Wild type	Wild type; *mat A*	FGSC 2489
2	ORS-SL6a	Wild type	Wild type; *mat a*	FGSC 4200
3	13040	04898	Δ*trm-9*::*hph*; *mat A*	FGSC 13040
4	13071	04736	Δ*nca-2*::*hph*; *mat A*	FGSC 13071
5	*ras-1*^{bd}	08823	*ras-1*^{bd}; *mat a*	FGSC 1858
6	*ras-1*^{bd}	08823	*ras-1*^{bd}*; mat A*	FGSC 1859
6	20	20	Δ*trm-9*::*hph*; *mat a*	Laxmi and Tamuli, 2015
7	23	20	Δ*nca-2*::*hph*; *mat a*	Laxmi and Tamuli, 2015

8	12	12	Δ*trm-9*::*hph*Δ*nca-2*::*hph; mat A*	Laxmi and Tamuli, 2015
9	19	19	Δ*trm-9*::*hph*Δ*nca-2*::*hph; mat a*	Laxmi and Tamuli, 2015
10	24	24	Δ*trm-9*::*hph*Δ*cax*::*hph; mat A*	Our laboratory
11	29	29	Δ*trm-9*::*hph*Δ*cax*::*hph; mat a*	Our laboratory
12	52-4-9	00077	Δ*mus-52*::*nat*; *mat A*	FGSC 2479
13	51-IV-8	Homokaryotic	Δ*rid-1*::*nat*; Δ*mus-51*::*nat*; *mat a*	FGSC 23148
14	11249	07075	Δ*cax*::*hph*; *mat A*	FGSC 11249
15	11248	07075	Δ*cax*::*hph*; *mat a*	FGSC 11248
16	6032	03139	*his-3*; *mat A*	FGSC 6032
17	*upr-1* (34-97-3a)	NCU01951	*upr-1*^{Rip}; *mat a*	Tamuli *et al.* 2006
18	pccg-1_GFP	Homokaryotic	Δ*pan-2*::P_{ccg-1}::*5xGly*::*V5*::*gfp*; *mat a*	Borkovich Lab (UCR, USA) (Ouyang *et al.*, 2015)
19	559	Homokaryotic	Δ*crz-1*::*hph;* Δ*pan-2*$^{-}$::P_{tcu-1}::*crz-1*::*5xGly*::*V5*::*gfp*; *mat a*	Borkovich Lab (UCR, USA)
20	599 A	Homokaryotic RIP	Δ*cnb1::hph;*Δ*pan2::*P_{tcu-1}*::cnb-*	Tamuli et al. 2016

			1^{RIP}*::5xGly::V5::gfp; mat A*	
21	600 A	Homokaryotic RIP	Δ*cnb1::hph;*Δ*pan2::*P_{tcu-1}*::cnb-1*^{RIP}*::5xGly::V5::gfp; mat A*	Tamuli et al. 2016
22	602 A	Homokaryotic RIP	Δ*cnb1::hph;*Δ*pan2::*P_{tcu-1}*::cnb-1*^{RIP}*:: 5xGly::V5::gfp; mat A*	Tamuli et al. 2016
23	Δ*cnb-1*; *cnb-1*^{RIP}; *ras-1*^{bd} (599-1)	Heterokaryotic	*ras-1*^{bd} ; Δ*cnb-1*:: *hph*; Δ*pan-2*::P_{tcu-1}::*cnb-1*^{RIP}:: 5xGly::*V5*::*gfp*; *mat A*	Our laboratory
24	Δ*cnb-1*; *cnb-1*^{RIP}; *ras-1*^{bd} (600-8)	Heterokaryotic	*ras-1*^{bd}; Δ*cnb-1*:: *hph*; Δ*pan-2*::P_{tcu-1}:: *cnb-1* ^{RIP}:: 5xGly::*V5*::*gfp*; *mat A*	Our laboratory
25	Δ*cnb-1*; *cnb-1*^{RIP}; *ras-1*^{bd} (602-82)	Heterokaryotic	*ras-1* ^{bd} *;* Δ*cnb-1:: hph;* Δ*pan-2:: *P_{tcu-1}*::cnb-1* ^{RIP}*:: 5xGly::V5::gfp; mat a*	Our laboratory

2.1.3 Plasmid vector used in this study

pRS426PVG/ptcu-1_1.5 kb: This vector consists of the backbone from the yeast/*E. coli* shuttle vector pRS426PVG (Ouyang *et al.* 2015). The pRS426PVG/ptcu-1_1.5 kb vector (Fig. 2.1) confer pantothenate auxotrophy in *N. crassa*, uracil prototrophy to *S. cerevisae ura-3* mutant (URA3) and ampicillin resistance (Ap^R) in *E. coli*. The pRS426PVG/ptcu-1_1.5 kb vector contains the 5' flanking region of the *N. crassa pan-2* (NCU10048) ORF followed by

the *N. crassa* copper regulated *tcu-1* (NCU00830) promoter (P_{tcu-1}), a MCS, a 5xGly linker, a V5 peptide tag, the *gfp* gene, and 3' flanking region of the *N. crassa pan-2* (NCU10048) ORF. It also contains *bar* gene as the selection marker which confers resistance to Glufosinate ammonium commonly known as Basta® or Ignite® (Pall, 1993). P_{tcu-1} is repressed by the addition of $CuSO_4$ and induced by the addition of BCS (Lamb *et al.* 2013; Ouyang *et al.* 2015).

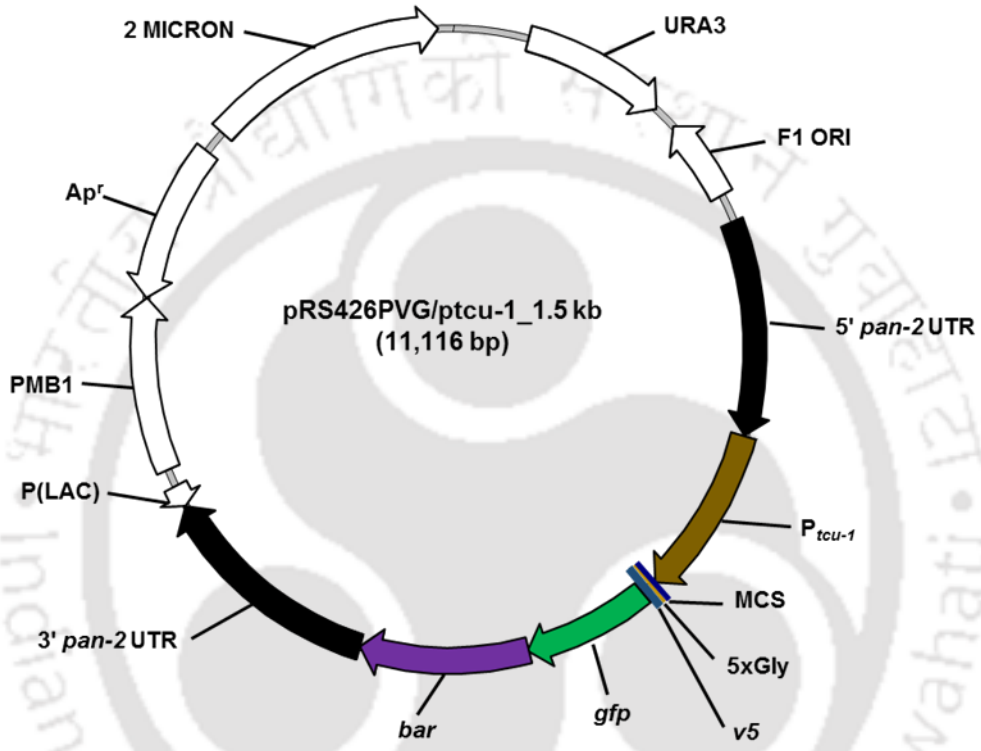

Fig. 2.1. Schematic of the pRS426PVG/ptcu-1_1.5 kb vector. The vector size is 11,116 bp and arrow heads indicates 5′→3′ direction of the cloned genes or fragments (adapted from Ouyang *et al.* 2015).

2.1.4 Bacterial strain used in the study

The *Escherichia coli DH5α* strain with genotype *SupE*44 Δ*lac*U169 (φ80*lacZ* ΔM15) *hsdR*17 *recA*1 *end A*1 *gyrA*96 *thi*-1 *relA*1 (Sambrook and Russel, 2001) was used for all routine bacterial cloning and transformations, plasmid growth and isolation, and selection of the recombinants. The *E. coli DH5 α* is a recombination deficient nonsense (amber) suppressing

strain with the φ80 *lacZ* ΔM15 mutation which allows α-complementation with the *β*-galactosidase amino terminus encoded in the pUC vectors (Sambrook and Russel, 2001).

2.1.5 Media components, antibiotics for growth of bacterial strains and other reagents for common use

1. **Bacterial media:** LB agar and broth, Terrific broth, SOB and SOC media were purchased from Himedia (Mumbai, India) and were made ready for use by dissolving in distilled water as per the manufacturer's protocol. All the bacterial media were sterilized by autoclaving.
2. **Hygromycin B:** Hygromycin B was procured from Himedia (Mumbai, India) as a ready-to-use solution having a concentration of 50 mg/ml.
3. **Ampicillin:** A stock solution of ampicillin (100 mg/ml) was prepared by dissolving 200 mg ampicillin powder in 2 ml sterilized water and stored in 200 µl aliquots at minus 20 °C.
4. **Glufosinate ammonium/Basta®:** Glufosinate ammonium also known as Basta® was purchased from Sigma Aldrich (St. Louis, USA). A stock solution of 100 mg/ml was prepared by dissolving 100 mg glufosinate ammonium in 1 ml sterile distilled water and stored as aliquots of 200 µl at minus 20°C.
5. **BCS solution:** 0.2 M stock solution was prepared by dissolving 113 mg BCS in 1 ml sterile distilled water.
6. **1 M glucose:** 16.02 g D-glucose was dissolved in 70 ml distilled water and volume was adjusted to 100 ml. The stock was stored by sterilized by filtering through a 0.45-µm syringe filter and stored at room temperature.
7. **1 M sorbitol:** 18.21 g sorbitol was dissolved in 70 ml distilled water and the final volume was adjusted to 100 ml by adding distilled water and sterilized by autoclaving.

8. **10 N NaOH:** 40 g NaOH pellet was slowly dissolved in 80 ml of distilled water, stirring continuously in a glass beaker placed on ice, the volume was adjusted to 100 ml and stored at room temperature.
9. **8 M LiCl:** 33.9 g LiCl was dissolved in a final volume of 100 ml of DEPC treated sterile distilled water and sterilized by autoclaving.
10. **3 M Na-acetate (pH 5.2):** 24.61 g Na-acetate was dissolved in 70 ml distilled water and pH was adjusted to 5.2 by adding glacial acetic acid. Volume was adjusted to 100 ml by adding water.
11. **5 M $CaCl_2$:** 73.5 g of $CaCl_2.2H_2O$ was dissolved in distilled water to a final volume of 100 ml. The solution was sterilized by autoclaving.
12. **2 M KCl:** 14.9 g of KCl was dissolved in 80 ml of distilled water, and the volume was adjusted to 100 ml and stored at room temperature.
13. **1 M sorbitol:** 18.21 g sorbitol was dissolved in 70 ml distilled water and the final volume was adjusted to 100 ml by adding distilled water and sterilized by autoclaving.
14. **10% SDS:** 10 g SDS was dissolved in 90 ml distilled water and heated at 68 °C by stirring in a magnetic stirrer cum heater. The volume was adjusted to 100 ml and stored at room temperature.
15. **EtBr:** A stock solution of EtBr (10 mg/ml) was prepared by dissolving 10 mg EtBr in 1 ml distilled water and stored at 4 °C.
16. **1 M glycine:** 7.5 g glycine was dissolved in 70 ml distilled water and volume was adjusted to 100 ml and stored at room temperature.
17. **0.5 M EDTA (pH 8.0):** 18.61g EDTA was dissolved in 70 ml distilled water, pH was adjusted to 8.0 by adding NaOH pellets, and volume was adjusted to 100 ml and sterilized by autoclaving.

18. **1 M Tris-HCl (pH 7.5):** 12.11 g Tris base was dissolved in 70 ml distilled water, adjusted pH to 7.5 by adding concentrated HCl, and adjusted the volume to 100 ml with distilled water and sterilized by autoclaving.
19. **1 M Tris-HCl (pH 8.0):** 12.11 g Tris base was dissolved in 70 ml of distilled water, adjusted pH to 8.0 by adding concentrated HCl, and adjusted the volume to 100 ml with distilled water and sterilized by autoclaving.
20. **Proteinase K:** Proteinase K was dissolved at a concentration of 20 mg/ml in 50 mM Tris-HCl (pH 8.0), 10 mM $CaCl_2$, and stored at minus 20 °C.
21. **1 M $MgCl_2$:** 20.33g $MgCl_2.6H_2O$ was dissolved in 80 ml distilled water, the volume was adjusted to 100 ml and sterilized by autoclaving.
22. **50X TAE:** 1 L of the 50X TAE stock solution was prepared by adding 242 g Tris base, 57.1 ml of glacial acetic acid and 100 ml of 0.5 M EDTA (pH 8.0) and adjusting the volume to 1 L by adding distilled water. The solution was stored at 4 °C.
23. **1X TE:** The solution was prepared by adding 10 mM Tris-HCl (pH 8.0) and 1 mM EDTA (pH 8.0) from their respective stocks and stored at 4 °C.
24. **10X MOPS buffer:** The stock solution of 10X MOPS for 100 ml contains 4.18 g of MOPS (0.2 M), 2 ml 1 M Na-acetate solution (20 mM), and 2 ml 0.5 M EDTA (10 mM). After dissolving, 4.18 g of MOPS in DEPC-treated water, 3 M Na-acetate solution and 0.5 M EDTA were added in the indicated volume. The pH was adjusted to 7.0 with 10 N NaOH. Solution was sterilized by filtering through a 0.45 µm syringe filter and stored at room temperature protected from light.
25. **1 M HEPES buffer (pH 7.5):** 2.38 g HEPES was dissolved in 6 ml distilled water and pH was adjusted to 7.5 by adding 10 N NaOH solution and adjusted the volume to 10 ml. The solution was sterilized by filtering through a 0.45 µm syringe filter and stored at minus 20 °C.

26. **10X TBE buffer (pH 8.0):** 10.8 g Tris base and 5.5 g boric acid were dissolved in 50 ml distilled water. 4 ml 0.5 M EDTA (pH 8.0) was added and volume was adjusted to 100 ml by adding distilled water.
27. **0.5 M $NaHCO_3$:** 0.21 g $NaHCO_3$ was dissolved in 8 ml distilled water, the volume was adjusted to 10 ml and stored at room temperature.
28. **10% Na-deoxycholate:** 1 g Na-deoxycholate was dissolved in 8 ml distilled water. The volume was adjusted to 10 ml and stored at room temperature.
29. **100 mM DTT:** 0.15 g DTT was dissolved in 1 ml 100 mM HEPES buffer (pH 7.5) and stored at minus 20 °C protected from light.
30. **Alkaline lysis Solution I:** Alkaline lysis Solution I consists of 50 mM glucose, 25 mM Tris-Cl (pH 8.0), and 10 mM EDTA (pH 8.0).
31. **Alkaline lysis Solution II:** Alkaline lysis Solution II comprises of 0.2 N NaOH and 1% SDS. The solution was freshly prepared just prior to use.
32. **Alkaline lysis Solution III:** For a volume of 100 ml solution, 60 ml of 5 M potassium acetate, 11.5 ml of glacial acetic acid, and 23.5 ml of distilled water were mixed together. The solution was sterilized by autoclaving and stored at 4 ºC.
33. **Inoue transformation buffer:** The Inoue transformation buffer (Ninomiya et al. 2004) consists of 55 mM $MnCl_2$, 15 mM $CaCl_2$, 250 mM KCl and 10 mM PIPES buffer (pH 6.7).
34. **Lysis buffer for *N. crassa* genomic DNA isolation:** The lysis buffer comprises of 10 mM Tris HCl (pH 7.5), 0.5 M NaCl, 10 mM EDTA, 1% SDS, and 1% CTAB.
35. **Lysis buffer for *N. crassa* RNA isolation:** The lysis buffer consists of 100 mM Tris HCl (pH 8.0), 0.6 M NaCl, 10 mM EDTA (pH 8.0), 4.5 % SDS, and 2 % β-mercaptoethanol.

36. ***N. crassa* native protein isolation buffer:** The protein isolation buffer contains 50 mM Tris-HCl (pH 7.5), 1 mM EDTA (pH 8.0), 6 mM $MgCl_2$, 2.5 mM PMSF, and 0.1% fungal protease inhibitor cocktail (FPIC, Sigma Aldrich, USA).

2.1.6 Stock Solutions for growth, crossing and maintenance of *N. crassa* strains

(i) Trace element solution: Trace element solution was prepared by dissolving the following chemicals sequentially in 90 ml of distilled water with constant stirring.

$C_6H_8O_7.H_2O$	5.00 g
$ZnSO_4.7H_2O$	5.00 g
$Fe(NH_4)_2(SO_4)_2.6H_2O$	1.00 g
$CuSO_4.5H_2O$	0.25 g
$MnSO_4.1H_2O$	0.05 g
H_3BO_3	0.05 g
$Na_2MoO_4.2H_20$	0.05 g

The final volume was adjusted to 100 ml, 1 ml of chloroform was added as a preservative and stored at room temperature.

(ii) Biotin solution: 5 mg biotin was dissolved in 100 ml 50% (v/v) ethanol, stored at 4 °C.

(iii) Vogel's Medium N (VGN): A 50X stock of Vogel's Medium N (Vogel, 1956; Vogel, 1964) was prepared by adding following chemicals sequentially in 75 ml distilled water with constant stirring.

$Na_3C_6H_5O_7.2H_2O$	12.5 g
KH_2PO_4	25 g
NH_4NO_3	10 g
$MgSO_4.7H_2O$	1 g

$CaCl_2.2H_2O$	0.5 g
(Pre-dissolved in 2 ml H_2O)	
Biotin solution	500 µl
Trace element solution	500 µl
Chloroform	300 µl

The volume of the solution was adjusted to 100 ml and the chloroform was added as a preservative.

(iv) 4X Synthetic crossing medium (SCM): 4X strength synthetic crossing medium (SCM) was prepared by dissolving the following chemicals sequentially in 80 ml distilled water with constant stirring.

KNO_3	0.4 g
K_2HPO_4	0.28 g
KH_2PO_4	0.2 g
$MgSO_4.7H_2O$	0.2 g
$CaCl_2.2H_2O$	40 mg
NaCl	40 mg
Biotin solution	20 µl
Trace element solution	20 µl

The volume of the solution was adjusted to 100 ml and sterilized by autoclaving.

(v) Vogel's glucose media (VG):

Vogel's Medium N	1X
Glucose	1.5%(w/v)

(v) VGM agar:

Vogel's Medium N	1X
Glucose	1.5%(w/v)
Agar	2% (w/v)

(vii) SCM agar:

SCM	1X
Glucose	1.5% (w/v)
Agar	2% (w/v)

(viii) 10X FGS (Fructose, glucose, and sorbose) stock: 10X FGS stock was prepared by dissolving the following chemicals in 80 ml distilled water.

Fructose	5% (w/v)
Glucose	5% (w/v)
Sorbose	20% (w/v)

The volume of the solution was adjusted to 100 ml and sterilized by autoclaving.

(ix) FGS agar:

FGS	1X
Vogel's Medium N	1X
Agar	2% (w/v)

(x) Top agar:

FGS	1X
Vogel's Medium N	1X

(xi) Media for circadian clock study:

Vogel's Medium N	1X
Glucose	0.1% (w/v)
Arginine	0.17% (w/v)
Biotin	50 ng/ml
Agar	1.5% (w/v)

2.1.7 Reagents for SDS-polyacrylamide gel electrophoresis

(i) Resolving gel (10 ml)

Acrylamide percentage	10%	12%
H_2O	3.8 ml	3.2 ml
Acrylamide/Bis-acrylamide (30%/0.8% w/v)	3.4 ml	4 ml
1.5 M Tris-HCl (pH 8.8)	2.6 ml	2.6 ml
10% w/v SDS	100 µl	100 µl
10% w/v APS	100 µl	100 µl
TEMED	10 µl	10 µl

(ii) Stacking gel (5 ml)

H_2O	2.975 ml
Acrylamide/Bis-acrylamide (30%/0.8% w/v)	0.67 ml
0.5 M Tris-HCl (pH 6.8)	1.25 ml
10% w/v SDS	50 µl
10% w/v APS	50 µl
TEMED	5 µl

(iii) 1X running buffer (1000 ml)

Glycine	15 g
1 M Tris-HCl (pH 8.0)	25 ml
10% w/v SDS	100 ml
H_2O	875 ml

(iv) 5X SDS-PAGE sample buffer (10 ml; Krystofova and Borkovich, 2005)

0.5 M Tris-HCl (pH 6.8)	1.25 ml
Bromophenol blue (1% w/v stock)	50 µl
10% w/v SDS	2 ml
β-mercaptoethanol	100 µl
H_2O	6.6 ml

(v) Staining solution (100 ml)

Coomassie Brilliant Blue	100 mg
Methanol	50 ml
Glacial acetic acid	10 ml
H_2O	40 ml

(vi) Destaining solution

Methanol	10 ml
Glacial acetic acid	7 ml
H_2O	83 ml

2.1.8 Buffers for Chromatin Immunoprecipitation (ChIP)

(i) CHIP lysis buffer (10 ml)

1 M HEPES (pH 7.5)	500 µl
0.5 M EDTA (pH 8.0)	20 µl
5 M NaCl	180 µl
Triton X-100	100 µl
10% Na-deoxycholate	100 µl
100 mM PMSF	100 µl
FPIC	10 µl
H_2O	8.99 ml

(ii) RIPA buffer (10 ml)

1 M Tris-HCl (pH 8.0)	500 µl
0.5 M EDTA (pH 8.0)	40 µl
5 M NaCl	300 µl
10% w/v SDS	100 µl
10% w/v Na-deoxycholate	100 µl
NP-40	100 µl
H_2O	8.86 ml

(iii) Low salt wash buffer (10 ml)

1 M Tris-HCl (pH 8.0)	200 µl
0.5 M EDTA (pH 8.0)	40 µl
5 M NaCl	300 µl
10% w/v SDS	100 µl
Triton X-100	100 µl
H_2O	9.26 ml

(iv) High salt wash buffer

1 M Tris-HCl (pH 8.0)	200 µl
0.5 M EDTA (pH 8.0)	40 µl
5 M NaCl	300 µl
10% w/v SDS	100 µl
Triton X-100	100 µl
H_2O	9.26 ml

(v) LiCl wash buffer (10 ml)

1 M Tris-HCl (pH 8.0)	200 µl
0.5 M EDTA (pH 8.0)	40 µl
5 M NaCl	300 µl
10% w/v SDS	100 µl
Triton X-100	100 µl
H_2O	9.26 ml

(v) LiCl wash buffer (10 ml)

1 M Tris-HCl (pH 8.0)	100 µl
0.5 M EDTA (pH 8.0)	20 µl
3 M LiCl	100 µl
10% w/v Na-deoxycholate	2 ml
NP-40	100 µl
H_2O	7.68 ml

(vi) Elution buffer (10 ml)

10% w/v SDS	100 µl
0.5 M $NaHCO_3$	2 ml
H_2O	7.9 ml

2.1.9 Primers used in study

Table 2.2 The list of primers used for the study

Sl No.	Primer Name	Sequence (5'-3')	Reference
1	NCU04898-5F	GGTTAGTGAGCTTTGAGTCG	Our laboratory (Laxmi and Tamuli, 2015)
2	Cax AR-Fw HI	CGCCACCGGAATTACAATACC	Our laboratory
3	5HPHR	ATCCACTTAACGTTACTGAAATC	Our laboratory (Deka et al. 2011)
4	P_{tcu}-CaM-RIP-FP-3	TTGAGAACGAATCCTTCATC	Our laboratory (Laxmi and Tamuli, 2017)
5	HI-CNBFW-AR Fw	GCATTTGCTGGTCGTCATAG	Our laboratory
6	RT-FRQ-F	GAATCGACATCGCAGAGGAG	Our laboratory
7	RT-FRQ-R	GCCCGTCGACATAGAGTTGT	Our laboratory
8	RT-WC-1-F	GCGGGAATCGAGATCTATGC	Our laboratory
9	RT-WC-1-R	TGAGTTCTTGGTAGCGGTGG	Our laboratory
10	q-B-tub-FW	CCCAAGAACATGATGGCTGC	Our laboratory (Barman and Tamuli, 2017)
11	q-B-tub-Rv	TTGTTCTGAACGTTGCGCATC	Our laboratory (Barman and Tamuli, 2017)

12	Hsp80RT-Fw	CGAACAAGACCCTCACCATC	Our laboratory
13	Hsp80RT-Rv	GAGCGGGCAATAGTACCAAG	Our laboratory
14	Hsp60 ARrt Fw	GTCCTCATCGAGTCCAGCTT	Our laboratory
15	Hsp60 ARrt Rv	CCGAGGTTCTCGAACTTGTC	Our laboratory
16	RT-CNB-1-F	GGCAACAAGGAGCAGAAGCT	Our laboratory
17	RT-CNB-1-R	CCTCCATGATCGTCTTGTCG	Our laboratory
18	RT-NCU07952-F	GATGTCTCTTCGGTAGCCCA	Our laboratory
19	RT-NCU07952-R	CGTCCGACAGACTGAAGTTG	Our laboratory
20	RT-NCU04898-F	CCTCTCTACCTCCACGCCTA	Our laboratory (Laxmi and Tamuli, 2016)
21	RT-NCU04898-R	CCAAACAAAGGTCCATTCCT	Our laboratory (Laxmi and Tamuli, 2016)
22	RT-NCU04736-F	GAGATGACTCCTCTCCAGTC	Our laboratory (Laxmi and Tamuli, 2016)
23	RT-NCU04736-R	GGAGTGTGCTGTGATTTGGG	Our laboratory (Laxmi and Tamuli, 2016)
24	1F	CATCGAATTCTGTTGCTGGC	Our laboratory
25	1R	GAGAAGCTGAGAGATCTCAG	Our laboratory
26	2F	ACCCGGTGATTTGGAGTTGA	Our laboratory
27	2R	ATTGGGAAGACTGAGGGAAC	Our laboratory
28	3F	AGGCTTCTTGAAACAGGCAG	Our laboratory

29	3R	GGGAACTGAAATGACTCCAG	Our laboratory
30	4F	GCCTCGAGGATTCTGGATC	Our laboratory
31	4R	CCCTGTTTGTCGTGTGTAGT	Our laboratory
32	5F	AAGAGGGACCTGCCCCTC	Our laboratory
33	5R	CCATCCGCATTCCTCAGCT	Our laboratory
34	Chip 1F Hsp60	AAATTTCATGCTAGGGGACG	Our laboratory
35	Chip 1R Hsp60	TTTGGGGGTATTGTGTGAAG	Our laboratory
37	ChIP NCA-2 1F	GACAGCAACAGCGACCTGAC	Our laboratory
38	ChIP NCA 1R	GATAGCTGGCACTCAAGGGC	Our laboratory
39	EMSA_ hsp80 1F	GGCCGCAAACGAATCAGAG	Our laboratory
40	EMSA_hsp80 1R	GTTGCTTGCTATCCCCACAT	Our laboratory
41	Duplex Hsp80_1	GGACGTTAGCACGCGCAGCACCGAGGGCAC	Our laboratory
42	Duplex Hsp80_1 comp	CCTGCAATCGTGCGCGTCGTGGCTCCCGTG	Our laboratory
43	Duplex Hsp80_2	ACCTGCCCCTCAGCGGAGCGATTTGGACGG	Our laboratory
44	Duplex Hsp80_2 comp	TGGACGGGGAGTCGCCTCGCTAAACCTGCC	Our laboratory
45	Duplex Hsp80_1 Mut	GGACGTTAGCAATATACTAACCGAGGGCAC	Our laboratory

46	Duplex Hsp80_1 Mut comp	CCTGCAATCGTTATATGATTGGCTCCCGTG	Our laboratory
47	Duplex Hsp80_2 Mut	ACCTGCCCCTCCTATTCTAGATTTGGACGG	Our laboratory
48	Duplex Hsp80_2 Mut comp	TGGACGGGGAGGATAAGATCTAAACCTGCC	Our laboratory
49	EMSA NCA-2 Fw	AGCAACGCGTACATTCGAACA	Our laboratory
50	EMSA NCA-2 Rv	CAGCTCAGGCGAACTCTGTT	Our laboratory
51	Duplex NCA-2_1	TGGCTCTGTCTACCGCGCCTCGATTTTCGA	Our laboratory
52	Duplex NCA-2_1C	ACCGAGACAGATGGCGCGGAGCTAAAAGCT	Our laboratory
53	Duplex NCA-2_2	GAGTCTGCCCTTGCGCAGCTGACGGGTTGC	Our laboratory
54	Duplex NCA-2_2C	CTCAGACGGGAACGCGTCGACTGCCCAACG	Our laboratory
55	Duplex NCA-2_1 Mut	TGGCTCTGTCTCAATATAATCGATTTTCGA	Our laboratory
56	Duplex NCA-2_1 Mut C	ACCGAGACAGAGTTATATTAGCTAAAAGCT	Our laboratory

57	Duplex NCA-2_2 Mut	GAGTCTGCCCTGTATACTATGACGGGTTGC	Our laboratory
58	Duplex NCA-2_2 Mut C	CTCAGACGGGACATATGATACTGCCCAACG	Our laboratory

2.2 Methods

2.2.1 Growth conditions

N. crassa strains were cultured and maintained as described previously (Davis and de Serres, 1970). Strains were cultured routinely on 1X Vogel's glucose medium N (VG) for vegetative growth (Vogel, 1956; Vogel, 1964), on 1X synthetic crossing medium (SCM) for crossing and sexual development (Westergaard and Mitchell, 1947) and FGS agar media for germination of ascospores (Davis and de Serres, 1970). Inositol and pantothenic acid stocks were prepared and added to the growth media at a concentration of 0.05 and 0.01 and mg/ml, respectively, for culturing the respective auxotrophs (http://www.fgsc.net/methods/stanford.html; Murray and Perkins, 1963). For the selection of the *N. crassa* transformants, FGS agar media supplemented with Basta® or Ignite® (Pall, 1993) at a concentration of 400 µg/ml was used. For the selection of the *N. crassa* knockout mutants generated using the *hph* cassette, hygromycin was supplemented to the growth medium at a concentration of 220 µg/ml (Colot *et al.* 2006).

2.2.2 Setting up crosses and harvesting ascospores

Crosses among *N. crassa* strains of opposite matting type were performed as described previously (Westergaard and Mitchell, 1947; Davis and de Serres, 1970). Crosses were performed by inoculation of the agar plugs from respective strains on SCM agar in 55 mm Petri dishes. Further, these crosses were incubated at 22 °C in a BOD incubator for three to four weeks. Then, ascospores obtained from the crosses were harvested by washing the lids with 1

ml sterile water. Next, these ascospores were plated on FGS agar plates, germination was triggered by heat shock at 65 °C for 30-60 min in a shaking water bath, and germinated colonies were picked underneath a dissection microscope by cutting out a small agar block bearing the ascospore and subsequently transferred onto a slant having minimal or selective media followed by incubation at 30 °C for growth.

2.2.3 Maintenance of *N. crassa* strains

Silica stocks were prepared for long term preservation of the *N. crassa*. Strains were grown in VG agar slants for 3 days in constant dark at 30 °C and then for 4 days at room-temperature under light. Silica (6-12 Mesh, Grade 40) was sterilized by autoclaving and dried at 60 °C and cooled to room temperature before use. Cryo tubes (4.5 ml) were filled with dried silica. For each strain, 1 ml of 5% autoclaved skimmed milk was added to the culture tube and vortexed vigorously. Spore suspension was drawn up by using a Pasteur pipette and dispensed into the pre-chilled silica gel in the cryo tubes placed in ice and vortexed vigorously for 5 min, to break up any clumps in the process. Tubes were regularly vortexed for 8-10 days and the tubes were stored at minus 20 °C until further use.

2.2.4 Conidial cell count

For quantification, conidia scrapped from the agar surface with sterile distilled water and vortexed briefly for making conidial suspension. Conidial cells were counted using a haemocytometer under a trinocular inverted microscope (AxioVert A1 FL, Carl Zeiss, Germany).

2.2.5 Scoring for antibiotic resistance in *N. Crassa*

To score antibiotic resistance conidia were streaked onto 1.5% VG agar plates supplemented with the antibiotic. The antibiotics used were hygromycin B (220 µg /ml from 100 mg/ml stock in water), and Basta® or Ignite® (400 µg/ml from 100 mg/ml stock in water).

2.2.6 Calcium stress tolerance assay

For performing the Ca^{2+} stress tolerance assay using the *N. crassa* strains, the agar plugs from 3 days old culture were inoculated in the centre of the 90 mm Petri dish containing VG agar supplemented with increasing concentrations of $CaCl_2$ (0.2, 0.3, and 0.4 M) and incubated at 30 °C. Colony diameter (cm) was measured after 12 h at regular interval of 3 h over a period of 24 h. The average colony growth rate (cm h^{-1}) was calculated based on the data obtained from three independent experiments for each strain. Average colony growth rate percentage (%) was calculated relative to the colony diameter of the strains in VG without $CaCl_2$ (0 M) considered as 100%

2.2.7 Assay for the visualization of hyphal septation in the *N. crassa* strains

For visualization of septation in the growing hyphae, strains were initially grown in VG agar on a glass slide for 12 h in dark at 30 °C. Then the agar plugs containing the growing hyphal tips were cut and after staining with CFW were incubated in dark for about 10 minutes. After that visualization was done under a Trinocular inverted fluorescence microscope (Axio Vert A1 FL, Carl Zeiss) using DAPI filters with an exposure of 100-150 ms.

2.2.8 Assay for the visualization of intracellular Ca^{2+} distribution

For visualization of the intracellular Ca^{2+} distribution in *N. crassa*, strains were grown on VG agar in glass slides for 8 h at 30 °C. Then the media was replaced with VG agar supplemented with 200 M chlortetracycline hydrochloride (CTC) dissolved in 0.1 % dimethyl sulphoxide (DMSO). Fluorescence from the growing hyphae was observed using a Trinocular inverted fluorescence microscope (Axio Vert A1 FL, Carl Zeiss) using DAPI filters with an exposure of 100-150 ms.

2.2.9 Osmotic stress assay

N. crassa strains were grown for three days and then agar plug of diameter ~1 cm was cut and was placed in the middle of 90 mm -Petri dishes containing VG agar medium supplemented with or without increasing concentrations (0.5, 1, and 1.5 M) of Sorbitol. The strains were then incubated at 30 °C and colony diameter was measured after 12 h with an interval of 3 h over a period of 24 h. The radial growth rate was calculated as cm/h.

2.2.10 Thermotolerance Assay

For measuring thermotolerance three-day old conidia were inoculated into VG liquid medium at a concentration of ~1 X 10^6 cells/ ml and germinated for 2 h with shaking at 200 rpm at 30 °C. These germlings were exposed to different heat treatment condition in two sets one set was held at 30 °C for uninduced condition and the other set was set at 44 °C for induced condition for 30 min, then one set of each were given a lethal heat shock at 52 °C for 20 min (Kumar and Tamuli, 2014). After these the conidia were spread in 1X FGS agar plate incubated at 30 °C for 1 day. Percent survival was obtained by dividing the number of viable colonies on plates held at 30 °C (control) and multiplying by 100.

2.2.11 Assessment of Carotenoid accumulation

For carotenoid accumulation, ~1X10^6 conidia/ml were inoculated in petri plate containing 50 ml VG media supplemented with calcium D-pantothenic acid and 0.2% tween 80 as a wetting agent to avoid conidiation (Zalokar et.al. 1954). Cultures were initially incubated at 30 °C for 48 h and then exposed the different sets to 30 °C, 22 °C, and 8 °C. Mycelia was filtered, lyophilized and pulverized into fine powder. 50 mg from each sample was taken into 1.5 ml Eppendorf and 1 ml of acetone was added. It was kept on rotantiomixer for 5 h and centrifuged at 12,000 rpm for 10 min. Supernatant were collected in a new 1.5 ml Eppendorf tube. Stored

in -80 °C deep freezer for two h. Samples were then placed into incubator at 30 °C overnight with open caps of the tubes. 1 ml of hexane was added to extracted carotenoid in the Eppendorf tube and the absorbance was taken at OD_{470} nm. Total carotenoid content (µg/g) was calculated by following formulae:

Total carotenoid content (µg/g) = [Absorbance X 1 ml (total volume)] x [10^4/Absorption coefficient (2500) x sample weight (g)] as described earlier (Rodriguez-Amaya and Kimura, 2004)

2.2.12 Ultraviolet (UV) radiation sensitivity assay

For quantitative UV radiation sensitivity assay strains were grown in flasks containing Vogel's glucose medium at 30 °C for 3 days in dark followed by 3 days under constant light at room temperature. Strains were harvested, washed with sterile water and finally resuspended in sterile water. The conidial suspension of ~1 X 10^6 conidial cells were taken and ~100 conidia cells were plated on Vogel's sorbose agar medium and irradiated with UV (253 nm wavelength) doses of 100, 200 and 300 J/m^2 with no UV treated plate was taken as a control. The plates were then incubated at 30 °C in the dark for 24- 48 h and the number of viable colonies on each plate was counted.

2.2.13 Submerged conidiation assay

For observation of conidiation in submerged condition, about 1 X 10^6 cells/ml from conidial suspension of strains were inoculated in liquid VG supplemented with or without 2% peptone (w/v) followed by incubation for 16 h in dark with shaking at 180 rpm at 30 °C. Around 10 µl of the culture is taken from each conical flask and imaged at 20X magnification using a Trinocular inverted microscope (AxioVert A1 FL, Carl Zeiss) to analyze the formation of conidiophores (Yang et al. 2002).

2.2.14 Circadian regulated conidiation study

Strains were initially grown in 55 cm Petri dish on VG agar medium for three days at 30 ºC and fresh conidia were inoculated at one end of 40 cm long race tube comprising of circadian media and kept at 20 ºC, 25 ºC, and 30 ºC under light for 24 h. After 24 h, the growth front was marked and the race tubes were transferred to continuous darkness. After every 24 h, the growth front was marked under red safe light for 5 days. Then, the period lengths were calculated by multiplying the distance between conidial bands by the inverse of slope. The slope is the distance/hour determined from plot of distance between growth fronts versus 24-hour days (http://www.fgsc.net/teaching/circad.htm).

2.2.15 Isolation of *N. crassa* genomic DNA

The strain of interest was cultured in VG liquid at 30 °C for 3 days with shaking at 200 rpm. The mycelial mass harvested by filtration was lyophilized and were grinded with glass beads (0.2 mm in diameter) to a fine powder using a mortar and a pestle. Approximately, 150 mg of the mycelia powder was taken in a 2 ml microfuge tube and 1 ml of lysis buffer was added. The tube was heated at 65 °C for 30 min, followed by centrifugation for 10 min at 12,000 x *g*. The supernatant was transferred to a 2 ml microfuge tube and added 500 µl of phenol: chloroform: isoamyl alcohol mixture (25:24:1). The tube was rotated for 15 min in a rotary mixer and centrifuged for 10 min at 12,000 x *g*. The aqueous phase was collected in a 1.5 ml tube and 600 µl of chloroform was added to remove last traces of phenol. The tube was centrifuged for 10 min at 12,000 x *g*. The aqueous phase was taken in a 1.5 ml microfuge tube and genomic DNA was precipitated by adding 1 ml absolute ethanol. The tube was gently inverted few times and the genomic DNA was pelleted by centrifuging at 12,000 x *g* for 10 min. The pellet was washed with 70% ethanol by centrifuging for 2 min at 12,000 x *g*. The genomic DNA pellet was air dried at room temperature for 15 min. Finally, the dried pellet

was dissolved in 30 µl of 1X TE buffer (pH 8.0) and stored at 4 ºC. All centrifugation steps were performed at room temperature.

2.2.16 Agarose gel electrophoresis

For loading 1 µl DNA sample was mixed with 1 µl of Blue Gel Loading Dye (6X) and 4 µl 1X TAE. The samples based on the size of the DNA to be resolve were loaded on 0.7% to 1.5% agarose gels prepared using 1X TAE containing 0.5 µg/ml ethidium bromide. Electrophoresis was performed in 1X TAE running buffer at 5 Vcm^{-1}. For estimation of DNA fragment sizes standard DNA size markers were run alongside the sample. The DNA samples stained with ethidium bromide were visualized in a gel documentation system (Bio print ST4, Vilber Lormat, France). RNA samples were resolved in 1.2% agarose gel containing 1X MOPS buffer, 2.2 M formaldehyde, and 0.5 µg/ml ethidium bromide.

2.2.17 Quantification of nucleic acids

The nucleic acid concentration was estimated by measuring the OD at 260 nm in a spectrophotometer (BioSpectrometer® Kinetic, Eppendorf, Germany). The following empirical relationships were used to calculate the concentrations. An OD_{260} of 1 corresponds to ~50 µg/ml of double stranded DNA, 40 µg/ml of single-stranded DNA and RNA, ~20 µg/ml of single-stranded oligonucleotides. The purity of nucleic acids was estimated by calculating the OD_{260}/OD_{280} ratio. Pure preparations of RNA and DNA have OD_{260}/OD_{280} values of 2.0 and 1.8 respectively.

2.2.18 Polymerase chain reaction (PCR)

The routine polymerase chain reaction (PCR) reaction was performed by using Taq DNA polymerase (Cat no. M0273S, New England Biolabs, USA) as per the manufacturer's protocol. For cloning purposes, Phusion® High-Fidelity DNA polymerase (Cat. no. M0530S, New England Biolabs, USA) was used as normal Taq DNA polymerase isolated from *Thermus*

aquaticus lacked proofreading activity (3′-5′ exonuclease activity). The PCR conditions varied according to the size of the product and annealing temperature of the primers. All PCRs were performed with a thermal cycler (Arktik Thermal Cycler, Thermo Fisher Scientific, USA).

2.2.19 RNA isolation from *N. crassa* strains

RNA was isolated from *N. crassa* strains as described previously (http://www.fgsc.net/fgn37/sokol.html). For RNA the isolation, ~1 x 10^7 conidia of the strain of interest were inoculated in 10 ml of VG liquid medium, and incubated at 30 °C with constant 180 rpm shaking for 16 h. Mycelia harvested by filtration was crushed in a mortar and pestle to fine powder using liquid nitrogen. The mycelial powder (~25 mg) was immediately transferred into a 2 ml microfuge tube containing 300 µl TRIzol™ reagent (Cat. no. 15596026, Life Technologies, USA), and further added 750 µl RNA lysis buffer and 750 µl phenol: chloroform: isoamyl alcohol (25:24:1) mixture. The tube was rotated in a rotary mixer for 20 min and centrifuged for 10 min at 10,000 x *g*. The upper aqueous phase was taken in a 2 ml microfuge tube and 750 µl of 8 M LiCl was added. The mixture was stored at 4 °C for 12-15 h. The mixture was vortexed briefly and centrifuged for 10 min at 10,000 x *g*. The isolated pellet was suspended in 300 µl double distilled DEPC treated water, mixed with 30 µl of 3 M Na-acetate (pH 5.2) and 750 µl of absolute ethanol was added. The mixture was stored at minus 20 °C for 2 h and centrifuged for 10 min at 10,000 x *g*. The RNA pellet was washed with 70% ethanol. The RNA pellet was dried for 10-15 min at room temperature and finally dissolved in 30 µl RNAase free water. The RNA was stored at minus 80 °C. All centrifugation steps were carried out at room temperature.

2.2.20 Reverse transcription PCR for cDNA synthesis

Reverse transcription PCR (RT-PCR) was used for cDNA synthesis for performing gene expression study. The cDNA synthesis was performed by using Verso cDNA synthesis kit

(Cat. no. AB-1453/A, Thermo Fisher Scientific, USA). About 1 µg of total RNA was used in each 20 µl reaction. The cycling condition for cDNA synthesis was 50 °C for 45 min followed by 95 °C for 2 min for 1 cycle.

2.2.21 Real time quantitative PCR (qRT-PCR)

Total RNA isolated from *N. crassa* was used for real time quantitative PCR (qRT-PCR) for gene expression studies. qRT-PCR was performed in a real time PCR system (ABI 7500 Fast, Applied Biosystems, USA) using SYBR® select master mix (Cat. No. 4472903, Life Technologies, USA) in a final reaction volume of 15 µl. In general, 15 µl reaction mixture contained 7 µl of cDNA (~100 ng), 0.5 µl of forward primer, 0.5 µl of reverse primer, and 7 µl of SYBR® select master mix. The PCR reaction condition used was as follows: 95 °C for 10 min followed by 40 cycles of 95 °C for 15 s and 60 °C for 1 min. The relative expressions of the target genes were calculated by $2^{-\Delta\Delta C}{}_{T}$ method (Livak and Schmittgen, 2001), and the expression level of β-tubulin was used as the endogenous control.

2.2.22 DNA fragments purification from agarose gels

DNA which is to be used for cloning, sequencing, and transformation was amplified by PCR and then resolved on agarose gels. DNA bands to be eluted was excised by visualizing in a UV transilluminator and transferred to a 1.5 ml microfuge tube. DNA from the gel slice was purified from the agarose gel slices using a Gel Extraction Kit (Qiagen, USA) according to the manufacturer's protocol.

2.2.23 Protein isolation and purification

The NCS-1::5xGly::V5::GFP, CRZ-1::5xGly::V5::GFP, and 5xGly::V5::GFP proteins were isolated the $P_{nit\text{-}6}$::*ncs-1* (21), $P_{tcu\text{-}1}$::*crz-1* (559), and pccg-1_GFP strains (Table 2.1) respectively. The strains were cultured in VG liquid medium containing appropriate

supplements for 16 h at 30 °C and 180 rpm shaking. The mycelial mass was harvested from the culture by filtration and then crushed into a fine powder in a mortar and pestle using liquid nitrogen. Roughly 150 mg of mycelial powder from each sample was suspended in 400 µl native protein extraction buffer [50 mM Tris-HCl (pH 7.5), 1 mM EDTA, 6 mM $MgCl_2$, 2.5 mM phenylmethylsulphonyl fluoride (PMSF) and 0.1% fungal protease inhibitor cocktail (FPIC, Cat. No. P8215-1ML, Sigma Aldrich, USA) in 2 ml microfuge tube. The tubes were centrifuged for 10 min at 6000 x g at 4 ºC to isolate the crude proteins. 50 µg of the Dynabeads® Protein A magnetic beads (Cat. No. 10001D, Life Technologies, USA) conjugated and cross-linked with mouse anti-V5 monoclonal antibody (Cat. No. R960-25, Life Technologies, USA) was added to the crude protein samples and incubated overnight at 4 ºC on a rocking platform. 30 µl non-denaturing elution buffer [50 mM glycine (pH 2.8)] was added to the beads to elute the bounded protein and the acidic pH was neutralized by adding 5 µl of 1M Tris-HCl (pH 7.5). The purity was checked by resolving an aliquot of 5 µl eluted protein on a 10% SDS-PAGE gel and staining with Coomassie Brilliant Blue dye (Himedia, India). The Bradford assay was used for quantification of protein concentration.

2.2.24 Dynabeads® Protein A magnetic beads preparation

Dynabeads® Protein A magnetic beads (Cat. No. 10001D, Life Technologies, USA) were prepared as per the manufacture's protocol. To every 50 µl of beads (~1.5 mg), 10 µg of antibody was conjugated and cross-linked using DMP (Cat No. D8388-250MG, Sigma Aldrich, USA).

2.2.25 Chromatin immunoprecipitation (ChIP)

N. crassa germlings were grown for 5 h old under Ca^{2+} stress conditions to perform chromatin immunoprecipitation (ChIP) assay. Approximately 5 x 10^6 conidia/ml were inoculated in two 250 ml flasks one containing 50 ml standard VG liquid, another containing VG supplemented

with 0.2 M $CaCl_2$, and cultured at 30 ºC and 180 rpm shaking for 5 h. To perform ChIP under heat shock stress conditions, 5 x 10^6 conidia/ml were inoculated in two 250 ml flasks both containing 50 ml standard VG liquid and cultured at 30 ºC and 180 rpm shaking for 14 h and after that one of the flasks was shifted to 48 ºC with shaking at 170 rpm for 1 h more. Both the cultures were supplemented with 10 µg/ml pantothenic acid and 50 µM BCS. Chemical crosslinking was performed by incubating the germlings in 1% formaldehyde solution for 1 h at room temperature with shaking at 180 rpm. 125 mM glycine was added and incubated for 20 min at room temperature to quench the reaction. Germlings were harvested by centrifuging for 10 min at 3000 x *g* and 4 ºC. The harvested germlings were washed two times with 1X PBS (pH 7.4) and pellet was suspended in 1.2 ml CHIP lysis buffer. Chromatin shearing was performed by sonicating the germlings in a sonicator (Vibra cell sonics, USA) on ice using the parameters as amplitude: 33%, ON pulse: 8 s, OFF pulse: 10 s, cycles: 120, and time: 20 min. The sonicated samples were centrifuged for 8 min at 12,000 x *g* and 4 ºC to remove the cell debris, and then the supernatant having the sheared DNA was run on 1 % agarose gel to confirm the shearing and further quantified using a spectrophotometer (BioSpectrometer® Kinetic, USA). To precipitate CRZ-1::5xGly::V5::GFP bounded to the *nca-2* and *hsp80* promoter fragments, the sonicated chromatin was incubated with mouse anti-V5 monoclonal antibody (Cat. No. R960-25, Life Technologies, USA) using 1 µg antibody per 25 µg DNA. The samples treated with antibody and the input control (without antibody treatment) were incubated overnight with pre-blocked 50 µl Dynabeads® Protein A magnetic beads (Cat. No. 10001D, Life Technologies, USA) on a rocking platform in a cold-room. The beads were washed first with RIPA buffer and then the beads were sequentially given one low salt, one high salt and one LiCl wash. For each washing step, about 100 µl of respective buffers were used. The chromatin bounded to the bead was eluted using 120 µl of elution buffer after vortexing gently for 15- 20 min and eluted samples were incubated overnight after addition of

4.8 µl of 5 M NaCl at 65 ºC for de-crosslinking. After de-crosslinking, chromatin was treated with RNAse A (Cat. No. A7973, Promega, USA) for 1 h at 65 ºC and then proteinase K (Cat. No. V3021, Promega, USA) for 5- 6 h at 45 ºC. PCR Purification Kit (Cat. No. 28104, Qiagen, Germany) was used to purify chromatin and was quantified using a spectrophotometer (BioSpectrometer® Kinetic, Eppendorf, Germany).

2.2.26 Duplex DNA probe synthesis

Duplex DNA probes of 30 bp in size were generated from the complementary primer pairs or nucleotide strands, Duplex Hsp80_1, Duplex Hsp80_1 comp, Duplex Hsp80_2, Duplex Hsp80_2 comp, Duplex Hsp80_1 Mut, Duplex Hsp80_1 Mut comp, Duplex Hsp80_2 Mut, Duplex Hsp80_2 Mut comp, Duplex NCA-2_1, Duplex NCA-2_1C, Duplex NCA-2_2, Duplex NCA-2_2C, Duplex NCA-2_1 Mut, Duplex NCA-2_1 Mut C, Duplex NCA-2_2 Mut and Duplex NCA-2_2 Mut C (Table 2.2). The primer pairs were first denatured at 95 °C for 45 min, and then annealed at 55 °C for 50 min using a buffer [10 mM HEPES (pH 7.5), 0.1 mM EDTA, 0.1 M NaCl, and 5 mM $MgCl_2$], in a thermal cycler (Arktik, Thermo scientific, USA).

2.2.27 Electrophoretic mobility shift assay (EMSA)

Electrophoretic mobility shift assay (EMSA) was performed using a Molecular Probes™ EMSA Kit (Cat no. E33075, Life Technologies, USA) as per the manufacturer's protocol. The individual DNA probes (5 µM) were incubated with the purified protein (50 µM) to test protein-DNA binding. To resolve protein-DNA complexes, non-denaturing polyacrylamide (30:0.8)/1 X TBE gels were used. Electrophoresis was performed at 200 volts for 1 h in 1X TBE running buffer. The gels were visualized in a gel documentation system (Bio-Print ST4, Vilber Lourmat, France).

2.2.28 SDS-polyacrylamide gel electrophoresis (SDS-PAGE)

Based on the protein size, 10-12% resolving gel was poured to the gap between the glass plates. The top was overlaid with isopropanol and the gel was allowed to polymerise for 45 min. The stacking gel was poured over the resolving gel after removing the isopropanol and the comb was placed. The gel was allowed to polymerise for 20-30 min. The comb was removed and the wells were rinsed with 1X running buffer to remove the unpolymerised acrylamide. The glass plates containing the gel was assembled in the electrophoresis apparatus. An aliquot of 8 µl of protein sample and 2 µl of 5X SDS-PAGE sample buffer were mixed in a micro centrifuge tube and was heated to 90 °C for 5 min. The samples were loaded into the gel contained in 1X running buffer and electrophoresis was performed at 70 mA current and 80 V voltage for the stacking gel, while 120 V voltage for the resolving gel. Staining was carried out for 2 hours with shaking at room temperature. Destaining was done by soaking the gel in destaining solution on a slowly rocking platform for 8-12 h.

2.3 Databases and software programs used

1. **Basic Local Alignment Search Tool (BLAST):** BLAST (Altschul *et al.*, 1990; Altschul *et al.*, 1997; Altschul *et al.*, 2005) was used to compare nucleotide or protein sequences to sequence databases. This is available at http://blast.ncbi.nlm.nih.gov/Blast.cgi.
2. **Clustal X:** Clustal X (Thompson *et al.*, 1997) software was used for multiple sequence alignment of DNA and protein sequences. Clustal X is available online at http://www.clustal.org/clustal2/#Webservers.
3. **ExPasy Translate tool:** The ExPasy Translate tool was used for translating DNA sequences to protein sequences. It is available at http://web.expasy.org/tools/DNA.

4. **Conserved Domain Database (CDD):** CDD (Marchler-Bauer and Bryant, 2004; Marchler-Bauer *et al.*, 2008) was used to identify conserved domains in the proteins. This is available at http://www.ncbi.nlm.nih.gov/Structure/cdd/wrpsb.cgi.
5. **GeneDoc:** GeneDoc software (Nicholas, 1997) was used for finding conserved domains among aligned sequences of DNA or protein. It is available at http://www.nrbsc.org/gfx/genedoc/.
6. **RestrictionMapper:** This was used for restriction mapping of DNA sequences. It is available at http://www.restrictionmapper.org/.
7. **Molecular Evolutionary Genetic Analysis Version 6 (MEGA 6):** The MEGA software (Tamura *et al.*, 2013) was used to depict the evolutionary relationship among the organisms or gene sequences. It is available at http://www.megasoftware.net/.
8. ***Neurospora crassa* genome databases:** Genome resource for *Neurospora* is available at http://fungidb.org. The web site for the Fungal Genetics Stock Center is http://www.fgsc.net/.
9. **NCBI:** NCBI at http://www.ncbi.nlm.nih.gov/ was used to retrieve the proteins or nucleic acid sequences.
10. **EMBL:** EMBL at http://embl.org/was used to retrieve the primary sequence of proteins or nucleic acid.
11. **UniProt:** UniProt at https://www.uniprot.org/ was used to retrieve the primary sequence of proteins.
12. **Primer3:** Primer3 was used for analysis of the secondary structure of oligonucleotide primers. It is available at http://bioinfo.ut.ee/primer3-0.4.0/.
13. **Site for reverse-complement:** The sequence manipulation suite (SMS) software package was used to convert a DNA sequence into reverse-complement sequence. It is available at http://www.bioinformatics.org/sms/index.html.

14. **DNA binding site predictor for Cys_2His_2 Zinc Finger Proteins**: DNA binding site predictor for Cys_2His_2 Zinc Finger Proteins" (Persikov *et al.*, 2008; Persikov and Singh, 2013) was used for prediction of the CRZ-1 binding sites. It is available at http://zf.princeton.edu.
15. **Search Tool For The Retrieval Of Interacting Genes/Proteins (STRING):** To predict the functional protein association networks STRING version 10.0 (Szklarczyk et al. 2015) was used.
16. **SigmaPlot:** The linear and bar graphs representing data from the various sets of experiments were plotted using SigmaPlot version 11.0 (Systat software, San Jose, California, USA) available at www.systatsoftware.com.
17. **IBS (illustrator of biological sequences):** It is a software package used for the organizing the different proteins or nucleotide sequences in an efficient and precise manner giving different colours to different domains and also scaling can be adjusted according to the length of the sequences (Liu et al. 2015).

Chapter 3

Cell functions and regulatory mechanism of calcineurin B (CNB-1) subunit

3.1 Introduction

Calcineurin is a eukaryotic Ca^{2+} and calmodulin-dependent serine/threonine protein phosphatase (Rusnak & Mertz, 2000). Calcineurin, also known as protein phosphatase 2B or PP2B of the PPP family, is a heterodimer consisting of one catalytic subunit Calcineurin A (CNA-1) and one regulatory subunit Calcineurin B (CNB-1) (Guerini, 1997). It was first detected as a Ni-NTA column fraction that inhibited the calmodulin dependent cyclic nucleotide phosphodiesterase (Wang and Desai, 1976). As suggested by the protein sequence and confirmed by the crystallographic structure, the catalytic subunit of calcineurin (CNA-1) has high sequence homologies with other protein phosphatases while calcineurin B (CNB-1), the regulatory subunit of calcineurin, is a Ca^{2+}-binding protein with four "EF-hand" Ca^{2+}-binding sites and a myristylation motif (Aitken et al. 1982). The secondary structure of CNB-1 is determined by multidimensional NMR, is similar to that of calmodulin (Anglister et al. 1993). The calcineurin B subunit is also highly conserved throughout evolution, with mammalian calcineurin B showing 86% amino acid sequence identity with the calcineurin B identified in insect including *Drosophila melanogaster* and 54% identity with calcineurin B from *S. cerevisiae*. This high degree of conservation allows functional interchange of calcineurin B subunits between mammalian and *N. crassa* catalytic subunits (Kincaid and Ueki, 1993). The gene for mammalian calcineurin B encodes a protein of 170 amino acids containing four Ca^{2+}-binding EF-hand motifs (Cohen et al. 1993)

CNB-1 plays many important cell functions from lower to higher eukaryotes, including Ca^{2+} homeostasis and Ca^{2+} mediated cell cycle arrest in *Saccharomyces cerevisiae* (Cyert, 1993; Thorner et al. 1993), polarized growth, septation and spindle body formation in *Schizosaccharomyces pombe* (Rasmussen et al. 1995; Moir et al. 1989). In *Cryptococcus neoformans*, CNB-1 has a role in the temperature sensitive growth and virulence (Heitman et al. 1997). In *N. crassa*, CNB-1 is necessary for hyphal growth/conidiation, maintenance of

apical Ca^{2+} gradient, proper septation (Free et al. 1998; Barthelmes et al. 1997). In higher eukaryotes like *Nicotiana tabacum* and *Arabidopsis thaliana*, mutation of CNB-1 leads to salt tolerance (Hasegawa et al. 1998) and sensitivity to Na^{+} ions (Zhu et al. 1998). In humans, mutations in CNB-1 results in osteoclast bone resorption, cardiac hypertrophy, immunosuppressant induced hypertrophy (Victor et al. 1996; Mak et al. 1998).

Because *cnb-1* is an essential gene in *N. crassa*, conventional gene knockout or site-directed mutagenesis of key residues is not feasible due to the lethal effect of the deletion or mutation. Therefore, *cnb-1* mutants were generated in a previous study (Tamuli et al. 2016) using a gene silencing mechanism known as repeat-induced point (RIP) mutation in *N. crassa* (Cambareri et al. 1989). The *cnb-1*^{RIP} mutants revealed mutations in several important amino acid residues (Tamuli et al. 2016) (Table 3.1) responsible for the both sexual and asexual developmental stages, and survival under the stress conditions in *N. crassa* (Tamuli et al. 2016; Kumar et al. 2019). I further investigated the cellular roles of the CNB-1 and its associated proteins in different stress conditions and development in *N. crassa*.

Table. 3.1 Type of mutations in the *cnb-1*^{RIP} mutants

Strain Name	Type of mutations in EF-hand domains	References
599	M31I (ATG→ATA) in EF1 domain	Tamuli et al. 2016
600	M31I (ATG→ATA) in EF1 domain, D103N (GAC→ AAC), D107N (GAC→ AAC) and M121I (ATG → ATA) in EF3	Tamuli et al. 2016
602	M31I (ATG→ATA) in EF1 domain and D105N (GAC→AAC) in EF3	Tamuli et al. 2016

3.2 Results

3.2.1 High concentration of Ca^{2+} affects growth of the *cnb-1*^{RIP} mutants

Calcineurin is involved in stress response pathway, including Ca^{2+} stress in *S. cerevisiae*, in filamentous fungi. Therefore, I studied the phenotypes of the *cnb-1*^{RIP} mutants under the Ca^{2+} stress condition. I tested Ca^{2+} sensitivity of the *cnb-1*^{RIP} mutants on the medium supplemented with various concentration of Ca^{2+} (200 mM, 300 mM, and 400 mM) using the Ca^{2+} stress assay method as described in Chapter 2. Among the four *cnb-1*^{RIP} mutants, bearing the mutations in the different EF-hand domains as described earlier (Table 3.1) only the 602 mutant showed a significant reduction (~64.3%) in growth compared to the wild type at Ca^{2+} concentration of 400 mM. This suggests that *cnb-1* may have a role in the Ca^{2+} stress tolerance in *N. crassa*.

Table3.2 Average colony growth rate expressed in percentage of the wild type and *cnb-1*^{RIP} mutants 599A, 600A and 602A strains at various concentrations of $CaCl_2$.

Strains	**[+]Relative average growth rate (%) at various concentrations of $CaCl_2$ (M)**			
	0	0.2	0.3	0.4
Wild type	100 ± 0.0	93.7 ± 1.5	83.8 ± 2	71.3 ± 2.2
599A	100 ± 0.0	90.8 ± 1.2	88.1 ± 1.8	69.8 ± 2
600A	100 ± 0.0	90.6 ± 1.5	89.4 ± 1.9	67.4 ± 2.3
602A	100 ± 0.0	84.9 ± 1.6	70.4 ± 2	45.9 ± 2.4

[+] Data are expressed as the mean ± standard deviation for three independent experiments.

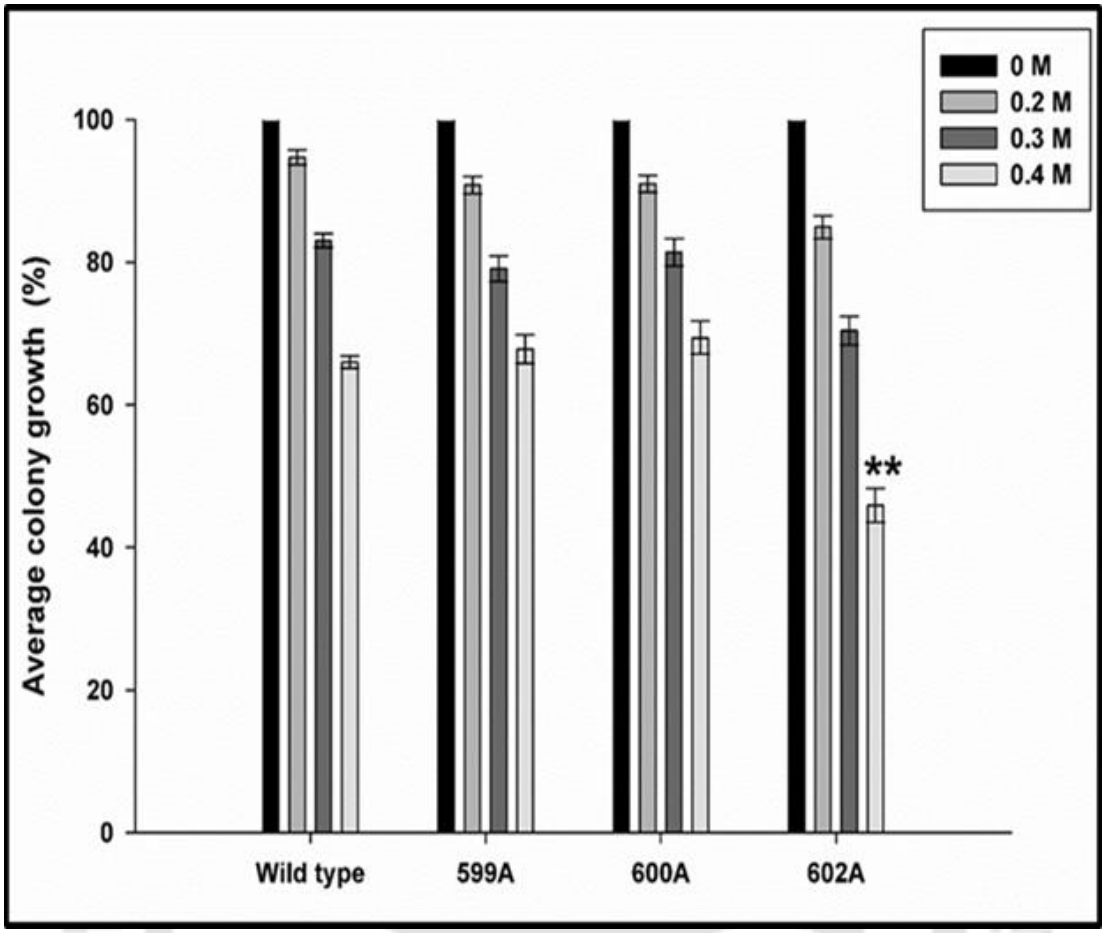

Fig 3.1 Average colony growth rate of the *cnb-1*^{RIP} mutants in the presence of high Ca^{2+} concentration in *N. crassa*. The *N. crassa cnb-1*^{RIP} mutants were grown at various concentrations of $CaCl_2$ (0.2 M, 0.3 M and 0.4 M), however, only the 602A strain shows restricted growth at highest concentration of $CaCl_2$ (0.4 M) in comparison to the wild type strain. Error bars indicate the standard deviation calculated from three independent experiments (n = 3) with *P* values<0.05 (*), <0.01 (**), <0.001 (***) and otherwise non-significant (*ns*) as measured by one-way ANOVA test.

3.2.2 Growth defect of the *cnb-1*^{RIP} mutants were related to improper cell wall formation and hyphal septation

3.2.2.1 Septation studies in the hyphae of the *cnb-1*^{RIP} mutants

Septation is a major phenomenon during the vegetative growth of the filamentous fungi (Alvarez et al. 2014). In *N. crassa*, Rho family of GTPase Rho-4 is responsible for the septation of hyphae during vegetative phase (Molloy, 2007). The *cnb-1*^{RIP} mutants possess morphological defects in terms of slower apical growth, reduced aerial hyphae (Tamuli et al. 2016). Therefore, I examined if, the slow growth phenotype is linked with a defect in hyphal septation using calcofluor white (CFW) stain, a fluorescent dye which selectively binds to the chitin and cellulose of the cell wall in fungi (Fig. 3.2 A; Rasconi et al. 2009). Among the three *cnb-1*^{RIP} mutants, 600 and 602 mutants, showed major difference in septation from to that of the wild type (Fig. 3.2 B). In the 600 and 602 mutants, lesser amount of the CFW appears to bind, indicating that chitin and cellulose content of the cell wall were altered. Therefore, mutations in the EF-hand domains of 600 and 602 mutants lead to slow growth pattern and defect in the cell wall formation.

(A)

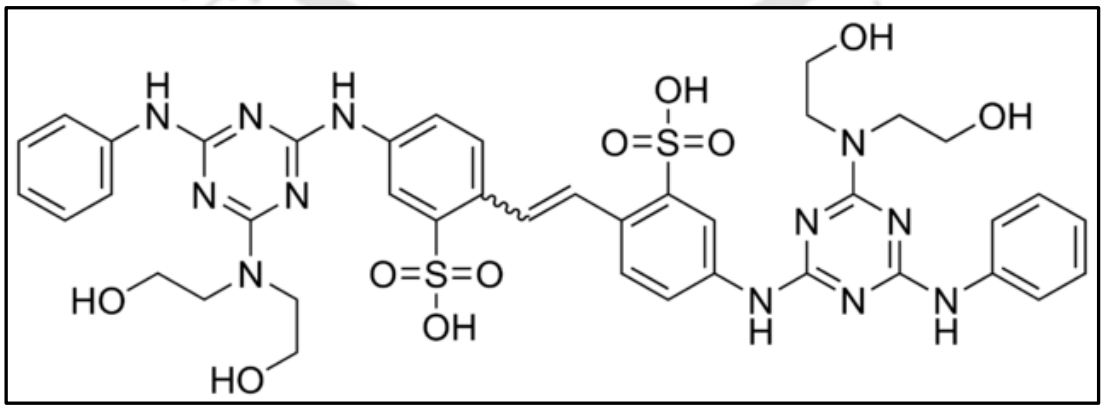

(B)

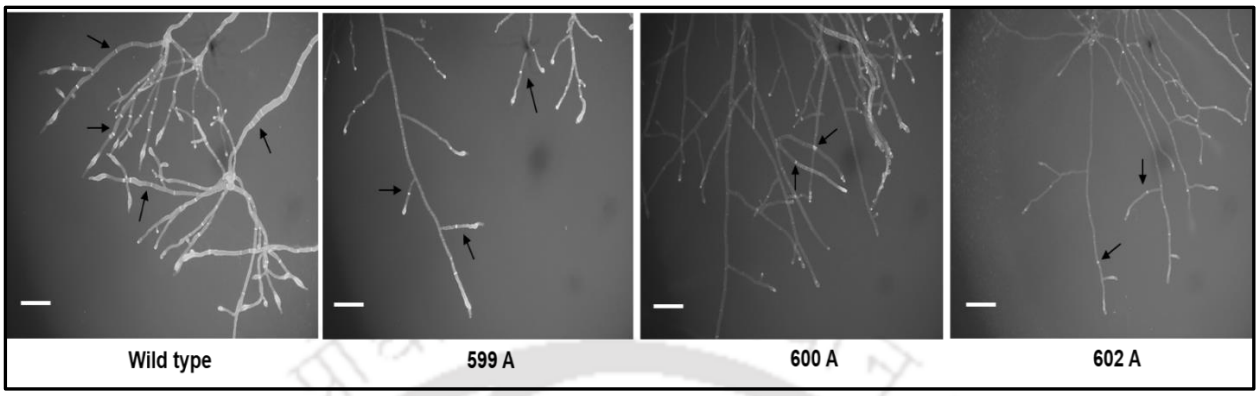

Fig. 3.2 Assay for the visualization septation in hyphae. The calcofluor white (CFW) has an excitation at 355 nm and emission at 420 nm and its structure is available at (https://www.sigmaaldrich.com/catalog/product/sigma/f3543?lang=en&region=IN) (B) The hyphae of the *cnb-1*^{RIP} strains along with the wild type was grown in VG agar and stained with CFW to stain the septa in the hyphae. The slides were kept in dark for 10 mins and fluorescence was observed in which the wild type showed distinct septation whereas the *cnb-1*^{RIP} mutants showed reduced hyphal septation when observed with the help of an inverted fluorescence microscope (AxioVert A1 Fl, Carl Zeiss, Germany) using DAPI filter setting the exposure time of 300-400 ms and using scale bar of 20 µm.

3.2.2.2 Visualization of the internal distribution of Ca^{2+} in the *cnb-1* mutants

In most of the filamentous fungi, including *N. crassa*, hyphal growth depends on the Ca^{2+} gradient in the cytoplasm. The entry of the Ca^{2+} ions in the cytoplasm occurs via the Ca^{2+} channels activated by IP_3 (Silverman-Gavrila and Lew, 2003). Therefore, Ca^{2+} concentration has a direct effect on the hyphal tip growth in *N. crassa*. In the *N. crassa* Ca^{2+}-ATPase mutant *vma-1*, which is localized to the vacuoles, defect in the vacuolar Ca^{2+} uptake affected Ca^{2+} homeostasis, colony growth, aerial hyphae, and female fertility (Bowman et al. 2000). The *cnb-*

1^{RIP} mutants also displayed growth defect, reduced aerial hyphae, and female sterility (Tamuli et al. 2016). Therefore, I performed microscopy analysis using chlortetracycline (CTC), dye which selectively binds to Ca^{2+} stores and thereby exhibits fluorescence, to visualize if, the mutations affected the hyphal growth by altering the internal Ca^{2+} gradient across the hyphae in comparison with the wild type (Fig. 3.3 A) (Schimd and Harold, 1988). The enhanced intensity of fluorescence indicates greater binding of the dye to the membrane enabling better visualization of the accumulated Ca^{2+} stores present in the vesicles (Bowman et al. 2000). The *N. crassa* wild type and the *cnb-1*^{RIP} mutant strains were analyzed using this assay in comparison with the wild type (Fig. 3.3 B). The microscopy analysis using CTC revealed that there was less fluorescence intensity owing to reduced Ca^{2+} concentration across the hyphae, which complements the growth, hyphal defect as discussed earlier regarding the *cnb-1* mutants (Tamuli et al. 2016).

(A)

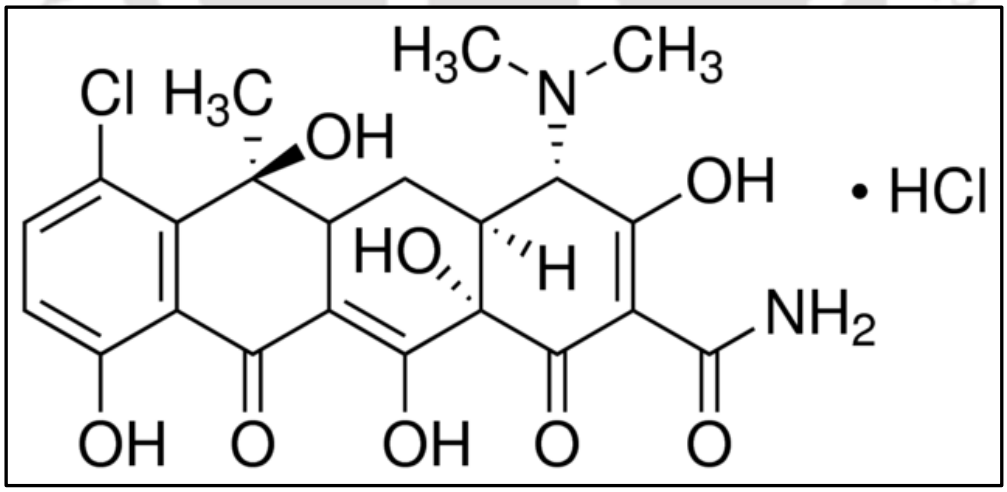

(B)

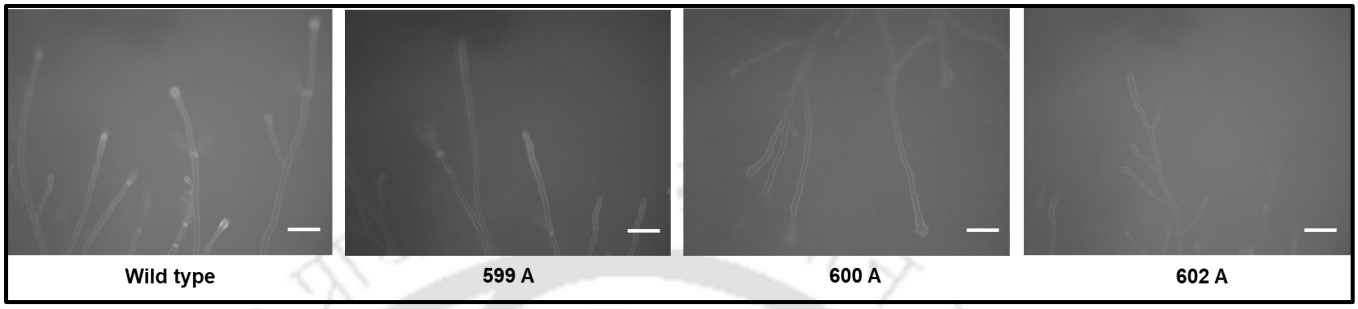

Fig. 3.3 Assay for the internal distribution of Ca^{2+}. (A) The chlortetracycline hydrochloride (CTC) has an excitation at 400 nm and emission at 470 nm and its structure is available at (https://www.sigmaaldrich.com/catalog/product/sigma/c4881?lang=en&region=IN.) (B) The hyphae of the *cnb-1*^{RIP} strains along with the wild type was grown in VG agar supplemented with CTC dissolved in 0.1% dimethyl sulphoxide (DMSO) and fluorescence was observed with the help of an inverted fluorescence microscope (AxioVert A1 Fl, Carl Zeiss, Germany) using DAPI filter setting the exposure time of 300-400 ms and using scale bar of 20 µm.

3.2.3 High concentration of sorbitol inhibits growth of the *cnb-1*^{RIP} mutants

High concentration of salts causes osmotic stress that inhibits fungal growth. In most eukaryotes, high concentrations of Ca^{2+}, sodium chloride, sorbitol cause osmotic stress. Therefore, I tested the sensitivity of the *cnb-1*^{RIP} mutants to increasing concentrations of NaCl and sorbitol (500 mM, 1000 mM, and 1500 mM) using methods described in osmotic stress assay in Chapter 2. Although, there is no significant difference among the mutants compared to wild type in growth rate with increasing concentration of NaCl but the growth rate of the *cnb-1*^{RIP} mutant strains 599A and 600A were reduced by ~20% and ~22% compared to the wild type in 1.5 M concentration of sorbitol. This result suggested that the amino acid residues

in the EF-hand domains as mentioned earlier in this Chapter (Table 3.1) are important for survival under osmotic stress conditions.

Table 3.3 Average colony growth rate of the wild type and *cnb-1*^{RIP} mutants 599 A, 600 A and 602 A strains at various concentrations of sorbitol.

Strains	**Relative average growth rate (%) at various concentrations of Sorbitol (M)**$^{+}$			
	0	0.5	1	1.5
Wild type	100 ± 0	80.8 ± 0.02	56.38 ± 0.01	38.68 ± 0.05
599 A	100 ± 0	70 ± 0.01	44.47 ± 0.04	32.33 ± 0.02
600 A	100 ± 0	68 ± 0.01	47.22 ± 0.09	30.44 ± 0.03
602 A	100 ± 0	79.33 ± 0.09	55.30 ± 0.03	37.80 ± 0.02

$^{+}$Data are expressed as the mean ± standard deviation for three independent experiments.

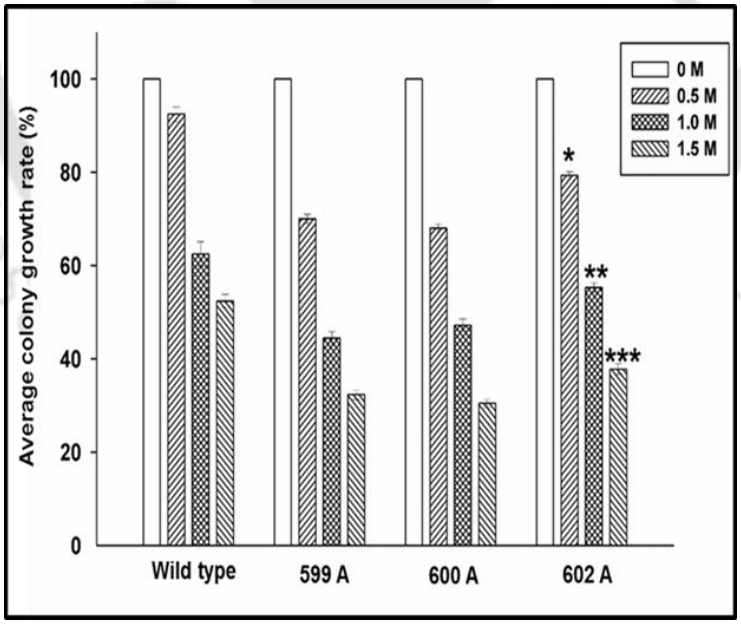

Fig 3.4 Osmotic stress assay for the *cnb-1*^{RIP} mutants in *N. crassa*. The *cnb-1*^{RIP} mutants were grown in the increasing concentrations of sorbitol (0.5 M, 1 M and 1.5 M) and their growth rate was compared to the wild type strain. Only two *cnb-1*^{RIP} mutants, 599A and 600A

showed reduced growth rate and shown in the figure. Error bars indicate the standard deviation calculated from three independent experiments (n = 3) with *P* values<0.05 (*), <0.01 (**), <0.001 (***) and otherwise non-significant (*ns*) as measured by one-way ANOVA test.

3.2.4 Calcineurin regulatory subunit is involved in heat shock stress tolerance

Since the response pathway to different stress signaling pathways are interrelated in *N. crassa* (Kapoor et al. 1990). I investigated the role of the *cnb-1*^{RIP} mutants in thermotolerance. Induced thermotolerance is the increased survival of cells pre-incubated at a sub lethal (heat shock) temperature after subsequent exposure to a lethal temperature, whereas uninduced thermotolerance is the survival of the cells after exposure to a lethal temperature, without pre-incubation at a heat shock temperature (Kapoor et al. 1990). Incubation of *N. crassa* cells to a sub lethal temperature before exposure to lethal temperature promotes synthesis of heat shock proteins, which protects the cells from lethal temperature (Kapoor et al. 1995; Yang and Borkovich, 1999). To determine thermotolerance of *cnb-1*^{RIP} mutants, I determined the viability of mutant colonies after exposure to a lethal temperature with or without pre-exposure to sub lethal temperature 44 °C. Percent survival was determined and number of viable colonies were counted. The *cnb-1*^{RIP} mutants 599 and 600 showed a significant decrease in survival percent compared to other *cnb-1*^{RIP} mutants and wild type under the induced condition. However, survival of the mutants was similar to the wild type under the uninduced condition. This result suggested a role for the calcineurin in survival at lethal temperature mediated by prior expression of heat shock proteins.

Table 3.4 Percent survival of the wild type, *cnb-1*^{RIP} mutants – 599 A, 600 A, and 602 A upon heat shock. Data are expressed as the mean ± standard deviation for three independent experiments.

Strains	Percent survival upon exposure to heat shock (52 ^{0}C) ± SD	
	Induced (44 °C)	Uninduced (30 °C)
Wild type	40.56 ± 0.90	1.40 ± 0.23
599 A	15.07 ± 1.08	0.90 ± 0.47
600 A	29.13 ± 1.02	0.83 ± 0.45
602 A	40.23 ± 0.55	1.40 ± 0.37

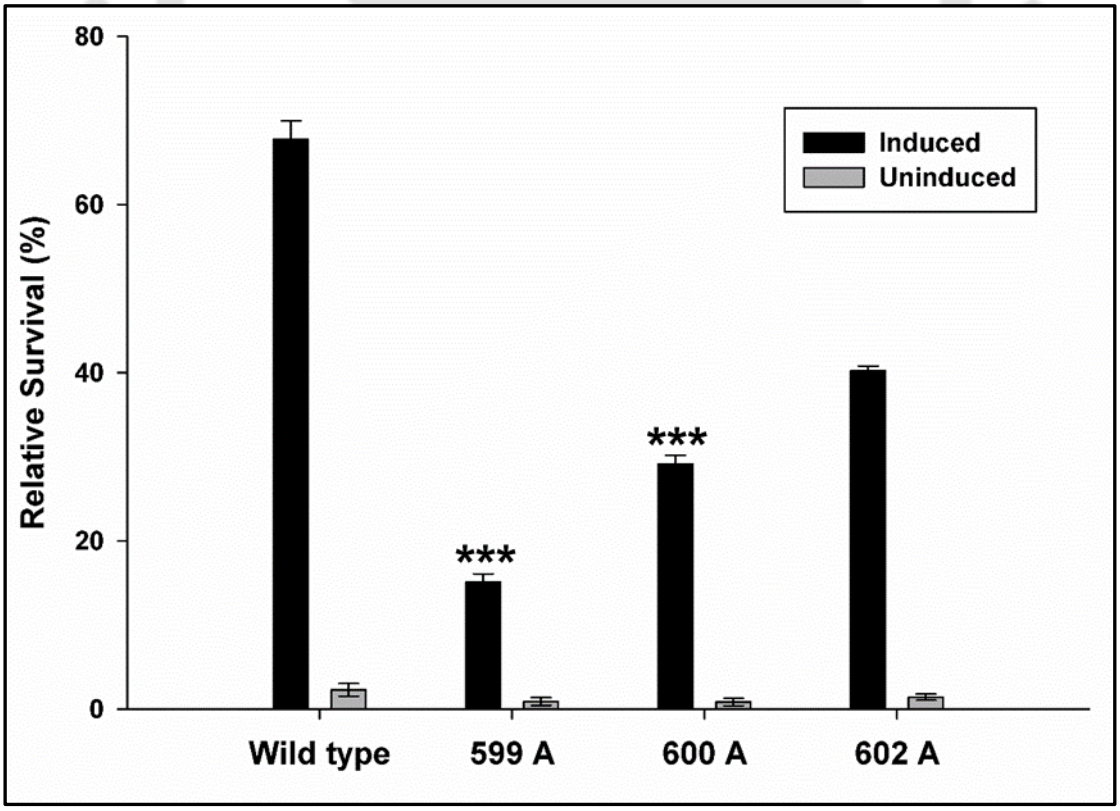

Fig. 3.5 Thermotolerance assay for the *cnb-1*^{RIP} mutants. Germlings of the wild type, *cnb-1*^{RIP} mutants 599, 600 and 602 were exposed to 52 °C lethal temperature with (induced) or

without (uninduced) pre-exposure to a sublethal heat shock temperature 44 °C and percent survival determined. The standard deviation was calculated from the data of three individual experiments (n = 3) with *P* values<0.05 (*), <0.01 (**), <0.001 (***) and otherwise non-significant (*ns*) as measured by one-way ANOVA test.

3.2.5 Carotenoid accumulation was not affected in the *N. crassa cnb-1*^{RIP} mutants

For carotenoid accumulation,~ 1X10^6 conidia/ml were inoculated in Petri plate containing 50 ml VG liquid media supplemented with calcium D-pantothenic acid and 0.2% tween 80 as a wetting agent to avoid conidiation (Zalokar, 1954). Cultures were initially incubated at 30 °C for 48 h and then exposed the individual sets to 30 °C, 22 °C, and 8 °C. Mycelia was filtered, lyophilized and pulverized into fine powder. 50 mg from each sample was taken into 1.5 ml eppendorf and 1 ml of acetone was added. It was kept on rotantiomixer for 5 h and centrifuged at 12,000 rpm for 10 min. Supernatant were collected in a new 1.5 ml Eppendorf tube, stored in -80 °C deep freezer for 2 h, and incubated at 30 °C for overnight keeping the lids of the tubes open. 1 ml of hexane was added to extracted carotenoid in the Eppendorf tube and the absorbance was taken at OD_{470} nm. Total carotenoid content (µg/g) was calculated by following formulae (Rodriguez-Amaya and Kimura, 2004):

Total carotenoid content (µg/g) = Absorbance X 1 ml (total volume) x10^4/Absorption coefficient (2500) x sample weight (g)

Cultures of *N. crassa* possess a characteristic orange pigment due to accumulation of xanthophyll neurosporoxanthin and variable amounts of carotenoid precursors in mycelia and conidia (Zalokar, 1954; Avalos et al. 2013). Carotenoid acts as a protective layer against various environmental stress conditions like UV-radiation. Carotenoid accumulation in the *cnb-1*^{RIP} mutants were compared with the wild type strains. Accumulation of carotenoid varies under various conditions, including change in temperature. In *N. crassa*, low temperature

causes and increase in carotenoid accumulation, the amount of carotenoid accumulation was increased 8 °C then at 30 °C (Harding et al. 1969; Estrada et al. 2008; Diaz-Sanchez et al. 2011; Barman and Tamuli, 2015). However, there was no significant difference in carotenoid accumulation among the *cnb-1*^{RIP} mutants compared to the wild type (Table 3.5; Fig. 3.6). Therefore, it signifies that *cnb-1* does not have a role in carotenoid accumulation in *N. crassa*.

Table 3.5 Carotenoid accumulation at three different temperatures (8 °C, 22 °C and 30 °C) in the *N. crassa* wild type (WT) and *cnb-1*^{RIP} mutant (599 A, 600 A and 602 A) strains

Strains	Carotenoids (µg /g dry weight)					
	8 °C		22 °C		30 °C	
	Light	Dark	Light	Dark	Light	Dark
WT	159.93 ±7.78	33.06 ±1.22	58.63 ±8.58	30.23 ±1.27	46.48 ±5.78	20.83 ±1.34
599 A	160.73 ±13.03	44.07 ±7.70 (***)	56.16 ±4.79	34.40 ±11.31 (*)	44.52 ±4.01	31.09 ±14.8 (***)
600 A	171.52 ±18.02 (***)	57.82 ±1.55 (*)	59.06 ±5.25	38.18 ±7.14 (***)	46.51 ±5.28	27.41 ±9.72 (*)
602 A	152.17 ±7.82 (*)	40.06 ±6.42	52.57 ±5.55	44.91 ±15.07	36.64 ±5.24	30.52 ±0.54 (***)

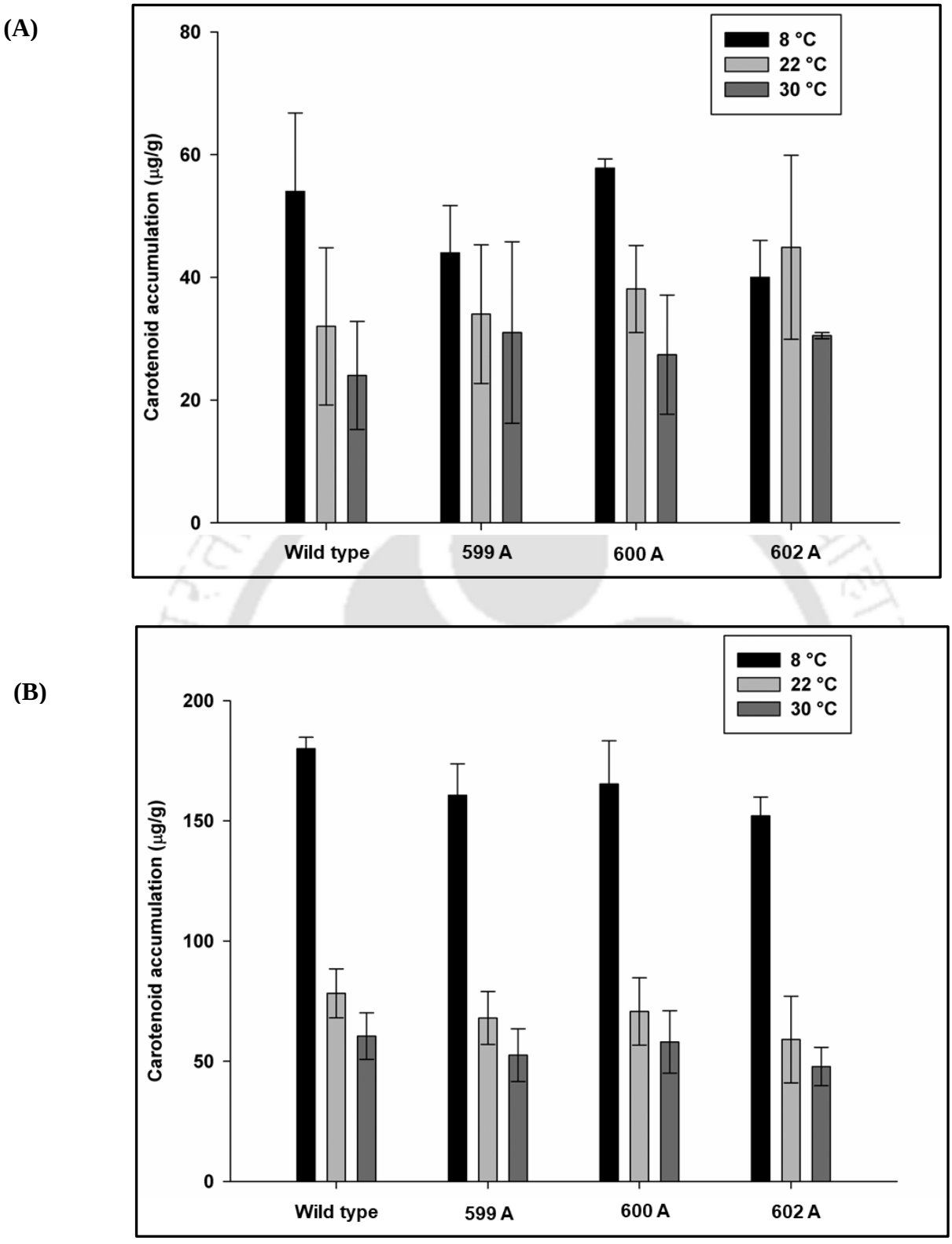

Fig. 3.6 Carotenoid accumulation in the *cnb-1*^{RIP} mutants. The *cnb-1*^{RIP} strains 599 A, 600 A, 602 A and wild type were grown on Petri dishes for 48 h in VG liquid medium at 30 °C in

dark and then the plates were incubated under continuous (A) dark or (B) light condition for 24 h. Error bars indicate standard deviation calculated from the data of three independent experiments (n = 3).

3.2.6 The UV sensitivity of the *cnb-1*^{RIP} mutants is like the wild type strain

Increased carotenoid accumulation renders antioxidant effect and protects the fungal cells and human tissues against the ultraviolet (UV) irradiation (Luque et al. 2012). I also tested the UV sensitivity of the *cnb-1*^{RIP} mutants. For UV sensitivity assay, strains were grown in flasks containing VG agar media at 30 °C for 3 days in dark followed by 3 days under constant light at room temperature. Strains were harvested, washed with sterile water and finally resuspended in sterile water. The conidial suspension of~ 1 X 10^6 conidial cells were taken and ~100 conidia cells were plated on Vogel's sorbose agar medium and irradiated with UV (253 nm wavelength) doses of 0 (control), 100, 200 and 300 Joule/m^2 in a UVC 500 cross linker (Hoefer, UK). The plates were then incubated at 30 °C in the dark for 24 h and the number of viable colonies on each plate was counted.

The survival percentage of the *cnb-1*^{RIP} mutants were similar to the wild type strains. The *upr-1* strain was one of the first isolated mutagen sensitive mutant in *N. crassa* whose homolog in budding yeast is *REV-3* and *upr-1* mainly have a role in the DNA translesion synthesis and DNA- damaged induced mutagenesis (Sakai et al. 2002). This *upr-1* was used as a reference mutant strain for the UV irradiation (Fig. 3.7). This suggests that the mutations in the different EF- hand domains of the *cnb-1*^{RIP} mutant isolates does not involve in the protective role.

Table.3.6 Relative UV sensitivity of the *cnb-1*^{RIP} mutants

Strains	% Survival of the *cnb-1*^{RIP} mutants under various dosages of UV irradiation (J m^{-2})			
	0	**100**	**200**	**300**
Wild Type	100.0 ± 0.0	65.0 ± 1.3	17.2 ± 0.7	1.9 ± 0.2
upr-1	100.0 ± 0.0	13.8 ± 0.8	0.8 ± 0.1	0.0 ± 0.0
599	100.0 ± 0.0	64.0 ± 1.2	14.8 ± 0.9	1.5 ± 0.3
600	100.0 ± 0.0	65.0 ± 0.6	13.7 ± 0.5	1.6 ± 0.2
602	100.0 ± 0.0	63.9 ± 1.6	13.5 ± 0.4	1.3 ± 0.1

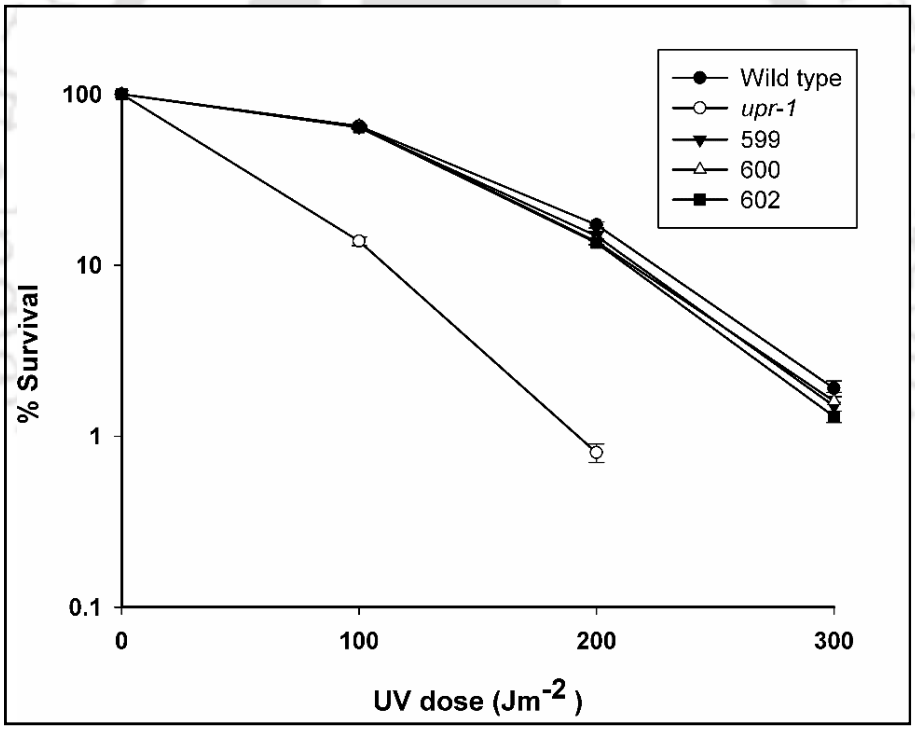

Fig. 3.7 UV sensitivity assay for the *cnb-1*^{RIP} mutants. Dose response curves of the Wild type, *upr-1*, and the *cnb-1*^{RIP} mutants 599, 600, and 602. Each data point represents the mean of at least three independent experiments (n = 3).

3.2.7 *Cnb-1* does not have a role in conidiation under submerged condition

In *N. crassa*, life cycle progression takes place by formation of both sexual and asexual spores. Asexual spores, also known as conidia, are of two types macroconidia and microconidia that are produced by the aerial hyphae formed in the air-water interface (Fig. 3.8; Kays et al. 2000). But, nitrogen or carbon limiting conditions and other stress factors leads to conidiation is submerged condition in *N. crassa* (Cortat and Turian, 1974; Guignard et al. 1974). The *cnb-1*^{RIP} mutants displayed reduced length of aerial hyphae compared to the wild type strains (Tamuli et al. 2016). Therefore, to test if, *cnb-1* has a role in submerged conidiation, ~1 X 10^6 cells/ml were inoculated in VG liquid and VG liquid supplemented with 2% peptone and incubated at 30 °C for 16 h in dark with shaking at 180 rpm. An aliquot of ~10 µl of the culture was taken from each conical flask and observed under a microscope (Trinocular inverted microscope; AxioVert AI FL, Carl Zeiss) at 20X magnification. Both the wild type and *cnb-1*^{RIP} mutant strains have shown hyphal growth in submerged condition, therefore mutations in *cnb-1* did not impact conidiation under the submerged condition (Fig. 3.9).

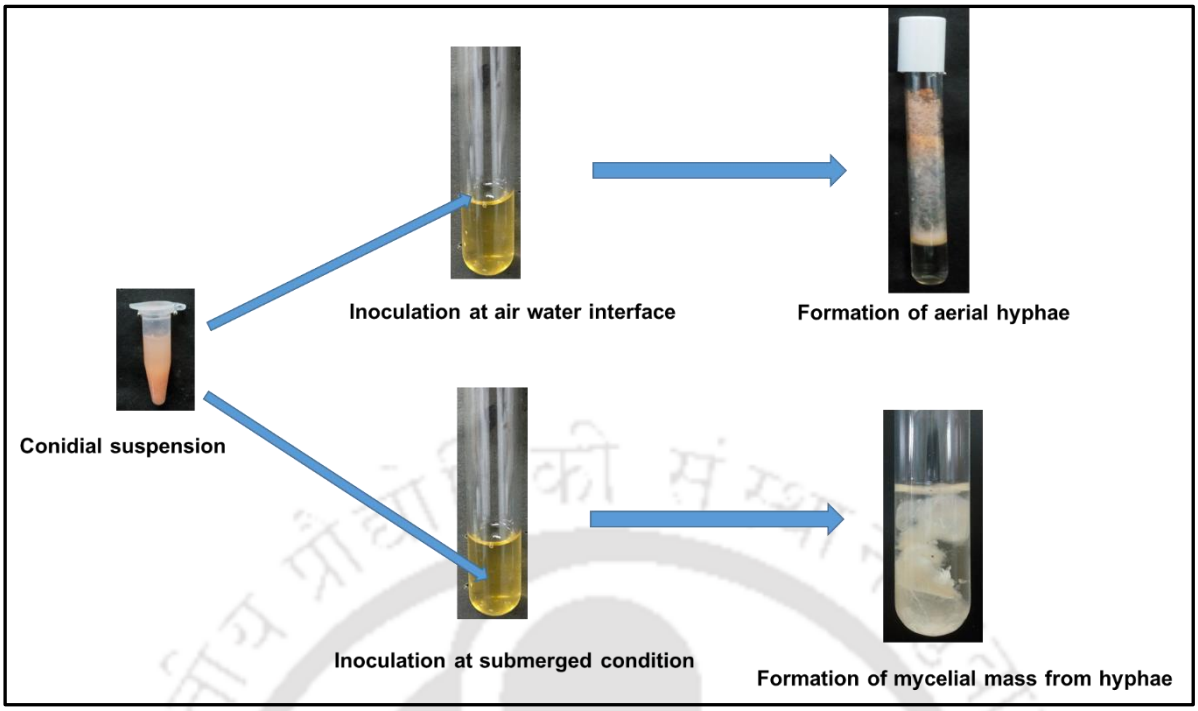

Fig. 3.8 Pictorial representation of difference between conidiation in aerial hyphae and submerged conidiation. For aerial hyphae, the conidial suspension is inoculated at the air-water interface so that there is formation of aerial hyphae. For submerged conidiation, conidia are inoculated in submerged condition that affect conidiation and form a mycelial mass.

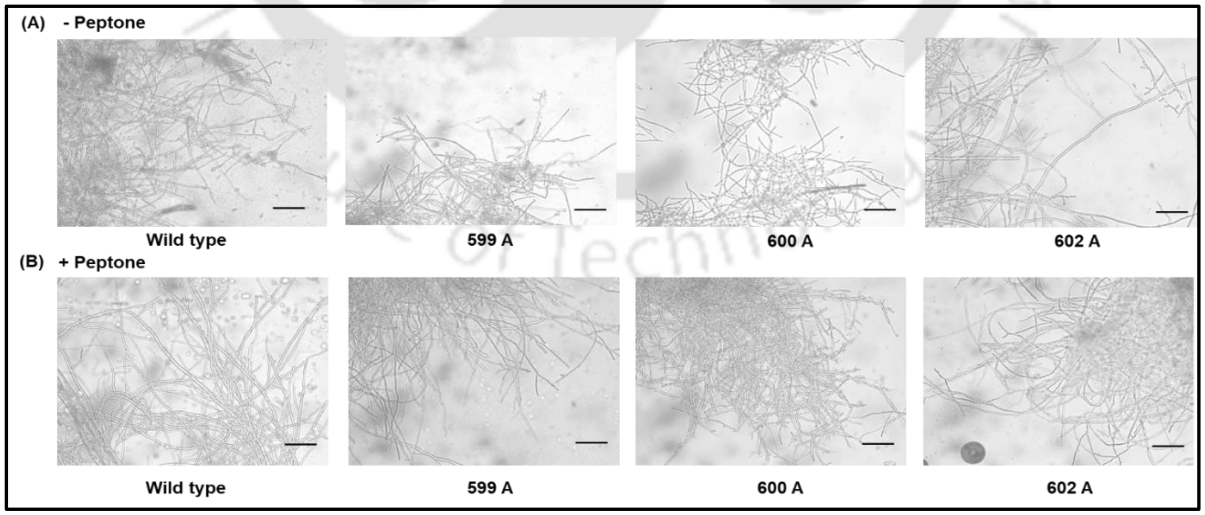

Fig 3.9 Submerged culture conidiation for the *cnb-1*^{RIP} mutants. The *N. crassa* cultures were inoculated at a concentration of ~1 X 10^{6} cells/ml and incubated for 16 h in (A) liquid

VG and (B) VG supplemented with 2% peptone. The cultures were incubated at 30 °C in dark with shaking at 180 rpm for 16 h. Wild type was used as a control strain. Scale used 10 µm.

3.2.8 Generation of Δ*trm-9*Δ*cax* strain

To generate Δ*trm-9*Δ*cax* double mutant, individual single mutants, generated during the *N. crassa* genome project, were crossed (Fig. 3.10). Ascospores obtained from the cross were harvested after 21 days and germination was performed at a temperature of 60 °C for 45 min on Vogel's sorbose agar media. After about 12-14 h, germinated progenies were transferred to tubes containing minimal media and incubated at 30 °C for 72 h. The progenies were screened for resistance to the hygromycin. The DNA from the Hyg^R progenies was isolated and presence of the Δ*trm-9* and Δ*cax* alleles were confirmed by PCR analysis using the NCU04898-5F and Cax AR-Fw HI forward primer and the common 5HPHR reverse primer. amplification to observe amplification of ~1.2 kb and ~1.0 kb when resolved in a 0.8 % agarose gel (Fig. 3.11).

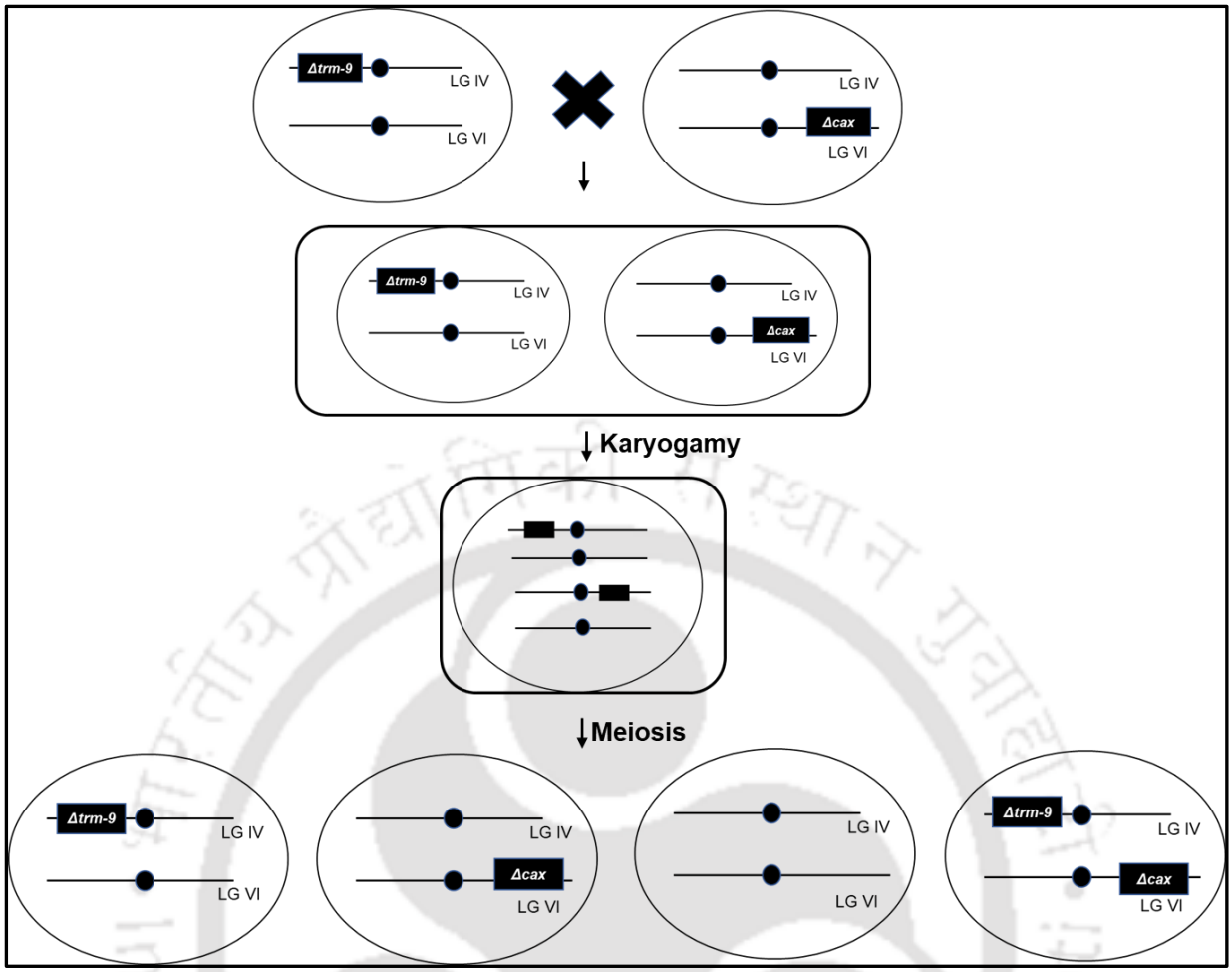

Fig 3.10 Strain generation for Δ*trm-9*Δ*cax* double mutant. The opposite mating types of the Δ*trm-9* and Δ*cax* single mutants were crossed; during the sexual cycle, fertilization followed by karyogamy and meiosis would generate progenies of four different types 1) progeny with Δ*trm-9* allele, 2) progeny with Δ*cax* allele 3) wild type progeny, and 4) the Δ*trm-9*Δ*cax* double mutant.

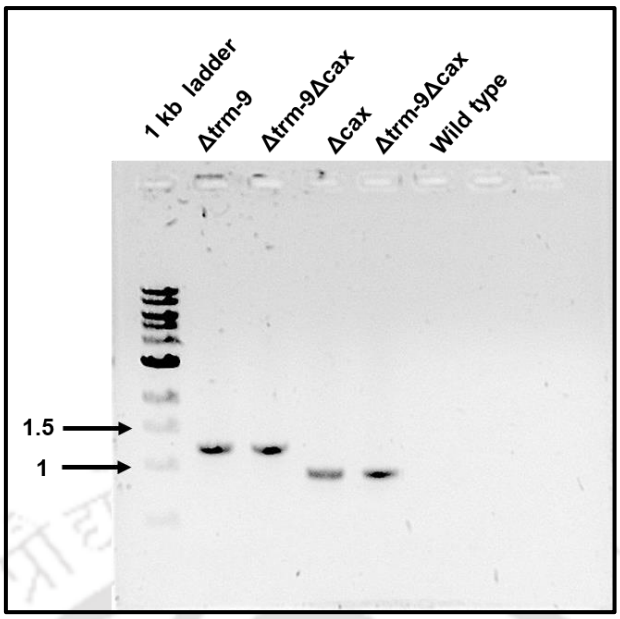

Fig. 3.11 PCR confirmation of the Δ*trm-9*Δ*cax* double mutants. The Δ*trm-9*Δ*cax* double mutants were verified by using forward primers NCU04898-5F and Cax AR-Fw HI, and common 5HPHR reverse primer (Deka et al. 2011). Amplification of ~1.2 kb and ~ 1.0 kb confirmed the presence of both Δ*trm-9* and Δ*cax* knockout allele in the Δ*trm-9*Δ*cax* double mutant. The wild type strain was used as a control, and the PCR products were resolved using a 0.8 % agarose gel along with 1 kb (NEB) ladder as reference.

3.2.9 Ca^{2+} ATPases Δ*cax*, Δ*trm-9* and Δ*trm-9*Δ*cax* impacts conidiation in submerged cultures

The *N. crassa* Ca^{2+} ATPases TRM-9 and Ca^{2+} exchanger CAX have previously shown to have a role in various developmental processes, including apical growth, development of aerial hyphae and conidia, carotenoid accumulation, and survival under stress conditions such as heat shock, Ca^{2+} stress, and ultraviolet (UV) irradiation (Laxmi and Tamuli, 2015). I tested if, *trm-9* and *cax* have a role in the conidial germination under submerged condition. The Ca^{2+}-cation ATPase mutants *cax*, *trm-9* and their double mutant were grown in VG agar, and ~1 X 10^6 conidia/ml were inoculated in VG liquid and VG liquid supplemented with 2% peptone for 16 h in dark with shaking at 180 rpm. Then about 10 µl of the culture was taken from each conical

flask and observed under a microscope at 20X magnification (Trinocular inverted microscope; Axiovert AIFL, Carl Zeiss). Wild-type strain showed hyphal growth in submerged condition, whereas the Δ*cax*, Δ*trm-9* and Δ*trm-9*Δ*cax* mutants showed submerged conidiation (Fig. 3.12). Moreover, supplementation of nutrient rich peptone shown to suppress conidiation in submerged cultures, however, the Δ*cax*, Δ*trm-9* and Δ*trm-9*Δ*cax* mutants showed submerged conidiation even in the medium supplemented with peptone. Conidiation in submerged cultures is known to correlate with the inappropriate expression of conidiation specific gene *con-10* (Madi et al. 1997; Kays et al. 2000).

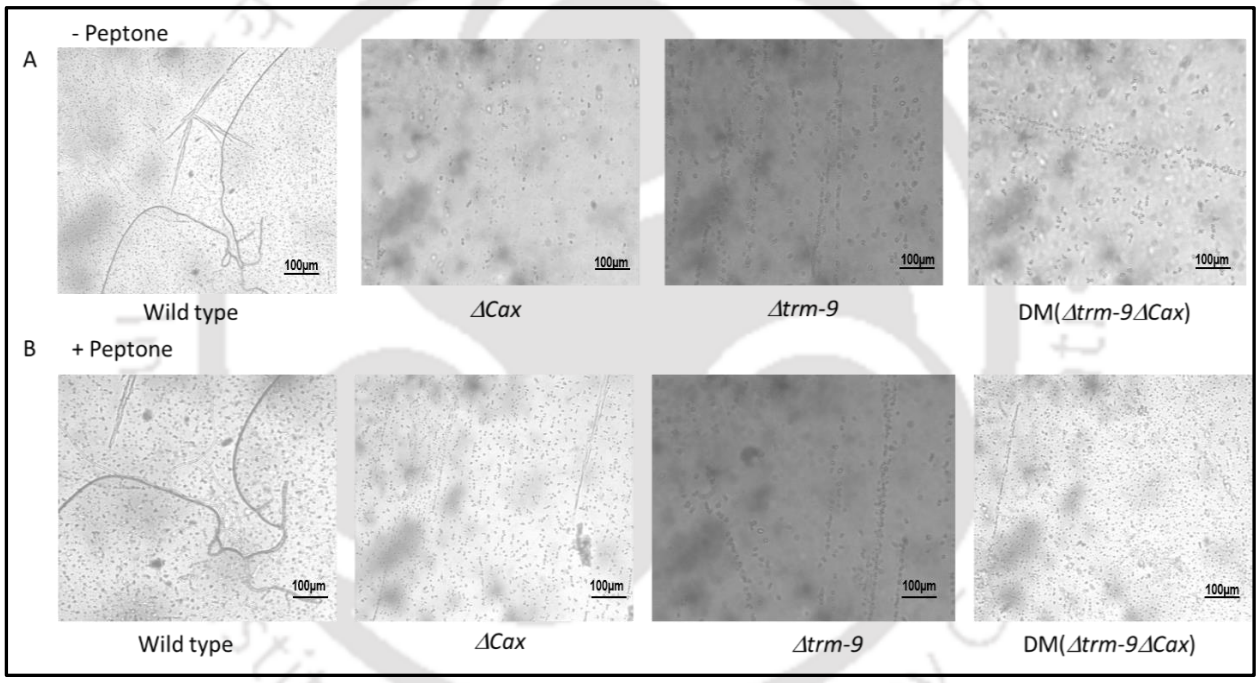

Fig 3.12 Submerged culture conidiation for the Δ*cax*, Δ*trm-9* and Δ*trm-9*Δ*cax* mutants.

The *N. crassa* cultures were inoculated at a concertation of ~1 X 10^6 conidia/ml and incubated for 16 h in (A) liquid VG, and (B) VG supplemented with 2% peptone. The cultures were incubated at 30 °C in dark under shaking at 180 rpm for 16 h. Wild type strain used as control. Scale used 10 µm.

3.2.10 Prediction of CNB-1 interacting partners using STRING analysis

An important search tool used to predict the interaction between proteins/genes is known as STRING (Szlarczyk et al. 2015). It is a biological database comprising of both known and predicted protein-protein interactions inclusive of both direct (physical) and indirect (functional) link. The STRING repository covers about 9,643,763 proteins derived from 2,031 organisms (Szlarczyk et al. 2015). This repository provides important information regarding the interactions on the basis of experimental evidences as well as computational predictions and high throughput data analysis. The predicted interactions provide understanding of the cellular processes controlled by the network of different proteins, and how the interactions among the different proteins impacts the structure, and function of proteins. I predicted interacting partners of the CNB-1 protein that identified Ca^{2+} ATPases such as NCA-2 and NCA-3, which are localized to the plasma membrane and play a role in the sequestering of the excess Ca^{2+} ions into the vacuoles (Bowman et al. 2011). Earlier phenotypic studies revealed that *cnb-1* has a role in the Ca^{2+} stress response (Kumar et al. 2019). Therefore, I investigated if, NCA-2 is linked to the CNB-1 mediated molecular pathway for Ca^{2+} tolerance. Previous work in our laboratory identified cell functions of CNA-1 and CNB-1 using a novel expression system containing a copper relatable *tcu-1* promoter, and demonstrated a direct interaction between CNA-1 and CNB-1 (Tamuli et al. 2016). Again, activation of calcineurin complex causes dephosphorylation of its one of the downstream targets CRZ-1 for its subsequent nuclear localization and activation of target genes (Kumar et al. 2019). The STRING generated network of interacting partners (Fig. 3.13; Table 3.7) suggested interactions of CNB-1 with CNA-1, CRZ-1, NCA-2, and other proteins.

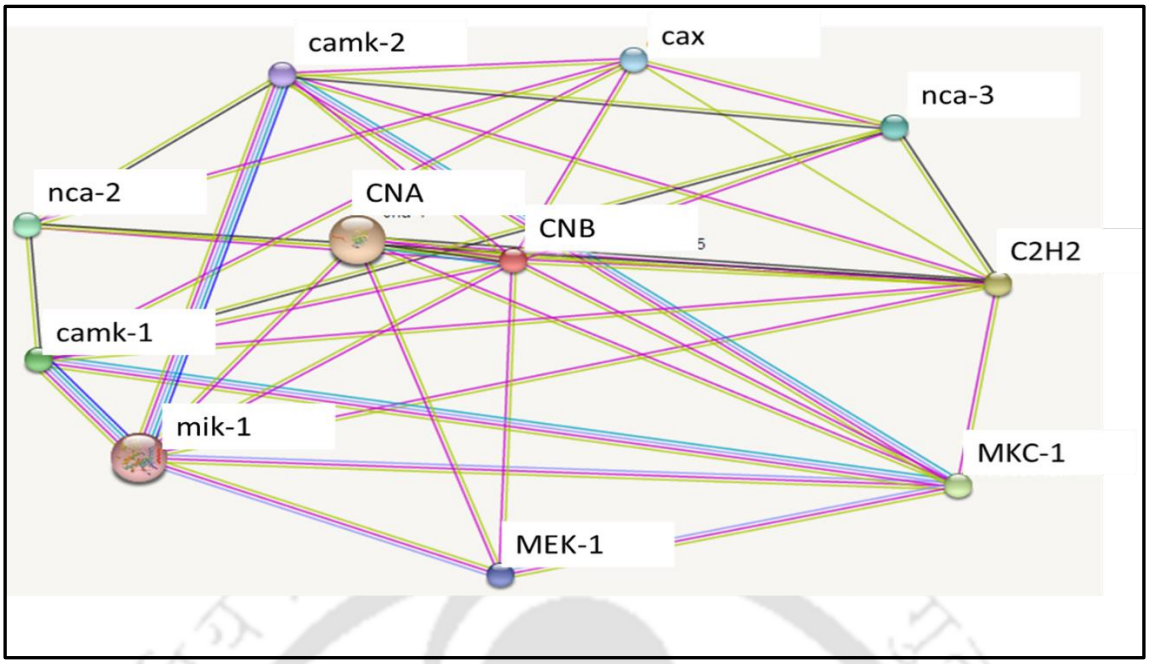

Fig 3.13 Schematic representation of network of interacting partners of CNB-1 using STRING analysis in *N. crassa*. The edges represent the specific protein-protein that corresponds to functionality, which might not be a direct (physical) interaction. The smaller nodes indicate those proteins having unknown 3D structure, whereas the larger nodes represent the proteins with solved 3D structure. The colored nodes depict the query proteins and the first shell of interacting partners, while the white nodes represent the second shell of interactors. In the above network, the interaction of CNB-1 with its putative interacting partners such as CNA-1 (calcineurin catalytic subunit), NCA-2 (Ca^{2+} P-type ATPase 2), NCA-3 (Ca^{2+} P-type ATPase 3), CAX (Calcium exchanger), Camk-2 (Ca^{2+}/calmodulin dependent kinase-2), Camk-1 (Ca^{2+}/calmodulin dependent kinase-1), Crz-1 (C_2H_2 type zinc finger domain containing transcription factor), mkc-1(Mitogen activated protein kinase -1) and mik-1 (Mitogen activated protein kinase kinase kinase (MEK kinase -1) have been predicted.

Table 3.7 Predicted interacting proteins of CNB-1

Gene Name	NCU No.	Protein
cna-1	NCU03804	Serine/ threonine protein phosphatase 2B catalytic subunit
nca-2	NCU04736	Ca^{2+} P-type ATPase 2
nca-3	NCU05154	Ca^{2+} P-type ATPase 3
cax	NCU07075	Calcium exchanger
camk-2	NCU02283	Ca^{2+}/calmodulin dependent kinase-2
camk-1	NCU09123	Ca^{2+}/calmodulin dependent kinase-1
crz-1	NCU07952	C_2H_2 type zinc finger domain containing transcription factor
mkc-1	NCU09842	Mitogen activated protein kinase -1
mik-1	NCU02234	Mitogen activated protein kinase kinase kinase (MEK kinase -1)

3.2.11 Generation of *cnb-1*^{RIP};*ras-1*^{bd} mutants

To generate Δ*cnb-1; cnb-1*^{RIP}*; ras-1*^{bd} *(599-1),* Δ*cnb-1; cnb-1*^{RIP}*; ras-1*^{bd} *(600-8)* and Δ*cnb-1; cnb-1*^{RIP}*; ras-1*^{bd} *(602-82)* double mutants, each of the three *cnb-1*^{RIP} strains were crossed with *ras-1*^{bd} of opposite mating type (Fig. 3.14) and ascospores from these crosses were harvested after 21 days, and germinated on Vogel's sorbose agar medium by heat shock at 60 °C for 45 min. Progenies were then transferred to VG agar medium and incubated for two days at 30 °C and one day under light. The f_1 progenies were first screened for pantothenate auxotrophy and then for the resistance to hygromycin B (Hyg^R). The Hyg^R strains were checked for the presence of the *ras-1*^{bd} mutation by screening them on race tube for the *ras-1*^{bd} allele. The *ras-1*^{bd} mutation causes circadian-regulated conidiation in race tube despite the accumulation of CO_2 (Sargent and Kaltenborn, 1972; Belden et al. 2007). DNA from the *cnb-1*^{RIP} mutants with *ras-1*^{bd} mutations showing distinct conidial band was isolated, and then PCR verified for

both the ectopic and endogenous copy using $P_{tcu\text{-}1}$-CAM-RIP- FP and GFP-Rv primers, whereas the endogenous copy was confirmed using the HI-CNBFW-AR Fw forward and 5HPHR reverse primers. The size of the ectopic copy was 1.5 kb (Fig. 3.15 A), while the size of the endogenous copy was 1.2 kb (Fig. 3.15 B); PCR amplification of these copies confirmed the integration of the Δ*pan-2::*$P_{tcu\text{-}1}$*::cnb-1*^{RIP}*::5xGly::V5::gfp* allele in the *pan-2* locus, whereas the Δ*cnb-1::hph* copy was present in the endogenous locus.

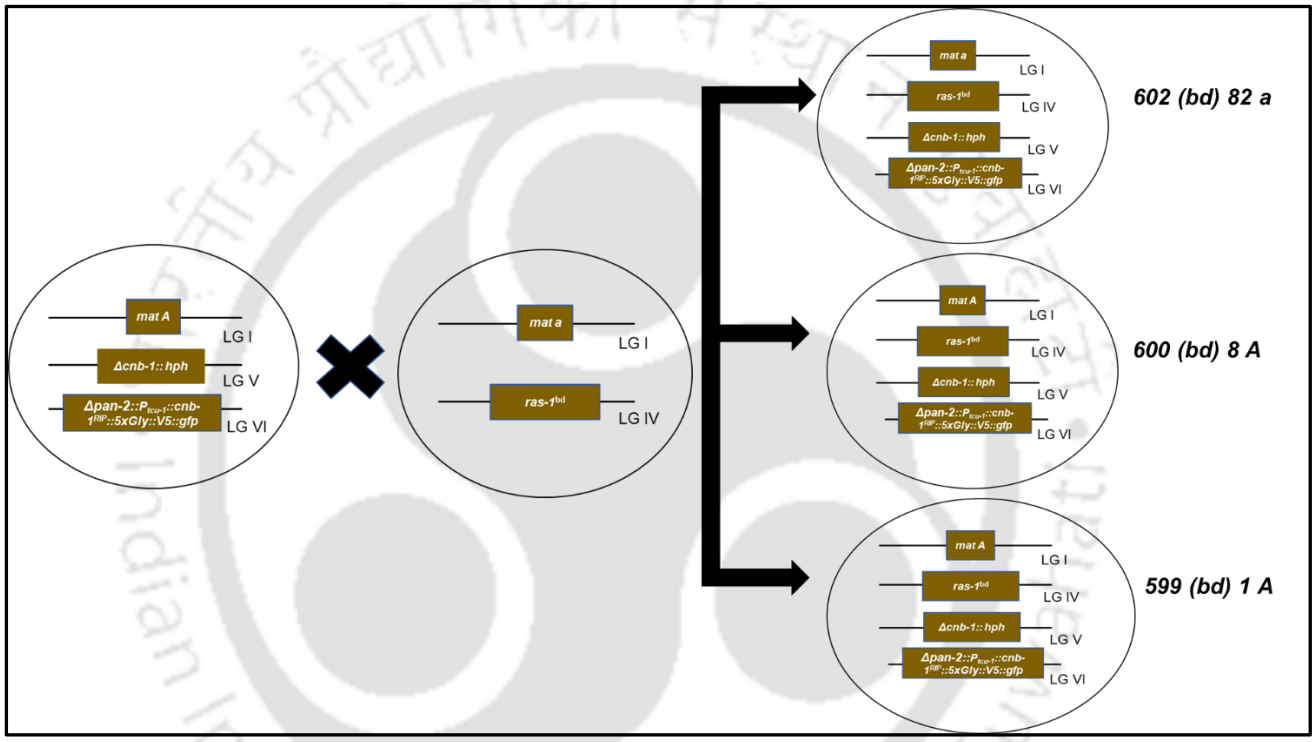

Fig 3.14 Generation of the *cnb-1*^{RIP} strains with *ras-1*^{bd} mutations. The double mutant strains of *cnb-1*^{RIP} with *ras-1*^{bd} mutations were generated by crossing of the opposite mating types and further screened for *pan-2* auxotroph and resistance to hygromycin.

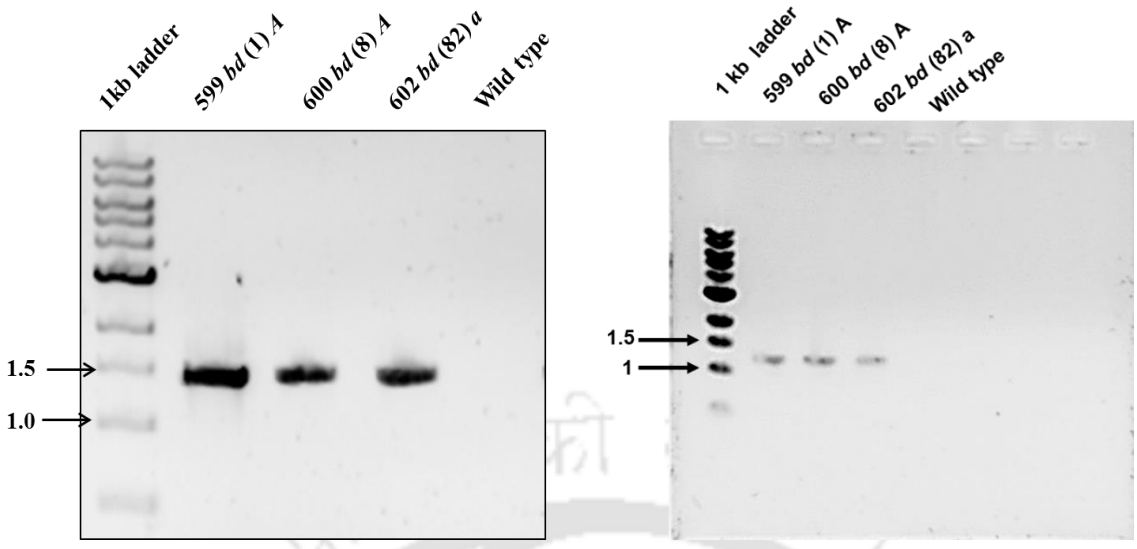

(A) **(B)**

Fig 3.15 PCR amplification to confirm the *cnb-1*^{RIP} mutants with *ras-1*^{bd} mutations.

(A) Ectopic copy of *cnb-1* was amplified (1.5 kb) and resolved in 0.8% agarose gel alongwith 1 kb DNA ladder (NEB). (B) Endogenous copy of *cnb-1* was amplified (1.2 kb) and resolved in 0.8% agarose gel.

3.2.12 The mutations in *cnb-1* affected the circadian clock in *N. crassa*

Circadian rhythms are universal biological oscillations with an approximately 24 h period, which controls diverse phenomena including cell division, homeostasis, immunity, physiology, and sleep-wake cycle in eukaryotes, including fungi and mammals (Mehra et al. 2009). Circadian clock shows three characteristics, (1) a regular period of about 24 h, (2) sensitivity to light, reflecting the ability to adjust its phase to the phase of the environment, (3) and the relative insensitivity of its period to the growth temperature, which is known as temperature compensation (Mattern et al. 1982). In *N. crassa*, Ca^{2+} signaling genes play an important role in maintaining Ca^{2+} homeostasis, asexual and sexual development (Tamuli et al. 2011; Kumar and Tamuli, 2014; Barman and Tamuli, 2017). To check the role of *cnb-1* in the regulation of *N. crassa* circadian rhythm, I crossed the *cnb-1*^{RIP} mutants with the *ras-1*^{bd} strain. The *cnb-1*^{RIP};*ras-1*^{bd} double mutants as mentioned in Chapter 2 (Table 2.1) were

used for circadian regulated conidiation assay (Fig. 3.16) in three different temperatures (20 ºC, 25 ºC, and 30 ºC). The period lengths of all the strains was found to be decreased with increasing temperatures compared to the control *ras-1*^{bd} strain (Table 3.8). Circadian clock shows insensitivity of its period length in response to variation in the growth temperature, a phenomenon known as temperature compensation (Q_{10}). On calculating the Q_{10} values (Table 3.9), it was revealed that these *cnb-1*^{RIP};*ras-1*^{bd} double mutants were able to perform temperature compensation across different range of temperature. The Q_{10} of circadian rhythms normally range between 0.8 and 1.2 (Mattern et al. 1982).

Table 3.8 Period length of the *N. crassa cnb-1*^{RIP} mutants at 20 ºC, 25 ºC and 30 ºC

Sl. No.	Strains	Period lengths ± SD (h)		
		20 °C	**25 °C**	**30 °C**
1	*ras-1*^{bd}	23.5 ± 0.1	22.0 ± 0.2	20.4 ± 0.1
2	599 *; ras-1*^{bd} (1)	21.8 ± 0.3	20.9 ± 0.4 (*)	19.6 ± 0.6 (***)
3	600 *; ras-1*^{bd} (8)	21.5 ± 0.2 (***)	20.5 ± 0.5 (*)	19.5 ± 0.1 (***)
4	602 *; ras-1*^{bd} (82)	21.7 ± 0.5(***)	20.4 ± 0.2 (**)	19.3± 0.1 (***)

Results are shown as mean ± standard deviation (SD) for three independent experiments (n = 3) with *P* values < 0.05(*), <0.01 (**), and <0.001 (***) compared with the *ras-1*^{bd} strain as measured by one-way ANOVA test.

Table 3.9 Q_{10} values of the *cnb-1*^{RIP} mutants between 20 °C and 30 °C

Sl. No.	Strains	Q_{10} values T1 = 20 °C, T2 = 30 °C
1	*ras-1*^{bd}	0.9
2	599 ; *ras-1*^{bd} (1)	0.9
3	600 ; *ras-1*^{bd} (8)	0.9
4	602 ; *ras-1*^{bd} (82)	0.9

Calculation of Q_{10} (Waterhouse et al. 2005)

$$Q_{10} = \left(\frac{R_2}{R_1}\right)^{10/(T_2-T_1)}$$

R_1 and R_2 are period lengths at T_1 and T_2 temperatures, respectively.

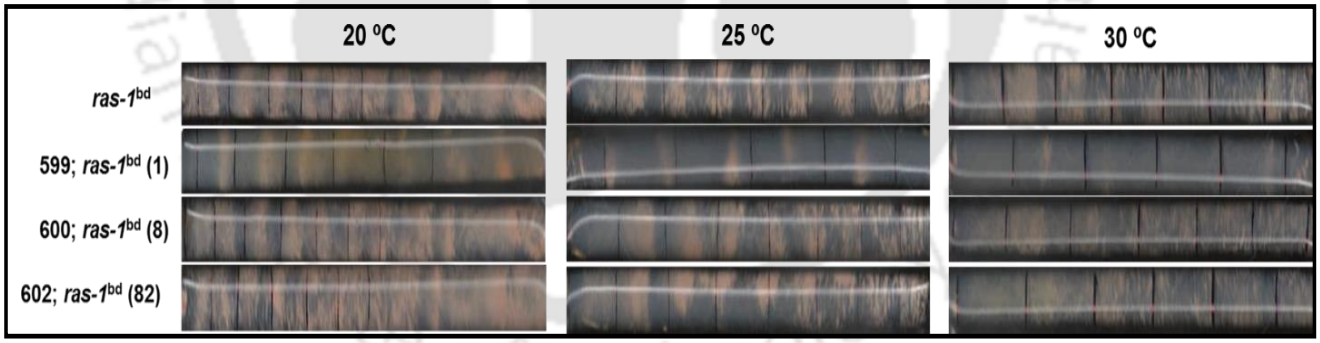

Figure 3.16 Circadian regulated conidiation in *cnb-1*^{RIP} mutants. The *N. crassa* strains showing distinct conidial bands at a regular interval in the race tube like the control *ras-1*^{bd} strain. The banding pattern was observed at three different temperatures 20, 25, and 30 °C. The black mark indicates the growth front. Conidial bands were measured till 144 hours for all the strains.

3.3 Discussion

In this Chapter, I described phenotypic effect of various mutations in the different EF-hand domains of the *cnb-1* (Table. 3.1) generated using RIP (Tamuli et al. 2016). This study revealed that CNB-1 plays an important role in the development and tolerance to stress conditions in *N. crassa*. Previous work also identified that *cnb-1* has a role in the vegetative growth in *N. crassa* (Kothe and Free, 1998). In addition, work in our laboratory showed cnb-*1* role in hyphal growth and fertility (Tamuli et al. 2016). CNB-1 possesses four EF-hand domains for binding to Ca^{2+}, and act as a Ca^{2+} sensor similar to CaM (Rusnak and Mertz 2000; Klee et al. 1998). I also studied the growth of the *cnb-1*^{RIP} mutants in media supplemented with increasing concentrations of Ca^{2+} (Fig. 3.1). Ca^{2+} is also required for hyphal extension (Jackson and Heath, 1993), therefore, I performed microscopy studies to visualize the Ca^{2+} concentration in growing hyphae in the *cnb-1* mutants. The microscopy studies revealed a defect in the deposition of Ca^{2+} in the hyphal tips (Fig. 3.3 B) and also defective septation of the hyphae (Fig. 3.2 B). In *N. crassa*, growth occurs by means of apical extension of tubular cells known as hyphae (Alvarez et al. 2014). Hyphal septation a unique feature (Molloy, 2007) in *N. crassa* has important implications such as – provides structural integrity to the hyphae, and helps in the cell differentiation (Bracker, 1967). Furthermore, osmotic stress using different concentrations of sorbitol showed reduced growth in the *cnb-1*^{RIP} mutants (Fig. 3.4). Another characteristic features of *N. crassa* is its characteristic orange pigment as a result of the carotenoid content (Zalokar, 1954). The carotenoid pigment plays an important role in the protection against ultraviolet (UV) stress (Luque et al. 2012). However, the *cnb-1*^{RIP} mutants did not affect the carotenoid accumulation (Fig. 3.6), or the survival under the UV stress conditions (Fig. 3.7). In one of the pathogenic fungi *Cryptococcus neoformans*, calcineurin has a role in growth in the increasing temperature condition (Odom et al. 1997; Cruz et al. 2001). I also studied for the *cnb-1*^{RIP} mutants for thermotolerance, which showed reduced viability for the *cnb-1*^{RIP}

mutants in high temperature (Fig. 3.5). *N. crassa* produces both asexual and sexual spores, the asexual spores also known as conidia formed in the tip of the aerial hyphae (Kays et al. 2000). Previous work in our laboratory showed reduced aerial hyphae under both BCS induced and $CuSO_4$ suppressing conditions in the *cnb-1*^{RIP} mutants (Tamuli et al. 2016). I studied the submerged conidiation in the *cnb-1*^{RIP} mutants that produced similar kind to hyphal network under both nitrogen limiting and nitrogen rich media when supplemented with peptone (Fig. 3.9). Ca^{2+}, an important ubiquitous secondary messenger, also plays an important role in regulating circadian rhythm (O'Neill and Reddy, 2012). The *N. crassa* circadian rhythm is important for its vegetative spore formation i.e. conidia (Sadakane and Nakashima, 1996; Suzuki et al. 1996). I also studied if, calcineurin has a role in the regulation of the circadian clock in *N. crassa*. I investigated the role of *cnb-1* in circadian rhythm at three different temperature conditions. Temperature is one of the abiotic factors, which impact the rhythm (Buhr et al. 2010). I observed a shift in the period length across all the *cnb-1*^{RIP} mutants in comparison to the *ras-1*^{bd} control strain (Table. 3.8; Fig. 3.16). However, the Q_{10} value of the *cnb-1*^{RIP} mutants was 0.9 (Table. 3.9), which falls in the normal temperature compensation range (0.8-1.2) for the circadian rhythm, suggesting a temperature compensation in the *cnb-1*^{RIP} mutants (Saunders, 1977; Mattern et al. 1982).

A part of the results from this chapter have been published in Archives of Microbiology (Kumar et al. 2019), and also presented as posters in (i) XL All India Cell Biology Conference & International Symposium on Functional Genomics and Epigenomics, Jiwaji University, Gwalior, November, 2016 (ii) National Conference on Fungal Biology: Recent Trends and Future Prospects and 44th Annual meeting of the Mycological Society of India (MSI), University of Jammu, Jammu, November, 2017.

In the next Chapter, I discuss genetic interaction and the molecular players of *cnb-1* pathway. This will have a better understanding of cross talk between the molecular pathways linked to the calcineurin stress response pathway.

Chapter 4

Understanding the *cnb-1* transcriptional regulation and mechanism of action

4.1 Introduction

Calcineurin is a phosphatase involved in diverse cell functions, including growth, Ca^{2+} stress, osmotic stress, circadian clock regulation, survival in higher temperature and virulence in different filamentous fungi including *Neurospora crassa*. Calcineurin, dephosphorylates one of its downstream target calcineurin responsive zinc finger-1 (CRZ-1) protein that transcriptionally regulate many stress response genes in filamentous fungi (Steinbach et al. 2007; Juvvadi et al. 2014). In *Cryptococcus neoformans*, CRZ-1 has been essential gene for the survival at 37 °C in the host and also for virulence. Calcineurin have also shown its role in Ca^{2+} homeostasis (Mendoza et al. 1994; Mendoza et al. 1996; Marquina et al. 2012), thermotolerance (Liu et al. 1991) in *Saccharomyces cerevisiae* whereas hyphal growth, dimorphic switch (Sanglard et al. 2003), virulence (Blankenship et al. 2003; Bader et al. 2006) in *Candida albicans*. In *Aspergillus fumgiatus* calcineurin important for cation homeostasis (Cramer et al. 2008; Dinamarco et al. 2012), resistance to echinocandins (Lamoth et al. 2013a). Several important molecular players namely- *frequency* (*frq*) and the *white collar* genes (*wc-1* and *wc-2*) have been identified regulating the circadian clock of *N. crassa* (Dunlap and Loros, 2004; Liu and Bell-Pedersen, 2006) and as discussed in chapter 3 *cnb-1* have a role in circadian clock regulation but whether *frq* and *wcc* are the molecular players involved in the regulation of clock in *cnb-1* is still not known. Also, as discussed in Chapter 3 *cnb-1* have a role in Ca^{2+} stress, thermotolerance (Kumar et al. 2019) and earlier work from our laboratory have indicated role of CRZ-1 in the upregulation of *ncs-1* during Ca^{2+} stress and also in that signaling pathway there was possibility that CRZ-1 can also upregulate *nca-2* (Gohain and Tamuli, 2019), a Ca^{2+} ATPase transporter responsible for sequestering Ca^{2+} into the vacuoles (Bowman et al. 2011) during Ca^{2+} stress to maintain Ca^{2+} homeostasis. But still information regarding the exact molecular players involved with *cnb-1* in *N. crassa* for the different stress response phenotypes as described in Chapter 3 earlier has been limited. Therefore, in this Chapter I tried to identify

the probable molecular targets and weave the calcineurin stress signaling pathway in accordance with the molecular players to find the answer how calcineurin alongwith its downstream target CRZ-1 activates the important stress response genes and cross talk with their respective signaling cascade in response to different abiotic stress conditions.

4.2 Results

4.2.1 The CNB-1 plays an important role in the expression of the *frq1* and *wc1* genes that are critical for the circadian clock in *N. crassa*

The core components of the *N. crassa* circadian clock have been identified; however, the role of Ca^{2+} signaling genes for the regulation of the circadian rhythm has remained largely unknown. Therefore, I investigated function of the Ca^{2+} signaling gene *cnb-1* in circadian clock under different temperature conditions. The *cnb-1*^{RIP} mutants showed reduced period length compared to the control *ras-1*^{bd} strain under different temperatures (Table 3.8, Chapter 3). Additionally, expressions of one of the key clock regulators *frq* gene was reduced in the *cnb-1*^{RIP} mutants displaying reduced period length (Fig. 4.1).

In Chapter 3, I discussed how the period lengths in the *N. crassa cnb-1*^{RIP} strain shifts with variation in temperature compared to those of the *ras-1*^{bd} control (Table 3.8; Fig 3.16). I determined the period length at three different temperatures (20 °C, 25 °C and 30 °C) to test whether the period length shows temperature compensation over a physiological range of temperatures. The period length of the clock in the *ras-1*^{bd} control strain was greater at 20 °C as compared to that at 25 °C and 30 °C. The *cnb-1*^{RIP} mutants (Strain 599, 600, and 602) showed exhibited shorter periods shortening at all the temperatures, 20 °C, 25 °C, and 30 °C. The *frq*, *wc-1*, and *wc-2* genes are core molecular regulators of the *N. crassa* circadian clock (Dunlap et al. 2006; Liu and Bell-Pedersen 2006). The alteration in the period length may be associated with the transcriptional regulation of *frq* and *wc-1* in the *cnb-1*^{RIP} mutants.

Henceforth, I performed the expression studies of *frq* and *wc-1* in the *cnb-1*^{RIP} mutants at two different temperatures of 20 °C and 25 °C using qRT-PCR (Fig. 4.1, Fig. 4.2).

In *N. crassa*, CNB-1 binds to the calcineurin-dependent response element (CDRE), possibly to regulate target gene expression (Kumar et al. 2006). Therefore, the altered *frq* expression in the *cnb-1*^{RIP} mutants could result from the mutations in the key amino acid residues in the CNB-1 subunit. CNB-1 is required for dephosphorylation of the white collar (WCC), which directly affects FRQ levels (Schafmeier et al. 2005). The mutated CNB-1 was unable to dephosphorylate WC-1, resulting in WC-1 hyperphosphorylation by kinases (Yang et al. 2004), and rendering its low binding affinity to the *frq* promoter and reduced *frq* transcription. It is possible that the CNB-1^{RIP} protein also has low affinity for the *frq* promoter, causing low levels of *frq* transcript (Fig. 4.1), and the observed corresponding decreased period length.

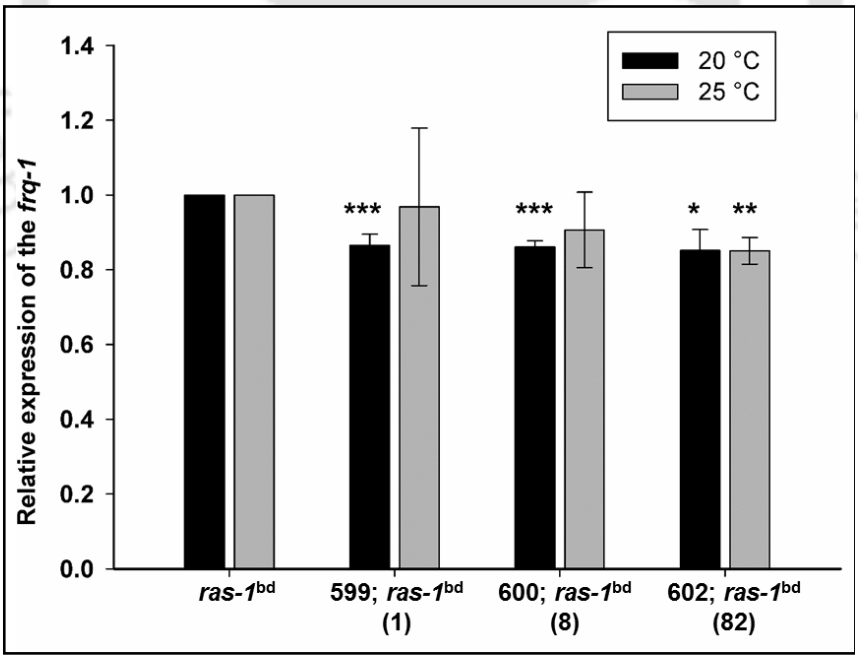

Fig. 4.1 Relative expression of *frq-1* in the *cnb-1*^{RIP} mutants under the conditions used for the circadian conidiation at different temperatures. Relative expression of *frq-1* under the conditions used for the circadian conidiation at different temperatures. Fold changes were

calculated using $2^{-\Delta\Delta C_T}$ method (Livak and Schmittgen, 2001) by taking control (*ras-1*^{bd}) as calibrator and *β*-tubulin as endogenous control. The Standard deviation was calculated from the data of three individual experiments each with three triplicates (n = 9) with *P* values <0.05 (*), <0.01 (**), <0.001 (***), and otherwise non-significant (ns) as measured by one-way ANOVA test.

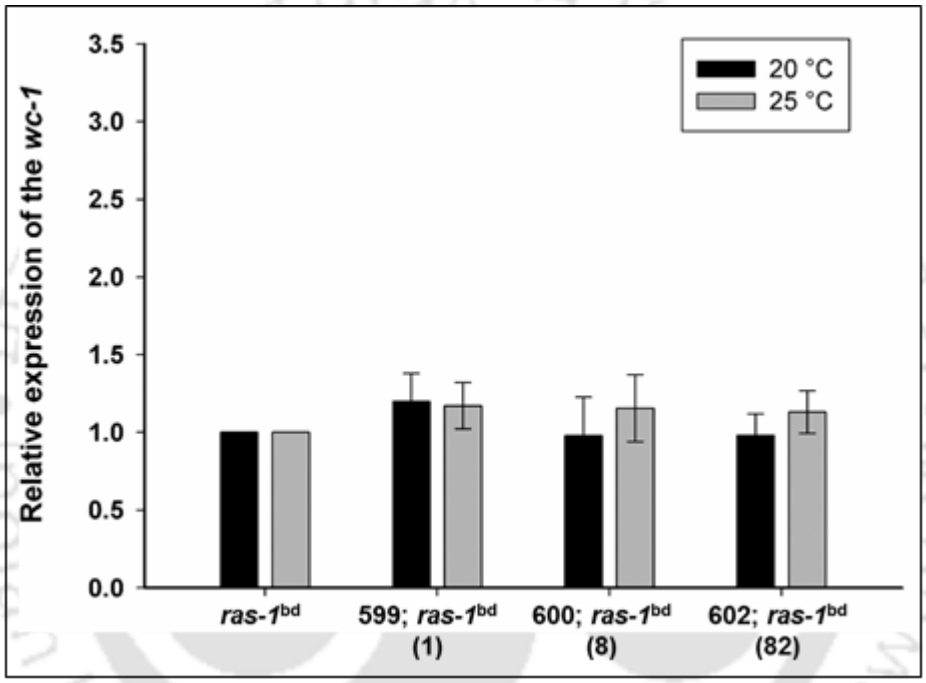

Fig. 4.2 Relative expression of *wc-1* under the conditions used for the circadian conidiation at different temperatures. Relative expression of *wc-1* under the conditions used for the circadian conidiation at different temperatures. Fold changes were calculated using $2^{-\Delta\Delta C_T}$ method (Livak and Schmittgen, 2001) by taking control (*ras-1*^{bd}) as calibrator and *β*-tubulin as endogenous control. The Standard deviation was calculated from the data of three individual experiments each with three triplicates (n = 9) with *P* values<0.05 (*), <0.01 (**), <0.001 (***) and otherwise non-significant (ns) as measured by one-way ANOVA test

4.2.2 Promoter analysis of *hsp80* to predict CRZ1 regulatory sequences for the survival under the heat shock stress in *N. crassa*

Hsp90, a client molecular chaperone, is conserved throughout from lower to higher eukaryotes. In pathogenic fungi, Hsp90 plays a major role in virulence and drug resistance (Singh et al. 2009). Hsp90 is also responsible for the activation of calcineurin in *Candida albicans* and inhibition of Hsp90 causes decreased transcript levels of calcineurin, and thereby, results in the disruption of the downstream signaling cascade.

Calcineurin signaling is important in the regulation of different stress responses, including heat stress in fungi. The *cnb-1*^{RIP} mutants showed a reduced cell survival in thermotolerance (Table 3.4, Chapter 3); therefore, I investigated the molecular link between the calcineurin and Hsp80. Hsp80 belongs to the family of hsp90 heat shock family of protein, and the interaction between calcineurin and Hsp90 was important in *C. albicans* for the antifungal drug resistance against echinocandins- a class of drug which inhibits cell wall biosynthesis in fungi (Singh et al. 2009). The repression of Hsp90 results in the inactivation of calcineurin which further downstream inhibits CRZ1 which has an essential role in the activation of echinocandin (Singh et al. 2009).

The promoter analysis of *hsp80* identified a sequence for CRZ-1 binding.

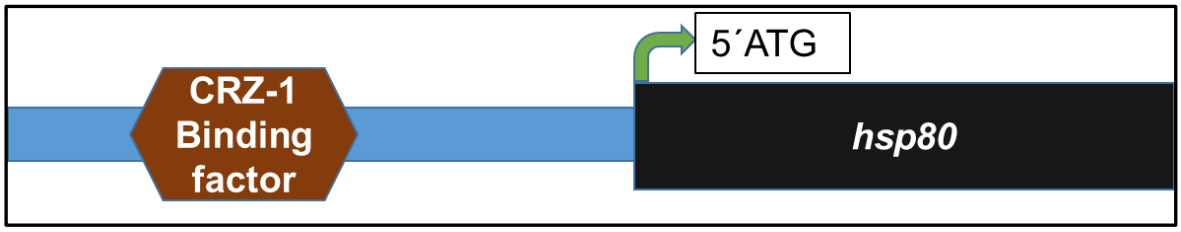

Fig.4.3 Promoter analysis of *hsp80*. The promoter analysis of *hsp80* revealed the presence of a CRZ-1 binding factor at about~1380 bp upstream of the *hsp80* gene. Therefore, it signifies that the heat shock stress pathway in *N. crassa* is mediated through calcineurin-CRZ-1 signaling pathway.

Table.4.1 Promoter analysis of *hsp80* using Genomatix

Sl. No.	**Name of the upstream element**	**Sequence (5'→3')**
1	Ribosomal RNA processing element	ATCTCTTTTTCATACT
2	pH responsive regulators	CACCGCCAAGTGCTATA
3	Yeast heat shock factors	GATTCTGCCTGTTTCAAGAAGCCTCTGTGATTG
4	Pheromone response elements	TCTTGAAACAGGC
5	Calcineurin-responsive zinc finger 1 binding factor	GTGGCTG
6	Yeast stress response elements	GGACCCAGGGGCCGG
7	Repressor of hypoxic genes	CCCATCGTTCAGC
8	Regulator of Drug Sensitivity	TTGCGGCCGTTGC

4.2.3 Transcriptional regulation of *hsp80* has a role in the survival under the heat shock stress

In Chapter 3, I described that the *cnb-1*^{RIP} mutants displayed decreased viability on exposure to lethal heat shock of 52 °C (Kumar et al. 2019). The heat shock protein families are classified according to the molecular weights. Earlier studies identified Hsp60 and Hsp90 as two important family of Hsps involved in important stress responses ranging from antifungal drug resistance in *S. cerevisiae*, *C. albicans* (Cowen and Lindquist, 2005; Cowen et al. 2009) to sexual and asexual developments in *Fusarium graminearum* (Bui et al. 2016). Moreover, the interaction of Hsp90 with Cna have been established in *C. albicans* (Gong et al. 2017), and the cross talk between Hsp90 and calcium-calcineurin pathway important for conferring resistance to antifungal drugs in *C. albicans* (Liu et al. 2015), therefore, Hsp90 have been targeted for antifungal drug development (Gong et al. 2017). In the pathogenic fungi *A. fumigatus*, Hsp90 been responsible for conidiation and cell wall integrity (Lamoth et al. 2012). In *N. crassa*, only the expression levels of the heat shock proteins have been characterized under different time periods after exposure to heat shock temperature of 48 °C (Kapoor et al. 1995). In *N. crassa* hsp80 belongs to the family of hsp90 family of Hsps (Borkovich et al. 2004). But, whether the calcineurin-CRZ-1 mediated regulation of Hsps occurs in in *N. crassa* is not known. Therefore, I studied the expression of *hsp80* during heat shock stress, and the role of calcineurin-CRZ-1 in the expression of *hsp80* under the heat shock stress conditions. I performed qRT- PCR of the *cnb-1*^{RIP} mutants under lethal heat shock temperature of 48 °C to check the expression of both *hsp60* and *hsp80* in comparison to the wild type control, using the protocol and primers described in Chapter 2. For the expression studies of *hsp60* and *hsp80* cells were grown under normal growth temperature of 28 °C for 14 h and then after exposure to the lethal heat shock temperature of 48 °C for 1 h RNA was isolated. The fold change of the *hsp60* and *hsp80* in the *cnb-1*^{RIP} mutants, were compared to the wild type control under heat shock conditions. The

expression of *hsp60* in the *cnb-1*^{RIP} mutants was not altered (Fig. 4.4) compared to wild type control under heat shock condition, whereas the expression of *hsp80* was decreased by ~ 0.4, ~ 0.3 and ~ 0.2-fold (Fig. 4.5) among the *cnb-1*^{RIP} mutants. This results further supports cell viability under the heat shock stress (Table 3.4) discussed in Chapter 3. Therefore, calcineurin has a role in the *hsp80* mediated heat shock stress response in *N. crassa*.

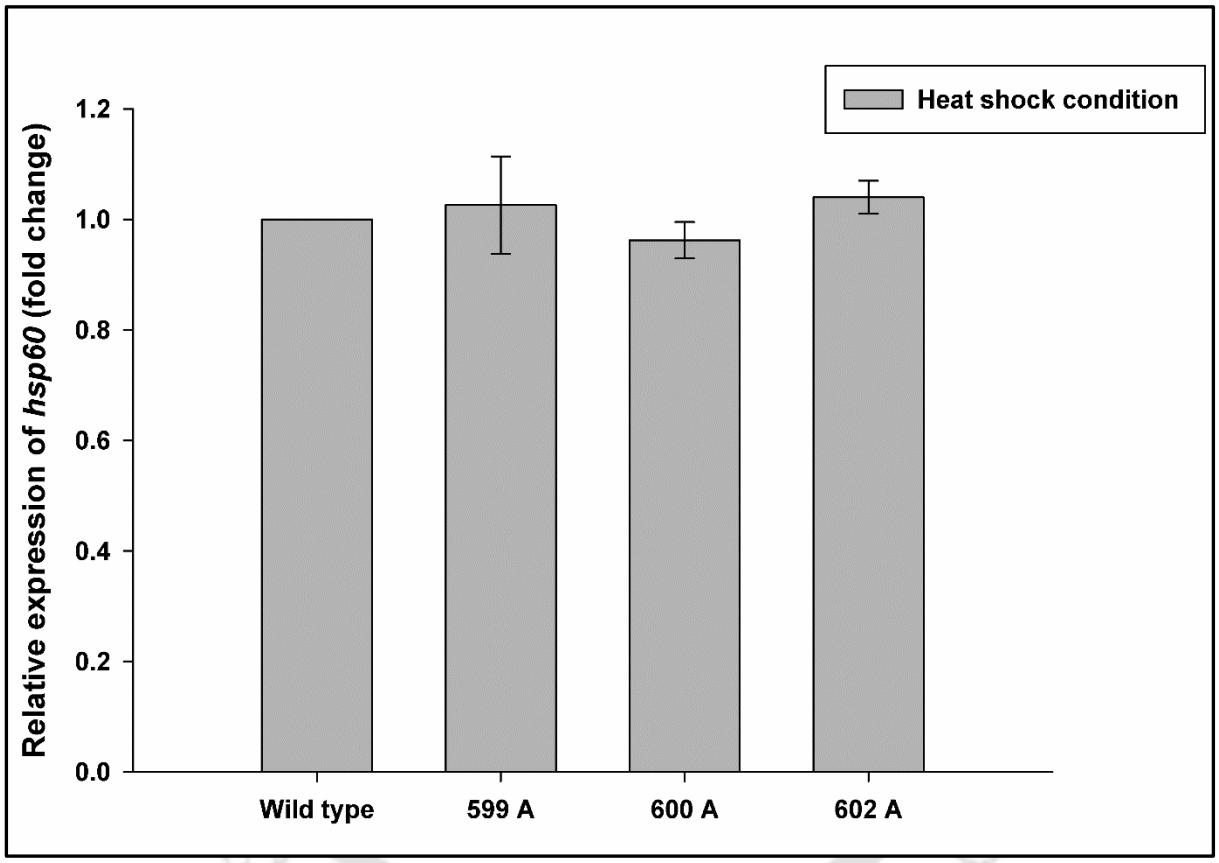

Fig 4.4 Relative expression of *hsp60* in the *cnb-1*^{RIP} mutants under heat stress conditions. The expression of *hsp60* in the *cnb-1*^{RIP} mutants was analysed being subjected to thermal stress conditions. Fold changes were calculated using $2^{-\Delta\Delta C}{}_T$ method (Livak and Schmittgen, 2001) by taking control (wild type with heat shock) as calibrator and *β*-tubulin as the endogenous control. The standard deviation was calculated from the data of three individual experiments each with three triplicates (n = 9).

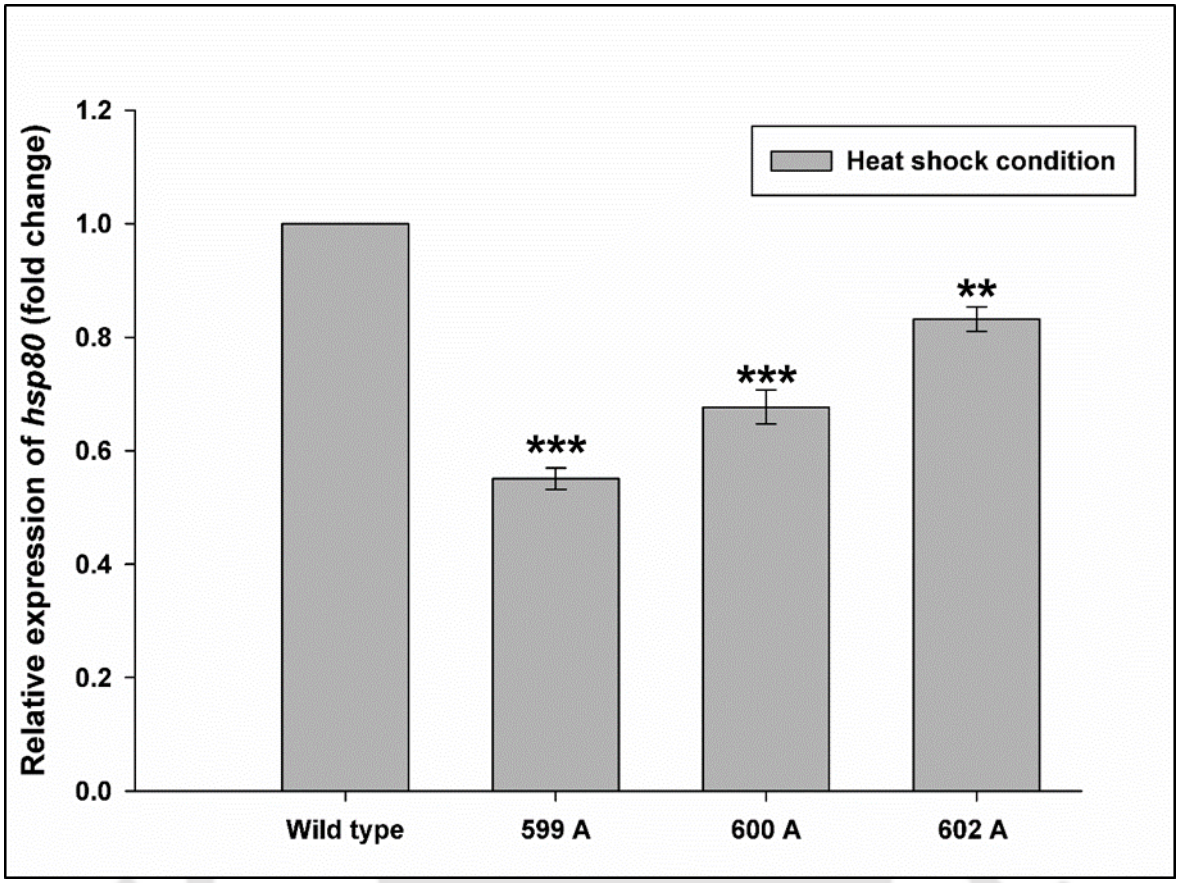

Fig.4.5 Relative expression of *hsp80* in the *cnb-1*^{RIP} mutants under heat stress conditions. The expression of *hsp80* in the *cnb-1*^{RIP} mutants was analysed being subjected to thermal stress conditions. Fold changes were calculated using $2^{-\Delta\Delta C}{}_{T}$ method (Livak and Schmittgen, 2001) by taking control (wild type with heat shock) as calibrator and *β*-tubulin as endogenous control. The standard deviation was calculated from the data of three individual experiments each with three triplicates (n = 9) with *P* values <0.05 (*), <0.01 (**), <0.001 (***), and otherwise non-significant (ns) as measured by one-way ANOVA test.

4.2.4 Expression studies of the *hsp60, hsp80, cnb-1* and *crz-1* in the wild type using calcineurin inhibitor FK506

In *C. albicans*, calcineurin interacts with Hsp90, and Crz-1 downstream target of calcineurin responsible for the Hsp90 mediated drug resistance (Cowen et al. 2006) and also regulates apoptosis in *C. albicans* (Phillips et al. 2003). In addition, the expression level of *hsp80*, a

homolog of hsp90, was reduced in the *cnb-1*^{RIP} mutants under the heat shock condition (Fig. 4.5). Therefore, I tested if, Hsp80 signaling pathway is regulated by the calcineurin- CRZ-1 pathway in *N. crassa* like in the *C. albicans* and performed qRT-PCR for the *cnb-1*, *hsp60*, *hsp80*, and *crz-1* in the wild type strain grown in VG liquid media supplemented with FK506, a potent inhibitor of calcineurin (Peng et al. 2014), under the heat shock conditions. Isolation of RNA, cDNA preparation, and qRT-PCR were performed using the manufacturers protocol and using the specific primers as mentioned in Chapter 2 (Table 2.2). The transcript levels of *cnb-1*, *hsp80*, and *crz-1* were increased by ~1.7, 2.1, 1.9-fold (Fig. 4.6) under heat shock and reduced by ~0.8, ~0.6 and ~0.8 fold (Fig. 4.6) on supplementation of media with FK506 in comparison with the wild type control without heat shock condition (Fig. 4.6). However, the fold change in the expression level of *hsp60* was not significant (Fig. 4.6), and similar to *hsp60* expression the *cnb-1*^{RIP} mutants (Fig. 4.4). Therefore, the expression analysis indicates the involvement of the calcineurin-CRZ-1 signaling pathway in the hsp80 mediated heat shock stress response in *N. crassa*.

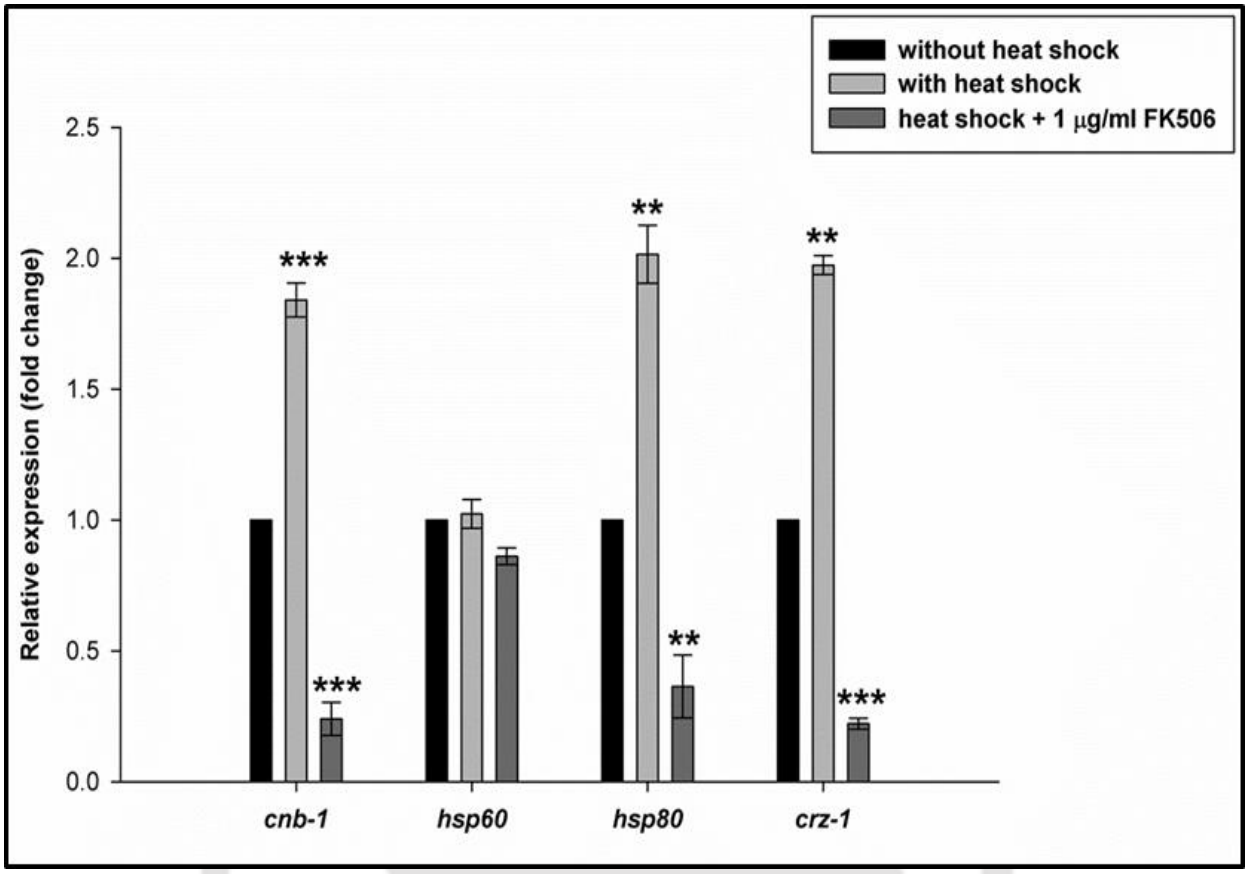

Fig. 4.6 Relative expression studies for *cnb-1*, *hsp60*, *hsp80* and *crz-1* in the wild type strain under heat shock conditions. The expression studies were performed in VG liquid media supplemented with FK506 as indicated. Fold changes were calculated using $2^{-\Delta\Delta Ct}$ method (Livak & Schmittgen, 2001) by taking control wild type (without heat shock) as calibrator and β-tubulin as endogenous control. The standard deviation was calculated from the data of three individual experiments each with three triplicates (n=9) with P values<0.05 (*), <0.01 (**), <0.001 (***) and otherwise non-significant (ns) as measured by one-way ANOVA test.

4.2.5 Transcriptional analysis of *hsp60* and *hsp80* in the *trm-9*, *nca-2*, and their respective double mutants under heat shock conditions

The calcineurin-CRZ-1 signaling pathway was shown to upregulate *ncs-1*, a Ca^{2+} sensor, in response to Ca^{2+} stress (Gohain and Tamuli, 2019). In addition, calcineurin-CRZ-1 signaling

pathway also upregulate *nca-2*, a Ca^{2+} ATPase transporter localized to the vacuoles, under Ca^{2+} stress conditions in *N. crassa* (Roy and Tamuli, unpublished). Moreover, the *trm-9*, another Ca^{2+} ATPase, and *nca-2* were studied in our laboratory, the Δ*trm-9*Δ*nca-2* double mutant showed decreased cell survival to the heat stress condition (Laxmi and Tamuli 2015). I studied if *hsp60* and *hsp80* are involved in Δ*trm-9*, Δ*nca-2*, and the Δ*trm-9*Δ*nca-2* double mutants for heat shock response. The expression of *hsp80* in the Δ*trm-9*Δ*nca-2* double mutant was ~0.6-fold reduced compared to the wild type strain under heat shock conditions (Fig. 4.8). However, expression of *hsp60* in the *cnb-1*^{RIP} mutants were not significantly different from the wild type strain (Fig. 4.7). Therefore, the expression studies suggested that Hsp80 is a major heat shock protein necessary for coping up the heat shock stress in *N. crassa*.

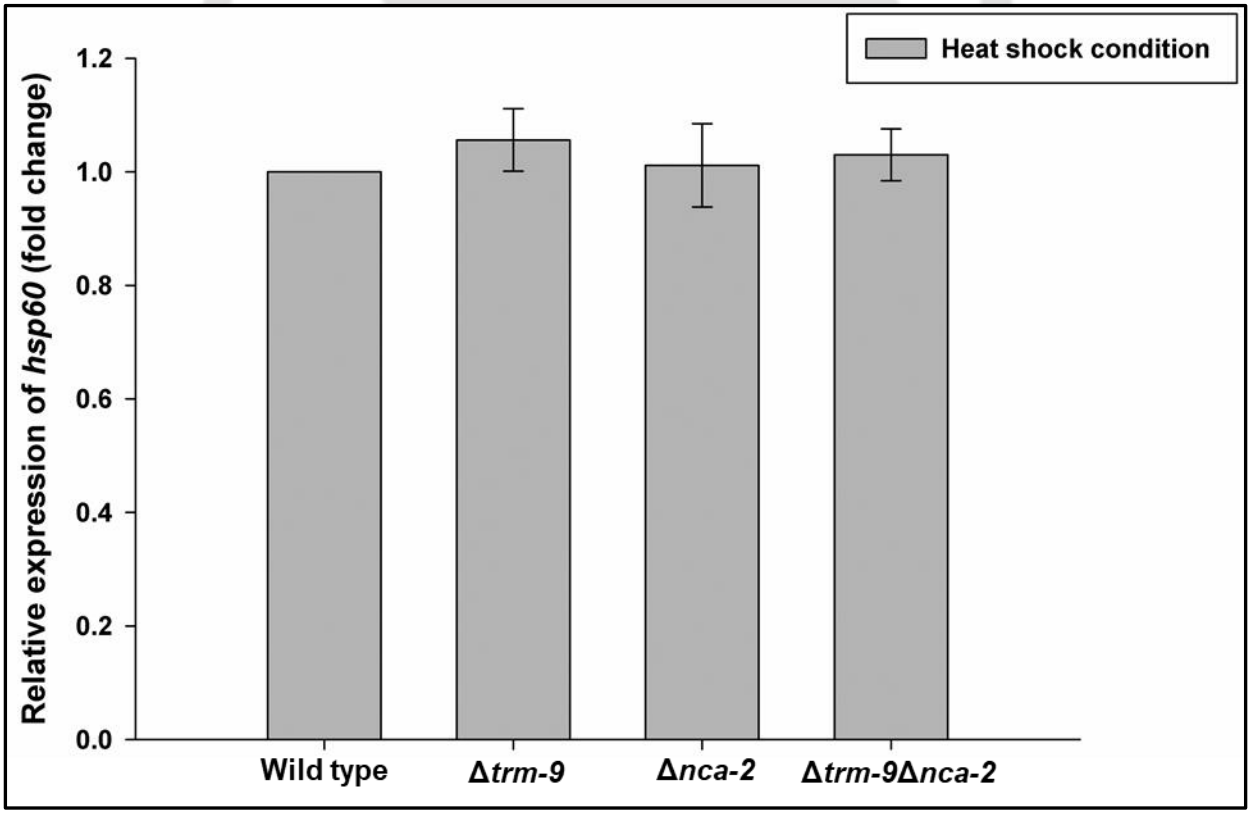

Fig. 4.7 Relative expression of *hsp60* in wild type, Δ*trm-9*, Δ*nca-2*, and the Δ*trm-9* Δ*nca-2* double mutant strains under the heat shock condition. Fold changes were calculated using

$2^{-\Delta\Delta C_T}$ method (Livak and Schmittgen, 2001) by taking control (wild type with heat shock) as calibrator and *β*-tubulin as endogenous control. The standard deviation was calculated from the data of three individual experiments each with three triplicates (n = 9).

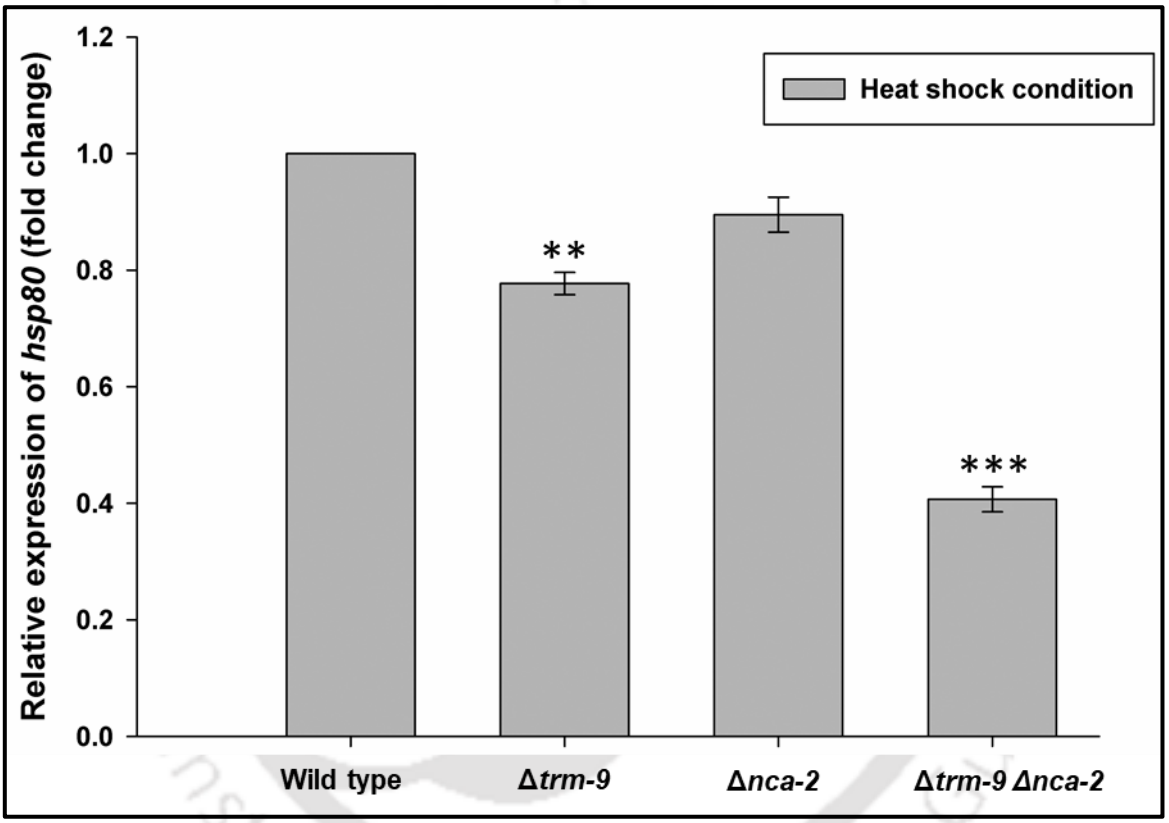

Fig.4.8 Relative expression of *hsp80* in wild type, Δ*trm-9*, Δ*nca-2*, and the Δ*trm-9* Δ*nca-2* double mutant strains under the heat shock condition. Fold changes were calculated using $2^{-\Delta\Delta C_T}$ method (Livak and Schmittgen, 2001) by taking control (wild type with heat shock) as calibrator and *β*-tubulin as endogenous control. The standard deviation was calculated from the data of three individual experiments each with three triplicates (n = 9) with *P* values <0.05 (*), <0.01 (**), <0.001 (***), and otherwise non-significant (*ns*) as measured by one-way ANOVA test.

4.2.6 Expression studies of *trm-9* and *nca-2* in the wild type under heat shock conditions

In our laboratory, previous studies on Δ*trm-9*, Δ*nca-2*, and Δ*trm-9*Δ*nca-2* double mutants in response to heat shock conditions exhibited the requirement of both *trm-9* and *nca-2* genes for cell survival under heat shock (Laxmi and Tamuli, 2015). Also, the expression studies of *hsp60* and *hsp80* across the *cnb-1*^{RIP,} Δ*trm-9*, Δ*nca-2*, and Δ*trm-9*Δ*nca-2* mutant strains revealed that hsp80 is the major heat shock family of protein has a role in the heat shock stress tolerance in *N. crassa*. Further, to complement the results observed from the phenotypic studies from thermotolerance assay of Δ*trm-9*, Δ*nca-2*, and Δ*trm-9*Δ*nca-2* mutants (Laxmi and Tamuli, 2015) and to analyze whether *trm-9* and *nca-2* genes are itself important for survival under heat shock stress similar to *cnb-1* gene (Fig. 4.6) I performed expression analysis of *trm-9* and *nca-2* in the wild type background under the heat shock stress conditions (Fig. 4.9). The expressions *trm-9* and *nca-2* were increased by ~2 and ~2.7-fold under heat shock conditions in comparison with the control (wild type without the heat shock condition) (Fig. 4.9), suggesting that the *trm-9* and *nca-2* genes are involved in the heat shock stress tolerance pathway.

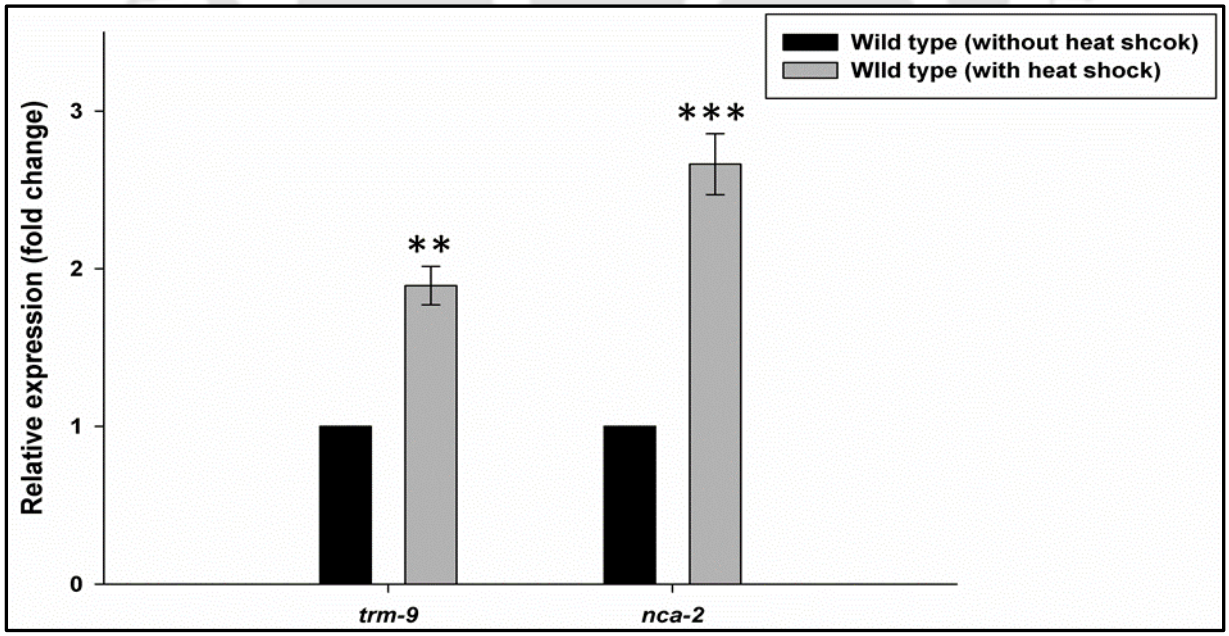

Fig. 4.9 Relative expression of *trm-9 and nca-2* in thermotolerance conditions using qRT-PCR. Fold changes were calculated using $2^{-\Delta\Delta C_T}$ method (Livak and Schmittgen, 2001) by

taking control (wild type without heat shock) as calibrator and *β*-tubulin as endogenous control. The standard deviation was calculated from the data of three individual experiments each with three triplicates (n = 9) with *P* values <0.05 (*), <0.01 (**), <0.001 (***), and otherwise non-significant (*ns*) as measured by one-way ANOVA test.

4.2.7 The transcription of *nca-2* is controlled by calcineurin-crz-1 pathway under Ca^{2+} stress conditions

The P-type Ca^{2+} ATPase, NCA-2 localized to the plasma membrane, has a role in growth in response to increased Ca^{2+} concentration and fertility in *N. crassa* (Bowman et al. 2011; Deka and Tamuli, 2013). In *S. cerevisiae*, transcript levels of *nca-2* is increased under the Ca^{2+} stress and osmotic stress conditions (Benito et al. 2000). In *N. crassa*, Δ*nca-2* mutant has restricted growth in response to elevated extracellular Ca^{2+} levels, indicating a defect in Ca^{2+} homeostasis in the mutant (Hamam and Lew, 2012). Besides, work in our laboratory revealed *nca-2* role in the Ca^{2+} stress, growth, and other stress responses (Laxmi and Tamuli, 2015). Furthermore, CRZ-1, an important downstream target of calcineurin, might transcriptionally upregulate *nca-2* in response to high Ca^{2+} concentrations (Gohain and Tamuli, 2019). I described the role of *cnb-1* in Ca^{2+} stress in Chapter 3 (Kumar et al. 2019). Further, I performed the qRT-PCR analysis to determine the transcript levels of *nca-2* in the *cnb-1*^{RIP} mutants under Ca^{2+} stress. I found ~0.2-fold reduction of *nca-2* transcript levels in the 599 and 600, and ~0.4-fold reduction in the 602 mutant strains compared to the wild type control (Fig. 4.10). I also performed qRT-PCR analysis for the *cnb-1*, *nca-2* and *crz-1* in the wild type strain grown in standard VG liquid media (0.68 mM $CaCl_2$) as control and wild type supplemented with FK506, a potent inhibitor of calcineurin (Peng et al. 2014) under Ca^{2+} stress conditions. The RNA isolation, cDNA preparation, and qRT-PCR were performed using the manufacturer's protocol and the specific primers (Table 2.2) as mentioned in Chapter 2. The expressions of *cnb-1*, *nca-2*, and *crz-1* were increased by ~2, ~3.5 and ~3-fold in the VG liquid supplemented with 200 mM $CaCl_2$, whereas

on supplementation with 1 µg/ ml FK506 under Ca^{2+} stress conditions, the *cnb-1*, *nca-2* and *crz-1* transcript levels were reduced by ~0.4, ~0.6, ~0.4- fold compared to the wild type strain in standard VG liquid (0.68 mM $CaCl_2$) (Fig. 4.11). Therefore, *nca-2* is a major player of the Ca^{2+} stress response, and regulated via the calcineurin-CRZ-1 via pathway.

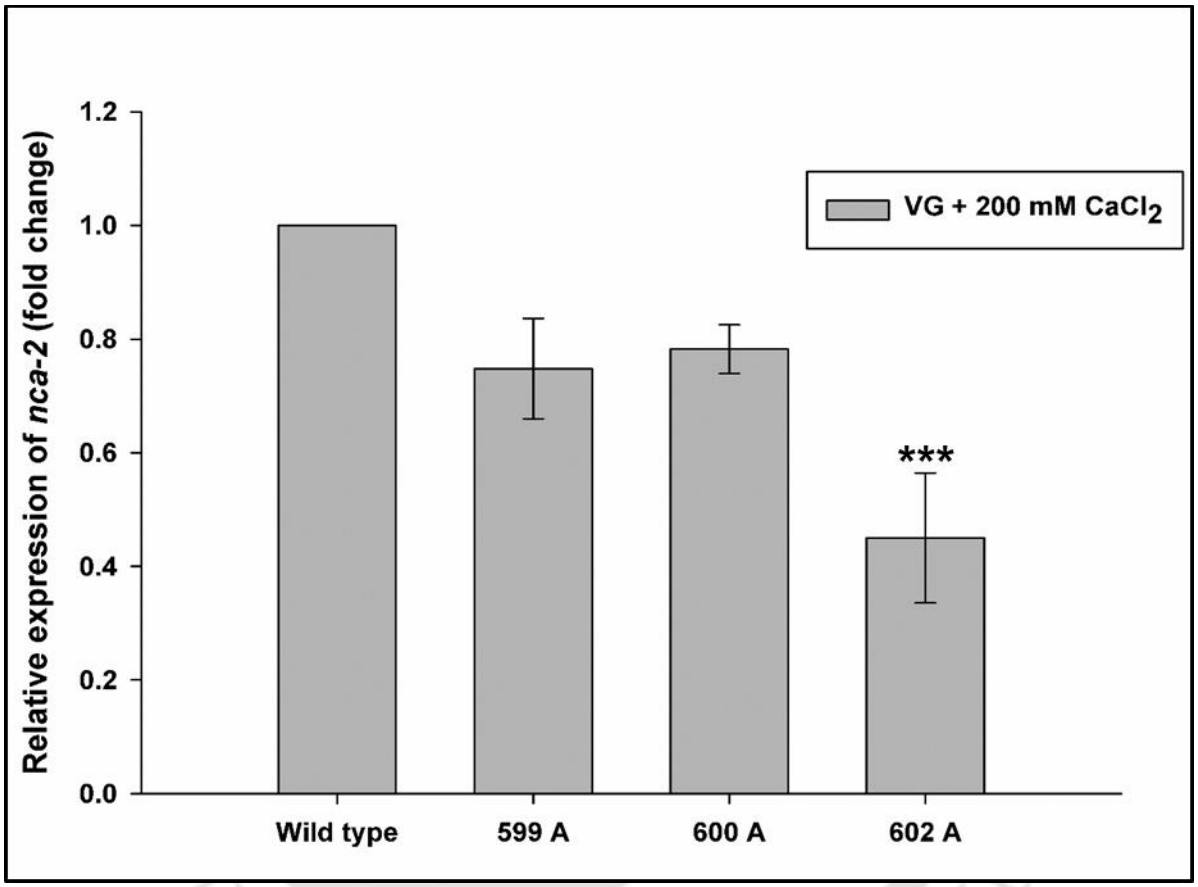

Fig. 4.10 Relative expression of *nca-2* in the wild type and the *cnb-1*^{RIP} mutant strains under Ca^{2+} stress conditions determined by qRT-PCR analysis. Fold changes were calculated using $2^{-\Delta\Delta C}{}_T$ method (Livak and Schmittgen, 2001) by taking control (wild type with 200 mM $CaCl_2$ stress) as calibrator and *β*-tubulin as endogenous control. The standard deviation was calculated from the data of three individual experiments each with three triplicates (n = 9) with *P* values<0.0 5 (*), <0.01 (**), <0.001 (***) and otherwise non-significant (*ns*) as measured by one-way ANOVA test.

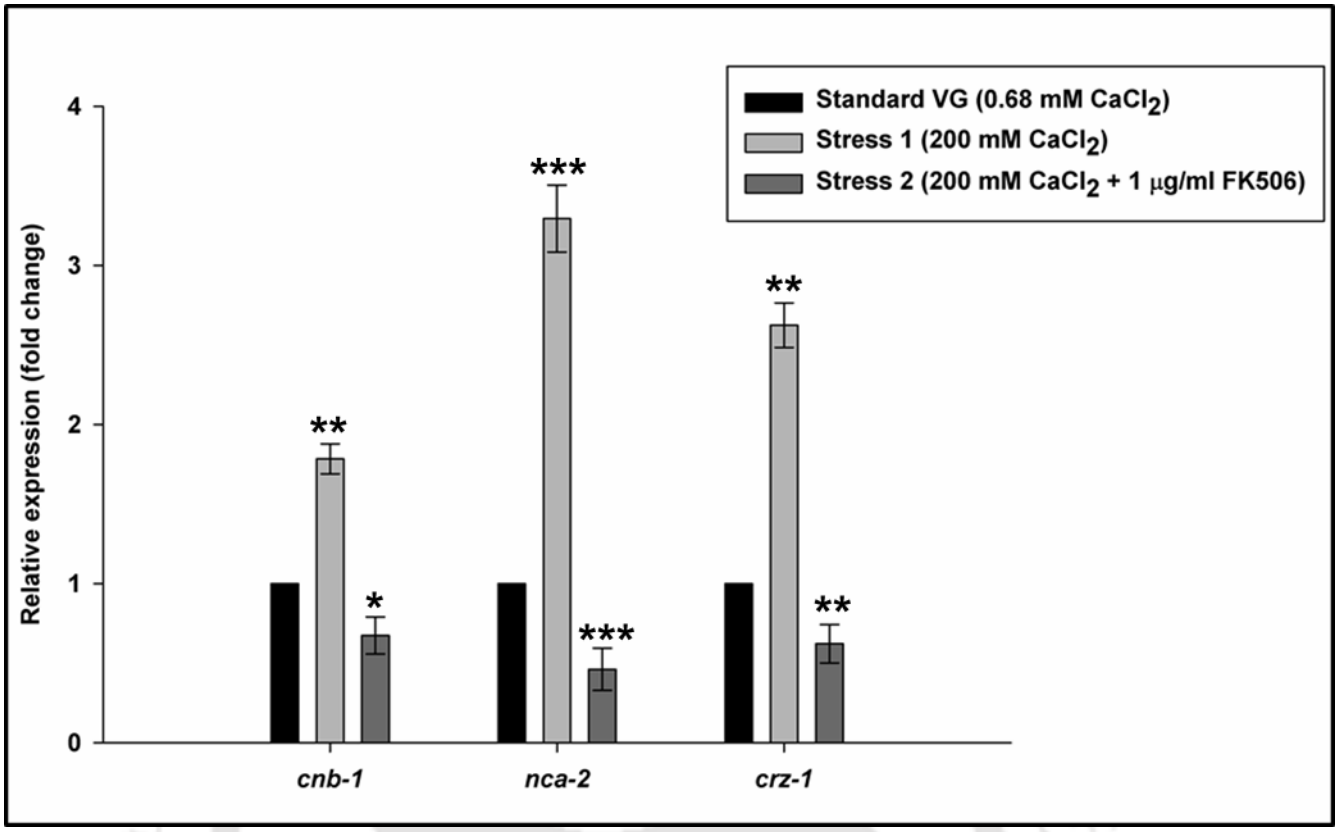

Fig. 4.11 Relative expression of *cnb-1, nca-2 and crz-1* under Ca^{2+} stress conditions with or without supplementation with calcineurin inhibitor FK506. Fold changes were calculated using $2^{-\Delta\Delta C}{}_T$ method (Livak and Schmittgen, 2001) by taking control (wild type in standard VG with 0.68 mM $CaCl_2$) as calibrator and *β*-tubulin as endogenous control. The Standard deviation was calculated from the data of three individual experiments each with three triplicates (n = 9) with *P* values <0.05 (*), <0.01 (**), <0.001 (***) and otherwise non-significant (*ns*) as measured by one-way ANOVA test.

4.3 Discussion

In this Chapter, I investigate the molecular components of calcineurin signaling pathway using the *N. crassa cnb-1*^{RIP} mutants. Previous Chapter describes the roles of *cnb-1* roles regulating circadian clock, thermotolerance and Ca^{2+} mediated stress response in *N. crassa* (Kumar et al. 2019). In eukaryotes, circadian clock acts as an internal timekeeper for the daily regulation of different biological processes. The ubiquitous second messenger molecule Ca^{2+} is important

for the regulation of circadian clock in higher eukaryotes (O'Neill and Reddy, 2012). In *N. crassa*, several molecular components like *frequency* (*frq*) and *white-collar genes* (*wc-1* and *wc-2*) play critical role in the circadian clock (Dunlap and Lorros, 2004; Liu and Bell-Pedersen, 2006). I tested if, *frq*, *wc-1*, and *wc-2* interacts with *cnb-1* to regulate the circadian clock in *N. crassa*. I performed expression analysis of the *frq* and *wc-1* genes in the *cnb-1*^{RIP} mutants strains. The transcript level of *frq* was reduced across the *cnb-1*^{RIP} mutants at 20 °C (Fig. 4.1), which is relatively a stress condition for *N. crassa* that grows at an optimum temperature of 30 °C. Although both WC-1 and WC-2 are modulated by phosphorylation (Baker et al. 2009), depending on phosphorylation of WC-1, FRQ is regulated (Huang et al. 2007) and *frq* level increases by binding of WC-1 to its promoter. Whereas WC-2 remains constant (Baker et al. 2012), and it majorly assists WC-1 for the WCC mediated light signaling pathway in *N. crassa* (Cheng et al. 2002). However, *wc-1* transcript levels were not significantly different across the *cnb-1*^{RIP} mutants in comparison with the *ras-1*^{bd} control at 20 °C and 25 °C (Fig. 4.2). Calcineurin, plays an essential role in the survival of pathogenic fungi *C. neoformans* (Odom et al. 1997) and *Candida glabrata* (Chen et al. 2012), and parasitic protozoa *Leishmania donovani* (Naderer et al. 2011) in the human host at about 37 °C and higher temperature. Therefore, calcineurin is responsible for the virulence of the pathogenic organisms in the host. Studies on the calcineurin signal cascade revealed its possible interaction with one of the downstream targets CRZ-1, which regulates thermotolerance and pathogenesis in mammals (Chen et al. 2012). Hsp90 is an essential and highly conserved family of molecular chaperones (Juvvadi et al. 2016) in most fungal species. In *C. albicans*, Hsp90 was shown to interact with calcineurin for proper cell function regulation including thermotolerance, virulence, and growth (Hill et al. 2015; Deizmann et al. 2015; Singh et al. 2012). In *A. fumigatus*, repression of GFP tagged Hsp90 by use of inhibitors has unraveled its role in transcriptional regulation by localization to the nuclei (Lamoth et al. 2012). The *N. crassa* genome sequencing and

analysis identified Hsp80, a member of the Hsp90 family of heat shock proteins (Borkovich et al. 2004). In Chapter 3, I discussed about the role of *cnb-1* in the heat shock stress tolerance. Furthermore, I investigated the expression levels of both *hsp60* and *hsp80* in the *cnb-1*^{RIP} mutants, which revealed no significant change in the expression level of *hsp60* in the *cnb-1*^{RIP} mutants (Fig.4.4). Whereas, the *hsp80* expression was reduced by ~0.4- fold in the 599 and 600 *cnb-1*^{RIP}mutants, and ~0.2-fold reduction in the 602 *cnb-1*^{RIP} mutant compared to the wild type (Fig. 4.5). I also determined the expression of *hsp80*, *hsp60*, *cnb-1*, and *crz-1*, a downstream target of calcineurin having a role in the heat shock stress tolerance in fungi (Chen et al. 2012). The *N. crassa* strains were grown in VG and VG supplemented with FK506, a potent inhibitor of calcineurin (Peng et al. 2016) with or without heat shock stress. The fold change for *hsp60* was not significant, but the expressions of *cnb-1*, *crz-1*, and *hsp80* were increased by ~1.7, 2.1, 1.9-fold in VG and decreased by ~0.8 and ~0.6-fold in the VG supplemented with FK506 under heat shock conditions in comparison with the wuld type without heat shock (Fig. 4.6). Besides, previous studies in our laboratory identified the role of *trm-9* and *nca-2* for survival under the heat shock conditions (Laxmi and Tamuli, 2015). I determined the expressions of *hsp60* and *hsp80* in the Δ*trm-9*, Δ*nca-2*, and Δ*trm-9*Δ*nca-2* mutants. There was no change in the expression *hsp60* was (Fig. 4.7), but the expression of *hsp80* was reduced by ~0.2-fold in the *Δtrm-9,Δnca-2* mutants (Fig. 4.8). Furthermore, the expression of *hsp80* was and reduced by ~0.6-fold in the *Δtrm-9Δnca-2* double mutant (Fig. 4.8). Also, the expression levels of *trm-9* and *nca-2* were increased by ~2-and ~2.7-fold, respectively, under the heat shock conditions (Fig. 4.9). This results further supports the previous findings that genetic interaction of *trm-9* and *nca-2* are required for the survival under thermotolerance condition in *N. crassa* (Laxmi and Tamuli, 2015).

The *cnb-1* gene also plays a role in the Ca^{2+} stress tolerance (Kumar et al. 2019). In addition, the calcineurin activated CRZ-1 binds to the *ncs-1* promoter to upregulate its

expression in response to high Ca^{2+} concentrations (Gohain and Tamuli 2019). The *N. crassa* Ca^{2+} transporters are responsible for regulating the Ca^{2+} entry and exit into the various internal Ca^{2+} stores (Tamuli et al. 2013). Previous work in our laboratory also showed that *nca-2* plays a role in Ca^{2+} stress tolerance (Deka and Tamuli, 2013), and the calcineurin-CRZ-1 signaling pathway might transcriptionally regulate *nca-2* expression in response to high Ca^{2+} concentrations (Gohain and Tamuli, 2019). To further investigate the *nca-2* role in the calcineurin mediated Ca^{2+} stress tolerance pathway, I determined the expression of *nca-2* in the *cnb-1*^{RIP} mutants grown in VG supplemented with 200 mM $CaCl_2$. The transcript levels of *nca-2* was reduced by ~0.2-fold in the 599 and, 600 and ~0.3-fold in the 602 *cnb-1*^{RIP} mutant strains (Fig. 4.10). Furthermore, I determined the transcript levels of *cnb-1*, *nca-2*, and *crz-1* using wild type in the standard VG (contains 0.68 mM $CaCl_2$) control, VG supplemented with 200 mM supplementation of $CaCl_2$, and VG with 200 mM $CaCl_2$ supplemted with 1 ug/ml of FK506. The expression levels of *cnb-1*, *nca-2*, and *crz-1* were increased by ~2, ~3.5, and ~3-fold in the VG supplemented with 200 mM $CaCl_2$, and reduced by ~0.3, ~0.6, and ~0.4- fold in the VG supplemented with FK506 (Fig. 4.11). These results further suggested that of *nca-2* is transcriptionally regulated via the calcineurin-CRZ-1 pathway during Ca^{2+} stress in *N. crassa*.

A part of the results described in this Chapter was presented (i) as a poster and flash talk in the 11th International Conference on Biology of Yeast and Filamentous Fungi, University of Hyderabad, India, 26-29 November, 2019, and (ii) in the poster session at the EMBO symposium on Calcium signaling: Molecular mechanisms to role in health and diseases, National Center for Biological Sciences (NCBS), Bangalore, 26-29 January, 2020.

In the next Chapter, I discuss how CRZ-1, a transcription factor regulated by calcineurin, regulates expressions of *hsp80* and *nca-2* in response to heat shock and Ca^{2+} stress conditions in *N. crassa*.

Chapter 5

The calcineurin-CRZ-1 signaling pathway is required for the heat shock and calcium stress responses in *N. crassa*

5.1 Introduction

In the previous Chapter, I described that heat shock stress results in increased expression of *hsp80* via the calcineurin-CRZ-1 signaling pathway. In *C. albicans*, Hsp90 interacts with Cna-1 and the calcium-calcineurin mediated signaling pathway was targeted for antifungal drug development (Gong et al. 2017). In Chapter 4 (Table 4.1) promoter analysis of *hsp80* revealed a putative sequence GTGGCTG located 1206 bp upstream responsible for binding of CRZ-1 to the promoter of *hsp80* in *N. crassa*. In this Chapter, I described identification of the nucleotide sequence responsible for the binding of CRZ-1 in the promoter of *hsp80*, and unveiled the molecular mechanism of calcienruin-CRZ-1 mediated *hsp80* activation during heat shock stress in *N. crassa*.

In the previous Chapter, I also described increased expression of *nca-2* in response to the increasing Ca^{2+} concentration. The Ca^{2+} ATPase transporter NCA-2 is localized to the plasma membrane and vacuoles having a role in sequestering of Ca^{2+} ions into the vacuolar stores thereby maintain the Ca^{2+} homeostasis (Bowman et al. 2009, 2011; Deka and Tamuli, 2013). In addition, previous studies in our laboratory indicated that the calcineurin-CRZ-1 signaling pathway might upregulate *nca-2* expression under high Ca^{2+} concentrations (Gohain and Tamuli, 2019). In this Chapter, I identified the nucleotide sequence responsible for the binding of CRZ-1 to the promoter of *nca-2*, and demonstrated that the intensity of CRZ-1 binding to the *nca-2* promoter sequence increases with an increase in the intracellular Ca^{2+} concentration. Therefore, transcriptional upregulation of *nca-2* could be mediated via the calcineurin-CRZ-1 signaling pathway under Ca^{2+} stress conditions.

5.2 Results

5.2.1 Chromatin immunoprecipitation revealed that CRZ-1 binds to the promoter of *hsp80* under heat shock condition

Chromatin immunoprecipitation (ChIP) assay for binding of CRZ-1 to the promoter of *hsp80* and *hsp60* was performed using 14 h old germlings of the 559 strain (Table 2.1, Chapter 2). For ChIP assay, the conidia were inoculated at a concentration of ~5 x 10^6 conidia/ml in a 250 ml flask consisting of 50 ml standard VG liquid, supplemented with BCS (50 µM) and pantothenic acid (10 µg/ml), and grown for 15 h at 28 ºC and shaking at 180 rpm. Another 250 ml flask ~5 x 10^6 conidia/ml were inoculated in 50 ml standard VG liquid, supplemented with BCS (50 µM) and pantothenic acid (10 µg/ml), and grown for 14 h at 28 ºC and shaking at 180 rpm, then subjected to heat shock for 1 h at 48 ºC in shaking water bath at 180 rpm. The germlings were harvested and washed twice with 1X phosphate-buffered saline (PBS, pH 7.4), then 1% formaldehyde was added to the cultures and incubated at room temperature on a rotating platform for 30 min for chemical crosslinking. The reaction was quenched by the addition of 125 mM glycine and was incubated for 10 min at room temperature. Germlings were harvested and washed twice with 1X PBS and suspended in ChIP lysis buffer. Chromatin was sheared by sonication in a sonicator (Vibra cell sonics, USA) on ice. The parameters for the sonication were 33% amplitude, 8 s ON pulse, 10 s OFF pulse, 120 cycles, and 20 min time. Five pairs of overlapping PCR primers, 1F and 1R, 2F and 2R, 3F and 3R, 4F and 4R, 5F and 5R were used covering the entire 1261 bp of the *hsp80* promoter region, to PCR amplify five overlapping fragments of different sizes (Fig. 5.1) were designed for determining the binding position of the CRZ-1 to the *hsp80* promoter. All the PCRs were performed by using Phusion® High-Fidelity DNA polymerase (Cat. No. M0530S, New England Biolabs, USA) using the reaction conditions- 98 ºC for 30 s, 25 cycles of 98 ºC for 10 s, 60 ºC for 30 s and 72 ºC for 30 s, and then 72 ºC for 5 min. The PCR products were run on 1.2 % agarose gel

containing EtBr (0.5 µg/ml) and visualized in a Gel Doc (Bio-Print ST4, Vilber Lourmat, France).

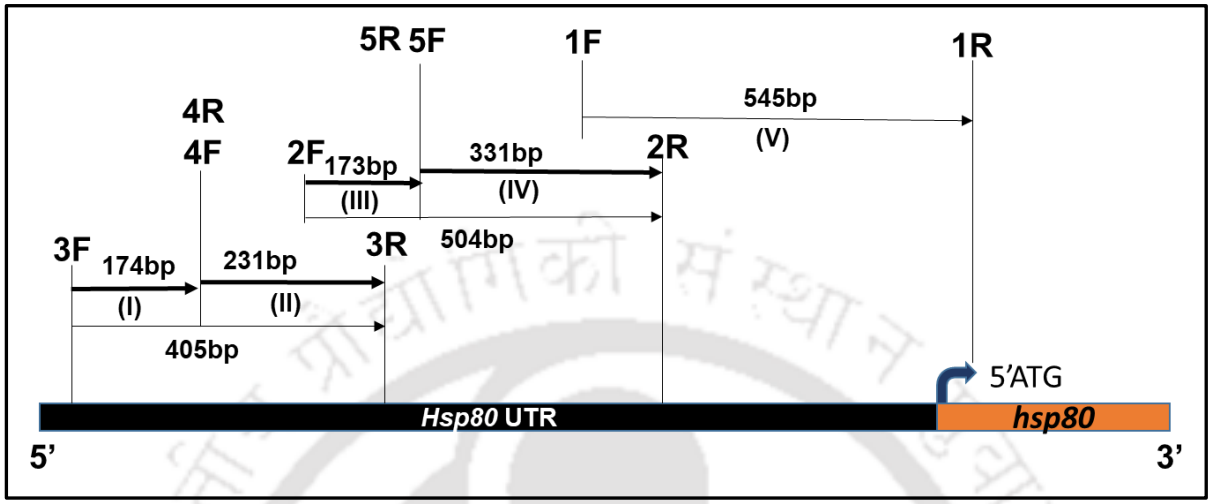

Fig. 5.1 Schematic representation of the primer pairs and their position for *hsp80* ChIP analysis. Five pairs of primers were designed to perform PCR for the *hsp80* promoter region using the DNA template obtained in the ChIP are located between the 5' UTR of the *hsp80* gene and the *hsp80* ORF. The primers 1F and 1R were used to PCR amplify fragment (V) of 545 bp size, Chip 5F and 2R to amplify 331 bp fragment (IV), 4F and 3R to amplify 231 bp fragment (II), 3F and 4R to amplify 174 bp fragment (I) and 2F and 5R to amplify 173 bp fragment (III) as indicated in the diagram (Fig. 5.1).

In the ChIP analysis, positive PCR bands were observed only for the 331 bp fragment (iv) and 174 bp fragment (i), amplified using the primers 5F and 2R, and 3F and 4R, respectively (Fig. 5.2). The band intensity of the positive ChIP was higher for both the fragments (i) of 174 bp and fragment (iv) of 331 bp. This confirmed that the CRZ-1 transcription factor binds to the *hsp80* promoter. Moreover, there was ~3-fold increase in the band intensity of the positive ChIP for the strain grown in heat shock condition compared to the strain grown in the normal VM, suggesting that binding of CRZ-1 to the *hsp80* promoter was increased during heat shock.

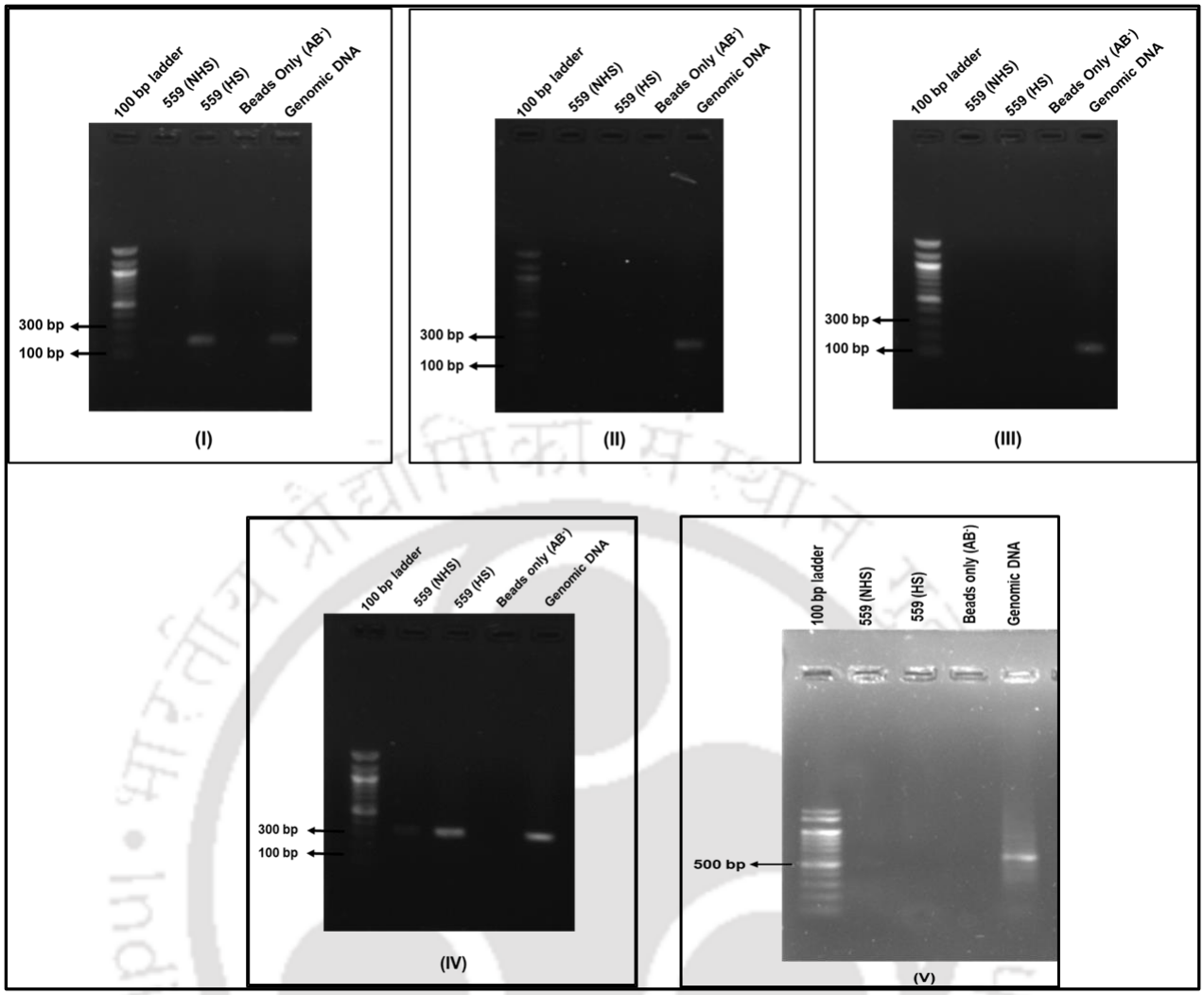

Fig. 5.2 ChIP assay to determine the binding of CRZ-1 to the *hsp80* promoter sequence. PCR products were analyzed using a 1.2% agarose gel to identify the CRZ-1 binding region in the *hsp80* promoter sequence. The PCR amplification for each of the five fragments (I to V) is indicated in the gel. The analysis of the PCR revealed a positive product for the fragment I and IV of 174 bp and 331 bp, respectively, and the band intensity was further enhanced when the 559 strain was grown in the presence of heat shock stress condition. The antibody control (Ab^-) indicates the control PCR for the sample, where only beads were used for immunoprecipitation. The wild type genomic DNA has used a positive PCR control for amplification of all the five fragments. (NHS - Non heat shock, HS - Heat shock)

In addition, to determine if, CRZ-1 binds to the promoter of *hsp60*, ChIP analysis was performed using the primers Chip 1F HSP60 and Chip 1R HSP60 mapping about 1161 bp of the promoter region of the *hsp60* gene.

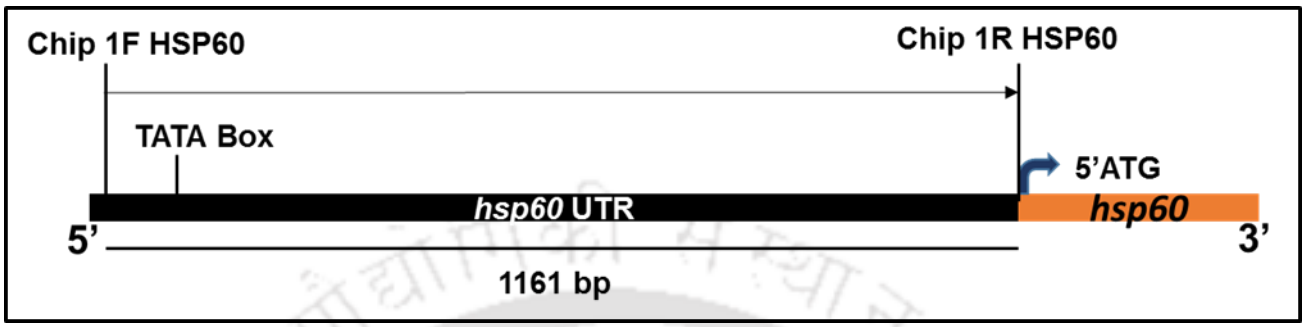

Fig. 5.3 Schematic representation of the primer pairs and their positions for *hsp60* ChIP analysis. The primers designed to perform PCR for the *hsp60* promoter region using the DNA template obtained in the ChIP are located between the 5' UTR of the *hsp60* gene and the *hsp60* ORF. The primers Chip 1F HSP60 and Chip 1R HSP60 were used to PCR amplify a fragment of 1161 bp size as indicated in the diagram.

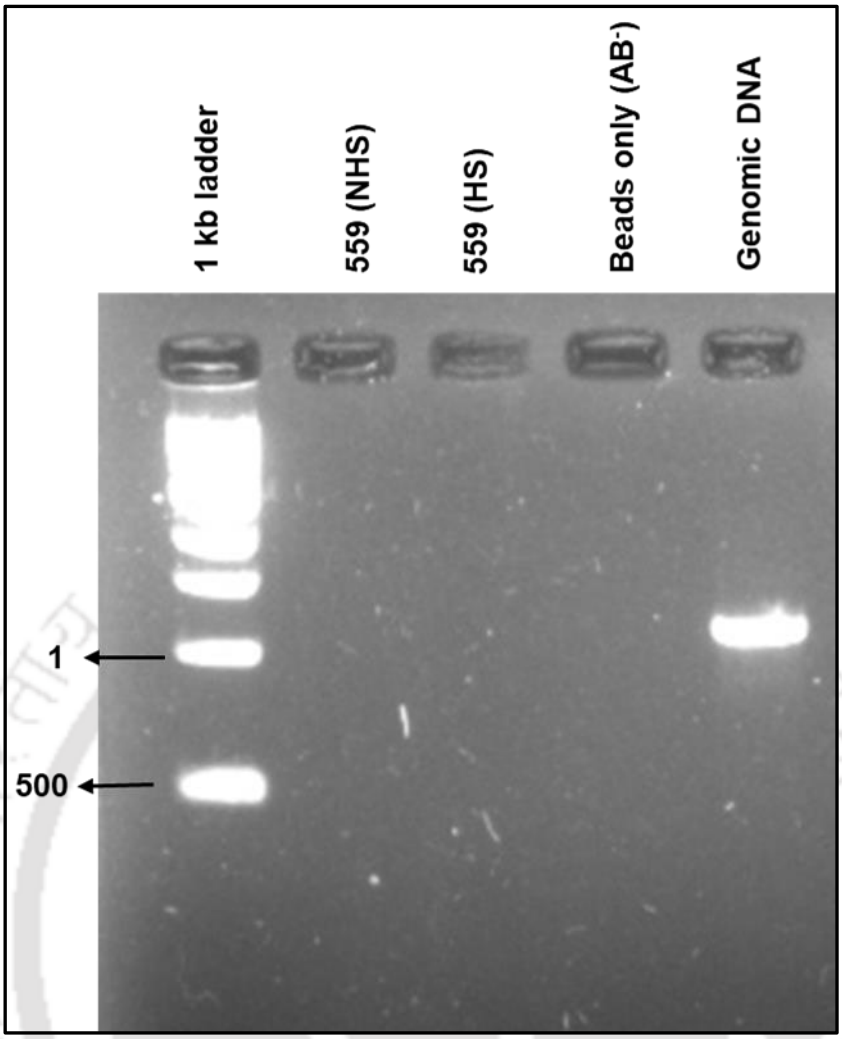

Fig. 5.4 ChIP assay to determine the binding of CRZ-1 to the *hsp60* promoter sequence. PCR products were analyzed using a 1.2% agarose gel to identify the CRZ-1 binding region in the *hsp60* promoter sequence. No PCR amplification was observed in the gel at 400 bp for both normal and also when the strain 559 was subjected to heat shock stress. The antibody control (Ab^-) indicates the control PCR for the sample, where only beads were used for immunoprecipitation. The wild type genomic DNA has used a positive PCR control for amplification of the fragment. (NHS - Non heat shock, HS - Heat shock)

In the ChIP assay for *hsp60*, no such prominent CRZ-1 binding region was identified, which is consistent with the previous findings that the expression of *hsp60* is not significantly different in the *cnb-1*^{RIP} mutants in comparison with the wild type strain under heat shock stress.

Furthermore, I performed electrophoretic mobility shift assay (EMSA) of the purified CRZ-1 protein to identify the exact binding sequence of CRZ-1 to the promoter of *hsp80*.

5.2.2 The electrophoretic mobility shift assay revealed CRZ-1 binding site in the *hsp80* promoter

The ChIP assay revealed that the CRZ-1 transcription factor binds to the *hsp80* promoter and the binding increases under heat shock conditions. But, the binding sequence in the *hsp80* promoter for CRZ-1 remains unknown. Therefore, to determine the CRZ-1 binding sequence, I designed and performed an electrophoretic mobility shift assay (EMSA). EMSA was performed using a Molecular probes™ EMSA Kit (Cat no. E33075, Life Technologies, USA) as per the manufacturer's protocol. In the ChIP analysis, it was observed that the probability of CRZ-1 binding could be in the fragment (i) and fragment (iv) (Fig. 5.1) about 997 bp and 270 bp upstream of the start codon (ATG). I designed two new DNA probes by equally dividing fragment (iv) (Fig. 5.1) where binding was seen in ChIP of sizes 161 bp and 170 bp and along with it used the earlier ChIP primers to check binding in fragment (i) and in the larger fragment (iv) for EMSA (Fig. 5.5). The DNA probes were prepared by PCR from the wild type *N. crassa* genomic DNA using the PCR primers 3F, 4R, 5F, EMSA_hsp80 1R, EMSA_hsp80 1F and 2R in appropriate pairs (Table 2.2; Fig. 5.5), and Phusion® High-Fidelity DNA polymerase (Cat. no. M0530S, New England Biolabs, USA). The PCR products were analyzed in a 1.2% agarose gel and later purified by using a PCR purification kit (Cat. No. 28104, Qiagen, Germany). The CRZ-1::5xGly::V5::GFP (~105 kDa) and V5::GFP (~28 kDa) proteins were isolated and purified from the 559 and P*ccg-1*::GFP strains (Table 2.1) as described in Chapter 2 and were

run on a 10% SDS- polyacrylamide (30:1) gel to check the purity. To test protein-DNA binding, the purified CRZ-1::5xGly::V5::GFP protein with concentration 3.2 mg/ml was incubated with the respective DNA probes (i), (iv), (vi), (vii), and (viii) of 240 µg/ml, 320 µg/ml, 720 µg/ml, 160 µg/ml and 200 µg/ml concentrations respectively along with EMSA 5 X binding buffer composition of which has been provided in Chapter 2 as provided in the EMSA kit for 2 h at 30 °C**.** Protein-DNA complexes were resolved in a 5% non-denaturing polyacrylamide (30:0.8)/1X TBE gel at 180 volts for 25 min in 1 X TBE running buffer and stained with SYBR® Green provided with the EMSA kit. The gel was visualized in a gel doc (Bio-Print ST4, Vilber Lourmat, France). Band shifts were observed only for the probes I (174 bp), IV (331 bp), and VII (161 bp) in the EMSA (Fig. 5.7). Therefore, CRZ-1 binds to multiple sites located within the174 bp (I) and 161 bp (VI) fragments within the 331 bp larger fragment (IV) in the promoter of *hsp80* (Fig. 5.5) where binding has been observed earlier in ChIP.

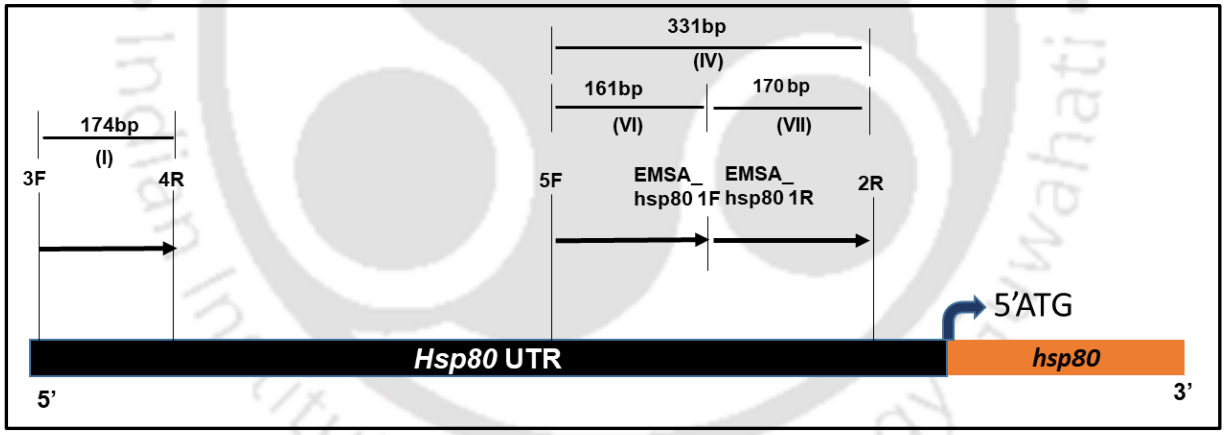

Fig. 5.5 Schematic representation showing the position of the PCR primers to map the CRZ-1 binding sequence in the fragments I and IV of the *hsp80* promoter. The primers, indicated using arrows, were used for PCR amplification of four different DNA probes, (I), (IV), (VI), and (VII) of indicated size (bp) for the EMSA.

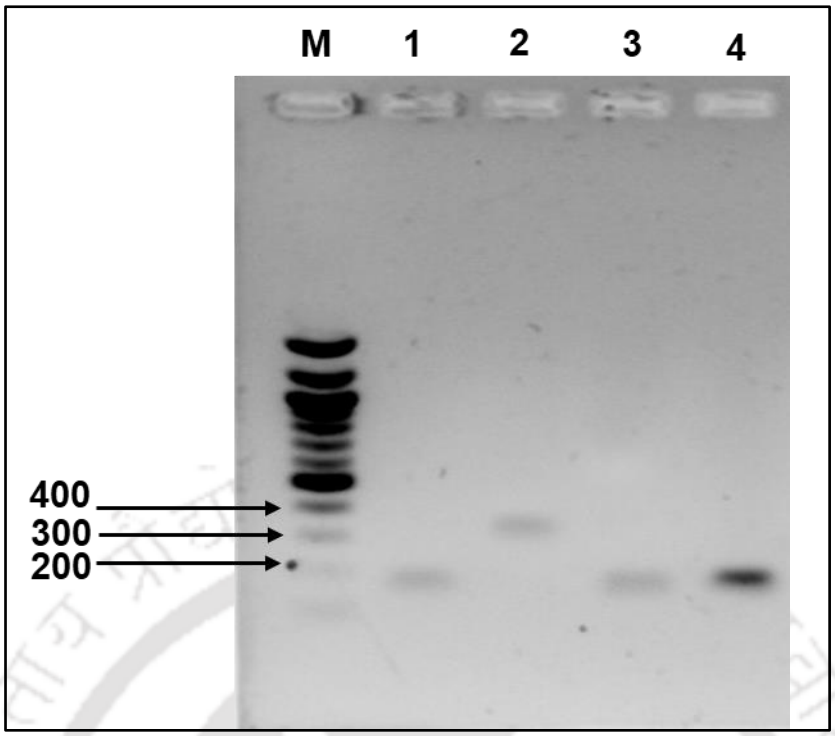

Fig. 5.6 Verification of the DNA probes for binding to the promoter of *hsp80* obtained by PCR. The four DNA probes (i), (iv), (vi), and (vii) were obtained by PCR amplification using the *N. crassa* wild type (FGSC4200) genomic DNA as a template and the primers 3F, 4R, 5F, EMSA_hsp80 1R, EMSA_hsp80 1F, and 2R in appropriate combination same as shown in Fig. 5.5. The probes were verified by running on a 1.2 % agarose gel using 100 bp NEB DNA ladder (New England Biolabs, USA) indicated as M. Lanes 1, 2, 3, and 4 indicate the DNA probes I, IV, VI, and VII, respectively.

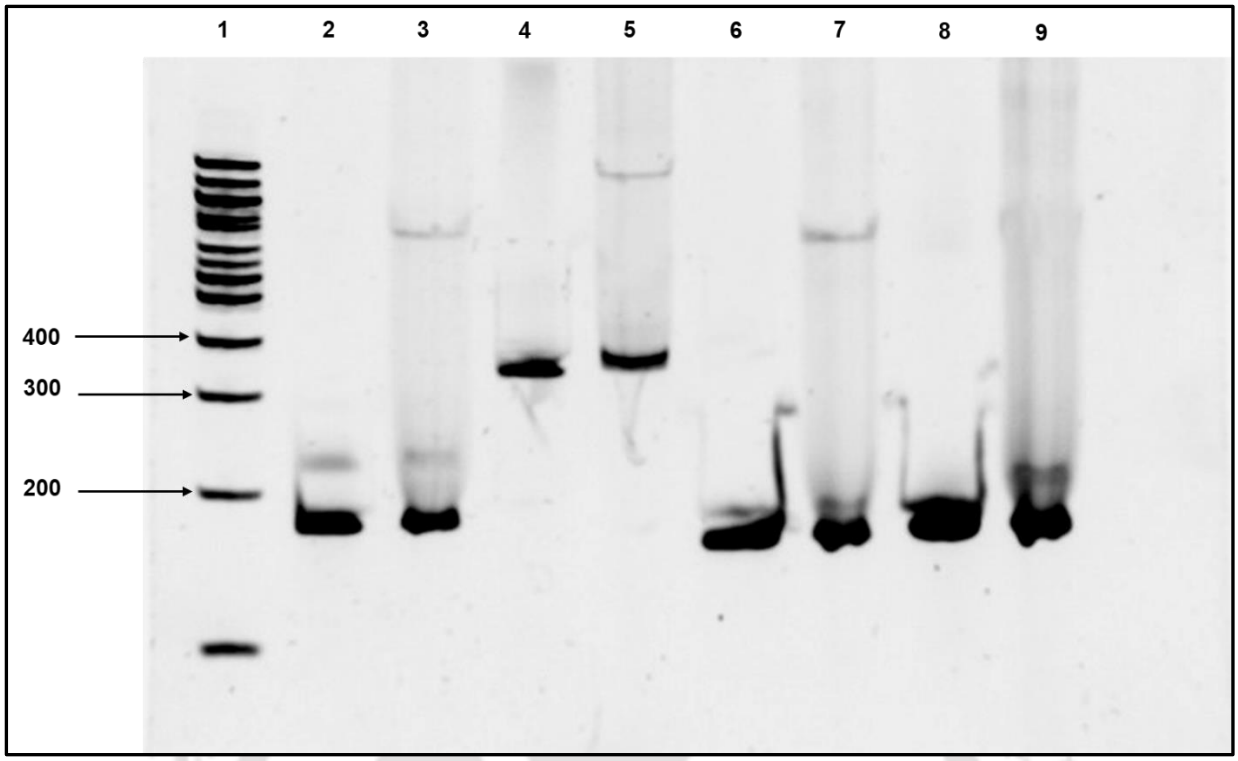

Fig. 5.7 CRZ-1 binding to the specific DNA probes in the promoter of *hsp80*. The 100 bp DNA ladder (lane 1; New England Biolabs, USA), DNA probes only controls (lanes 2, 4, 6, and 8), and the reaction mixture containing both the DNA probe and the CRZ-1::5xGly::V5::GFP protein (lanes 3, 5, 7, and 9) were resolved in a 5% non-denaturing polyacrylamide gel and stained with SYBR® Green. The DNA probe I (lanes 2 and 3), IV (lanes 4 and 5), VI (lanes 6 and 7), and VII (lanes 8 and 9) were used either alone or with the protein as described above. The gel shifts were observed for the probes I of 174 bp (lane 3) and VI of 161 bp (lane 7), which falls within the larger probe IV of 331 bp, which has also shown a shift (lane 5); hence it maps that CRZ-1::5xGly::V5::GFP protein has two binding regions in the *hsp80* promoter.

5.2.3 Prediction of the nucleotide binding sites of CRZ-1 in the promoter of *hsp80* for designing duplex probes

The EMSA revealed that the CRZ-1 binding site in the *hsp80* promoter is located within the 174 bp and 331 bp fragments upstream of start codon ATG. To identify the specific nucleotide sequence essential for CRZ-1 binding within this 174 bp and 331 bp regions in the *hsp80* promoter, 10 putative binding sites of 8 bp in size were predicted (Table 5.1) using the online tool "DNA binding site predictor for Cys_2His_2 Zinc Finger Proteins" (http://zf.princeton.edu; Persikov *et al.*, 2008; Persikov and Singh, 2013). Based on the predicted results (Table 5.1), I designed two 30 bp duplex DNA probes (Fig. 5.8) containing the first two putative nucleotide sequences with the highest support vector machine (SVM) score and the lowest *p*-value for performing the second round of EMSA. Total of four probes were designed of which two were normal probes (1 and 2) the remaining two were mutated probe (3 and 4) which was to be used as negative control. The 30 bp duplex DNA probes were prepared from the complementary primer pairs, Duplex Hsp80_1, Duplex Hsp80_1 comp, Duplex Hsp80_2, Duplex Hsp80_2 comp, Duplex Hsp80_1 Mut, Duplex Hsp80_1 Mut comp, Duplex Hsp80_2 Mut and Duplex Hsp80_2 Mut comp (Table 2.2) as described in Chapter 2. The duplex probes were run on a 20% non-denaturing polyacrylamide (30:0.8)/1 X TBE gel at 200 volts for 1 h in 1 X TBE running buffer and stained with EtBr to test whether the probes were generated properly (Fig. 5.9).

Table. 5.1 CRZ-1 binding regions in *hsp80* promoter scored by linear SVM

DNA Binding regions (5′ → 3′)	Sequential position in original DNA	SVM score	p-Value
CGCGCAGC	89-96	15.8457	0.000
AGCGGAGC	485-492	12.5510	0.000

CCTGCGGA	569-576	10.5510	0.001
CCTGCCCC	475-482	10.2435	0.004
GCTGCCCA	207-214	10.0202	0.004
TCTGCCCA	196-203	10.0202	0.004
GCTGCCCT	747-754	10.0202	0.004
AGCCCAGG	701-708	9.8283	0.005
AGCGCAAG	542-549	9.4583	0.006
TGTGAAGG	273-280	9.3403	0.006

p-values were calculated using following background nucleotide Probabilities-*P*(a)=0.2500: *P*(c)=0.2500: *P*(g)=0.2500: *P*(t)=0.2500

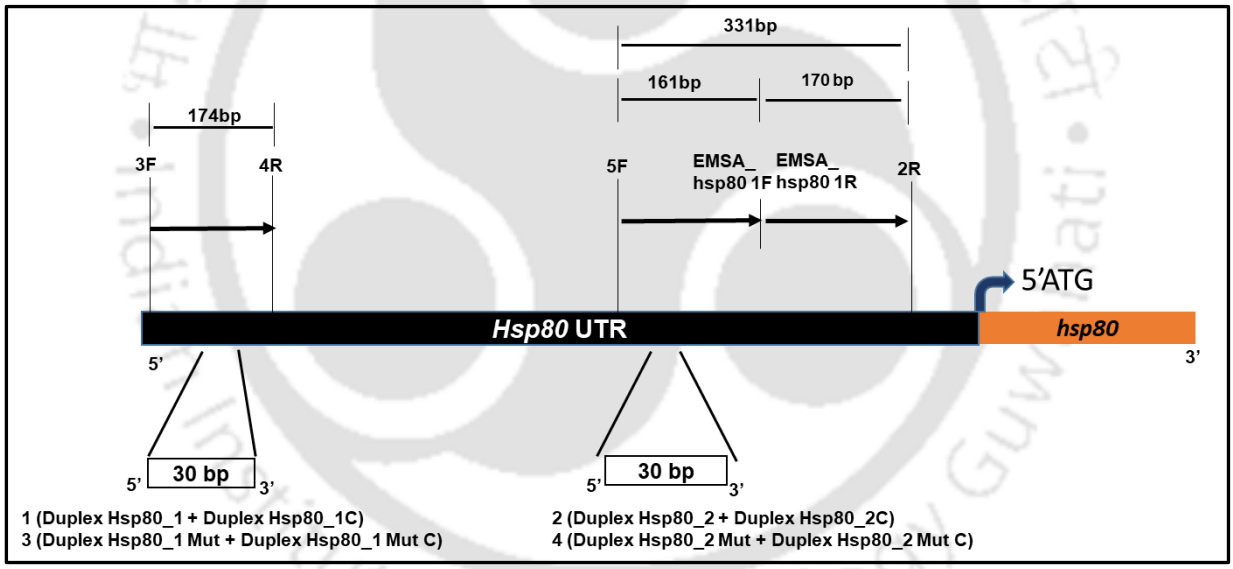

Fig. 5.8 Schematic representation of the position for the duplex DNA probes in the CRZ-1 binding fragments of size 174 bp and 161 bp in the *hsp80* promoter. The positions of the two duplex DNA probe 1 and 2 of 30 bp each is indicated below the *hsp80* promoter. The position of mutated probes 3 and 4 are the same as that of 1 and 2. The primers to obtain each of the probes are indicated in the parentheses for the respective probe.

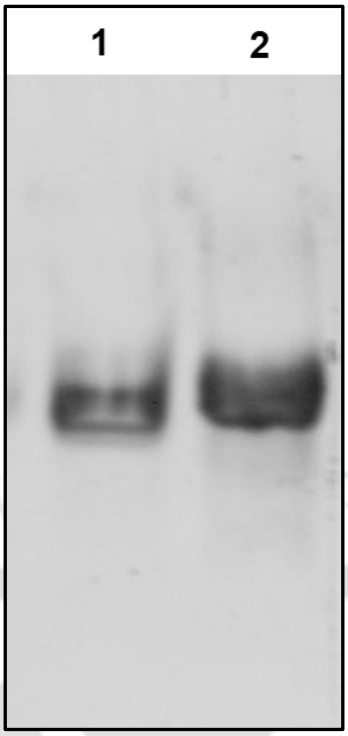

Fig. 5.9 Verification of the synthesis of the duplex DNA probes to identify the CRZ-1 binding site upstream of *hsp80*. The two 30 bp DNA probes were run on a 20% non-denaturing polyacrylamide (30:0.8)/1 X TBE gel at 200 volts for 1 h in 1 X TBE running buffer and visualized using ethidium bromide (EtBr) staining. Lanes 1, 2 were loaded with probes 1 and 2, respectively, and a single band in each lane shows the successful synthesis of probes.

5.2.4 Identification of an 8 bp fragment essential for the CRZ-1 binding to the *hsp80* promoter

An EMSA was performed using the purified CRZ-1::5xGly::V5::GFP protein and the respective duplex DNA probes as described in Chapter 2. Additionally, the purified V5::GFP protein was also incubated with the probes as a control. Protein-DNA complexes were resolved in a 20% non-denaturing polyacrylamide (30:0.8)/1 X TBE gel at 200 volts for 1 h in 1 X TBE running buffer and stained with SYBR® Green provided in the EMSA kit. The gel was visualized in a Gel Doc (Bio-Print ST4, Vilber Lourmat, France). Band shift was observed for the probes 1 and 2 containing the sequences 5′-CGCGCAGC-3′ and 5′- AGCGGAGC -3′ (Fig.

5.10), suggesting that CRZ-1 has two binding sequences which are present in probes 1 and 2. Furthermore, no shift was observed for either of the probes 3, where 8 bp sequence 5′-CGCGCAGC-3′ mutated to 5′-ATATACTA-3′, or the probe 4, where the 8 bp 5′-AGCGGAGC-3′ nucleotide sequence was mutated to 5′-CTATTCTA-3′ (Fig. 4.15). Therefore, *N crassa* CRZ-1 specifically binds to 8 bp nucleotide sequences 5′-CCTTCACA-3′ and 5′-AGCGGAGC-3′ located 1075 bp and 679 bp upstream of the ATG start codon. Based on the ChIP and EMSA binding results and the expression studies described in the previous section, I concluded that CRZ-1 binds to a specific 8 bp nucleotide sequences in the *hsp80* promoter for transcriptional upregulation of *hsp80* under the heat shock stress.

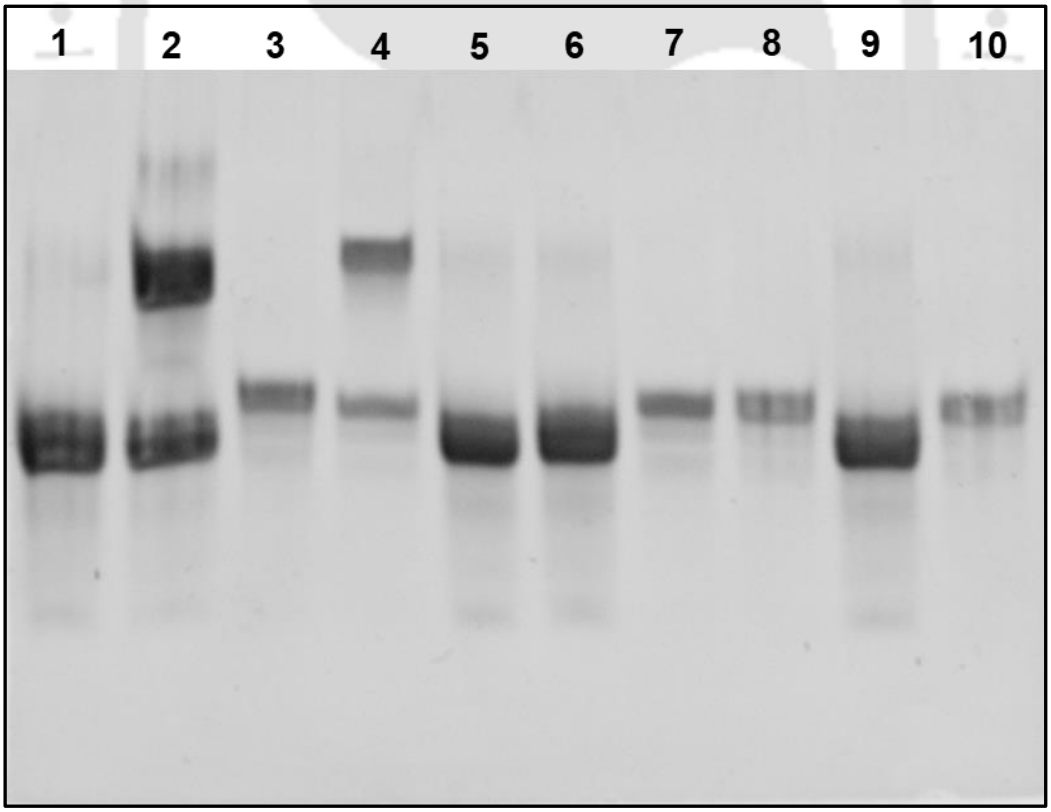

Fig. 5.10 Identification of the CRZ-1 binding sequence in the *hsp80* promoter region. The DNA probes 1and 2 were used alone as controls (lanes 1 and 3, respectively) or together with

the CRZ-1::5xGly::V5::GFP protein (lanes 2 and 4, respectively). Shift was observed when probes 1 and 2 were used together with the protein (lanes 2 and 4), showing that CRZ-1::5xGly::V5::GFP binds to probes 1 and 2, containing the predicted CRZ-1 binding sequence sites 5´-CCTTCACA-3´and 5′-AGCGGAGC-3′. The shift was not observed for probes 3 and 4 containing mutations in the predicted CRZ-1 binding sites (lanes 6 and 8). In lanes 9 and 10, 5xGly::V5::GFP protein with probes 1 and 2 was used as a negative control, and no shift was observed.

5.2.5 CRZ-1 binds to *nca-2* promoter in response to Ca^{2+} stress response

Previous work in our laboratory demonstrated that CRZ-1 is involved in the transcriptional regulation of *ncs-1* under the high Ca^{2+} concentrations (Gohain and Tamuli, 2019). In addition, calcineurin, which dephosphorylates CRZ-1, is also involved in the survival under the high Ca^{2+} concentrations (Gohain and Tamuli, 2019). Furthermore, NCA-2, a Ca^{2+} ATPase, has a distinct role in the uptake of Ca^{2+} in the vacuoles (Bowman et al. 2011) is transcriptionally downregulated when calcineurin is inhibited by FK506 (Fig. 4.11, Chapter 4). Therefore, I designed primer pairs Chip NCA-2 1F and Chip NCA-2 1R (Table 2.2, Chapter 2) to map the CRZ-1 binding regions in the promoter of *nca-2* (Fig. 5.11).

For ChIP analysis, ~1 x 10^6 conidia/ml were inoculated in 50 ml standard VG liquid (0.68 mM), and VG supplemented with 0.2 M $CaCl_2$, and grown for 5 h at 30 ºC with shaking at 180 rpm. Both the growth media were supplemented with 50 µM BCS and 10 µg/ml pantothenic acid. Then 1% formaldehyde was added to the cultures and incubated at room temperature on a rotating platform for 1 h at 30 ºC for chemical crosslinking. To quench the reaction, 125 mM glycine was added and incubated at 30 ºC for 30 min. Germlings were harvested and washed twice with 1X PBS (pH 7.4) and suspended in ChIP lysis buffer. Chromatin was sheared by sonication in a sonicator (Vibra Cell Sonics, USA) on ice. The

parameters for the sonication were 33% amplitude, 8 s ON pulse, 10 s OFF pulse, 120 cycles, and 16 min time. ChIP was performed as described in Chapter 2. The 400 bp region in the *nca-2* promoter was amplified using the PCR primer pairs Chip NCA-2 1F and Chip NCA-2 1R (Table 2.2, Chapter 2; Fig. 5.12) to determine the CRZ-1 binding position in the *nca-2* promoter. The PCR was performed using Phusion® High-Fidelity DNA polymerase (Cat. No. M0530S, New England Biolabs, USA), and the reaction conditions were 98 ºC for 30 s, 25 cycles of 98 ºC for 10 s, 63 ºC for 30 s, and 72 ºC for 30 s, and then 72 ºC for 5 min. The PCR products were run on 1.2% agarose gel containing EtBr (0.5 µg/ml) and visualized in a gel doc (Bio-Print ST4, Vilber Lourmat, France).

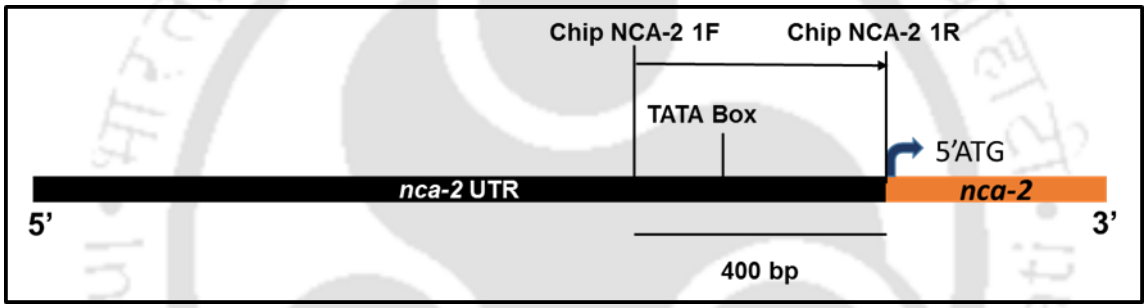

Fig. 5.11 Schematic showing the positions of the primer pairs in the *nca-2* promoter for ChIP analysis. The primers designed to perform PCR for the *nca-2* promoter region using the DNA template obtained in the ChIP are located between the 5′ UTR and the ORF of *nca-2*. The primers Chip NCA-2 1F and Chip NCA-2 1R were used to PCR amplify a fragment of 400 bp size as indicated in the figure.

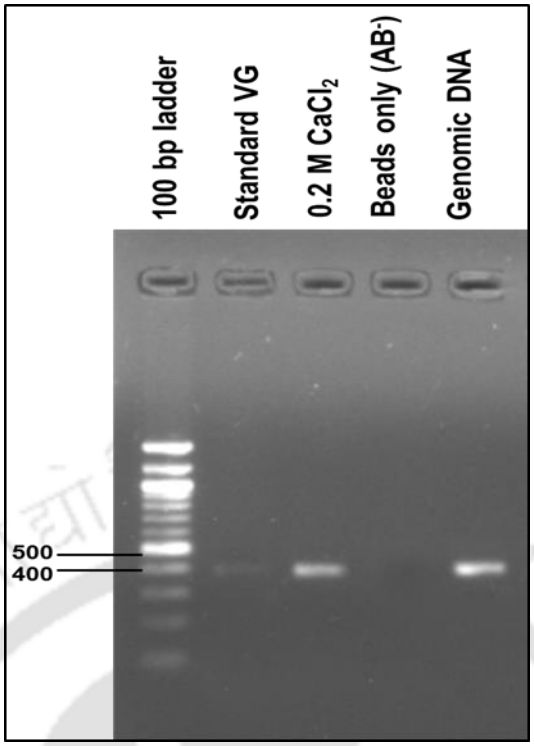

Fig. 5.12 ChIP assay to determine the binding of CRZ-1 to the *nca-2* promoter sequence. PCR products were analyzed using a 1.2% agarose gel to identify the CRZ-1 binding region in the *nca-2* promoter sequence. The analysis of the PCR revealed a positive product for the fragment of 400 bp in size, and the band intensity was further enhanced when the 559 strain was grown in the presence of 0.2 M $CaCl_2$ stress condition. The antibody control (Ab^-) indicates the control PCR for the sample, where only beads were used for immunoprecipitation. The wild type genomic DNA has used a positive PCR control for amplification.

In the ChIP analysis, positive PCR bands were observed for the 400 bp fragment, amplified using the primers Chip NCA-2 1F and Chip NCA-2 2R, respectively (Fig. 5.12). The band intensity of the positive ChIP was ~3-fold higher than the control strain grown in standard VG containing 0.68 mM $CaCl_2$. This confirmed that the CRZ-1 transcription factor binds to the *nca-2* promoter, thereby plays a role in the calcineurin mediated Ca^{2+} stress tolerance pathway mediated.

5.2.6 The electrophoretic mobility shift assay revealed that the CRZ-1 binding site located upstream of the TATA box in the *nca-2* promoter

The ChIP assay revealed that the CRZ-1 transcription factor binds to the *nca-2* promoter, and the binding increases with the increasing Ca^{2+} concentration. Furthermore, I performed an electrophoretic mobility shift assay (EMSA) to identify the CRZ-1 binding sequence. EMSA was performed using a Molecular probes™ EMSA Kit (Cat No. E33075, Life Technologies, USA) as per the manufacturer's protocol. The TATA box, present 359 bp upstream of the start codon (ATG), is within the 400 bp fragment identified by the ChIP analysis (Fig. 5.12). I designed three DNA probes of sizes 400 bp, 220 bp, and 179 bp for EMSA. (Fig. 5.13). The TATA box falls within the 220 bp fragment of the total 400 bp candidate region earlier identified for CRZ-1 binding in ChIP (Fig. 5.12), and the remaining 179 bp fragment lies downstream of the TATA box (Fig. 5.13). The DNA probes were prepared by PCR from the wild type *N. crassa* genomic DNA using the PCR primers Chip NCA-2 1F, Chip NCA-2 2R, Chip NCA-2 1F, EMSA NCA-2 Rv, EMSA NCA-2 Fw, and Chip NCA-2 2R (Fig. 5.14) in appropriate pairs (Table 2.2, Chapter 2), using Phusion® High-Fidelity DNA polymerase (Cat. No. M0530S, New England Biolabs, USA). The PCR products were analyzed in a 1.2% agarose gel, and then purified by using a PCR Purification Kit (Cat. No. 28104, Qiagen, Germany). The CRZ-1::5xGly::V5::GFP (~105 kDa) and V5::GFP (~28 kDa) proteins were isolated and purified from the 559 and P*ccg-1*::GFP strains (Table 2.1) as described in Chapter 2. To test protein-DNA binding, ~ 4.8 mg/ml of the purified CRZ-1::5xGly::V5::GFP protein was incubated with the respective DNA probes (I), (II), and (III) at a concentration of 161 µg/ml, 224 µg/ml, and 320 µg/ml, respectively, along with EMSA 5 X binding buffer (described in Chapter 2) for 2 h at 30 °C**.** Protein-DNA complexes were resolved in a 5% non-denaturing polyacrylamide (30:0.8)/1 X TBE gel at 180 volts for 25 min in 1 X TBE running buffer and stained with SYBR® Green provided with the EMSA Kit. The gel was visualized

in a Gel Doc (Bio-Print ST4, Vilber Lourmat, France). Band shifts were observed only for the probes I (400 bp) and II (220 bp) in the EMSA (Fig. 5.15). Therefore, CRZ-1 binding site is located within the 220 bp fragment, which includes the TATA box, upstream of the *nca-2* promoter.

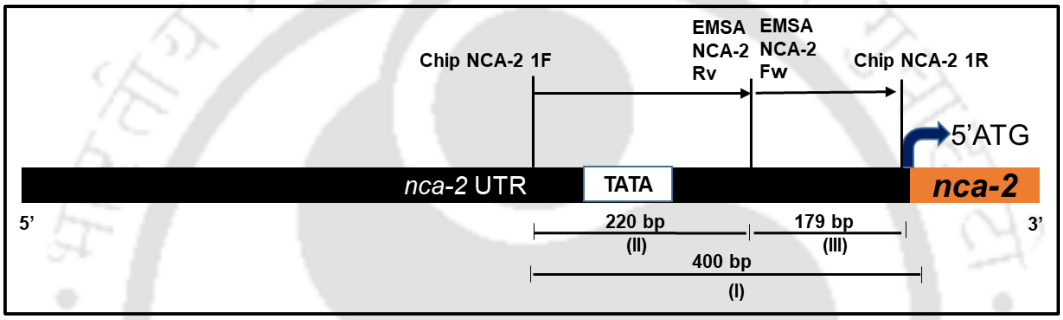

Fig. 5.13 Schematic showing the position of the PCR primers to map the CRZ-1 binding sequence in the *nca-2* promoter. The primers, indicated using arrows, were used for PCR amplification of three different DNA probes (I), (II), and (III) of indicated size (bp) for the EMSA. The relative position of the TATA box with respect to the primer position is shown.

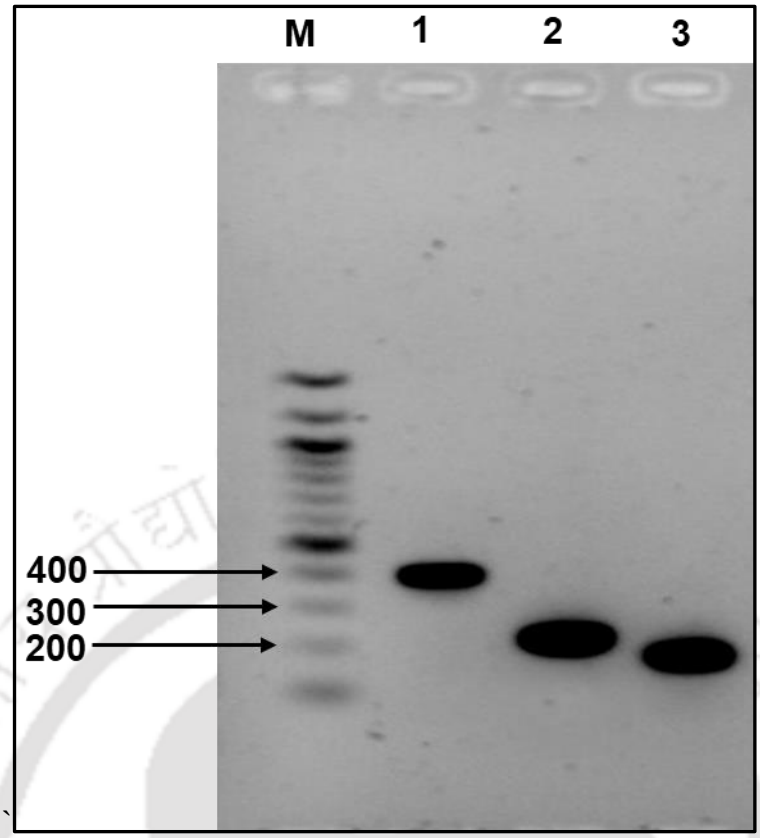

Fig. 5.14 PCR verification of the DNA probes for binding to the *nca-2* promoter. The three DNA probes (I), (II), and (III) were PCR amplified using the *N. crassa* wild type (FGSC 4200) genomic DNA as a template and the primers Chip NCA-2 1F, Chip NCA-2 2R, Chip NCA-2 1F, EMSA NCA-2 Rv, EMSA NCA-2 Fw and Chip NCA-2 2R in appropriate combination as shown in the Fig. 5.13. The PCR-amplified probes were verified by running on a 1.2% agarose gel. Lane M indicates 100 bp NEB DNA ladder (New England Biolabs, USA). Lanes 1, 2, and 3 indicate the DNA probes I, II, and III, respectively.

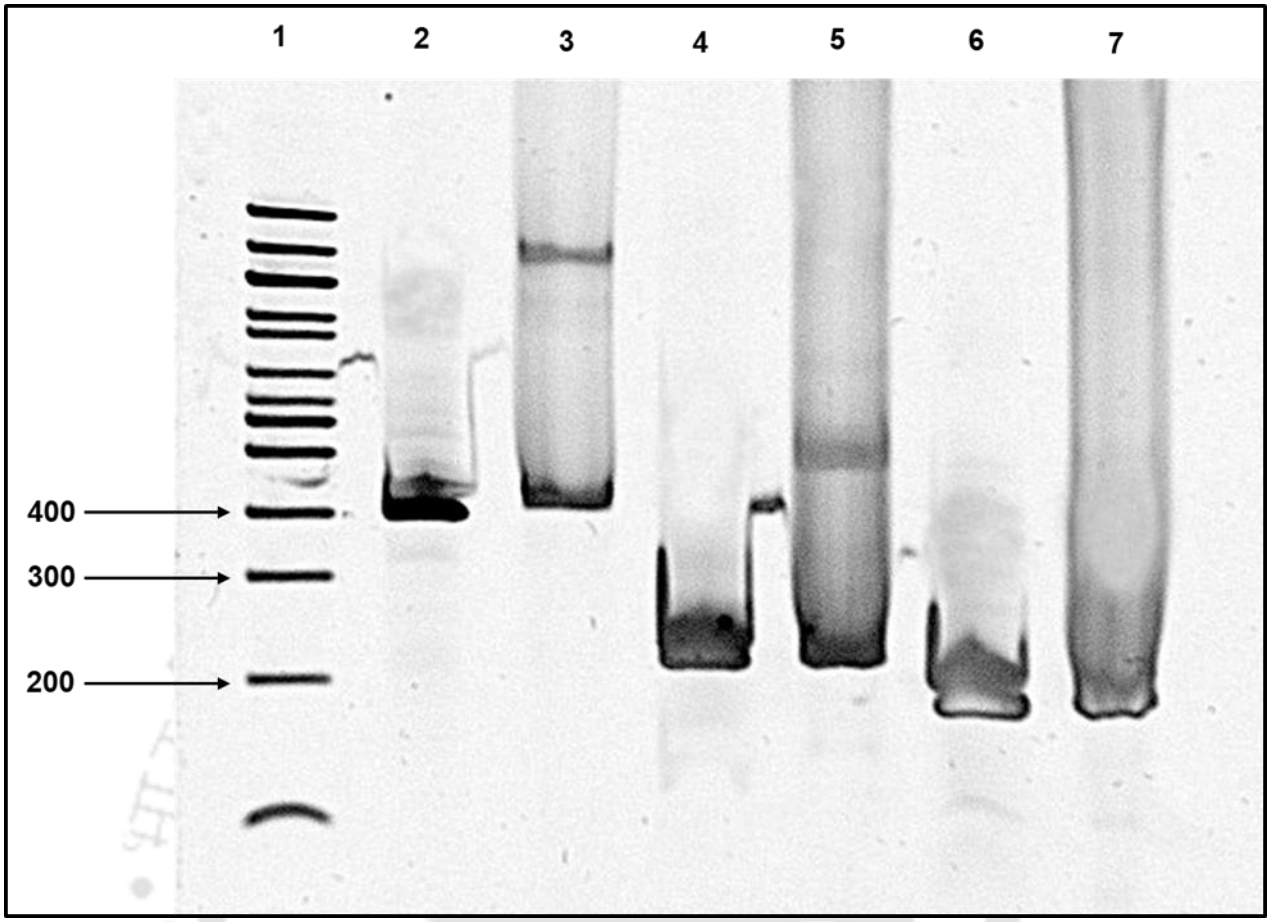

Fig. 5.15 CRZ-1 binding to the specific DNA probe in the promoter of *nca-2*. The 100 bp DNA ladder (New England Biolabs, USA) (lane 1), DNA probes only controls (lanes 2, 4, and 6), and the reaction mixture containing both the DNA probe and the CRZ-1::5xGly::V5::GFP protein (lanes 3, 5, and 7) were resolved in a 5% non-denaturing polyacrylamide gel and stained with SYBR® Green. The DNA probe I (lanes 2 and 3), II (lanes 4 and 5), and III (lanes 6 and 7) were used either alone or with the protein as described above. The gel shifts were observed for probes I comprising of entire 400 bp candidate region in ChIP (lane 3) and II of 220 bp (lane 5), which further maps the CRZ-1::5xGly::V5::GFP protein binding region in the *nca-2* promoter.

5.2.7 Prediction of the nucleotide binding sites of CRZ-1 in the promoter of *nca-2* for designing duplex probes

The EMSA revealed that the CRZ-1 binding site in the *nca-2* promoter is located upstream of start codon ATG within the 220 bp fragment and the TATA box falls within this fragment. To identify the specific nucleotide sequence essential for CRZ-1 binding within this 220 bp region in the *nca-2* promoter, 10 putative binding sites of 8 bp in size were predicted (Table 5.2) using the online tool "DNA binding site predictor for Cys_2His_2 Zinc Finger Proteins" (http://zf.princeton.edu; Persikov *et al.*, 2008; Persikov and Singh, 2013). Based on the predicted results (Table 5.2), I designed two 30 bp duplex DNA probes (Fig. 5.16) containing the first two putative nucleotide sequences with the highest support vector machine (SVM) score and the lowest *p*-value for performing the second round of EMSA. Among the four probes, two were normal probes (A and B) the remaining two were mutated probe (C and D) which was to be used as negative control. The 30 bp duplex DNA probes were prepared from the complementary primer pairs, Duplex NCA-2_1 and Duplex NCA-2_1C, Duplex NCA-2_1, Duplex NCA-2_2C, Duplex NCA-2_Mut 1 and Duplex NCA-2_Mut 1C (Table 2.2) as described in Chapter 2. The duplex probes were run on a 20% non-denaturing polyacrylamide (30:0.8)/1 X TBE gel at 200 volts for 1 h in 1 X TBE running buffer and stained with EtBr to test whether the probes were generated properly (Fig. 5.17).

Table. 5.2 CRZ-1 binding regions in *nca-2* promoter scored by linear SVM

DNA Binding regions (5′ → 3′)	Sequential position in original DNA	SVM score	p-Value
ACCGCGCC	158-165	15.8457	0.000
TGCGCAGC	279-286	13.9859	0.000
TCTCCGCT	30-37	12.5510	0.001

ACTGCCA	97-104	10.0202	0.003
TCTGCCCT	271-278	10.0202	0.003
CTTGCGCA	277-284	9.4583	0.005
CCTGAGCT	212-219	8.6034	0.007
GCTGAGCA	217-224	8.3801	0.008
GCAACGCG	222-229	8.0419	0.009
AGTTCGCC	206-213	7.4007	0.011

p-values were calculated using following background nucleotide Probabilities-*P*(a)=0.2500: *P*(c)=0.2500: *P*(g)=0.2500: *P*(t)=0.2500

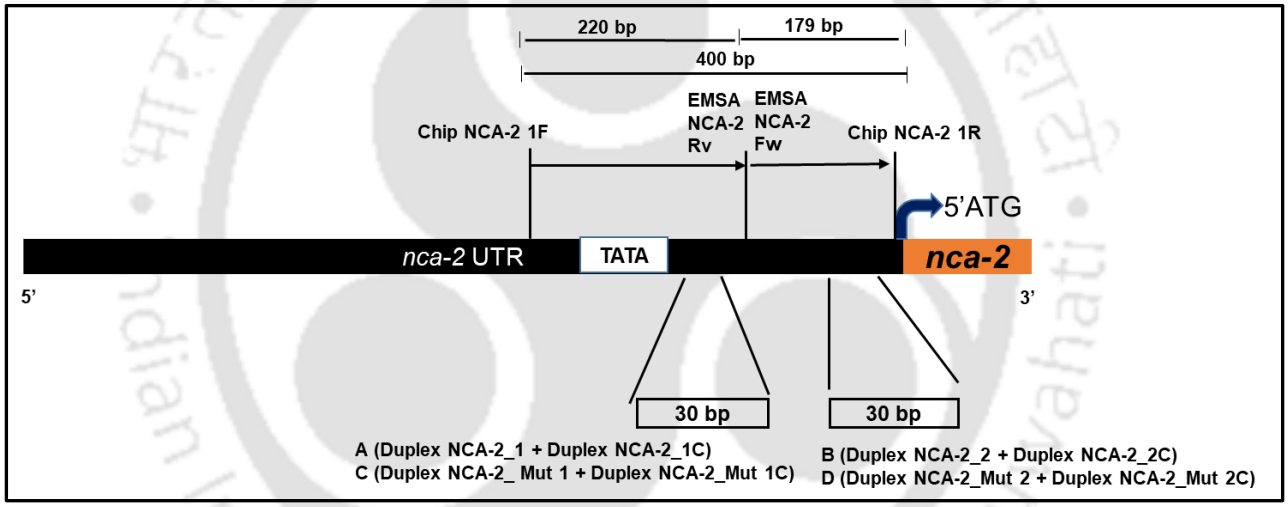

Fig. 5.16 Schematic showing the position of the duplex DNA probes in the CRZ-1 binding 147 bp fragment of the *nca-2* promoter. The positions of the two duplex DNA probe A and B of 30 bp each are indicated below the *nca-2* promoter. The position of mutated probes C and D is the same as that of A and B. The primers to obtain each of the probes are indicated in the parentheses for the respective probe.

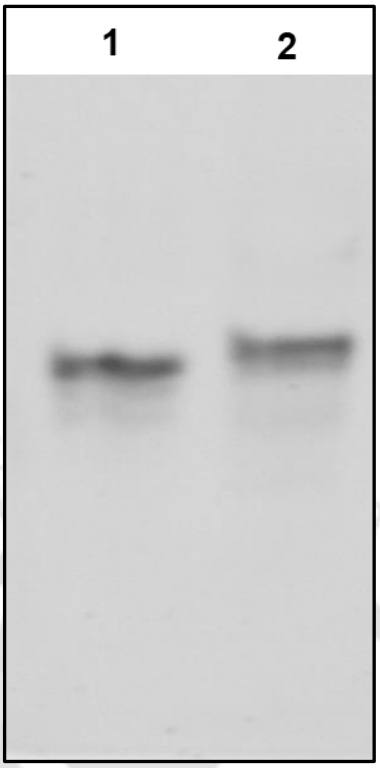

Fig. 5.17 Verification of the synthesis of the duplex DNA probes to identify the CRZ-1 binding site upstream of *nca-2*. The three 30 bp DNA probes were run on a 20% non-denaturing polyacrylamide (30:0.8)/1 X TBE gel at 200 volts for 1 h in 1 X TBE running buffer and visualized using ethidium bromide (EtBr) staining. Lanes 1 and 2 were loaded with probes A and B, respectively, and a single band in each lane shows the successful synthesis of all the probes.

5.2.8 Identification of an 8 bp fragment essential for the CRZ-1 binding to the *nca-2* promoter

An EMSA was performed using the purified CRZ-1::5xGly::V5::GFP protein and the respective duplex DNA probes as described in Chapter 2. Additionally, the purified V5::GFP protein was also incubated with the probes as a control. Protein-DNA complexes were resolved in a 20% non-denaturing polyacrylamide (30:0.8)/1 X TBE gel at 200 volts for 1 h in 1 X TBE running buffer and stained with SYBR® Green provided in the EMSA Kit. The gel was visualized in a Gel Doc (Bio-Print ST4, Vilber Lourmat, France). Band shift was observed for

the probe A containing the sequence 5′-ACCGCGCC-3′ (Fig. 5.18), suggesting the CRZ-1 binding to the probe A. Furthermore, no shift was observed either for the probe B containing the 8 bp sequence 5′-TGCGCAGC-3′, or the probe C in which the 8 bp 5′- ACCGCGCC-3′ nucleotide sequence was mutated to 5′-CAATATAA-3′ and the probe D in which the probe B was mutated to the sequence 5′-GTATACTA-3′ (Fig. 5.18). Thus, *N crassa* CRZ-1 specifically binds to an 8 bp nucleotide sequence 5′-ACCGCGCC-3′, located 234 bp upstream of the ATG start codon. Therefore, extrapolating the data from the expression studies discussed in Chapter 4, ChIP and EMSA assays, I concluded that binding of CRZ-1 binds to the promoter of *nca-2* thereby upregulates its expression during Ca^{2+} stress.

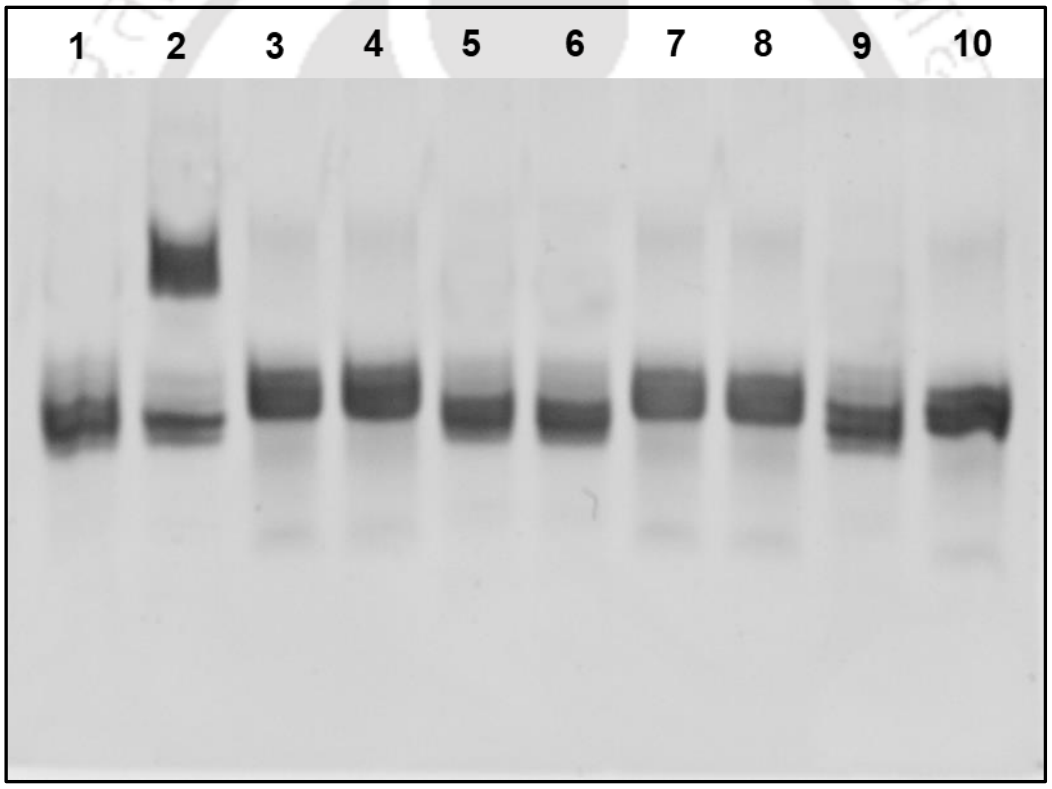

Fig. 5.18 Identification of the CRZ-1 binding sequence in the *nca-2* promoter region. The DNA probes A, B, C, and D were used alone as controls (lanes 1, 3, 5, and 7, respectively) or together with the CRZ-1::5xGly::V5::GFP protein (lanes 2, 4, 6, and 8, respectively). A shift was observed when probe A was used together with the protein (lane 2), showing that CRZ-1::5xGly::V5::GFP binds to probe A that contains the predicted CRZ-1 binding sequence site

5′-ACCGCGCC-3′. The shift was not observed either for the probe B having the sequence 5′-TGCGCAGC-3′ or probe C containing mutations in the predicted CRZ-1 binding site as mentioned in probe A (lanes 4 and 6). No binding was observed in lane 8 containing probe D, which is the mutated version of probe B. In lane 9, 5xGly::V5::GFP protein with probe A and was used as a negative control, and no shift was observed. Similarly, in lane 10, 5xGly::V5::GFP protein with probe B was used, and there was no shift.

5.3 Discussion

In this Chapter, I discussed the molecular mechanism of heat shock and Ca^{2+} stress tolerance via the calcineurin-CRZ-1 signaling pathway in *N. crassa*. The ChIP analysis revealed that CRZ-1, a transcription factor activated by calcineurin, binds to the promoter of *hsp80*, thereby upregulates its expression during heat shock stress tolerance. In addition, ChIP analysis revealed that CRZ-1 binds to the promoter of *nca-2* in response to Ca^{2+} stress. The NCA-2 Ca^{2+} ATPase transporter assists in sequestering Ca^{2+} into the vacuoles, thereby maintain Ca^{2+} homeostasis (Bowman et al. 2009, 2011). Therefore, upregulation of *nca-2* expression during Ca^{2+} stress would be necessary to maintain resting level of $[Ca^{2+}]_c$ in response to cellular stresses for Ca^{2+} homeostasis and cell survival.

Studies in *S. cerevisiae* showed that dephosphorylation of CRZ-1 homolog *TCN1/CRZ-1* causes its nuclear localization and regulates the transcription of the target genes under different cellular stress conditions (Stathopoulos and Cyert, 1997). In *N. crassa*, the binding intensity of CRZ-1 to the promoters of both *hsp80* and *nca-2* were increased under heat shock and with an increased concentration of Ca^{2+}. Earlier experimental evidences proved the interaction of Hsp90 with Cna-1 in *C. albicans*, and the calcineurin signaling cascade has been targeted for antifungal drug development (Gong et al. 2017). I described in the Chapter 4 that in *N. crassa*, HSP80, belonging to the family of HSP90, is upregulated under heat shock

conditions. Moreover, to understand the molecular mechanism of HSP80 upregulation, I mapped the promoter of *hsp80* using ChIP analysis and identified two regions of 174 bp and 331 bp, which are ~1167 bp and ~ 679 bp upstream of the ATG start codon, responsible for CRZ-1 binding under heat shock conditions (Fig. 5.2). However, CRZ-1 binding to the *hsp60* promoter was not observed (Fig. 5.4). Furthermore, I performed EMSA, and identified two separate CRZ-1 binding sequences 5´-CCTTCACA-3´ and 5′-AGCGGAGC-3′, located in the 174 bp and 331 bp upstream of *hsp80* (Fig. 5.10). In general, transcription factors may have multiple binding sites within the promoter of specific target genes to regulate different cell functions. Earlier, computational studies in *S. cerevisiae* revealed that a single transcription factor can have more than one binding sites in the promoter without a specific consensus sequence (Harbison et al. 2004). The Reb1 transcription factor in *S. cerevisiae* binds to many different genes, but, there was a deviation in the consensus sequence, and more the number of binding sites on the same promoter greater is the deviation (Bilu and Barkai, 2005). A similar trend was observed in the CRZ-1 binding sites on the *hsp80* promoter, and altogether the binding sequences differed from the consensus sequence GTGGCTG found in the promoter analysis of *hsp80* as discussed in Chapter 4. Moreover, the *N. crassa* calcineurin dependent response element (CDRE) sequence - 5′-AGCCTC-3′ (Kumar et al. 2006) was not observed in the promoter of *hsp80*. Therefore, it indicates that the binding sites for the same transcription factor may vary across the genes within the same species.

The *cnb-1* also has a role in Ca^{2+} stress tolerance (discussed in Chapter 3), the growth rate of the *cnb-1*^{RIP} mutants decreases with increasing concentrations of Ca^{2+} in comparison with the wild type strain (Kumar et al. 2019). Previously, studies in our laboratory on the molecular mechanism of the Ca^{2+} stress tolerance revealed that CRZ-1 upregulates the *ncs-1* during Ca^{2+} stress by binding to an 8 bp nucleotide sequence 5′-CCTTCACA-3′ in the promoter, located about 216 bp upstream of the ATG start codon (Gohain and Tamuli, 2019).

Moreover, it was also hypothesized that CRZ-1 might upregulate the *nca-2* expression binding to its promoter (Gohain and Tamuli, 2019). I performed the expression studies of *nca-2* in the *cnb-1*^{RIP} mutants and the wild type strains using the calcineurin inhibitor FK506 (discussed in Chapter 4), and the expression data were consistent with the phenotypic data of the *cnb-1*^{RIP} mutants in response to Ca^{2+} stress (Kumar et al. 2019). Furthermore, I mapped the promoter of *nca-2* by ChIP analysis to locate the probable CRZ-1 binding sites and found that CRZ-1 binds to a 400 bp region upstream of ATG start codon and containing the TATA box (Fig. 5.12), and the binding intensity was enhanced with the increasing concentrations of Ca^{2+}. Further, to determine the nucleotide sequence of the CRZ-1 binding site, EMSA was performed and an 8 bp 5′-ACCGCGCC-3′ sequence located 234 bp upstream of ATG start codon was found necessary for the binding of CRZ-1 to the *nca-2* promoter (Fig. 5.18). However, the 5′-ACCGCGCC-3′ sequence differs from the 5'-[G/A]CACAGC[C/A]AC-3', (5'-GAAGATG[A/G]T[G/A]-3') CDRE sequences predicted for CRZ-1 binding to different stress response genes in *C. neoformans* (Chow et al. 2017). Therefore, taken together, it can be concluded that the CRZ-1 binding motifs vary in different species, and unique for a particular stress response gene regulating the cellular functions under stress conditions.

Finally, on the basis of the above described results, I derived a probable model governing the regulation of *hsp80* and *nca-2* via calcineurin-CRZ-1 pathway (Fig. 5.19). During the heat stress or Ca^{2+} stress, the influx of Ca^{2+} increases in the cytoplasm via the Ca^{2+}-ATPase transporters and the Ca^{2+} channel proteins such as NCA-2, present in the plasma membrane. When $[Ca^{2+}]_c$ rises above a threshold level of about 1 mM, then the Ca^{2+} signaling machinery gets activated, and the Ca^{2+} binds to one of the Ca^{2+} sensor CaM, which then activates calcineurin complex. The activated calcineurin dephosphorylates its downstream target CRZ-1, which shuttles into the nucleus from the cytoplasm to bind the promoter of both *hsp80* and *nca-2* at 679 and 234 bp, respectively, upstream of the ATG start codon. The HSP80

is necessary for cell survival under the thermotolerance condition. On the other hand, activated NCA-2 transports the excess Ca^{2+} into the internal store, including vacuoles, and also exports excess Ca^{2+} out of the cell to maintain Ca^{2+} homeostasis inside the cell (Bowman *et al.* 2009, 2011; Zelter et al. 2004). The calcineurin inhibitor FK506 disrupts calcineurin signaling, resulting in reduced expression of *nca-2*, *cnb-1*, *hsp80*, and *crz-1*. In *A. fumigatus*, *C. albicans*, and *C. neoformans*, HSP90 is necessary to confer antifungal drug resistance (Cordeiro Rde et al. 2016; Lamoth et al. 2016; Chatterjee and Tatu, 2017). Therefore, HSP90 could be a new target for increasing the efficacy of antifungal drugs. In *N. crassa*, HSP80 belongs to the HSP90 family of heat shock proteins and shares about 100% structural similarity to HSP90-domain containing protein, however, detailed information regarding the HSP80 regulation was remained limited (Galagan et al. 2003). Therefore, our findings will shed light on the regulation of HSP80 information in future, targeting the pathway of calcineurin-CRZ-1 mediated activation of HSP80, may unravel new strategies to combat the increasing drug resistance in different pathogenic fungi.

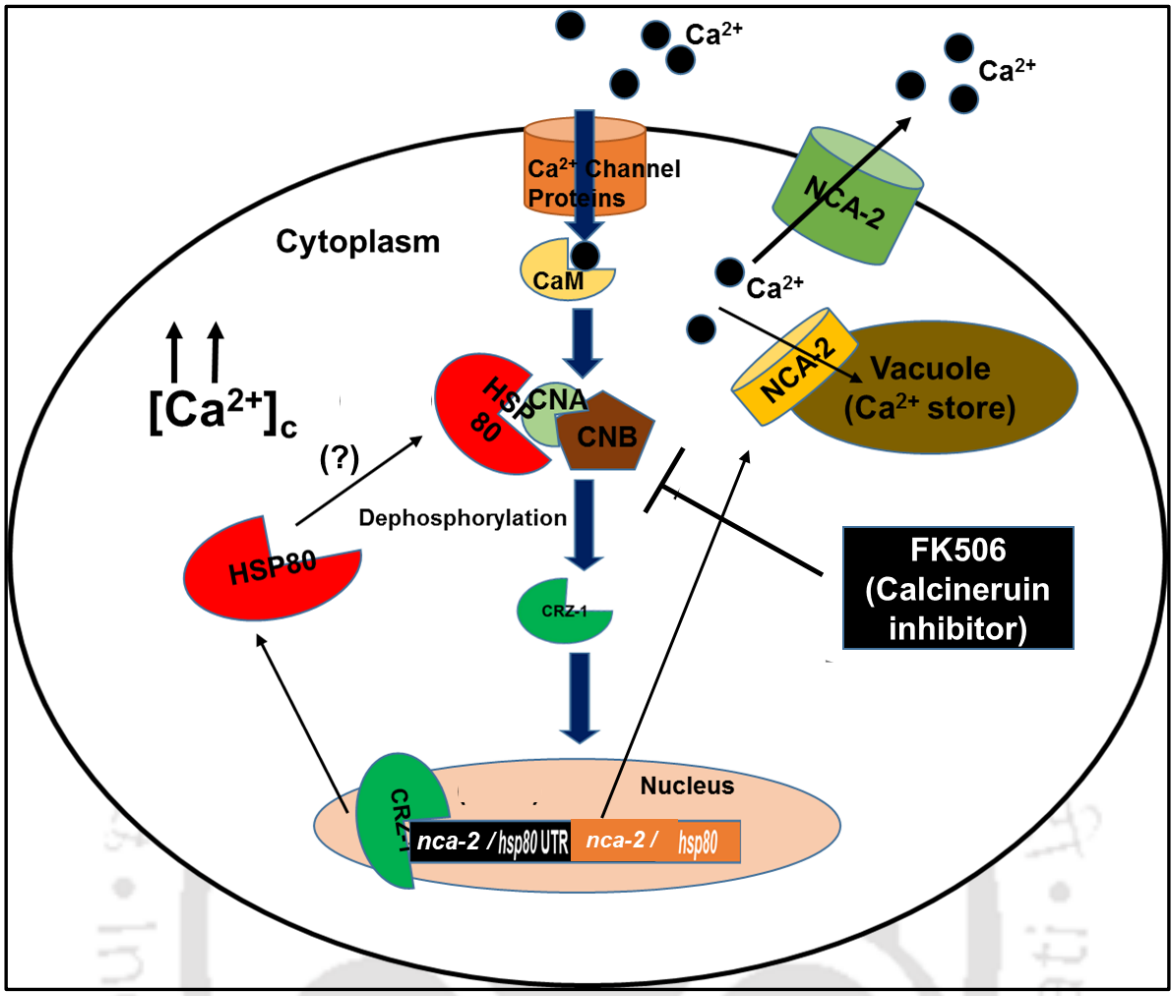

Fig. 5.19 Model depicting the mechanism of HSP80 and NCA-2 via calcineurin-CRZ-1 pathway in response to heat shock and Ca^{2+} stress tolerance in *N. crassa*. Ca^{2+} influx through Ca^{2+} channel proteins increase the level of $[Ca^{2+}]_c$ during stress conditions. Calmodulin, activated by $[Ca^{2+}]_c$, activates calcineurin, which dephosphorylates CRZ-1. Dephosphorylated CRZ-1 enters in the nucleus and increases the transcription of *hsp80 and nca-2*. The FK506, a calcineurin inhibitor, inhibits the activation of *hsp80* and *nca-2* by shutting down the calcineurin mediated activation of CRZ-1. Hsp80, after activated by $[Ca^{2+}]_c$, may shuttle into the cytoplasm, and might interact with CNA-1 for its activation as shown in *C. albicans* (Gong et al. 2017). NCA-2, another target of CRZ-1, also contributes to Ca^{2+} stress tolerance by pumping Ca^{2+} out of the cell and presumably into vacuole to reduce $[Ca^{2+}]_c$ (Bowman et al. 2009, 2011; Deka and Tamuli, 2013). A possible interaction between HSP80

and CNA-1, which has not yet been established in *N. crassa*, is indicated using question marks in the parentheses.

A part of the results described in this Chapter was presented as a poster and flash Talk in the (i) 11th International Conference on Biology of Yeast and Filamentous Fungi, University of Hyderabad, India, 26-29 November, 2019, and (ii) EMBO Symposium on Calcium signaling: Molecular mechanisms to role in health and diseases, National Center for Biological Sciences (NCBS), Bangalore, 26-29 January, 2020.

Conclusions and future perspectives

Major conclusions of this study

In this study, *cnb-1*, which is an essential gene in *N. crassa* has been studied for its role in different asexual and vegetative developmental stages in response to various environmental cues. I studied the *cnb-1* mutants generated using a gene silencing mechanism called repeat induced point (RIP) mutation. The *cnb-1*^{RIP} mutants showed defect in growth in response to increasing concentrations of $CaCl_2$, reduced survival under heat shock conditions in *N. crassa*. In addition, vegetative spore formation or conidiation in *N. crassa* has been shown to be regulated by circadian rhythm (Ruger-Herreros et al. 2020). I found that the mutations in the EF- hand domains of *cnb-1* resulted in reduced period length in the mutants, therefore, *cnb-1* plays a role in circadian regulated conidiation in *N. crassa*.

Further, to understand the molecular players of the *cnb-1* mediated signaling pathway, expressions of some of selected genes such as *frq-1, wc-1, hsp80, hsp60, nca-2* and *crz-1* were studied under different cellular stress conditions. Transcriptional analysis of these molecular players revealed that calcineurin regulate the heat shock and Ca^{2+} stress tolerance pathway via its well-known downstream target CRZ-1 in *N. crassa*.

Finally, ChIP analysis revealed that CRZ-1 binds to the promoter of *hsp80* and *nca-2* under heat shock and Ca^{2+} stress conditions and upregulates their expressions. Furthermore, CRZ-1 binding increases with higher intensity under heat shock and high concentrations of Ca^{2+}. Moreover, the EMSA analysis revealed that the 5´-CCTTCACA-3´ and 5′-AGCGGAGC-3′ sequences, which are located about 1167 bp and 679 bp upstream of the ATG start codon in the promoter of *hsp80*, were responsible for the CRZ-1 binding under the heat shock conditions. In addition, EMSA studies under the Ca^{2+} stress conditions revealed that CRZ-1 binds to an 8 bp nucleotide sequence 5′-ACCGCGCC-3′, located about 234 bp upstream of ATG start codon in the promoter of *nca-2* and upregulates its expression during the Ca^{2+} stress.

Future prospects of this research work

This thesis work opens up several new avenues such as (i) to determine the molecular interaction of Hsp80 and CNA-1, (ii) to identify additional molecular targets of calcineurin for its molecular mechanism behind the regulation of the circadian clock in *N. crassa*, and (iii) to gain insight into the structure-function relationship of CNB-1 using nuclear magnetic resonance (NMR), and (iv) to determine an extensive molecular signaling network of calcineurin in *N. crassa*.

References

Aitiken, A., Klee, C.B. and Cohen, P., 1984. The structure of the B subunit of calcineurin. *European journal of biochemistry*, *139*(3), pp.663-671.

Aitken, A., Cohen, P., Santikarn, S., Williams, D.H., Calder, A.G., Smith, A. and Klee, C.B., 1982. Identification of the NH2-terminal blocking group of calcineurin B as myristic acid. *FEBS letters*, *150*(2), pp.314-318.

Alessi, D.R., Street, A.J., Cohen, P. and Cohen, P.T., 1993. Inhibitor-2 functions like a chaperone to fold three expressed isoforms of mammalian protein phosphatase-1 into a conformation with the specificity and regulatory properties of the native enzyme. *European Journal of Biochemistry*, *213*(3), pp.1055-1066.

Alspaugh, J.A., Perfect, J.R. and Heitman, J., 1998. Signal Transduction Pathways Regulating Differentiation and Pathogenicity of *Cryptococcus neoformans*. *Fungal Genetics and Biology*, *25*(1), pp.1-14.

Altschul, S.F., Gish, W., Miller, W., Myers, E.W. and Lipman, D.J., 1990. Basic local alignment search tool. *Journal of molecular biology*, *215*(3), pp.403-410.

Altschul, S.F., Madden, T.L., Schäffer, A.A., Zhang, J., Zhang, Z., Miller, W. and Lipman, D.J., 1997. Gapped BLAST and PSI-BLAST: a new generation of protein database search programs. *Nucleic acids research*, *25*(17), pp.3389-3402.

Altschul, S.F., Wootton, J.C., Gertz, E.M., Agarwala, R., Morgulis, A., Schäffer, A.A. and Yu, Y.K., 2005. Protein database searches using compositionally adjusted substitution matrices. *The FEBS journal*, *272*(20), pp.5101-5109.

Anglister, J., Grzesiek, S., Ren, H., Klee, C.B. and Bax, A., 1993. Isotope-edited multidimensional NMR of calcineurin B in the presence of the non-deuterated detergent CHAPS. Journal of biomolecular NMR, 3(1), pp.121-126.

Avalos, J. and Corrochano, L.M., 2013. Carotenoid biosynthesis in Neurospora. *Neurospora: Genomics and Molecular Biology; Kasbekar, DP, McCluskey, K., Eds*, pp.227-241.

Ávalos Cordero, F.J., Díaz Sánchez, V., Estrada, A.F., Trautmann, D., Limón Mirón, M.D.C. and Al-Babili, S., 2011. Analysis of al-2 mutations in *neurospora*. *PLoS One, 6, e21948*.

Bader, T., Schröppel, K., Bentink, S., Agabian, N., Köhler, G. and Morschhäuser, J., 2006. Role of calcineurin in stress resistance, morphogenesis, and virulence of a *Candida albicans* wild-type strain. *Infection and immunity*, *74*(7), pp.4366-4369.

Baker, C.L., Kettenbach, A.N., Loros, J.J., Gerber, S.A. and Dunlap, J.C., 2009. Quantitative proteomics reveals a dynamic interactome and phase-specific phosphorylation in the *Neurospora* circadian clock. *Molecular cell*, *34*(3), pp.354-363.

Baker, C.L., Loros, J.J. and Dunlap, J.C., 2012. The circadian clock of *Neurospora* crassa. *FEMS microbiology reviews*, *36*(1), pp.95-110.

Barman, A. and Tamuli, R., 2015. Multiple cellular roles of *Neurospora crassa plc-1*, *splA2*, and *cpe-1* in regulation of cytosolic free calcium, carotenoid accumulation, stress responses, and acquisition of thermotolerance. *Journal of Microbiology*, *53*(4), pp.226-235.

Barman, A. and Tamuli, R., 2017. The pleiotropic vegetative and sexual development phenotypes of *Neurospora crassa* arise from double mutants of the calcium signaling genes plc-1, splA2, and cpe-1. *Current Genetics*, *63*(5), pp.861-875.

Barroso, M.R., Bernd, K.K., DeWitt, N.D., Chang, A., Mills, K. and Sztul, E.S., 1996. A novel Ca^{2+}-binding protein, p22, is required for constitutive membrane traffic. *Journal of Biological Chemistry*, *271*(17), pp.10183-10187.

Bates, S., MacCallum, D.M., Bertram, G., Munro, C.A., Hughes, H.B., Buurman, E.T., Brown, A.J., Odds, F.C. and Gow, N.A., 2005. *Candida albicans* Pmr1p, a secretory pathway P-type

Ca^{2+}/Mn^{2+}-ATPase, is required for glycosylation and virulence. *Journal of Biological Chemistry*, *280*(24), pp.23408-23415.

Beadle, G.W. and Tatum, E.L., 1941. Genetic control of biochemical reactions in *Neurospora*. *Proceedings of the National Academy of Sciences of the United States of America*, *27*(11), p.499.

Belden, W.J., Larrondo, L.F., Froehlich, A.C., Shi, M., Chen, C.H., Loros, J.J. and Dunlap, J.C., 2007. The band mutation in *Neurospora crassa* is a dominant allele of *ras-1* implicating RAS signaling in circadian output. *Genes & development*, *21*(12), pp.1494-1505.

Benito, B., Garciadeblás, B. and Rodríguez-Navarro, A., 2000. Molecular cloning of the calcium and sodium ATPases in *Neurospora crassa*. *Molecular microbiology*, *35*(5), pp.1079-1088.

Berridge, M.J., Bootman, M.D. and Lipp, P., 1998. Calcium-a life and death signal. *Nature*, *395*(6703), pp.645-648.

Berridge, M.J., Bootman, M.D. and Roderick, H.L., 2003. Calcium signalling: dynamics, homeostasis and remodelling. *Nature reviews Molecular cell biology*, *4*(7), pp.517-529.

Bilu, Y. and Barkai, N., 2005. The design of transcription-factor binding sites is affected by combinatorial regulation. *Genome biology*, *6*(12), p.R103.

Blankenship, J.R., Wormley, F.L., Boyce, M.K., Schell, W.A., Filler, S.G., Perfect, J.R. and Heitman, J., 2003. Calcineurin is essential for *Candida albicans* survival in serum and virulence. *Eukaryotic cell*, *2*(3), pp.422-430.

Bonnefoy-Berard, N., Genestier, L., Flacher, M. and Revillard, J.P., 1994. The phosphoprotein phosphatase calcineurin controls calcium-dependent apoptosis in B cell lines. *European journal of immunology*, *24*(2), pp.325-329.

Borkovich, K.A., Farrelly, F.W., Finkelstein, D.B., Taulien, J. and Lindquist, S., 1989. hsp82 is an essential protein that is required in higher concentrations for growth of cells at higher temperatures. *Molecular and cellular biology*, *9*(9), pp.3919-3930.

Borkovich, K.A., Alex, L.A., Yarden, O., Freitag, M., Turner, G.E., Read, N.D., Seiler, S., Bell-Pedersen, D., Paietta, J., Plesofsky, N. and Plamann, M., 2004. Lessons from the genome sequence of *Neurospora crassa*: tracing the path from genomic blueprint to multicellular organism. *Microbiology and molecular biology reviews*, *68*(1), pp.1-108.

Bootman, M.D., Collins, T.J., Peppiatt, C.M., Prothero, L.S., MacKenzie, L., De Smet, P., Travers, M., Tovey, S.C., Seo, J.T., Berridge, M.J. and Ciccolini, F., 2001, February. Calcium signalling—an overview. In *Seminars in cell & developmental biology* (Vol. 12, No. 1, pp. 3-10). Academic Press.

Bowman, B.J., Draskovic, M., Freitag, M. and Bowman, E.J., 2009. Structure and distribution of organelles and cellular location of calcium transporters in *Neurospora crassa*. *Eukaryotic cell*, *8*(12), pp.1845-1855.

Bowman, B.J., Abreu, S., Margolles-Clark, E., Draskovic, M. and Bowman, E.J., 2011. Role of four calcium transport proteins, encoded by *nca-1*, *nca-2*, *nca-3*, and *cax*, in maintaining intracellular calcium levels in *Neurospora crassa*. *Eukaryotic Cell*, *10*(5), pp.654-661.

Bracker, C.E., 1967. Ultrastructure of fungi. *Annual Review of Phytopathology*, *5*(1), pp.343-372.

Brini, M., Calì, T., Ottolini, D. and Carafoli, E., 2013. The plasma membrane calcium pump in health and disease. *The FEBS journal*, *280*(21), pp.5385-5397.

Brini, M., Calì, T., Ottolini, D. and Carafoli, E., 2013. Intracellular calcium homeostasis and signaling. *In Metallomics and the Cell* (pp. 119-168). Springer, Dordrecht.

Buhr, E.D., Yoo, S.H. and Takahashi, J.S., 2010. Temperature as a universal resetting cue for mammalian circadian oscillators. *Science*, *330*(6002), pp.379-385.

Burgoyne, R.D., O'Callaghan, D.W., Hasdemir, B., Haynes, L.P. and Tepikin, A.V., 2004. Neuronal Ca^{2+}-sensor proteins: multitalented regulators of neuronal function. *Trends in neurosciences*, *27*(4), pp.203-209.

Burgoyne, R.D., 2007. Neuronal calcium sensor proteins: generating diversity in neuronal Ca^{2+} signalling. *Nature Reviews Neuroscience*, *8*(3), pp.182-193.

Bui, D.C., Lee, Y., Lim, J.Y., Fu, M., Kim, J.C., Choi, G.J., Son, H. and Lee, Y.W., 2016. Heat shock protein 90 is required for sexual and asexual development, virulence, and heat shock response in *Fusarium graminearum*. *Scientific reports*, *6*(1), pp.1-11.

Cambareri, E.B., Jensen, B.C., Schabtach, E. and Selker, E.U., 1989. Repeat-induced GC to AT mutations in *Neurospora*. *Science*, *244*(4912), pp.1571-1575.

Case, R.M., Eisner, D., Gurney, A., Jones, O., Muallem, S. and Verkhratsky, A., 2007. Evolution of calcium homeostasis: from birth of the first cell to an omnipresent signalling system. *Cell calcium*, *42*(4-5), pp.345-350.

Carafoli, E., 2002. Calcium signaling: a tale for all seasons. *Proceedings of the National Academy of Sciences*, *99*(3), pp.1115-1122.

Chang, C.D., Mukai, H., Kuno, T. and Tanaka, C., 1994. cDNA cloning of an alternatively spliced isoform of the regulatory subunit of Ca^{2+}/calmodulin-dependent protein phosphatase (calcineurin Bα2). *Biochimica et Biophysica Acta (BBA)-Gene Structure and Expression*, *1217*(2), pp.174-180.

Chatterjee, S. and Tatu, U., 2017. Heat shock protein 90 localizes to the surface and augments virulence factors of *Cryptococcus neoformans*. *PLoS neglected tropical diseases*, *11*(8), p.e0005836.

Chen, Y.L., Kozubowski, L., Cardenas, M.E. and Heitman, J., 2010. On the roles of calcineurin in fungal growth and pathogenesis. *Current Fungal Infection Reports*, *4*(4), pp.244-255.

Chen, Y.L., Konieczka, J.H., Springer, D.J., Bowen, S.E., Zhang, J., Silao, F.G.S., Bungay, A.A.C., Bigol, U.G., Nicolas, M.G., Abraham, S.N. and Thompson, D.A., 2012. Convergent evolution of calcineurin pathway roles in thermotolerance and virulence in *Candida glabrata*. *G3: Genes, Genomes, Genetics*, *2*(6), pp.675-691.

Cheng, P., Yang, Y., Gardner, K.H. and Liu, Y., 2002. PAS domain-mediated WC-1/WC-2 interaction is essential for maintaining the steady-state level of WC-1 and the function of both proteins in circadian clock and light responses of *Neurospora*. *Molecular and Cellular Biology*, *22*(2), pp.517-524.

Chin, D. and Means, A.R., 2000. Calmodulin: a prototypical calcium sensor. *Trends in cell biology*, *10*(8), pp.322-328.

Chow, E.W., Clancey, S.A., Billmyre, R.B., Averette, A.F., Granek, J.A., Mieczkowski, P., Cardenas, M.E. and Heitman, J., 2017. Elucidation of the calcineurin-Crz1 stress response transcriptional network in the human fungal pathogen *Cryptococcus neoformans*. *PLoS genetics*, *13*(4), p.e1006667

Clapham, D.E., 2007. Calcium signaling. Cell, 131(6), pp.1047-1058.

Cornelius, G. and Nakashima, H., 1987. Vacuoles play a decisive role in calcium homeostasis in *Neurospora crassa*. Microbiology, 133(8), pp.2341-2347.

Cortat, M. and Turian, G., 1974. Conidiation of *Neurospora crassa* in submerged culture without mycelial phase. *Archives of Microbiology*, *95*(1), pp.305-309.

Cowen, L.E. and Lindquist, S., 2005. Hsp90 potentiates the rapid evolution of new traits: drug resistance in diverse fungi. *Science*, *309*(5744), pp.2185-2189.

Cowen, L.E., Carpenter, A.E., Matangkasombut, O., Fink, G.R. and Lindquist, S., 2006. Genetic architecture of Hsp90-dependent drug resistance. *Eukaryotic Cell*, *5*(12), pp.2184-2188.

Cowen, L.E., Singh, S.D., Köhler, J.R., Collins, C., Zaas, A.K., Schell, W.A., Aziz, H., Mylonakis, E., Perfect, J.R., Whitesell, L. and Lindquist, S., 2009. Harnessing Hsp90 function as a powerful, broadly effective therapeutic strategy for fungal infectious disease. *Proceedings of the National Academy of Sciences*, *106*(8), pp.2818-2823.

Cortés, J.C.G., Katoh-Fukui, R., Moto, K., Ribas, J.C. and Ishiguro, J., 2004. *Schizosaccharomyces pombe* Pmr1p is essential for cell wall integrity and is required for polarized cell growth and cytokinesis. *Eukaryotic Cell*, *3*(5), pp.1124-1135.

Colot, H.V., Park, G., Turner, G.E., Ringelberg, C., Crew, C.M., Litvinkova, L., Weiss, R.L., Borkovich, K.A. and Dunlap, J.C., 2006. A high-throughput gene knockout procedure for *Neurospora* reveals functions for multiple transcription factors. *Proceedings of the National Academy of Sciences*, *103*(27), pp.10352-10357.

Cramer, R.A., Perfect, B.Z., Pinchai, N., Park, S., Perlin, D.S., Asfaw, Y.G., Heitman, J., Perfect, J.R. and Steinbach, W.J., 2008. Calcineurin target CrzA regulates conidial germination, hyphal growth, and pathogenesis of *Aspergillus fumigatus*. *Eukaryotic cell*, *7*(7), pp.1085-1097.

Cunningham, K.W. and Fink, G.R., 1994. Calcineurin-dependent growth control in *Saccharomyces cerevisiae* mutants lacking PMC1, a homolog of plasma membrane Ca^{2+} ATPases. *Journal of Cell Biology*, *124*(3), pp.351-363.

Cruz, M.C., Fox, D.S. and Heitman, J., 2001. Calcineurin is required for hyphal elongation during mating and haploid fruiting in *Cryptococcus neoformans*. *The EMBO journal*, *20*(5), pp.1020-1032.

Cyert, M.S., 1993.The function of Ca^{2+}/calmodulin-regulated phosphatase in yeast. Advances Protein Phosphatases.

Davis, R.H. and de Serres, F.J., 1970. Genetic and microbiological research techniques for *Neurospora crassa*. In *Methods in enzymology* (Vol. 17, pp. 79-143). Academic Press.

Davis, R.H., 2000. *Neurospora*: contributions of a model organism. Oxford University Press.

Davis, R.H. and Perkins, D.D., 2002. *Neurospora*: a model of model microbes. *Nature Reviews Genetics*, *3*(5), pp.397-403.

Davies, S.A. and Terhzaz, S., 2009. Organellar calcium signalling mechanisms in Drosophila epithelial function. *Journal of Experimental Biology*, *212*(3), pp.387-400.

Deka, R., Kumar, R. and Tamuli, R., 2011. *Neurospora crassa* homologue of Neuronal Calcium Sensor-1 has a role in growth, calcium stress tolerance, and ultraviolet survival. *Genetica*, *139*(7), p.885.

Deka, R. and Tamuli, R., 2013. *Neurospora crassa ncs-1*, *mid-1* and *nca-2* double-mutant phenotypes suggest diverse interaction among three Ca^{2+}-regulating gene products. *Journal of genetics*, *92*(3), pp.559-563.

De Castro, P.A., Chiaratto, J., Winkelströter, L.K., Bom, V.L.P., Ramalho, L.N.Z., Goldman, M.H.S., Brown, N.A. and Goldman, G.H., 2014. The involvement of the Mid1/Cch1/Yvc1 calcium channels in *Aspergillus fumigatus* virulence. *PLoS One*, *9*(8), p.e103957.

de La Pompa, J.L., Timmerman, L.A., Takimoto, H., Yoshida, H., Elia, A.J., Samper, E., Potter, J., Wakeham, A., Marengere, L., Langille, B.L. and Crabtree, G.R., 1998. Role of the NF-ATc transcription factor in morphogenesis of cardiac valves and septum. *Nature*, *392*(6672), pp.182-186.

Decastro, E., Nef, S., Fiumelli, H., Lenz, S.E., Kawamura, S. and Nef, P., 1995. Regulation of rhodopsin phosphorylation by a family of neuronal calcium sensors. *Biochemical and biophysical research communications*, *216*(1), pp.133-140.

Delgado-Álvarez, D.L., Bartnicki-García, S., Seiler, S. and Mouriño-Pérez, R.R., 2014. Septum development in *Neurospora crassa*: the septal actomyosin tangle. *PloS one*, *9*(5), p.e96744.

de Aguiar Cordeiro, R., de Jesus Evangelista, A.J., Serpa, R., de Farias Marques, F.J., de Melo, C.V.S., de Oliveira, J.S., da Silva Franco, J., de Alencar, L.P., Bandeira, T.D.J.P.G., Brilhante, R.S.N. and Sidrim, J.J.C., 2016. Inhibition of heat-shock protein 90 enhances the susceptibility to antifungals and reduces the virulence of *Cryptococcus neoformans*/*Cryptococcus gattii* species complex. *Microbiology*, *162*(2), pp.309-317.

Dinamarco, T.M., Freitas, F.Z., Almeida, R.S., Brown, N.A., Dos Reis, T.F., Ramalho, L.N.Z., Savoldi, M., Goldman, M.H.S., Bertolini, M.C. and Goldman, G.H., 2012. Functional characterization of an *Aspergillus fumigatus* calcium transporter (PmcA) that is essential for fungal infection. *PLoS One*, *7*(5), p.e37591.

Diezmann, S., Leach, M.D. and Cowen, L.E., 2015. Functional divergence of Hsp90 genetic interactions in biofilm and planktonic cellular states. *PLoS one*, *10*(9), p.e0137947.

Dodge, B.O., 1939. Some problems in the genetics of the fungi. *Science*, *90*(2339), pp.379-385.

Dunlap, J.C., 2006. Proteins in the *Neurospora* circadian clockworks. *Journal of Biological Chemistry*, *281*(39), pp.28489-28493.

Dunlap, J.C., Loros, J.J. and DeCoursey, P.J., 2004. *Chronobiology: biological timekeeping*. Sinauer Associates.

Estrada, A.F., Youssar, L., Scherzinger, D., Al-Babili, S. and Avalos, J., 2008. The ylo-1 gene encodes an aldehyde dehydrogenase responsible for the last reaction in the *Neurospora* carotenoid pathway. *Molecular microbiology*, *69*(5), pp.1207-1220.

Galagan, J.E., Calvo, S.E., Borkovich, K.A., Selker, E.U., Read, N.D., Jaffe, D., FitzHugh, W., Ma, L.J., Smirnov, S., Purcell, S. and Rehman, B., 2003. The genome sequence of the filamentous fungus *Neurospora crassa*. *Nature*, *422(6934)*, pp.859-868.

Galimov, E.M., 2009. Concept of sustained ordering and an ATP-related mechanism of life's origin. *International Journal of Molecular Sciences*, *10(5)*, pp.2019-2030.

Girstmair, H., Tippel, F., Lopez, A., Tych, K., Stein, F., Haberkant, P., Schmid, P.W.N., Helm, D., Rief, M., Sattler, M. and Buchner, J., 2019. The Hsp90 isoforms from S. cerevisiae differ in structure, function and client range. *Nature communications*, *10*(1), pp.1-15.

Gifford, J.L., Walsh, M.P. and Vogel, H.J., 2007. Structures and metal-ion-binding properties of the Ca^{2+}-binding helix–loop–helix EF-hand motifs. *Biochemical Journal*, *405*(2), pp.199-221.

Gong, Y., Li, T., Yu, C. and Sun, S., 2017. Candida albicans heat shock proteins and Hsps-associated signaling pathways as potential antifungal targets. *Frontiers in cellular and infection microbiology*, *7*, p.520.

Gohain, D. and Tamuli, R., 2019. Calcineurin responsive zinc-finger-1 binds to a unique promoter sequence to upregulate neuronal calcium sensor-1, whose interaction with MID-1 increases tolerance to calcium stress in *Neurospora crassa*. *Molecular microbiology*, *111*(6), pp.1510-1528.

Griffith, J.P., Kim, J.L., Kim, E.E., Sintchak, M.D., Thomson, J.A., Fitzgibbon, M.J., Fleming, M.A., Caron, P.R., Hsiao, K. and Navia, M.A., 1995. X-ray structure of calcineurin inhibited by the immunophilin-immunosuppressant FKBP12-FK506 complex. *Cell*, *82(3)*, pp.507-522.

Guerini, D., Krinks, M.H., Sikela, J.M., Hahn, W.E. and Klee, C.B., 1989. Isolation and sequence of a cDNA clone for human calcineurin B, the Ca^{2+}-binding subunit of the Ca^{2+}/calmodulin-stimulated protein phosphatase. *Dna*, *8(9)*, pp.675-682.

Guerini, D., Krebs, J. and Carafoli, E., 1987. Stimulation of the erythrocyte Ca^{2+}-ATPase and of bovine brain cyclic nucleotide phosphodiesterases by chemically modified calmodulin. *European journal of biochemistry*, *170(1-2)*, pp.35-42.

Guignard, R., Grange, F. and Turian, G.T., 1984. Microcycle conidiation induced by partial nitrogen deprivation in *Neurospora crassa*. *Canadian journal of microbiology*, *30(10)*, pp.1210-1215.

Hamilton, S.L., 2005. Ryanodine receptors. Cell calcium, 38(3-4), pp.253-260.

Hamam, A. and Lew, R.R., 2012. Electrical phenotypes of calcium transport mutant strains of a filamentous fungus, *Neurospora crassa*. *Eukaryotic cell*, *11*(5), pp.694-702.

Harding, R.W., Huang, P.C. and Mitchell, H.K., 1969. Photochemical studies of the carotenoid biosynthetic pathway in *Neurospora crassa*. *Archives of Biochemistry and Biophysics*, *129*(2), pp.696-707.

Harbison, C.T., Gordon, D.B., Lee, T.I., Rinaldi, N.J., Macisaac, K.D., Danford, T.W., Hannett, N.M., Tagne, J.B., Reynolds, D.B., Yoo, J. and Jennings, E.G., 2004. Transcriptional regulatory code of a eukaryotic genome. *Nature*, *431*(7004), pp.99-104.

Heitman, J., 2005. A fungal Achilles' heel. *Science*, *309*(5744), pp.2175-2176.

Hill, J.A., O'Meara, T.R. and Cowen, L.E., 2015. Fitness trade-offs associated with the evolution of resistance to antifungal drug combinations. *Cell Reports*, *10*(5), pp.809-819.

Hoter, A., El-Sabban, M.E. and Naim, H.Y., 2018. The HSP90 family: structure, regulation, function, and implications in health and disease. *International journal of molecular sciences*, *19*(9), p.2560.

Huai, Q., Kim, H.Y., Liu, Y., Zhao, Y., Mondragon, A., Liu, J.O. and Ke, H., 2002. Crystal structure of calcineurin–cyclophilin–cyclosporin shows common but distinct recognition of immunophilin–drug complexes. *Proceedings of the National Academy of Sciences*, *99*(19), pp.12037-12042.

Huang, G., Chen, S., Li, S., Cha, J., Long, C., Li, L., He, Q. and Liu, Y., 2007. Protein kinase A and casein kinases mediate sequential phosphorylation events in the circadian negative feedback loop. *Genes & development*, *21*(24), pp.3283-3295.

Jackson, S.L. and Heath, I.B., 1993. Roles of calcium ions in hyphal tip growth. *Microbiology and Molecular Biology Reviews*, *57*(2), pp.367-382.

Jaiswal, J.K., 2001. Calcium—how and why? *Journal of biosciences*, *26*(3), pp.357-363.

Juvvadi, P.R., Lamoth, F. and Steinbach, W.J., 2014. Calcineurin as a multifunctional regulator: unraveling novel functions in fungal stress responses, hyphal growth, drug resistance, and pathogenesis. *Fungal biology reviews*, *28*(2-3), pp.56-69.

Kapoor, M., Curle, C.A. and Runham, C., 1995. The hsp70 gene family of *Neurospora crassa*: cloning, sequence analysis, expression, and genetic mapping of the major stress-inducible member. *Journal of bacteriology*, *177*(1), pp.212-221.

Kawasaki, H., Nakayama, S. and Kretsinger, R.H., 1998. Classification and evolution of EF-hand proteins. *Biometals*, *11*(4), pp.277-295.

Kays, A.M., Rowley, P.S., Baasiri, R.A. and Borkovich, K.A., 2000. Regulation of conidiation and adenylyl cyclase levels by the Gα protein GNA-3 in *Neurospora crassa*. *Molecular and Cellular Biology*, *20*(20), pp.7693-7705.

Kellermayer, R., Aiello, D.P., Miseta, A. and Bedwell, D.M., 2003. Extracellular Ca^{2+} sensing contributes to excess Ca^{2+} accumulation and vacuolar fragmentation in a pmr1Δ mutant of *S. cerevisiae*. *Journal of Cell Science*, *116*(8), pp.1637-1646.

Kim, H., Wright, S.J., Park, G., Ouyang, S., Krystofova, S. and Borkovich, K.A., 2012. Roles for receptors, pheromones, G proteins, and mating type genes during sexual reproduction in *Neurospora crassa*. Genetics, 190(4), pp.1389-1404.

Kissinger, C.R., Parge, H.E., Knighton, D.R., Lewis, C.T., Pelletier, L.A., Tempczyk, A., Kalish, V.J., Tucker, K.D., Showalter, R.E., Moomaw, E.W. and Gastinel, L.N., 1995. Crystal structures of human calcineurin and the human FKBP12–FK506–calcineurin complex. *Nature*, *378*(6557), pp.641-644.

Klee, C.B., Crouch, T.H. and Krinks, M.H., 1979. Calcineurin: a calcium-and calmodulin-binding protein of the nervous system. *Proceedings of the National Academy of Sciences*, *76*(12), pp.6270-6273.

Kothe, G.O. and Free, S.J., 1998. Calcineurin subunit B is required for normal vegetative growth in *Neurospora crassa*. *Fungal Genetics and Biology*, *23*(3), pp.248-258.

Kregel, K.C., 2002. Invited review: heat shock proteins: modifying factors in physiological stress responses and acquired thermotolerance. *Journal of applied physiology*, *92*(5), pp.2177-2186.

Krystofova, S. and Borkovich, K.A., 2005. The heterotrimeric G-protein subunits GNG-1 and GNB-1 form a Gβγ dimer required for normal female fertility, asexual development, and Gα protein levels in Neurospora crassa. *Eukaryotic Cell*, *4*(2), pp.365-378.

Kumar, A., Roy, A., Deshmukh, M.V. and Tamuli, R., 2019. Dominant mutants of the calcineurin catalytic subunit (CNA-1) showed developmental defects, increased sensitivity to stress conditions, and CNA-1 interacts with CaM and CRZ-1 in *Neurospora crassa*. *Archives of Microbiology*, pp.1-14.

Kumar, R. and Tamuli, R., 2014. Calcium/calmodulin-dependent kinases are involved in growth, thermotolerance, oxidative stress survival, and fertility in *Neurospora crassa*. *Archives of microbiology*, *196*(4), pp.295-305.

Kumar, K.S., Kumar, B.R., Siddavattam, D. and Subramanyam, C., 2006. Characterization of calcineurin-dependent response element binding protein and its involvement in copper-metallothionein gene expression in *Neurospora*. *Biochemical and biophysical research communications*, *345*(3), pp.1010-1013.

Kwon-Chung, K.J., Fraser, J.A., Doering, T.L., Wang, Z.A., Janbon, G., Idnurm, A. and Bahn, Y.S., 2014. *Cryptococcus neoformans* and *Cryptococcus gattii*, the etiologic agents of cryptococcosis. *Cold Spring Harbor perspectives in medicine*, *4*(7), p.a019760.

Lamb, T.M., Vickery, J. and Bell-Pedersen, D., 2013. Regulation of gene expression in *Neurospora crassa* with a copper responsive promoter. *G3: Genes, Genomes, Genetics*, *3*(12), pp.2273-2280.

Lamoth, F., Juvvadi, P.R., Fortwendel, J.R. and Steinbach, W.J., 2012. Heat shock protein 90 is required for conidiation and cell wall integrity in *Aspergillus fumigatus*. *Eukaryotic cell*, *11*(11), pp.1324-1332.

Lamoth, F., Juvvadi, P.R. and Steinbach, W.J., 2016. Heat shock protein 90 (Hsp90): a novel antifungal target against *Aspergillus fumigatus*. *Critical reviews in microbiology*, *42*(2), pp.310-321.

Lange, M. and Peiter, E., 2020. Calcium transport proteins in fungi: the phylogenetic diversity of their relevance for growth, virulence, and stress resistance. *Frontiers in microbiology*, *10*, p.3100.

Laxmi, V. and Tamuli, R., 2015. The *Neurospora crassa cmd*, *trm-9*, and *nca-2* Genes Play a Role in Growth, Development, and Survival in Stress conditions. *Genomics and Applied Biology*, *6*.

Laxmi, V. and Tamuli, R., 2017. The calmodulin gene in *Neurospora crassa* is required for normal vegetative growth, ultraviolet survival, and sexual development. *Archives of microbiology*, *199*(4), pp.531-542.

Lewit-Bentley, A. and Réty, S., 2000. EF-hand calcium-binding proteins. *Current opinion in structural biology*, *10*(6), pp.637-643.

Liu, W., Xie, Y., Ma, J., Luo, X., Nie, P., Zuo, Z., Lahrmann, U., Zhao, Q., Zheng, Y., Zhao, Y. and Xue, Y., 2015. IBS: an illustrator for the presentation and visualization of biological sequences. *Bioinformatics*, *31*(20), pp.3359-3361.

Liu, Y. and Bell-Pedersen, D., 2006. Circadian rhythms in *Neurospora crassa* and other filamentous fungi. *Eukaryotic cell*, *5*(8), pp.1184-1193.

Livak, K.J. and Schmittgen, T.D., 2001. Analysis of relative gene expression data using real-time quantitative PCR and the $2^{-\Delta\Delta CT}$ method. *methods*, *25*(4), pp.402-408.

Liu, S., Hou, Y., Liu, W., Lu, C., Wang, W. and Sun, S., 2015. Components of the calcium-calcineurin signaling pathway in fungal cells and their potential as antifungal targets. *Eukaryotic cell*, *14*(4), pp.324-334.

Lin, X. and Barber, D.L., 1996. A calcineurin homologous protein inhibits GTPase-stimulated Na-H exchange. *Proceedings of the National Academy of Sciences*, *93*(22), pp.12631-12636.

Li, Y., Zhang, Y. and Lu, L., 2019. Calcium signaling pathway is involved in non-CYP51 azole resistance in *Aspergillus fumigatus*. *Medical Mycology*, *57*(Supplement_2), pp.S233-S238.

Louvion, J.F., Abbas-Terki, T. and Picard, D., 1998. Hsp90 is required for pheromone signaling in yeast. *Molecular biology of the cell*, *9*(11), pp.3071-3083.

Luan, S., Kudla, J., Rodriguez-Concepcion, M., Yalovsky, S. and Gruissem, W., 2002. Calmodulins and calcineurin B–like proteins: Calcium sensors for specific signal response coupling in plants. *The Plant Cell*, *14*(suppl 1), pp.S389-S400.

Luque, E.M., Gutiérrez, G., Navarro-Sampedro, L., Olmedo, M., Rodríguez-Romero, J., Ruger-Herreros, C., Tagua, V.G. and Corrochano, L.M., 2012. A relationship between carotenoid accumulation and the distribution of species of the fungus *Neurospora* in Spain. *PLoS One*, *7*(3), p.e33658.

Madi, L., McBride, S.A., Bailey, L.A. and Ebbole, D.J., 1997. rco-3, a gene involved in glucose transport and conidiation in *Neurospora crassa*. *Genetics*, *146*(2), pp.499-508.

Marquina, M., González, A., Barreto, L., Gelis, S., Muñoz, I., Ruiz, A., Álvarez, M.C., Ramos, J. and Ariño, J., 2012. Modulation of yeast alkaline cation tolerance by ypi1 requires calcineurin. *Genetics*, *190*(4), pp.1355-1364.

Martin, D.C., Kim, H., Mackin, N.A., Maldonado-Báez, L., Evangelista, C.C., Beaudry, V.G., Dudgeon, D.D., Naiman, D.Q., Erdman, S.E. and Cunningham, K.W., 2011. New regulators of a high affinity Ca^{2+} influx system revealed through a genome-wide screen in yeast. *Journal of Biological Chemistry*, *286*(12), pp.10744-10754.

Marchler-Bauer, A., Anderson, J.B., Chitsaz, F., Derbyshire, M.K., DeWeese-Scott, C., Fong, J.H., Geer, L.Y., Geer, R.C., Gonzales, N.R., Gwadz, M. and He, S., 2009. CDD: specific functional annotation with the Conserved Domain Database. *Nucleic acids research*, *37*(suppl_1), pp.D205-D210.

Marchler-Bauer, A. and Bryant, S.H., 2004. CD-Search: protein domain annotations on the fly. *Nucleic acids research*, *32*(suppl_2), pp.W327-W331.

Mattern, D.L., Forman, L.R. and Brody, S., 1982. Circadian rhythms in *Neurospora crassa*: a mutation affecting temperature compensation. *Proceedings of the National Academy of Sciences*, *79*(3), pp.825-829.

McFerran, B.W., Graham, M.E. and Burgoyne, R.D., 1998. Neuronal Ca^{2+} sensor 1, the mammalian homologue of frequenin, is expressed in chromaffin and PC12 cells and regulates neurosecretion from dense-core granules. *Journal of Biological Chemistry*, *273(35)*, pp.22768-22772.

McCluskey, K., 2003. The fungal genetics stock center. *from molds to molecules*, *52*, pp.245-262.

McCluskey, K., Wiest, A. and Plamann, M., 2010. The Fungal Genetics Stock Center: a repository for 50 years of fungal genetics research. *Journal of biosciences*, *35*(1), pp.119-126.

Murray, N.E. and Perkins, D.D., 1963. Stanford *Neurospora* methods. *Neurospora News l4*, pp.21-25.

Mehra, A., Baker, C.L., Loros, J.J. and Dunlap, J.C., 2009. Post-translational modifications in circadian rhythms. *Trends in biochemical sciences*, *34*(10), pp.483-490.

Mendoza, I., Rubio, F., Rodriguez-Navarro, A. and Pardo, J.M., 1994. The protein phosphatase calcineurin is essential for NaCl tolerance of *Saccharomyces cerevisiae*. *Journal of Biological Chemistry*, *269*(12), pp.8792-8796.

Mendoza, I., Quintero, F.J., Bressan, R.A., Hasegawa, P.M. and Pardo, J.M., 1996. Activated calcineurin confers high tolerance to ion stress and alters the budding pattern and cell morphology of yeast cells. *Journal of Biological Chemistry*, *271*(38), pp.23061-23067.

Mikoshiba, K. and Hattori, M., 2000. IP3 receptor-operated calcium entry. *Science Signaling, 2000(51)*, pp.pe1-pe1.

Molloy, S., 2007. Differential regulation of septation. *Nature Reviews Microbiology*, *5*(9), pp.659-659.

Montagne, C., 1843. Quatrieme centurie plantes cellulaires exotiques nouvelles. Decades VIII, IX, X. *Ann. Sci. Nat. Bot., Ser. 2, 20*, pp.352-39.

Mukai, H., Chang, C.D., Tanaka, H., Ito, A., Kuno, T. and Tanaka, C., 1991. cDNA cloning of a novel testis-specific calcineurin B-like protein. *Biochemical and biophysical research communications, 179(3)*, pp.1325-1330.

Naderer, T., Dandash, O. and McConville, M.J., 2011. Calcineurin is required for *Leishmania* major stress response pathways and for virulence in the mammalian host. *Molecular microbiology*, *80*(2), pp.471-480.

Naik, U.P., Patel, P.M. and Parise, L.V., 1997. Identification of a novel calcium-binding protein that interacts with the integrin αIIb cytoplasmic domain. *Journal of Biological Chemistry*, *272*(8), pp.4651-4654.

Nakayama, S. and Kretsinger, R.H., 1994. Evolution of the EF-hand family of proteins. Annual review of biophysics and biomolecular structure, 23(1), pp.473-507.

Nargang, C.E., Bottorff, D.A. and Adachi, K., 1994. Isolation and characterization of a cDNA clone coding for the calcium-binding subunit of calcineurin from bovine brain: an identical amino acid sequence to the human protein. DNA Sequence, 4(5), pp.313-318.

Nanthakumar, N.N., Dayton, J.S. and Means, A.R., 1996. Role of Ca++/calmodulin binding proteins in *Aspergillus nidulans* cell cycle regulation. In *Progress in cell cycle research* (pp. 217-228). Springer, Boston, MA.

Nicholas, K.B., 1997. GeneDoc: analysis and visualization of genetic variation. *Embnew. news*, *4*, p.14.

Ninomiya, Y., Suzuki, K., Ishii, C. and Inoue, H., 2004. Highly efficient gene replacements in Neurospora strains deficient for nonhomologous end-joining. *Proceedings of the National Academy of Sciences*, *101*(33), pp.12248-12253.

Odom, A., Muir, S., Lim, E., Toffaletti, D.L., Perfect, J. and Heitman, J., 1997. Calcineurin is required for virulence of *Cryptococcus neoformans*. *The EMBO journal*, *16*(10), pp.2576-2589.

O'Neill, J.S. and Reddy, A.B., 2012. The essential role of cAMP/Ca^{2+} signalling in mammalian circadian timekeeping.

Ouyang, S., Beecher, C.N., Wang, K., Larive, C.K. and Borkovich, K.A., 2015. Metabolic impacts of using nitrogen and copper-regulated promoters to regulate gene expression in *Neurospora crassa*. *G3: Genes, Genomes, Genetics*, *5*(9), pp.1899-1908.

Pall, M.L., 1993. The use of Ignite (Basta; glufosinate; phosphinothricin) to select transformants of bar-containing plasmids in *Neurospora crassa*. *Fungal Genetics Reports*, *40*(1), p.58.

Papagianni, M., 2004. Fungal morphology and metabolite production in submerged mycelial processes. *Biotechnology advances*, *22*(3), pp.189-259.

Pardo, J.M., Reddy, M.P., Yang, S., Maggio, A., Huh, G.H., Matsumoto, T., Coca, M.A., Paino-D'Urzo, M., Koiwa, H., Yun, D.J. and Watad, A.A., 1998. Stress signaling through Ca^{2+}/calmodulin-dependent protein phosphatase calcineurin mediates salt adaptation in plants. *Proceedings of the National Academy of Sciences*, *95*(16), pp.9681-9686.

Payen, A.D., 1843. Extrait d'un rapport adresse a M. Le Marechal Duc de Dalmatie, Ministre de la Guerre, President du Conseil, sur une alteration extraordinaire du pain de munition. *Ann. Chim. Phys. 3rd Ser*, *9*, pp.5-21.

Perkins, D.D., 1992. *Neurospora*: the organism behind the molecular revolution. *Genetics*, *130*(4), p.687.

Persikov, A.V. and Singh, M., 2014. De novo prediction of DNA-binding specificities for Cys_2His_2 zinc finger proteins. *Nucleic acids research*, *42*(1), pp.97-108.

Peng, L., Ma, J., Cui, R., Chen, X., Wei, S.Y., Wei, Q.J. and Li, B., 2014. The calcineurin inhibitor tacrolimus reduces proteinuria in membranous nephropathy accompanied by a decrease in angiopoietin-like-4. *PloS one*, *9*(8), p.e106164.

Persikov, A.V., Osada, R. and Singh, M., 2009. Predicting DNA recognition by Cys2His2 zinc finger proteins. *Bioinformatics*, *25*(1), pp.22-29.

Phillips, A.J., Sudbery, I. and Ramsdale, M., 2003. Apoptosis induced by environmental stresses and amphotericin B in *Candida albicans*. *Proceedings of the National Academy of Sciences*, *100*(24), pp.14327-14332.

Pittman, J.K., 2011. Vacuolar Ca^{2+} uptake. *Cell calcium*, *50*(2), pp.139-146.

Plattner, H. and Verkhratsky, A., 2013. Ca2+ signalling early in evolution–all but primitive. *Journal of cell science*, *126*(10), pp.2141-2150.

Plesofsky-Vig, N., Light, D. and Brambl, R., 1983. Paedogenetic conidiation in *Neurospora crassa*. Experimental mycology, 7(3), pp.283-286.

Plochocka-Zulinska, D., Rasmussen, G. and Rasmussen, C., 1995. Regulation of calcineurin gene expression in *Schizosaccharomyces pombe* dependence on the ste11 transcription factor. *Journal of Biological Chemistry*, *270*(42), pp.24794-24799.

Ponnamperuma, C., Sagan, C. and Mariner, R., 1963. Synthesis of adenosine triphosphate under possible primitive earth conditions. Nature, 199(4890), pp.222-226.

Prokisch, H., Yarden, O., Dieminger, M., Tropschug, M. and Barthelmess, I.B., 1997. Impairment of calcineurin function in *Neurospora crassa* reveals its essential role in hyphal growth, morphology and maintenance of the apical Ca^{2+} gradient. *Molecular and General Genetics MGG*, *256*(2), pp.104-114.

Raju, N.B., 1980. Meiosis and ascospore genesis in *Neurospora*. European journal of cell biology, 23(1), pp.208-223.

Raju, N.B., 1992. Genetic control of the sexual cycle in *Neurospora*. Mycological research, 96(4), pp.241-262.

Remillard, S.P., Lai, E.Y., Levy, Y.Y. and Fulton, C., 1995. A calcineurin-B-encoding gene expressed during differentiation of the ameboflagellate *Naegleria gruberi* contains two introns. Gene, 154(1), pp.39-45.

Ruger-Herreros, C. and Corrochano, L.M., 2020. Conidiation in Neurospora crassa: vegetative reproduction by a model fungus. *International Microbiology*, pp.1-9.

Romano, N. and Macino, G., 1992. Quelling: transient inactivation of gene expression in *Neurospora crassa* by transformation with homologous sequences. Molecular microbiology, 6(22), pp.3343-3353.

Roy, A., Kumar, A., Baruah, D. and Tamuli, R., 2020. Calcium signaling is involved in diverse cellular processes in fungi. Mycology, pp.1-15.

Rodriguez-Amaya, D.B. and Kimura, M., 2004. *HarvestPlus handbook for carotenoid analysis* (Vol. 2). Washington: International Food Policy Research Institute (IFPRI).

Robbins, N., Uppuluri, P., Nett, J., Rajendran, R., Ramage, G., Lopez-Ribot, J.L., Andes, D. and Cowen, L.E., 2011. Hsp90 governs dispersion and drug resistance of fungal biofilms. *PLoS Pathog*, *7*(9), p.e1002257.

Rudolph, H.K., Antebi, A., Fink, G.R., Buckley, C.M., Dorman, T.E., LeVitre, J., Davidow, L.S., Mao, J.I. and Moir, D.T., 1989. The yeast secretory pathway is perturbed by mutations in PMR1, a member of a Ca^{2+} ATPase family. *Cell*, *58*(1), pp.133-145.

Rusnak, F. and Mertz, P., 2000. Calcineurin: form and function. *Physiological reviews*, *80*(4), pp.1483-1521.

Russell, D.W. and Sambrook, J., 2001. *Molecular cloning: a laboratory manual* (Vol. 1, p. 112). Cold Spring Harbor, NY: Cold Spring Harbor Laboratory.

Sanders, D., Pelloux, J., Brownlee, C. and Harper, J.F., 2002. Calcium at the crossroads of signaling. *The Plant Cell*, *14*(suppl 1), pp.S401-S417.

Sargent, M.L. and Kaltenborn, S.H., 1972. Effects of medium composition and carbon dioxide on circadian conidiation in *Neurospora*. *Plant Physiology*, *50*(1), pp.171-175.

Sadakane, Y. and Nakashima, H., 1996. Light-induced phase shifting of the circadian conidiation rhythm is inhibited by calmodulin antagonists in *Neurospora crassa*. *Journal of biological rhythms*, *11*(3), pp.234-240.

Saunders, D.S. and Thomson, E.J., 1977. 'Strong' phase response curve for the circadian rhythm of locomotor activity in a cockroach (*Nauphoeta cinerea*). *Nature*, *270*(5634), pp.241-243.

Sakai, W., Ishii, C. and Inoue, H., 2002. The *upr-1* gene encodes a catalytic subunit of the DNA polymerase ζ which is involved in damage-induced mutagenesis in *Neurospora crassa*. *Molecular Genetics and Genomics*, *267*(3), pp.401-408.

Schafmeier, T., Haase, A., Káldi, K., Scholz, J., Fuchs, M. and Brunner, M., 2005. Transcriptional feedback of *Neurospora* circadian clock gene by phosphorylation-dependent inactivation of its transcription factor. *Cell*, *122*(2), pp.235-246.

Schaad, N.C., De Castro, E., Nef, S., Hegi, S., Hinrichsen, R., Martone, M.E., Ellisman, M.H., Sikkink, R., Rusnak, F., Sygush, J. and Nef, P., 1996. Direct modulation of calmodulin targets by the neuronal calcium sensor NCS-1. *Proceedings of the National Academy of Sciences*, *93*(17), pp.9253-9258.

Schmid, J. and Harold, F.M., 1988. Dual roles for calcium ions in apical growth of *Neurospora crassa*. *Microbiology*, *134*(9), pp.2623-2631.

Senn, H., Shapiro, R.S. and Cowen, L.E., 2012. Cdc28 provides a molecular link between Hsp90, morphogenesis, and cell cycle progression in *Candida albicans*. *Molecular biology of the cell*, *23*(2), pp.268-283.

Serafin, C.F., Paris, A.P., Paula, C.R., Simão, R.C.G. and Gandra, R.F., 2017. Repression of Proteases and Hsp90 Chaperone Expression Induced by an Antiretroviral in Virulent Environmental Strains of *Cryptococcus neoformans*. *Microbial ecology*, *73*(3), pp.583-589.

Shapiro, R.S., Uppuluri, P., Zaas, A.K., Collins, C., Senn, H., Perfect, J.R., Heitman, J. and Cowen, L.E., 2009. Hsp90 orchestrates temperature-dependent *Candida albicans* morphogenesis via Ras1-PKA signaling. *Current Biology*, *19*(8), pp.621-629.

Shear, C.L. and Dodge, B.O., 1927. Life histories and heterothallism of the red bread-mold fungi of the *Monilia sitophila* group (pp. 1019-1042).

Shemarova, I.V. and Nesterov, V.P., 2005. Evolution of mechanisms of Ca^{2+}-signaling: role of calcium ions in signal transduction in prokaryotes. *Journal of Evolutionary Biochemistry and Physiology*, *41*(1), pp.12-19.

Shibasaki, F., Price, E.R., Milan, D. and McKeon, F., 1996. Role of kinases and the phosphatase calcineurin in the nuclear shuttling of transcription factor NF-AT4. *Nature*, *382*(6589), pp.370-373.

Shiu, P.K., Raju, N.B., Zickler, D. and Metzenberg, R.L., 2001. Meiotic silencing by unpaired DNA. *Cell*, *107*(7), pp.905-916.

Singh, S.D., Robbins, N., Zaas, A.K., Schell, W.A., Perfect, J.R. and Cowen, L.E., 2009. Hsp90 governs echinocandin resistance in the pathogenic yeast *Candida albicans* via calcineurin. *PLoS Pathog*, *5*(7), p.e1000532.

Silverman-Gavrila, L.B. and Lew, R.R., 2001. Regulation of the tip-high [Ca^{2+}] gradient in growing hyphae of the fungus *Neurospora crassa*. *European journal of cell biology*, *80*(6), pp.379-390.

Singh, S.D., Robbins, N., Zaas, A.K., Schell, W.A., Perfect, J.R. and Cowen, L.E., 2009. Hsp90 governs echinocandin resistance in the pathogenic yeast *Candida albicans* via calcineurin. *PLoS Pathog*, *5*(7), p.e1000532.

Singh-Babak, S.D., Babak, T., Diezmann, S., Hill, J.A., Xie, J.L., Chen, Y.L., Poutanen, S.M., Rennie, R.P., Heitman, J. and Cowen, L.E., 2012. Global analysis of the evolution and mechanism of echinocandin resistance in *Candida glabrata*. *PLoS Pathog*, *8*(5), p.e1002718.

Song, J., Liu, X., Zhai, P., Huang, J. and Lu, L., 2016. A putative mitochondrial calcium uniporter in *A. fumigatus* contributes to mitochondrial Ca^{2+} homeostasis and stress responses. *Fungal Genetics and Biology*, *94*, pp.15-22.

Springer, M.L., 1993. Genetic control of fungal differentiation: the three sporulation pathways of *Neurospora crassa*. *Bioessays*, *15*(6), pp.365-374.

Stathopoulos, A.M. and Cyert, M.S., 1997. Calcineurin acts through theCRZ1/TCN1-encoded transcription factor to regulate gene expression in yeast. *Genes & development*, *11*(24), pp.3432-3444.

Steinbach, W.J., Reedy, J.L., Cramer, R.A., Perfect, J.R. and Heitman, J., 2007. Harnessing calcineurin as a novel anti-infective agent against invasive fungal infections. *Nature Reviews Microbiology*, *5*(6), pp.418-430.

Suzuki, S., Katagiri, S. and Nakashima, H., 1996. Mutants with altered sensitivity to a calmodulin antagonist affect the circadian clock in *Neurospora crassa*. *Genetics*, *143*(3), pp.1175-1180.

Sze, H., Liang, F., Hwang, I., Curran, A.C. and Harper, J.F., 2000. Diversity and regulation of plant Ca^{2+} pumps: insights from expression in yeast. *Annual review of plant biology*, *51*(1), pp.433-462.

Szklarczyk, D., Franceschini, A., Wyder, S., Forslund, K., Heller, D., Huerta-Cepas, J., Simonovic, M., Roth, A., Santos, A., Tsafou, K.P. and Kuhn, M., 2015. STRING v10: protein–protein interaction networks, integrated over the tree of life. *Nucleic acids research*, *43*(D1), pp.D447-D452.

Tamuli, R., Kumar, R., Srivastava, D.A., and Deka, R. (2013) Calcium signaling. In: D.P. Kasbekar, and McCluskey, K. (eds.), *Neurospora Genomics and Molecular Biology* (pp 35–57). Norfolk: Caister Academic Press.

Tamuli, R., Deka, R. and Borkovich, K.A., 2016. Calcineurin subunits A and B interact to regulate growth and asexual and sexual development in *Neurospora crassa*. *PloS one*, *11*(3), p.e0151867.

Tamuli, R., Kumar, R. and Deka, R., 2011. Cellular roles of neuronal calcium sensor-1 and calcium/calmodulin-dependent kinases in fungi. *Journal of basic microbiology*, *51*(2), pp.120-128.

Tamura, K., Stecher, G., Peterson, D., Filipski, A. and Kumar, S., 2013. MEGA6: molecular evolutionary genetics analysis version 6.0. *Molecular biology and evolution*, *30*(12), pp.2725-2729.

That, T.T. and Turian, G., 1978. Ultrastructural study of microcyclic macroconidiation in *Neurospora crassa*. *Archives of microbiology*, *116*(3), pp.279-288.

Thewes, S., 2014. Calcineurin-Crz1 signaling in lower eukaryotes. *Eukaryotic cell*, *13*(6), pp.694-705.

Thompson, J.D., Gibson, T.J., Plewniak, F., Jeanmougin, F. and Higgins, D.G., 1997. The CLUSTAL_X windows interface: flexible strategies for multiple sequence alignment aided by quality analysis tools. *Nucleic acids research*, *25*(24), pp.4876-4882.

Tisi, R., Rigamonti, M., Groppi, S. and Belotti, F., 2016. Calcium homeostasis and signaling in fungi and their relevance for pathogenicity of yeasts and filamentous fungi.

Ton, V.K. and Rao, R., 2004. Functional expression of heterologous proteins in yeast: insights into Ca^{2+} signaling and Ca^{2+}-transporting ATPases. *American Journal of Physiology-Cell Physiology*.

Tsutsumi, S., Mollapour, M., Prodromou, C., Lee, C.T., Panaretou, B., Yoshida, S., Mayer, M.P. and Neckers, L.M., 2012. Charged linker sequence modulates eukaryotic heat shock protein 90 (Hsp90) chaperone activity. *Proceedings of the National Academy of Sciences*, *109*(8), pp.2937-2942.

Ueki, K., Muramatsu, T. and Kincaid, R.L., 1992. Structure and expression of two isoforms of the murine calmodulin-dependent protein phosphatase regulatory subunit (calcineurin B). Biochemical and biophysical research communications, 187(1), pp.537-543.

Ueki, K. and Kincaid, R.L., 1993. Interchangeable associations of calcineurin regulatory subunit isoforms with mammalian and fungal catalytic subunits. *Journal of Biological Chemistry*, *268*(9), pp.6554-6559.

Verkhratsky, A. and Parpura, V., 2014. Calcium signalling and calcium channels: evolution and general principles. European journal of pharmacology, 739, pp.1-3.

Victor, R.G., Thomas, G.D., Marban, E. and O'Rourke, B., 1995. Presynaptic modulation of cortical synaptic activity by calcineurin. *Proceedings of the National Academy of Sciences*, *92*(14), pp.6269-6273.

Vogel, H.J., 1956. A convenient growth medium for *Neurospora* (Medium N). *Microb. Genet. Bull.*, *13*, pp.42-43.

Vogel, H.J., 1964. Distribution of lysine pathways among fungi: evolutionary implications. *The American Naturalist*, *98*(903), pp.435-446.

Wang, J.H. and Desai, R., 1976. A brain protein and its effect on the Ca^{2+}-and protein modulator-activated cyclic nucleotide phosphodiesterase. *Biochemical and biophysical research communications*, *72(3)*, pp.926-932.

Westergaard, M. and Mitchell, H.K., 1947. *Neurospora* V. A synthetic medium favoring sexual reproduction. *American Journal of Botany*, pp.573-577.

Whitesell, L. and Lindquist, S.L., 2005. HSP90 and the chaperoning of cancer. *Nature Reviews Cancer*, *5*(10), pp.761-772.

Xu, Y., Zhan, C. and Huang, B., 2011. Heat shock proteins in association with heat tolerance in grasses. *International journal of proteomics*, 2011.

Yang, Q. and Borkovich, K.A., 1999. Mutational activation of a Gαi causes uncontrolled proliferation of aerial hyphae and increased sensitivity to heat and oxidative stress in *Neurospora crassa*. *Genetics*, *151*(1), pp.107-117.

Yang, Y., He, Q., Cheng, P., Wrage, P., Yarden, O. and Liu, Y., 2004. Distinct roles for PP1 and PP2A in the *Neurospora* circadian clock. *Genes & development*, *18*(3), pp.255-260.

Yu, A., Li, P., Tang, T., Wang, J., Chen, Y. and Liu, L., 2015. Roles of Hsp70s in stress responses of microorganisms, plants, and animals. *BioMed research international*, *2015*.

Zalokar, M., 1954. Studies on biosynthesis of carotenoids in *Neurospora crassa*. *Archives of Biochemistry and Biophysics*, *50*(1), pp.71-80.

Zeng, W., Mak, D.O.D., Li, Q., Shin, D.M., Foskett, J.K. and Muallem, S., 2003. A new mode of Ca^{2+} signaling by G protein-coupled receptors: gating of IP3 receptor Ca^{2+} release channels by Gβγ. *Current biology*, *13*(10), pp.872-876.

Zelter, A., Bencina, M., Bowman, B.J., Yarden, O. and Read, N.D., 2004. A comparative genomic analysis of the calcium signaling machinery in *Neurospora crassa*, *Magnaporthe grisea*, and *Saccharomyces cerevisiae*. *Fungal Genetics and Biology*, *41*(9), pp.827-841.

Zhu, D., Cardenas, M.E. and Heitman, J., 1995. Myristoylation of calcineurin B is not required for function or interaction with immunophilin-immunosuppressant complexes in the yeast Saccharomyces cerevisiae. *Journal of Biological Chemistry*, *270*(42), pp.24831-24838.

Zhu, Y. and Yakel, J.L., 1997. Calcineurin modulates G protein-mediated inhibition of N-type calcium channels in rat sympathetic neurons. *Journal of neurophysiology*, *78*(2), pp.1161-1169.

Publications, Conferences and Workshops

Publications

1. **Roy A,** Kumar A, Baruah D, Tamuli R. **(2020)** "Calcium signaling is involved in diverse cellular processes in fungi"**. Mycology: An International Journal of Fungal Biology P.P 1-15**

2. Kumar A, **Roy A**, Deshmukh MV and Tamuli R. **(2019)** "Dominant mutants of the calcineurin catalytic subunit (CNA-1) showed developmental defects, increased sensitivity to stress conditions, and CNA-1 interacts with CaM and CRZ-1 in *Neurospora crassa"* **Archives of Microbiology Vol. P.P 1-14**

3. Gohain D, **Roy A** and Tamuli R. **(2017)** "Calcium signalling proteins in human diseases and their potential as drug targets" **Annals of Pharmacology and Pharmaceutics 2: 1–3**

Conference Presentations

1. **Roy A and Tamuli R (2020)** "The calcineurin responsive zinc finger protein upregulates *hsp80* for survival under heat shock stress condition in *Neurospora crassa".* EMBO Symposium on Calcium Signaling: Molecular mechanisms to role in health and diseases, 26-29 January, 2020, National Centre for Biological Sciences (NCBS), Bangalore, India **(Poster presentation)**

2. **Roy A and Tamuli R (2019)** "Calcineurin pathway is responsible for upregulation of *hsp80* under heat shock condition in *Neurospora crassa*". 11th International Conference on Biology of Yeast and Filamentous fungi, 26- 28 November, 2019 University of Hyderabad, Hyderabad, India **(Flash Talk and Poster Presentation)**

3. **Roy A and Tamuli R (2017)** "Role of *cnb-1*^{RIP} mutants in stress tolerance, circadian rhythm and probable interaction with Calcium proton exchanger (CAX) regulating cell

functions in *Neurospora crassa"*. National conference on Fungal Biology, 16-18 Nov, University of Jammu **(Best Poster Presentation Award)**

4. **Roy A and Tamuli R (2016)** "Studies on the molecular mechanism of calcineurin regulatory subunit in *Neurospora crassa"*. XL All India Cell Biology conference, Jiwaji University, Gwalior, MP **(Poster Presentation)**

5. **Roy A and Tamuli R (2015)** "Studies on the the role of the calcium signaling genes in regulating cytosolic free calcium concentration in *Neurospora crassa"*. 9th International Conference on Yeast Biology, IACS, Kolkata, India **(Poster Presentation)**

Workshop

Roy A and Tamuli R (2018) "Investigating real time cytosolic calcium levels in *Neurospora crassa* using a novel fluorescence based biosensor" in 10th Bangalore Microscopy Course, 16-23 September, 2018, National Centre for Biological sciences (NCBS) and C-CAMP (Centre for Cell and Molecular Platforms), Bangalore, India